ACCURACY OF INTRA-OESOPHAGEAL DYNAMIC PRESSURE PROBES, AND THEIR VALIDITY IN DETERMINING DYNAMIC INTRA-PLEURAL PRESSURE

Craig Gordon Francis Hartford

A thesis submitted to the Faculty of Health Sciences, University of the Witwatersrand, Johannesburg, in fulfilment of the requirements for the degree of Doctor of Philosophy, 2000.

Johannesburg 2000

Declaration

I, Craig G Hartford, declare that this thesis is my own work. It is being submitted for the degree of Doctor of Philosophy at the University of the Witwatersrand, Johannesburg. It has not been published before for any degree or examination at this or any other University.

The format and style of this thesis is described in detail in the Preface section. In all Chapters the vast majority of the research ideas, preparation, execution, analysis, write-up, responses to reviewers and revisions for publication were initiated and performed by the candidate. This is reflected by the fact that the candidate is the first author on all publications arising from this thesis.

I certify that studies performed towards this thesis have the approval of the University of the Witwatersrand Animal Ethics Screening Committee, clearance number AESC 96/113/2b and modifications.

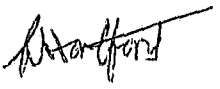

Signature of Candidate

.30 March 2000

CRAIG GORDON HARTFORD

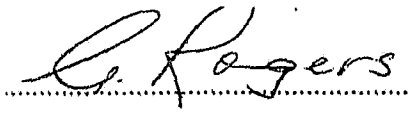

Signature of supervisor

30 March 2000

PROFESSOR GG ROGERS

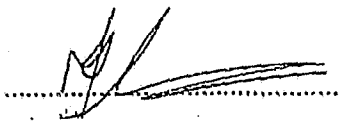

Signature of co-supervisor

30 March 2000

PROFESSOR MJ TURNER

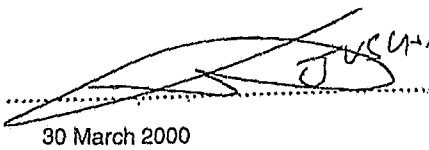

Signature of collaborator

30 March 2000

Dr J v SCHALKWYK

ABSTRACT

Oesophageal pressure (Pes) is often measured to estimate pleural pressure (Ppl) for the calculation of respiratory system elastance and resistance. High-fidelity dynamic Ppl estimation requires that Ppl waveforms be transmitted unchanged both across the Ppl-Pes tissue barrier and across Pes catheter-manometers.

In this study the frequency responses of liquid- and gas-filled catheter manometers used in clinical practice were examined in detail using the in vitro sine-wave technique. The assumption that fluid-filled catheter-manometer frequency responses fit a second order system was tested by comparing second order curve-fits to measured curves. An acute lung injury (ALI) model of human respiratory disease was developed in monkeys. In health and ALI direct Ppl and Pes were measured simultaneously to determine the Ppl-Pes tissue barrier amplitude frequency response. The relevant bandwidth of dynamic Pes waveforms was determined.

It is found that liquid-filled feeding catheters measure dynamic Pes within a 5% error up to a maximum respiratory rate (F_{RR}) of 82 breaths/min and are suitable for use only in subjects with low-frequency respiratory mechanics. F_{RR} differences exist between French Gauge sizes and differing catheter brands: French Gauge size is a poor predictor of Pes measurement suitability.

Infant air-balloon catheters' F_{RR} is up to 148 breaths/min. They possess superior frequency response characteristics compared to matching liquid-filled catheters, have lower frequency response variability within catheter samples, and are suited to dynamic Pes measurements during high-frequency respiratory mechanics.

Frequency responses of fluid-filled feeding catheters employed in Pes catheter-manometers do not adequately fit second order systems, casting doubt on the validity of applying second order mathematical models to predict catheter-manometer behaviour from step-responses.

Decreased dynamic lung compliance, reduced alveolar gas exchange and diffuse alveolar capillary leak similar to that of comparable humans evolves following oleic-acid administration in monkeys; the model is suitable for evaluation of pulmonary mechanics and gas exchange during ALI.

The Ppl-Pes tissue barrier has a uniform frequency response within the bandwidth of conventional Pes waveforms in healthy or diseased lungs, and does not attenuate Ppl-Pes waveform transmission between 1 - 40 Hz. At Pes frequencies higher than conventional regions of clinical interest the Ppl-Pes barrier resonates, is pressure amplitude dependent at low pressure offsets, and altered by ALI. During conventional ventilation for ALI, Pes-manometers require a uniform frequency response up to 8.5 Hz to achieve a $\leq$ 5% in vivo Pes waveform measurement error.

These findings advance the accuracy of pulmonary function studies in high frequency respiratory mechanics, such as conventional infant ventilation or high frequency ventilation.

PREFACE: THESIS STRUCTURE, FORMAT, PUBLICATIONS AND AWARDS

a). Rationale for structure.
b). Publications (international peer-reviewed) and their related conference abstracts, by Chapter.
c). Scholarly prizes attained in relation to research presented from thesis
d). Other publications in related (pressure and flow) biomedical engineering research.

a) **Rationale for structure.**

The Faculty of Health Sciences at the University of the Witwatersrand, Johannesburg, allows for the submission of Doctoral theses in the same format as published work where the manuscripts are published in international peer-reviewed journals and the candidate has previously written a full postgraduate dissertation. This candidate fulfills these criteria by already holding an MSc Med by dissertation in cardiovascular physiology, and all publications presented in this doctoral thesis are in reputable international, peer-reviewed and Science Citation Index listed journals. In all Chapters the research ideas, preparation, execution, analysis, write-up, responses to reviewers and revisions for publication were initiated and performed by the candidate (see Declaration page (i)). This is reflected by the candidate appearing as first author on all abstracts and papers arising from this thesis.

The body of this thesis is therefore submitted in the format of published research (Chapters 2, 3, 4, 6) and research under review for publication (Chapter 5). Chapters 2, 3 and 4 are identical in content and format to the submitted manuscripts already published. Chapter 5 is identical to the manuscript submitted for review for publication. Chapter 6 is a similar version to the published manuscript but includes additional information considered relevant to this thesis and is therefore longer than the published version. Reprints of the published papers (Chapters 2, 3, 4 and 6) are attached to the thesis for reference purposes (Section 9: Appendices).

A "linking comments" section is included at the start of each chapter to clarify the continuity between each chapter of the body of the thesis. An introduction (Chapter

1) and conclusion (Chapter 7) are also provided at the start and end of the body of published work (Chapters 2 - 6). References cited in the text are listed at the end of each chapter in the *same* format required by the published articles arising from each chapter. Where additional tables and figures are presented in the thesis for clarification over and above those published, these are marked as "*Supplemental, S*" in Chapters 2 - 6. Sources of material consulted for this thesis but which are not cited in the thesis text and not listed in the reference sections behind each chapter, are presented in the Bibliography section.

b) **Publications (international peer-reviewed) and their related conference abstracts, by Chapter.**

Thesis Chapter 2.

Published:

C.G. Hartford, G.G. Rogers, M.J. Turner

Correctly selecting a fluid-filled nasogastric infant feeding catheter to measure intra-esophageal pressure. ***Pediatric Pulmonology***. 1997;23:362-9.

Conference abstracts presented by student:

- Internationally presented abstract

  C.G. Hartford, G.G. Rogers, M.J. Turner

  Suitability of Polyvinyl Chloride Feeding Catheters in Catheter Manometer Systems. *Proceedings of the IEEE Engineering in Medicine and Biology Society, 18th Annual International Conference, Amsterdam, The Netherlands, 1996.* ISBN 90-9010005-9 (CD Rom), SOE 9609001, paper # 30

- Locally presented abstract

  C.G. Hartford, G.G. Rogers, M.J. Turner

  Frequency responses of liquid-filled infant nasogastric feeding catheters. Proceedings of the Annual Physiology Society of Southern Africa Conference, Cape Town, South Africa 1996.

Thesis Chapter 3.

Published:

C.G. Hartford, G.G. Rogers, Jv Schalkwyk, M.J. Turner

Frequency responses of infant air-balloon versus liquid-filled catheters for intra-esophageal pressure measurement. ***Pediatric Pulmonology***. 1997;Nov;24:353-363.

Conference abstract presented by student:

- International abstract

  C.G. Hartford and M.J. Turner

  Fidelity of infant air-balloon versus liquid-filled catheters for dynamic intra-esophageal pressure signal transmission. *Chest Southern Africa, South African Pulmonology Society, Windhoek, Namibia September 1997.*

Thesis Chapter 4.

Published:

C.G. Hartford, Jv Schalkwyk, GG Rogers, M.J. Turner

Predicting air-balloon and liquid-filled catheter frequency responses. Testing the validity of the assumption that fluid-filled catheters fit a second-order system. ***IEEE Engineering in Medicine and Biology***. 1997;May/June:27-33.

Thesis Chapter 5.

Under review:

C.G. Hartford, Jv Schalkwyk, GG Rogers, M.J. Turner

Stable diffuse acute lung injury model in vervet monkeys (*(Cercopithecus aephiops*). Under review in 2000.

Thesis Chapter 6.

Published:

C.G. Hartford, Jv Schalkwyk, GG Rogers, M.J. Turner

Primate pleuro-esophageal tissue barrier frequency response and esophageal pressure waveform bandwidth in health and acute lung-injury. ***Anesthesiology***. In Press. 1999.

Conference abstract presented by student:

- International abstract

  C.G. Hartford and M.J. Turner

  Frequency response of the pleuro-esophageal tissue barrier and esophageal waveform bandwidth in non-human primates. Proceedings-20th Annual International Conference-IEEE/EMBS Oct 29-Nov 1, 1998, Hong Kong. IEEE catalogue number 98CH36286C; ISBN 0-7803-5164-9/98 pp 3215-8.

c) **Scholarly Prizes attained in relation to research presented from thesis**

- CHAPTERS 2-4

  Institute of Electrical and Electronic Engineers (IEEE) Engineering in Medicine and Biology Society (EMBS) Student Whitaker Competition First Place Prize Winner, Amsterdam, 1996. (Appendix 9.6)

- CHAPTERS 5-6:

  Institute of Electrical and Electronic Engineers Engineering in Medicine and Biology Society IEEE Region 8 Finalist (student represented Europe, Africa and the Middle East in the finals), Hong Kong, 1998. (Appendix 9.6).

d). **Other publications in related (pressure and flow) biomedical engineering research, performed by the candidate during the tenure of this thesis (but not forming part of this thesis).**

Hartford CG, Marcos E, Rogers GG.
Non-invasive versus invasive blood pressure measurement in hypotensive baboons (Papio ursinus). *Laboratory Animal Science.* 1996;46;231-233.
Hartford CG and Rogers GG.
Correct technique of noninvasive auscultatory manometric blood pressure determination. *Journal of the South African Medical Students Association,* 1996;2;1:7-12.
Hartford CG, Maldonades C, Rogers GG
Inspired air humidity effect on respiratory function during exercise. *South African Journal of Sports Medicine,* 1995;2;2:24-7.

ACKNOWLEDGEMENTS

GENERAL

During my MB Bch and MSc Med I became acutely aware of the need for accurate dynamic measurements on which to base clinical interpretations and valid conclusions from data generated through medical instrumentation. My research interests therefore ventured into the field of biomedical engineering as a postgraduate student and I am grateful to the following persons:

SUPERVISOR SUPPORT

I gratefully acknowledge the assistance of my supervisors Professor G Rogers and Professor M Turner, whose tutoring enabled me to grasp the necessary essential principles of engineering and apply them to scientific and medical measurement techniques.

FINANCIAL SUPPORT

Grants:

The South African Foundation for Research and Development. Medical Research Council of South Africa. Iris Ellen grant. H.E. Griffin grant. University of the Witwatersrand Research Council and Medical Faculty Research Council grants. Levenberg Bequest South Africa. Skye Foundation. Pfizer Central Research United Kingdom.

Equipment donations:

Catheters; Erich-Jaeger, Selwyn Sher ElectroMed South Africa. Portex, the Boots Company South Africa. Portex United Kingdom. Ven Products South Africa. Vygon

(France), Art Medical Equipment South Africa. Sabax, Adcock Ingram South Africa. Ventilation equipment; SensorMedics 3100A, Sensormedics, The Netherlands; Manta Medical Systems, South Africa.
Anaesthetic agents; Janssen-Cilag, South Africa; Omnimed, South Africa, Roche products, South Africa.

PERSONNEL SUPPORT

I am grateful to Dr J van Schalkwyk for his intellectual input and practical assistance at the coalface of Chapters 5-6; Gavin Norton, Ernest Somya, Elizabeth Marcos, and the University of the Witwatersrand Central Animal Service, for technical assistance and interest in my biomedical engineering laboratory.

My father, Professor GF Hartford, for encouraging me whilst crossing disciplines between medicine, science and engineering.

TABLE OF CONTENTS

LIST OF FIGURES

LIST OF TABLES

NOMENCLATURE

In the style of this thesis, where required by the journals in which Chapters 2 - 6 are published, non-standard abbreviations are defined as a separate section at the beginning of each Chapter (Chapters 2, 3 and 6). Additionally, all abbreviations used are defined in the text where they first appear in each of Chapters 1 - 6.

CHAPTER 1.

1 INTRODUCTION

In the style of this thesis (by presentation of journal publications; see under Preface:Thesis Structure and Format) there are inevitable overlaps between this Introductory Chapter (Chapter One) and the introductions and methods sections at the start of each of Chapters 2 - 6. Thus Chapter One incorporates a discussion and review of the literature and key introductory points outlined in the body of the thesis (Chapters 2 -6), but provides unification for these across the Chapters. Chapter One also includes reference to relevant updated literature published subsequent to the journal publications of Chapters 2 - 6, and concludes the introduction by clarifying the collective rationale and objectives of this thesis.

1.1 Pulmonary Compliance Measurement

1.1.1 Intra-esophageal Pressure for Calculating Lung Compliance

The inappropriate mechanical ventilation of patients adversely affects their gas exchange and haemodynamics, and may result in lung barotrauma (Hirschl, 1999). It is estimated that up to two million infants worldwide require assisted ventilation each year, of which up to 70 000 are ventilated for respiratory distress syndrome (RDS) in

the United States alone (Wisweli and Mendolia, 1993). Many infant and adult patients die or have complications from acute RDS. For clinicians to select optimal mechanical ventilator settings, adequate quantitative information about the respiratory system is required on which to base sound clinical judgements (Roustan, 1995). Quantitative respiratory system information is also required to evaluate the effects of differing ventilation modes such as positive end expiratory pressure (PEEP) (Sohma et al. 1992) or high frequency oscillatory ventilation (HFOV) (Jackson et al. 1994) on gas exchange and the outcome of RDS. Intermittent positive pressure ventilation is associated with adverse haemodynamic effects (Greisen,1986). Although infant ventilators can usually be set to yield adequate gas exchange, it is not clear how to minimize barotrauma and the cardiovascular effects of positive pressure ventilation simultaneously (Platzker, 1986; Stahlman, 1989). Pulmonary function testing contributes to a better understanding of the pathophysiological mechanisms of pulmonary disease and is useful to optimise the clinical management of ventilated patients, including the selection of ventilation parameters which favour improved haemodynamics and gas exchange.

Current respiratory system monitoring for diseased patients includes the determination of dynamic respiratory system compliance. Measuring patients' dynamic intra-esophageal pressure (Pes) to estimate intra-pleural pressure (Ppl) is gaining popularity amongst researchers and clinicians as part of the pulmonary function work-up of sick infants and adults, particularly for the calculation of the elastic and resistive elements of the respiratory system, dynamically across the respiratory cycle (Beardsmore et al. 1989; Ratjen et al. 1992; Coates et al. 1996;

Nava and Rubini, 1999).

Accurate Ppl waveform representation is important for the construction of undistorted dynamic lung compliance loops and for resistance calculations in high frequency respiratory mechanics. High frequency waveforms are commonly encountered in pressure-limited conventional infant ventilation and during high frequency oscillatory ventilation (up to 50 Hz)(Chartrand et al. 1987; Peslin et al. 1993). The technical requirements for accurate respiratory measurements in newborns are elevated (Schmidt et al. 1998) and the measurement errors of commercial respiratory monitors increase with shortening of the respiratory system time constant (Hauschild et al. 1994). Measurement of dynamic respiratory mechanics during high frequency ventilation, in particular measurements of airway flow, airway pressure (Paw), dynamic intra-esophageal pressure (Pes) and intra-pleural pressure (Ppl) measurements at high applied respiratory frequencies (Schulze et al. 1991; Kalenga et al. 1998; Hernaiz et al. 1999) is becoming more important with the increasing use of high frequency ventilation (Donnelly and Bogue, 1998; McGettigan et al. 1998; Biarent, 1999; Hirschl, 1999).

Dynamic respiratory system compliance is given by

$$1/C_{RS} = 1/C_L + 1/Ccw,$$

where C_{RS} = total respiratory system compliance,

C_L = lung compliance,

C_{CW} = chest wall compliance.

Pes is used both in clinical practice and research to separate C_L from Ccw, and C_L is calculated from

$$C_L = \Delta V / \Delta TPP$$

where ΔV = change in lung volume,

ΔTPP = change in transpulmonary pressure

and

$$\Delta TPP = \Delta(Paw - Pes)$$

where Paw = proximal airway pressure.

Several factors influence the value of dynamic lung compliance ($C_L$dyn). In older children and adults $C_L$dyn is physiologically greater than dynamic respiratory system compliance (C_{RS}dyn), suggesting that the chest wall contributes significantly to C_{RS}dyn. This is unlike human newborns where the chest wall contributes only 20% to C_{RS}dyn (Prewitt et al. 1981). Thus C_{CW} of adults is lower than that of neonates. Positive end-expiratory pressure (PEEP) and respiratory rate (RR) may also affect $C_L$dyn (although $C_L$dyn frequency dependence is not reproducibly shown at under 60 breaths/min in infants (Beardsmore et al. 1989)). The type of analysis applied to the dynamic volume-pressure tracings (Coates et al. 1996) and the method of flow and pressure measurements (Turner et al. 1990; Turner et al. 1994) will affect $C_L$dyn. Further, the validity of the measurements made to estimate Ppl, and inter-alia the state of respiratory disease, affect $C_L$dyn.

High-fidelity non-invasive estimation of Ppl using Pes measurements requires that

the Ppl wave be transmitted unchanged across the tissues between the intra-pleural and intra-esophageal spaces, and further that the Pes wave be transmitted unchanged across the Pes catheter manometer systems. These two considerations are the foci of this thesis.

1.1.2 Clinical Procedure For Validating Pes Measurements

Current practice dictates that to site a Pes catheter manometer appropriately in the oesophagus to estimate Ppl an "occlusion test" should be used (Coates and Stocks, 1991; Stocks et al. 1996). The occlusion test, widely employed by clinicians, is currently the only means to verify Pes measurements in situ. In this test the ratio and lag of Pes to Paw is assessed during intra-thoracic isovolumia. A modification of this test exists for anaesthetised paralysed subjects (Lanteri et al. 1994).

The occlusion test is suitable for assessing the Pes measurement system intended for a relatively static response, such as that for use in conventional low frequency ventilation. To interpret the occlusion test in a valid fashion the following conditions should be met; (i) changes in pressure should be distributed evenly between the Paw, Ppl and Pes spaces and locally measured Pes should be similar to average Ppl; (ii) the Ppl and Pes compartments should be in an isovolumic chest; (iii) the patient should be able to deliver spontaneous respiratory efforts. An inadequate oesophageal wall frequency response (Chartrand et al. 1987), or non-instantaneous transmission of pressure from the alveoli to Paw, may influence the occlusion test results when used to validate an in situ Pes manometer for dynamic response.

The occlusion test is a relatively static procedure, and may not excite the pleural pressure and measurement system over a sufficiently wide frequency range. Further, it may not test Pes/Paw over all the amplitudes applied during mechanical ventilation. In anesthetised paralysed subjects the test pressure is applied in the reverse direction of conventional ventilation. The accurate representation of dynamic Ppl using Pes measurements depends in part on the amplitude and phase frequency response of the intra-pleural to intra-esophageal tissue barrier (Ppl-Pes tissue barrier), yet the frequency response of the oesophageal wall has not been adequately characterised to date.

The suggested optimal occlusion test value, based on the slope of the plot of Pes versus Paw is 0.95 - 1.05 (Coates and Stocks, 1991; Stocks et al. 1996). This figure is however dependent on lung condition and animal species (Coates and Stocks, 1991) and is not always achieved. For example, direct Ppl measurements in four rabbits yielded Pes to be 70 - 95% of Ppl during spontaneous respiration (Deen and Porcelijn, 1976). In sick and preterm infants as few as 8% (Thomson et al. 1983) and 75% (LeSouef et al. 1983) of Pes/Paw occlusion test ratios have been reported to fall between 0.90 - 1.10, and elsewhere only 33% fell within 0.95 - 1.05 (Heaf et al. 1986). Other researchers have reported Pes/Paw to lie between 0.9 - 1.1 in eight preterm subjects recovering from acute lung disease (Coates et al. 1989).

Thus the occlusion test is useful and widely applied to subjects with spontaneous respiratory efforts (with or without conventional mechanical ventilation), but the test has limitations in its application to validate high frequency dynamic Pes

measurements in mechanically ventilated patients or in patients without spontaneous respiratory efforts. For such subjects, the dynamic performance of Pes manometers, and the dynamic response of the Ppl-Pes tissue barrier, require empirical investigation, and these two factors are therefore the focus of this thesis.

1.2 Dynamic Intra-esophageal Catheter Manometers

1.2.1 Types of Pes Manometers

Options for measuring dynamic Pes include fluid-filled catheters or transducer micro-tip catheters. Traditional fluid-filled (liquid or gas) catheter manometer systems are likely to continue to be made use of extensively to estimate dynamic Ppl in clinical practice (Coates and Stocks, 1991; Coates et al. 1996; Karason et al. 1999). The use of micro-tip pressure transducer catheters to estimate Ppl is not validated (see below). Differing catheter types have relative advantages and disadvantages for Pes measurement:-

1.2.1.1 Liquid-filled Catheter Manometers

Commercial nasogastric liquid-filled feeding catheters are easily inserted and well tolerated (Asher et al. 1982; Coates and Stocks, 1991) and are readily available to clinicians as disposable and inexpensive alternatives to air-balloon (Heaf et al. 1986; Maxted et al. 1987; Beardsmore et al. 1989), and transducer-tip (Chartrand et al. 1987) catheters. In addition, feeding catheters are advantageous for Pes measurements in artificially ventilated infants because they are often in situ for long

term nasogastric feeding anyway and thus conveniently accessed. Liquid-filled Polyvinyl Chloride (PVC) catheters are also non-traumatic on insertion (Chartrand et al. 1987): the nasogastric water-filled catheters (WFC) and air-balloon catheters (ABC), by virtue of their flexibility, reduce the risk of esophageal trauma in newborns (Maxted et al. 1977; Kaplan et al. 1984). However, WFC absolute pressure measurements are altered when the vertical distance between the catheter-tip and transducer is changed, and they are sensitive to motion artifacts (Senterre and Geubelle, 1970).

1.2.1.2 Air-balloon Catheter Manometers

By virtue of their construction ABCs offer certain advantages over transducer micro-tip and WFCs (Coates and Stocks, 1991). The long ABC balloon measures mean intra-esophageal pressure over a larger portion of the esophagus than do WFCs or single micro-tip transducer catheters, making it more likely that the mean value of an unevenly distributed intra-thoracic pleural pressure is recorded (Baydur et al. 1982; LeSouef et al. 1983; Ratjen et al. 1992). ABCs are not subject to measurement errors related to the dissipation of liquid volume around WFC tips (Gerhardt et al. 1980), nor to worsened dynamic performance from introducing gas microbubbles into WFCs.

The recent advent of low cost disposable pressure transducers (Gardner, 1996) make ABCs and WFCs comparatively inexpensive for neonatal intensive care (Chartrand et al. 1991).

1.2.1.3 Transducer Micro-tip Catheter Manometers

Positive reports (Gappa et al. 1996) on the use of micro-tip catheters to estimate Ppl remain outweighed by the negative reports: Transducer micro-tip catheters can exhibit absolute pressure measurement inaccuracies (drift) with changes in light exposure, temperature and the fluid nature of the surrounding intra-esophageal medium (Chartrand et al. 1987). They are markedly more sensitive to intra-esophageal cardiac artifacts than air-balloon catheters (ABC) (Chartrand et al. 1991) and have been shown to overestimate dynamic pleural pressures in infants (Beardsmore et al. 1982). Their use in estimating dynamic Ppl has yet to be substantively validated

1.2.2 Catheter Manometer Dynamic Response Requirements

The high frequency respiratory mechanics encountered during artificial infant ventilation may require uniform catheter frequency responses up to 20 or 23 Hz (Senterre and Geubelle, 1970; Maxted et al. 1977; Turner et al. 1993; Chartrand et al. 1991), which few, if any, liquid-filled catheters demonstrate, and yet it is often necessary to introduce small FG size catheters for Pes measurement in neonates. Knowledge of the dynamic responses of Pes manometer systems is thus important for faithful Pes measurements in these settings.

1.2.2.1 Clinical Factors Affecting Catheter Manometer Resonance Properties

Resonance characteristics are dependent on the manometer compliance, inertance (liquid mass), viscous resistance and catheter wall hysteresis. In clinical practice factors which affect manometer volume displacement coefficients are (i) gas bubbles which increase the damping coefficient (D_c) but lower the resonance frequency (F_r) (the transparency of PVC catheters is advantageous here) (Milic-Emili et al. 1964; Gardner, 1981; Yeomanson and Evans, 1983); (ii) catheter wall compliance (Yeomanson and Evans, 1983); (iii) leaking connections, and (iv) the arrangement of stopcocks and transducer domes (Rothe and Kim, 1980). Manufacturing tolerances on the catheter inner diameter (ID) or length also affect F_r (Shapiro and Krovetz, 1970). The quality of pressure transducer employed in the Pes manometer directly affects resonance characteristics, and the liquid mass inertia and compliance of a Pes manometer depend on transducer dome size. Ideally a Pes manometer should have a high F_r, but a high F_r (or, more correctly, a high undamped natural frequency, F_o) by itself may be associated with overdamping and consequent reduced Pes manometer sensitivity at raised frequencies. Introducing damping systems to compensate for resonance in an underdamped Pes manometer is not usually practical, nor necessarily effective (Hipkins et al. 1989), therefore optimal damping ($D_c = 0.71$) accompanying a high F_r is desirable. Unfortunately, the potential for adverse Pes manometer responses is made more likely in the clinical setting where CO_2 flushing, degassing of water and reverse liquid flushing of WFCs are not possible.

1.2.2.2 Intra-esophageal Catheter Manometer Resonance Frequencies

Liquid-filled catheters are commonly used for intra-arterial pressure measurement, therefore extensive frequency response characterisation of these catheters exists. Large variations occur in the recorded frequency responses of these intravascular catheters (Shapiro and Krovetz, 1970; Rutten et al. 1987; Doyle, 1990), and discrepancies between manufacturer-claimed and experimentally observed resonant frequencies of liquid-filled catheters have also been documented (Rutten et al. 1987).

Data pertaining to WFCs and ABCs used for Pes measurement are sparse (Maxted et al. 1977; Beardsmore et al. 1980): Informal measurements on liquid-filled Pes catheters (usually performed with differing catheter lengths, brands and FG sizes between researchers, and using single samples) have demonstrated uniform frequency responses in a size 8 FG saline-filled catheter (2 mm ID and 38 cm long) up to 10 Hz (Coates et al. 1989) and in a similar catheter to > 10 Hz (Asher et al. 1982), while a 5 FG 1 mm ID catheter and a 6 FG catheter were also noted to be flat to 10 Hz (Asher et al. 1982; LeSouef et al. 1983). Researchers employing ABCs to measure Pes have noted "adequate" frequency responses to 10 Hz, 20 Hz and 22 Hz in a FG size 6 catheter ((Beardsmore et al. 1980; Heaf et al. 1986), (Baydur et al. 1982; Higgs et al. 1983) and (Baydur et al. 1987)), and to 5 Hz and 15 Hz in a FG size 8 catheter ((Bhutani et al. 1988; Wolfson et al. 1992) and (Dechmann et al. 1992)).

The above studies were not aimed at formally assessing the uniformity of the frequency responses of Pes catheters. Thus effects due to manufacturing tolerances within a catheter and balloon sample, and effects related to differing catheter tolerances between manufacturers for the same FG size were not judged. Details of catheter length, wall thickness, composition, brand, balloon length, balloon diameter and latex thickness, the definition of adequate frequency response used and the method of frequency response analysis were also not provided in most of the above reports.

Additionally, controversy exists in the literature as to the frequency responses of ABCs relative to WFCs: WFCs were qualitatively considered to have better frequency responses than ABCs (Chartrand et al. 1987), yet in another study ABCs were suggested to have better phase and amplitude characteristics than most WFCs (Maxted et al. 1977). In the latter study catheters of FG size 6 (unspecified length) only were tested.

In summary, studies employing WFCs or ABCs have concentrated on validating the in vivo estimation of pleural pressure by Pes (Beardsmore et al. 1980; Beardsmore et al. 1983) and do not present quantitative data on the dynamic response of differing catheter FG sizes and brands used for measuring Pes.

In this thesis studies are performed to characterise quantitatively the dynamic responses of Pes catheter manometer systems (liquid-filled and air-balloon) used in clinical practice to ascertain their suitability for transmitting dynamic pressure

waveforms accurately.

1.3 Frequency Response Measurement Techniques; Forced-oscillation Versus Square-wave Response

Currently, the accepted techniques for measuring catheter manometer frequency responses include deploying the in vitro swept sine-wave generator technique or the in vitro (free oscillation following a burst-balloon) or in vivo (fast-flush) square-wave response techniques. With in vitro techniques, superimposed in vivo peristaltic and cardiac waveform artifacts are absent (Gardner et al. 1991) which is an advantage since accurate interpretation of Pes manometer frequency responses calculated from the in vivo fast-flush test can be confounded by simultaneous pressure perturbations (Gardner, 1981). The swept sine wave frequency domain technique is suitable for a distributed parameter system (Gardner, 1981; Yeomanson and Evans, 1983), such as that encountered in catheter manometers used in clinical practice. It can also be set up to stimulate the catheter manometer at a predetermined amplitude over all frequencies, which is useful for detecting amplitude non-linearity in the manometer. The step-response approach always suffers from the disadvantage that the amplitude of the stimulation diminishes with increasing frequency. On the other hand, catheter whip, impact with the esophageal wall, physiological temperature and the surrounding intra-esophageal media may affect the response of in situ catheters, and these effects are largely ignored by in vitro techniques.

The square-wave response technique is used by clinicians to assess in vivo the

frequency response of underdamped catheter-manometer systems in situ, as well as in vitro by researchers who do not have ready access to suitable sine-wave pressure generators. The construction of an appropriate variable-frequency sine-wave generator with a uniform pressure amplitude response at varying frequencies is technically difficult (Fry, 1960; Yanof et al. 1963; Yeomanson and Evans, 1983), and requires the use of a chamber operating at physiological temperature, a variable pressure-amplitude and pressure-offset generator, and a high-fidelity temperature-compensated reference transducer. By virtue of the usual analysis methodology applied (see Second Order Systems below) when implementing step-response techniques (burst-balloon or fast flush tests), as opposed to the swept frequency forced-oscillation technique, step-response techniques are practically limited to underdamped systems (Gardner, 1981; Yeomanson and Evans, 1983) and are therefore typically unsuitable to assess potentially overdamped catheter manometers. Step-response techniques may also miss subtle differences in the undamped resonance frequency (Shapiro and Krovetz, 1970) and are open to measurement inaccuracies in the determination of the period and amplitude of the response (Gardner, 1981). In vivo fast flush tests are not practically applicable to ABCs, and the use of fast flush in vivo tests, in which there is a high inertia of the external flushing liquid, has been shown to overestimate catheter manometer damped resonance frequency (Rothe and Kim, 1980; Rutten et al. 1987; Hipkins et al. 1989).

1.4 Catheter Manometer Dynamic Responses As Second Order Systems

Where a catheter manometer's frequency response adequately fits a second order system, relatively simple mathematical equations which allow prediction of catheter frequency responses from square-wave response measurement techniques can be derived in order to estimate the catheter manometer's amplitude and phase frequency characteristics (Yanof et al. 1963; Hipkins et al. 1989). The theory surrounding the typical equations used to analyze square-wave responses, and hence to predict underdamped liquid-filled catheter frequency responses, is published in journals (Frank 1903; Hansen, 1950; Fry, 1960) and textbooks (Thomson, 1965; Kuo, 1966; Milhorn, 1966) extensively. The electrical correction of incorrect information from an imperfect catheter-manometer system may be accomplished using these second order system models.

The second order equations commonly used to model the dynamic behaviour of catheter-manometers are simple approximations of higher order models based on electrical transmission line theory in the manner of a distributed system (Hansen, 1950; Hansen and Warburg, 1950; Fry, 1960; Yeomanson and Evans, 1983). Simple second order models lump the distributed compliance, inertance and viscous resistance of the manometer into single parameters but ignore several important catheter-manometer properties which might influence the resulting theoretical frequency responses. These properties include the inertance associated with radial movements of the filling fluid and radial movements of the catheter manometer wall,

catheter manometer wall hysteresis and non-linearities associated with the catheter manometer compliance and fluid flow.

Although certain researchers have experimentally validated the second order system theoretical models for the resonant behaviour of a few intra-arterial blood pressure measurement systems (Hansen, 1949), and validated that of a more complex electrical transmission-line model (Yeomanson and Evans, 1983), other researchers have quantitatively shown such theoretical models to not be adequate for their intra-arterial catheters (Taylor, 1959; Latimer and Latimer, 1969; Billiet and Colardyn, 1992). Likewise, the similarity of frequency responses obtained with square-wave response techniques compared to those obtained from the sine-wave generator technique has been shown in some reports to be adequate (Scwhid, 1988; Sheahan et al. 1991) and in others to be inadequate (Hipkins et al. 1989; Billiet and Colardyn, 1992) for intra-arterial catheter-manometer systems.

Extrapolating the assumption of a second order system, shown to be valid in certain fluid-filled catheter-manometers, to fluid-filled catheter manometers of a different nature coupled to modern pressure transducers and domes, may be erroneous. Nevertheless, the square-wave response technique, typically reliant upon this assumption, has been used to determine frequency responses of Pes fluid-filled nasogastric catheters (LeSouef et al. 1983) and is widely applied to intra-arterial catheter manometers.

In this thesis a study is performed to investigate the validity of the assumption that

fluid-filled catheter (liquid and air-balloon) frequency responses fit a second-order system, thereby assessing the legitimacy of applying second order models to approximate the dynamic responses of Pes manometers.

1.5 Animal Models of Acute Lung Injury

Acute lung injury (ALI) animal models are useful for investigating respiratory system mechanics, barotrauma and gas exchange in respiratory distress syndromes (RDS) and for evaluating the effect of differing ventilation modes such as positive end expiratory pressure (PEEP) (Sohma et al. 1992) or high frequency oscillatory ventilation (HFOV) (Jackson et al. 1994) on gas exchange and the outcome of RDS. Intermittent positive pressure ventilation is associated with adverse haemodynamic effects (Greisen, 1986). Although infant ventilators can usually be set to yield adequate gas exchange, it is not clear how to minimize barotrauma and the cardiovascular effects of PEEP simultaneously (Stahlman, 1989). ALI models may therefore also be utilised to determine methods for assessing lung function parameters which will assist in choosing ventilator settings which reduce barotrauma but still maintain gas exchange and haemodynamics, and hence improve the long term outcome and cost-effectiveness of the treatment of pulmonary-diseased patients. One such approach would be to use ALI models to establish whether invasive or non-invasive haemodynamic variables can be reliably utilised to facilitate optimal adjustment of ventilator settings (Platzker, 1986). Additionally, certain ALI models may be useful for evaluating exogenous surfactant therapy (Lewis and Jobe, 1993), extra-corporeal membrane oxygenation (Dorrington et al. 1989), and liquid

lung ventilation (Hirschl et al. 1995).

Demand for ALI models not effected by premature delivery of foetuses has led to several modalities being employed; of note are the commonly used saline lung lavage, oleic acid infusion and hyperoxia exposure methods (Robertson, 1991). A successful saline lavage model has not been described in primates. ALI induced by hyperoxia requires specialised gas delivery systems and takes a few days to develop. In premature foetus delivery there are substantial staffing and cost implications (Jackson et al. 1986): specialised animal housing units and breeding programs are required with accurate knowledge of species gestation times, dates of conception (requiring frequent perineal skin change observations) (Meredith et al. 1989), ultrasound determination of gestational age, culminating in surgical hysterotomy. There may also be a delay to the onset of experimental data collection due to the gestation period (usually > 4 months in non-human primates). Oleic-acid induced ALI has been demonstrated in baboons (Johanson et al. 1982; Coalson et al. 1989) and used as a diffuse alveolar disease model to assess oxygen therapy (de los Santos et al. 1985). Oleic-acid induced ALI is thought to be due to toxic effects on the lung capillaries, the exact mechanism(s) of which are still unknown (Schuster, 1994).

Despite incompletely understood differences between non-human primate and human lung biochemistry, many experimentally relevant physiological and genetic characteristics are shared between humans and non-human primates (Kosch et al. 1979; Hessler et al. 1985; Juul et al. 1993; Van de Berg et al. 1996; Harroff, 1997).

In this thesis a new species model of oleic-acid induced ALI is developed (in Vervet monkeys), suitable for the pathophysiological evaluation of pulmonary mechanics and gas exchange following ALI.

1.6 In Vivo Intra-pleural Pressure Estimation

1.6.1 Specifying Intra-esophageal Catheter Manometer Dynamic Performance Requirements

Although extensive literature exists on the bandwidth of cardiovascular pressure waveforms (Paulsen, 1993) the literature pertaining to respiratory system pressure waveforms is scarce. Suggested minimum dynamic response requirements for proximal airway pressure (Paw, not Pes) measurement apparatus vary from up to the 5'th or 10'th harmonic frequency of the pressure waveform (Stocks et al. 1996), to 6 Hz and 20 Hz for 3% and 1% Paw errors respectively (Turner et al. 1993), and up to 23 Hz (Maxted et al. 1977).

Assumptions that Pes bandwidth during mechanical ventilation is the same as Paw bandwidth may be invalid since transmitted Paw frequency components may be amplified or attenuated in health and lung disease, and cardiac motion energy (not largely apparent in Paw waveforms) is added to Ppl and Pes waveforms.

One study of healthy intubated adult humans using FFT of Pes showed no significant harmonics above 5 Hz (Chartrand et al. 1991). Criteria and methods to

determine bandwidth were not detailed for this paper's subsection and waveform errors were not quantified. The determined bandwidth of respiratory system pressure waveforms is influenced by the calculation methods applied such as the type of transform used for frequency content analysis, characteristics of the filters implemented and the criteria for waveform error chosen. The Pes amplitude difference between end-inspiration and end-expiration (or between two points of zero gas flow) is currently most commonly used (Ahrens, 1991) for lung compliance calculations in clinical settings, therefore Pes waveform errors are best quantified based on these Pes reference points.

In this thesis the dynamic performance which is required of Pes manometers during mechanical ventilation is specified by determining Pes waveform bandwidth using appropriate Pes measurements.

1.6.2 Intra-pleural Intra-esophageal Tissue Barrier Transmission

Concerns surrounding the validity of in vivo Pes measurements to estimate Ppl are raised through findings such as the lung volume dependence and Paw-dependence of Pes changes in infants (Beardsmore et al. 1983; Silva-Neto et al. 1992) and adults (Baydur et al. 1987; Mergoni et al. 1997), and the frequency-dependence and Paw-dependence of lung compliance values in healthy adult monkeys (Wegner et al. 1984). Inaccuracy of Pes measurements has also been attributed to chest wall distortion producing uneven pleural pressure distribution (LeSouef et al. 1983). Additionally, it was shown recently that Ppl and Pes respond differently to changing

flow amplitudes at differing applied frequencies during high frequency ventilation in rabbits (Hernaiz et al. 1999). The mechanical properties of the esophageal wall and surrounding structures are a potential cause of signal alteration when estimating dynamic Ppl from Pes (Dechmann et al. 1992). Thus the dynamic range, amplitude-linearity and lung-condition dependence of the Ppl-Pes tissues which transmit pressure to the oesophagus require investigation.

Surveying the literature, one direct comparison of measured dynamic Ppl and Pes has been performed using validated Pes and Ppl catheters (Nagels et al. 1980); in 5 anesthetised paralysed (but healthy) dogs the amplitude frequency response did not deviate by > 10% from unity between 2 - 20 Hz, and variations in Paw offset had minimal effects on the observed frequency response. In healthy rabbits there was slight attenuation of Pes measured at discrete frequencies of 30, 40 and 50 Hz compared to Ppl measured via an (untested) chest drain (Kaplan et al. 1984). More recently, the response of non-dynamic Ppl and Pes to varying airway flow amplitudes at high frequencies was investigated in healthy rabbits (using the rib-capsule technique to estimate mean Ppl) (Hernaiz et al. 1999), demonstrating that, relative to Paw, Ppl and Pes had different phase frequency responses. One study in humans demonstrated systematic amplitude and phase differences between Pes and Paw during airway occlusion: however, Ppl was not measured directly in this study (Peslin et al. 1993).

Detecting amplitude-dependence of the Ppl-Pes barrier's frequency response by varying Paw amplitudes as well as by varying Paw pressure offsets is relevant to

lung pathologies requiring conventional artificial ventilation, where Paw offsets are often considerably raised due to PEEP requirements. Detecting amplitude-dependence may also become increasingly important with the advent of High Frequency Ventilation modes, which make extensive use of high Paw offsets with variable applied Paw amplitudes at high frequencies (Venegas and Fredberg, 1994).

To measure the specific transmission properties of the Ppl-Pes tissue barrier, effects due to the measurement manometers themselves must be diminished (Coates and Stocks, 1991; Murphy et al. 1998). Therefore the Pes manometer used must be capable of measuring Pes in a fashion similar to that performed in clinical practice, yet both the Pes and Ppl manometers must also possess a wide bandwidth considerably beyond that of conventional Pes manometers used in clinical practice, such that any non-uniformity in the responses is attributable to the Ppl-Pes barrier rather than to the measurement systems themselves. No such Pes or Ppl manometers have been described to date.

Therefore, prior to characterising the Ppl-Pes tissue barrier, this thesis develops a Pes and Ppl manometer for use in preclinical research which has an exceptionally wide bandwidth, is linear over a large amplitude, and yet measures dynamic pressure over a large portion of the esophagus and pleura.

1.7 Statement of the Problem: Rationale for Investigating High Frequency Respiratory Function Measurements

Inappropriate mechanical ventilation adversely affects gas exchange, haemodynamics, and lung barotrauma. For clinicians to select optimal mechanical ventilator settings, accurate quantitative information about the respiratory system is required on which to base sound clinical judgements.

Investigations to characterise the waveform transmission properties of the Ppl-Pes tissue barrier as well as of Pes manometers adequately, at low and high frequencies, are fundamental for the valid interpretation of respiratory pressure-flow curves derived from such measurements: the systems involved in non-invasive estimation of Ppl need to be characterised prior to looking for valuable interpretations from high frequency respiratory function measurements in clinical practice.

The dynamic performance of Pes measurement systems employed in clinical practice to estimate Ppl for the calculation of dynamic C_{RS}, C_L and C_{CW} have not been well characterised, at either low or high frequencies. There is discrepancy in the literature as to which of liquid-filled versus air-balloon catheters have superior frequency responses. The assumptions inherent to square-wave step-response techniques used to predict Pes catheter manometer frequency responses have not been tested. Additionally, in all animal species (including humans), in health and in

acute lung injury, the transmission properties of the Ppl-Pes tissue barrier have not been characterised, and the bandwidths of Pes waveforms have not been quantified.

The rationale for undertaking this thesis is that accurate pulmonary function measurements at high frequencies are, or will be, relevant in clinical practice. Certainly for conventional infant mechanical ventilation the accuracy of high frequency pulmonary function measurements is currently relevant in clinical practice. However, it cannot be predicted at this time of writing how widespread Pes measurements at high frequencies are likely to be, suffice to say that ventilation at high frequencies and with large Paw pressure offsets is increasingly used. Additionally, several authors from differing laboratories have recently published data from investigations of Pes measurements at high frequencies (see above), reflecting escalating interest in such measurements. Moreover, concerns pertaining to the accuracy of Pes measurements have also been raised by several authors (see above).

Therefore this thesis carefully characterises the dynamic responses of Pes manometers and of the Ppl-Pes tissue barrier, and places this characterisation in the context of Pes waveform bandwidths to enhance the clinical relevance of the data. These investigations have implications for potential measurements of lung function (compliance and resistance) derived from small signal detection and analysis of flow and pressure at higher frequencies and varied Paw offsets. Such waveforms are commonly encountered during conventional infant ventilation and High Frequency Ventilation, where respiratory waveforms are of variable frequency, Paw offset and

Paw amplitude. Concurrently, computer-aided analysis of pressure-volume loops is becoming more widespread, and the entire shape of the pressure-volume loop is becoming analysable in clinical practice: thus the potential for useful clinical interventions based on interpretations from shape alterations could be affected adversely if the higher frequencies of the Ppl waveforms are not represented accurately in the Pes estimate of the Ppl waveform (for example in the calculation of continuous dynamic pulmonary resistance).

1.8 Thesis Objectives

Collectively this thesis aims to:

- Characterise quantitatively the dynamic responses of Pes catheter manometer systems (liquid-filled and air-balloon) used in clinical practice to ascertain their suitability for monitoring dynamic pressure waveforms accurately
    - There-in, to develop in the laboratory an apparatus suitable for determining the dynamic frequency response of Pes manometers at pressure offsets applicable to clinical situations and at physiological temperatures.

- Test the validity of the assumption that fluid-filled catheter (liquid and air-balloon) frequency responses fit a second-order system.

- Develop and characterise a new species model of acute respiratory distress syndrome suitable for the pathophysiological evaluation of pulmonary mechanics and gas exchange in non-human primates.

- Investigate in detail the in vivo transmission properties of the primate pleuro-esophageal tissue barrier - report data on low and high frequency response uniformity, amplitude-linearity and lung-condition dependence:
  - There-in, to develop a Pes and Ppl manometer for use in preclinical research which exhibits an exceptionally wide bandwidth, is linear over a large amplitude, and yet measures dynamic pressure over a large portion of the esophagus and pleura, with which to characterise the Ppl-Pes tissue barrier.

- Specify the dynamic response requirements of Pes manometers by establishing the non-human primate relevant Pes waveform bandwidth.

1.9 Thesis Overview

High-fidelity non-invasive estimation of dynamic Ppl by using Pes measurements requires that the Ppl waveform be transmitted unchanged across the tissues between the intra-pleural and intra-esophageal spaces, and that the Pes waveform be transmitted unchanged across the Pes catheter manometer systems. These two requirements are the subject of investigation of Chapters 2 - 6 of this thesis, as follows:

In Chapter 2 the problem of selecting the correct type of water-filled catheter to measure Pes is addressed by assessing quantitatively the suitability of commercially available Pes catheter manometer systems, used in clinical practice, to transmit dynamic pressure waveforms accurately. Accordingly, the resonance frequency characteristics of a range of catheter brands, FG sizes and pressure transducers are measured, and the findings translated into the "maximum respiratory rate" (which is a measure meaningful to clinical practice) up to which differing feeding catheters may be utilised to measure Pes appropriately. It is concluded that liquid-filled feeding catheters are suitable for estimating pleural pressures in subjects mechanically ventilated without sharp inspiratory waveforms or high respiratory rates. However, judging the suitability of individual feeding catheters to measure dynamic intra-esophageal pressure based on catheter FG size alone is remarkably inappropriate.

In Chapter 3 the frequency response performances of infant air-balloon catheters are quantified and contrasted with those of new sets of matching water-filled catheters, using the swept-sine wave apparatus developed in Chapter 2. The dilemma as to which of liquid-filled versus air-filled catheters offer superior frequency responses is resolved. It is concluded that, compared to matching liquid-filled catheters, air-balloon catheters made to infant-appropriate specifications have significantly superior frequency response characteristics, lower frequency response variability within catheter samples, and are more suitable for accurate dynamic Pes measurements during high-frequency respiratory mechanics.

In Chapter 4 the validity of the assumption that fluid-filled catheter frequency

responses fit a second-order system is tested. It is concluded that the frequency responses of fluid-filled PVC catheters in catheter manometer systems do not adequately fit second order systems. Deviations of fit are significantly larger in liquid-filled than in air-balloon catheters. For compliant fluid-filled catheters, predicting Pes manometer frequency responses using the square-wave response technique is inaccurate and the swept sine-wave technique is preferred.

In Chapter 5 a new species model of non-human primate acute respiratory distress syndrome, suitable for the pathophysiological evaluation of pulmonary mechanics and gas exchange in acute lung injury, is developed. It is concluded that administration of oleic acid in monkeys rapidly results in stable acute lung injury characterised by decreased static and dynamic lung compliance, markedly reduced alveolar gas exchange and increased diffuse alveolar capillary leak. Advantageously, the healthy and sick monkey lung compliance values recorded are similar to comparable healthy and sick humans.

In Chapter 6 the transmission properties of the in vivo pleuro-esophageal tissue barrier are investigated in health and lung disease at low and high frequencies, and the relevant bandwidth of dynamic physiological intra-esophageal pressure waveforms is determined. From direct simultaneous Ppl and Pes measurements it is concluded that the Ppl-Pes tissue barrier has a uniform amplitude frequency response within the bandwidth of conventional Pes waveforms in healthy and diseased lungs, and does not significantly attenuate Ppl-Pes signal transmission between 1 - 40 Hz. However, at Pes frequencies higher than conventional clinical

regions of interest the Ppl-Pes barrier resonates significantly, is pressure amplitude dependent at low pressure offsets, and is significantly altered by lung disease.

These findings advance the accuracy of pulmonary function studies in high frequency respiratory mechanics, such as conventional infant mechanical ventilation or High Frequency Ventilation.

1.10 References to Introduction

Ahrens TS. Effects of mechanical ventilation on hemodynamic waveforms. Crit Care Nurse Clin North America 1991;3(4):629-39.

Asher MI, Coates AL, Collinge JM, Milic-Emili J. Measurement of pleural pressure in neonates. J Appl Physiol 1982;52:491-94.

Baydur A, Behrakis PK, Zin WA, Jaeger M, Milic-Emili J. A simple method for assessing the validity of the esophageal balloon technique. Am Rev Respir Dis 1982;126:788-91.

Baydur A, Cha E, Sassoon CSH. Validation of esophageal balloon technique at different lung volumes and postures. J Appl Physiol 1987;65:315-21.

Beardsmore CS, Helms P, Stocks J, Hatch DJ, Silverman M. Improved esophageal balloon technique for use in infants. J Appl Physiol 1980;49:735-42.

Beardsmore CS, Stocks J, Silverman M. Esophageal pressure in infants at elevated lung volumes and positive airway pressure. J Appl Physiol 1983;55:377-82.

Beardsmore CS, Stocks J, Helms P. Elastic properties of the respiratory system in infants. Eur Respir J 1989;2 Suppl:135s-139s.

Bhutani VK, Sivieri EM, Abbasi S, Shaffer TH. Evaluation of neonatal pulmonary mechanics and energetics. Pediatr Pulmonol 1988;4:150-58.

Biarent D. New tools in ventilatory support: high frequency ventilation, nitric oxide, tracheal gas insufflation, non-invasive ventilation. Pediatr Pulmonol 1999;18(Suppl):178-81.

Billiet E, Colardyn F. Hazardous information from bedside fast-flush device test for fluid-filled pressure monitoring systems. Angiology 1992;43(12):988-95.

Chartrand DA, Ye TH, Maarek JH, Chang HK. Measurement of pleural pressure at low and high frequencies in normal rabbits. J Appl Physiol 1987;63:1142-1146.

Chartrand DA, Jodoin C, Couture J. Measurement of pleural pressure with oesophageal catheter-tip micromanometer in anaesthetized humans. Can J Anaesth 1991;38:518-21.

Coalson JJ, King RJ, Winter VIT, et al. O2 and pneumonia-induced lung injury I. Pathological and morphometric studies. J Appl Physiol 1989;67(1):346-56.

Coates AL, Davis GM, Vallinis P, Outerbridge EW. Liquid-filled esophageal catheter for measuring pleural pressure in preterm neonates. J Appl Physiol 1989;67:889-93.

Coates AL, Stocks J. Esophageal pressure manometry in human infants. Pediatr Pulmonol 1991;11:350-60.

Coates AL, Stocks J, Gerhardt T. Esophageal manometry. In: Stocks J, Sly PD, Tepper RS, Morgan WJ, editors. Infant Respiratory Function Testing. John Wiley & Sons, Inc., 1996:241-58.

de los Santos R, Coalson J, Holcomb JR, et al. Hyperoxia exposure in mechanically ventilated primates with and without previous lung injury. Exp Lung Res 1985;9:255-75.

Dechman G, Sato J, Bates JHT. Factors affecting the accuracy of esophageal balloon measurement of pleural pressure in dogs. J Appl Physiol 1992;72:383-88.

Deen L, Porcelijn T. Oesophageal pressure measurement in rabbits and human infants using and air-filled balloon system. Br J Anaesth 1976;48:521-26.

Donnelly KM, Bogue CW. Use of high frequency and non-conventional ventilation for respiratory failure. Curr Opin Pediatr 1998;10:278-83.

Dorrington KL, McRae KM, Gardaz JP, et al. Randomized comparison of total extracorporeal CO2 removal with conventional mechanical ventilation in experimental hyaline membrane disease. Intensive Care Med 1989;15:184-91.

Doyle DJ. Resonance properties of 85-cm and 110-cm pulmonary artery catheters. J Cardiothorac Anesth 1990;4:781-82.

Egberts J, Beintema-Dubbeldam A, de Boers A. Phosphatidylinositol and not phosphatidylglycerol is the important minor phospholipid in rhesus-monkey surfactant. Biochim Biophys Acta 1987;919:90-2.

Fry DL. Physiologic recording of modern instruments with particular reference to pressure recording. Physiol Rev 1960;40:753-88.

Gappa M, Jackson E, Pilgrim L, Costeloe K, Stocks J. A new microtransducer catheter for measuring esophageal pressure in infants. Pediatr Pulmonol 1996;22:117-24.

Gardner RM. Direct blood pressure measurement-dynamic response requirements. Anesthesiology 1981;54:227-36.

Gardner RM. Accuracy and reliability of disposable pressure transducers coupled with modern pressure monitors. Crit Care Med 1996;24:879-82.

Gerhardt T, Bancalari E. Chestwall compliance in full term and premature infants. Acta Paediatr Scand 1980;69:359.

Greisen G. Cerebral blood flow in preterm infants during the first week of life. Acta Paediatr Scand 1986;75:43-51.

Hansen AT. Experimental examinations of the theory for the elastic liquid-containing membrane manometer. In: Pressure Measurement in the Human Organism. Thesis. Copenhagen, Teknisk Forlag, Acta Physiol Scand 1949:19:84-115.

Hansen AT, Warburg E. The theory for elastic liquid-containing membrane manometers: General part. Acta Physiol Scand 1950;19:306-32.

Hansen AT. The theory for elastic liquid-containing membrane manometers: Special part. Acta Physiol Scand 1950;19:333-43.

Harroff HH. Use of animal models in pediatric research. Advances in Pediatrics 1997;44:453-89.

Hauschild M, Schmalisch G, Wauer RR. Measuring accuracy of commercial respiratory function equipment and ventilation monitors for newborn infants. Klin Padiatr 1994;206:167-74.
Heaf DP, Turner H, Stocks J, Helms P. The accuracy of esophageal pressure

measurements in convalescent and sick intubated infants. Pediatr Pulmonol 1986;2:5-8.

Hernaiz MI, Fernandez P, Houtz P, Boynton BR, Lai-Fook SJ. Effect of frequency and tidal volume on pleural pressure in rabbits during high frequency ventilation. Lung 1999;177:21-36.

Hessler JR, Matinilla G, Kirkpatrick BV, et al. Asphyxia and hyaline membrane disease in neonatal monkeys. Am J of Perinatology 1985;2(2):101-8.

Higgs BD, Behrakis PK, Bevan DR, Milic-Emili J. Measurement of pleural pressure with esophageal balloon in anaesthetized humans. Anesthesiology 1983;59:340-43

Hipkins SF, Rutten AJ, Runciman WB. Experimental analysis of catheter-manometer systems in vitro and in vivo. Anesthesiology 1989;71:893-906.

Hirschl RB, Parent A, Tooley R, et al. Liquid ventilation improves pulmonary function, gas exchange and lung injury in a model of respiratory failure. Annals of Surgery 1995;(221)1:79-88.

Hirschl RB. Respiratory failure: current status of experimental therapies. Semin Pediatr Surg 1999;8:155-70.

Jackson CJ, Palmer S, Truog WE, et al. Surfactant quantity and composition during recovery from hyaline membrane disease. Pediatr Res 1986;20:1243-47.

Jackson CJ, Truog WE, Standaert TA, et al. Reduction in lung injury after combined surfactant and high frequency ventilation. Am J Respir Crit Care Med 1994;150:534-9.

Johanson Jr. WG, Holcomb JR, Coalson JJ. Experimental diffuse alveolar damage in baboons. Am. Rev. Respir. Dis. 1982;126:142-51.

Juul SE, Kinsella MG, Wight TN, et al. Alterations in nonhuman primate (M.nemestrina) lung proteoglycans during normal development and acute hyaline membrane disease. Am J Respir Cell Mol Biol 1993;8:299-310.

Kalenga M, Battisti O, Franccois A, Langhendries JP, Gertsmann DR, Bertrand JM. High frequency oscillatory ventilation in neonatal RDS: initial volume optimisation and respiratory mechanics. J Appl Physiol 1998;84:1174-7.

Kaplan M, Galioto FM, Ruttimann UE, Hamosh P, Avery GB. Evaluation of a gastric tube with esophageal balloon for neonatal use. Am J Perinatology 11984;355-59.

Karason S, Karlsen KL, Lundin S, Stenqvist O. A simplified method for separate measurements of lung and chest wall mechanics in ventilator treated patients. Acta Anaesthesiol Scan 1999;43:308-15.

Kosch C, Gillepsie JR, Berry JD. Respiratory mechanics in normal bonnet and rhesus monkeys. J Appl Physiol 1979;46(1):166-75.

Kuo FF. The Laplace transform; amplitude, phase and delay. In: Network Analysis and Synthesis. John Wiley & Sons Inc. New York, 1966:134-65,253-79.

Lanteri CJ, Kano S, Sly PD. Validation of the esophageal pressure occlusion test after paralysis. Pediatr Pulm 1994;17:56-62.

Latimer KE, Latimer RD. Measurements of pressure wave transmission in liquid-filled tubes used for intravascular blood pressure recording. Med Biol Eng 1969;7:143-48.

LeSouef PN, JM Lopes, SJ England, HM Bryan, CA Bryan. Influence of chest wall distortion on esophageal pressure. J Appl Physiol 1983;55:353-58.

Lewis JF, Jobe HJ. Surfactant and the adult respiratory distress syndrome. Am Rev Respir Dis 1993;147:218-33.

Maxted KJ, Shaw A, Macdonald TH. Choosing a catheter system for measuring intra-esophageal pressure. Med Biol Eng Comput 1977;15:398-401.

McGettigan MC, Adolph VR, Ginsberg HJ, Goldsmith JP. New ways to ventilate newborns in acute respiratory failure. Pediatr Clin North Am 1998;45:475-509.

Meredith KS, DeLemos RA, Coalson JJ, et al. Role of lung injury in the pathogenesis of hyaline membrane disease in premature baboons. J Appl Physiol 1989;66(5):2150-58.

Mergoni M, Martelli A, Volpi A, Primavera S, Zuccoli P, Rossi A. Impact of positive end expiratory pressure on chest wall and lung pressure volume curve in acute respiratory failure. Am J Respir Crit Care Med 1997;156:846-54.

Milhorn HT. Transient analysis of physical systems. In: The Application of Control Theory to Physiological Systems. WB Saunders Company, Philadelphia, 1966;78-91.

Milic-Emili J, Mead J, Turner JM, and Glauser EM. Improved technique for estimating pleural pressure from esophageal balloons. J Appl Physiol. 1964;19:207-211.

Murphy DJ, Renninger JP, Gossett KA. A novel method for chronic measurement of pleural pressure in conscious rats. J Pharmacol Toxicol Methods 1998;39:137-41.

Nagels J, Landser FJ, van de Linden L, Clement J, van Woestijne KP. Mechanical properties of lungs and chest wall during spontaneous breathing. J Appl Physiol 1980;49:408-16.

Nava S, Rubini F. Lung and chest wall mechanics in ventilated patients with end stage idiopathic pulmonary fibrosis. Thorax 1999;54:390-5.

Paulsen AW. Implications for clinical monitoring of intra-arterial blood pressure based on the frequency content of worst-case pressure waveforms. Biomedical Instrumentation and Technology 1993;May:217-34.

Peslin R, Navajas D, Rotger M, Farre R. Validity of the esophageal balloon technique at high frequencies. J Appl Physiol 1993;74(3):1039-44.

Platzker ACG. Congenital anomalies causing respiratory failure. In: Neonatal Pulmonary Care. Thibeault DW, Gregory GA (Eds). Appleton-Century-Crofts, Connecticut, 1986.

Prewitt RTM, McCarthy J, Wood LDH. Treatment of acute low pressure pulmonary edema in dogs. J Clin Invest 1981;67:409-418.

Ratjen FA, Wiesemann HG. Variability of dynamic compliance measurements in spontaneously breathing and ventilated newborn infants. Pediatr Pulmonol 1992;12:73-80.

Robertson B. Surfactant inactivation and surfactant replacement in experimental models of ARDS. Acta Anaesth Scand 1991;35(95):22-8.

Rothe CL, Kim KC. Measuring systolic arterial blood pressure; possible errors from extension tubes or disposable transducer domes. Crit Care Med 1980;8:683-89.

Roustan JP. High frequency jet ventilation combined with conventional mechanical ventilation in the treatment of adult respiratory distress syndrome. Ann Fr Anesth Reanim 1995;14:276-88.

Rutten AJ, Nancarrow C, Isley AH, Runciman WB. An assessment of six different pulmonary artery catheters. Crit Care Med 1987;15:250-55.

Schmidt M, Foitzik B, Hochmuth O, Schmalisch G. Computer simulation of the measured respiratory impedance in newborn infants and the effect of measurement equipment. Med Eng Phys 1998;20:220-8.

Schulze A, Schaller P, Dinger J, Winkler U, Gmyrek D. High frequency oscillatory ventilation near resonant frequency of the respiratory system in rabbits with normal and surfactant depleted lungs. Eur J Pediatr 1991;150:671-5.

Schuster DP. ARDS: Clinical lesion from the Oleic Acid Model of Acute Lung Injury. Am J Respir Crit Care Med 1994;149:245-60.

Scwhid HA. Frequency response evaluation of radial artery catheter-manometer systems: sinusoidal frequency analysis versus flush method. J Clin Monit 1988;4(3):181-85.

Senterre J, Geubelle F. Measurement of endoesophageal pressure in the newborns. Biol Neonate 1970;16:47-53.

Shapiro GG, Krovetz LJ. Damped and undamped frequency responses of underdamped catheter manometer systems. Am Heart J 1970;80:226-36.

Sheahan NF, Tuohy B, Kirkham R, et al. The fast flush test; evaluation in radial artery catheter-manometer systems. Clin Phys Physiol Meas 1991;12(3):247-53.

Silva-Neto G, Gerhardt T, Silberberg, A, Gerhardt T, Claure N, Duara S, Bancalari E. Nonlinear pressure/volume relationship and measurements of lung mechanics in infants. Pediatr Pulmonol 1992;12:146-52.

Sohma AE, Brampton WJ, Dunnill MS, et al. Effect of ventilation with positive end-expiratory pressure on the development of lung damage in experimental acid aspiration pneumonia in the rabbit. Intensive Care Med 1992;19:112-17.

Stahlman MT. Implications of research and high technology for neonatal intensive care. J. American Medical Association 1989;24:1791,1989.

Stocks J, Sly PD, Tepper RS, Morgan WJ, editors. Infant respiratory function testing. New York: Wiley-Liss, Inc., 1996.

Taylor MG. An experimental determination of the propagation of fluid oscillations in a tube with a visco-elastic wall; together with an analysis of the characteristics required in an electrical analogue. Phys Med Biol 1959;4:63-82.

Thomson A, Elliott J, Silverman M. Pulmonary compliance in sick low birthweight infants. Arch Dis Child 1983;58:891-96.

Thomson WT. Forced vibration with harmonic excursion. In: Vibration Theory and Applications. New Jersey, Prentice Hall Inc., Engelwood Cliffs, 1965:51-57.

Turner MJ, Macleod IM, Rothberg AD. Calibration of Fleisch and screen pneumotachographs for use with various oxygen concentrations. Med Biol Eng & Comput 1990;28:200-304.

Turner MJ, Davies VA, Ravel TJL. Bandwidths of respiratory gas flow and pressure waveforms in mechanically ventilated infants. Physiological Measurement 1993;14:419-31.

Turner MJ, MacLeod IM, Rothberg AD. Measurement of respiratory mechanics in a mechanically ventilated infant lung simulator: effects of variations in the frequency response of the flow measurement system. Med Biol Eng Comput 1994;32:49-54.

VandeBerg JL, Williams-Blangero S. Strategies for using nonhuman primates in genetic research on multifactorial diseases. Lab Anim Sci 1996;46(2):146-51.

Venegas JG, Fredberg JJ. Understanding the pressure cost of ventilation: why does high-frequency ventilation work? Crit Care Med 1994;22(Suppl):S49-47.

Wegner CD, Jackson AC, Berry JD, Gillepsie JR. Dynamic respiratory mechanics in monkeys measured by forced oscillations. Respiration Physiology 1984;55:47-61.

Wiswell TE, Mendiola J. Respiratory distress syndrome in the newborn: innovative therapies. Am Fam Physician 1993;47:407-14.

Wolfson FR, Greenspan JS, Deoras KS, Allen JL, Shaffer TH. Effect of position on mechanical interaction between rib cage and abdomen in preterm infants. J Appl Physiol 1992;72:1032-38.

Yanof HM, Rosen AL, McDonald NM, McDonald DA. A critical study of the response of manometers to forced oscillations. Phys Med Biol 1963;8(4):407-22.

Yeomanson CW, Evans DH. The frequency response of external transducer blood pressure measurement systems: a theoretical and experimental study. Clin Phys Physiol Meas 1983;4:435-49.

CHAPTER 2

2 CORRECTLY SELECTING A LIQUID-FILLED NASOGASTRIC INFANT FEEDING CATHETER TO MEASURE INTRA-ESOPHAGEAL PRESSURE

2.1 Linking Comments

Liquid-filled catheter manometer systems can be used to measure dynamic intra-esophageal pressure in order to estimate intra-pleural pressure. The commonly performed in vivo airway occlusion test helps to position clinical intra-esophageal pressure measurement catheters optimally by assessing the in situ intra-esophageal catheter's reflection of pleural pressure. However, this procedure does not adequately assess the ability of intra-esophageal pressure measurement catheters to respond accurately to dynamic pressure changes during artificial ventilation.

In Chapter Two a laboratory apparatus suitable for testing the in vitro frequency responses of a range of intra-esophageal pressure measurement catheters used in clinical practice, over pressure ranges encountered in clinical practice and at body temperature, is built in the laboratory. The suitability of liquid-filled infant feeding catheters available commercially to measure dynamic intra-esophageal pressure is quantified by determining their resonance-frequency amplitude and phase properties. Polyvinyl chloride infant nasogastric feeding catheters of four differing French Gauge sizes, three differing brands, attached to two pressure transducers of differing volumes, with six samples of each manufactured batch, are investigated using the in vitro sine-wave generator technique.

The findings for the liquid-filled catheters are translated into a "maximum respiratory rate", which is meaningful to clinicians, up to which feeding catheters of differing FG sizes may be utilised to measure intra-esophageal pressure appropriately.

[Comprehensive information is provided in Chapter Two's Abstract, Introduction and Discussion sections, which follow]:-

2.2 Summary

Polyvinyl chloride (PVC) nasogastric feeding catheters are used in clinical practice to measure intra-esophageal pressure as an estimate of pleural pressure for calculating lung compliance in infants. Pressure measurement accuracy of four French Gauge (FG) sizes and three brands of liquid-filled catheter manometer systems (CMS) was quantified by determining their resonance-frequency amplitude and phase properties. All CMS were underdamped and resonated. No CMS exhibited a uniform mean frequency response above 11 Hz. The maximum respiratory rate within which CMS could measure dynamic intra-esophageal pressure within a 5% error limit was determined (F_{rr}): The highest mean F_{rr} recorded in large diameter catheters was 82 breaths/min. Significant CMS accuracy differences existed between catheter FG sizes and between catheters of similar diameters but differing brands. Correlation (r^2) between catheter inner diameter and CMS F_{rr} was 0.66 across brands. F_{rr} values for differing catheter FG sizes and brands are presented. In conclusion, intra-esophageal PVC liquid-filled feeding catheters are suitable for estimating pleural pressures in subjects mechanically ventilated without sharp inspiratory waveforms or high respiratory rates. Quantitative frequency response characterisation of differing nasogastric catheter brands and diameters is mandatory prior to their utilisation.

KEYWORDS: apparatus and methods; lung compliance; pleural pressure; pressure; oesophageal manometry; respiratory mechanics.

2.3 Non-standard Nomenclature

A_r/A_0	Resonance amplitude ratio
Adc	Adcock Ingram catheter
CMS	Catheter Manometer System
D_c	Damping coefficient
F_{a5}	Frequency at A_0 + 5%
F_o	Undamped natural resonant frequency
F_r	Damped resonant frequency
F_{rr}	Maximum working respiratory rate
FG	French Gauge
Hz	Hertz
Mag	Linear magnitude gain
MANOVA	Multivariate analysis of variance
P_{a5}	Phase difference at F_{a5}
Por	Portex catheter
PVC	Polyvinyl chloride
SA	South Africa
UK	United Kingdom
USA	United States of America
WRMS	Root mean square Watts

2.4 Introduction

Measuring dynamic intra-esophageal pressure to estimate pleural pressure is gaining popularity amongst researchers and clinicians as part of the pulmonary function work-up of infants, particularly for the calculation of the elastic and resistive elements of the respiratory system.[1,2,3] Commercial nasogastric liquid-filled feeding catheters are easily inserted and well tolerated,[4,5] and are readily available to clinicians as disposable and inexpensive alternatives to balloon[2,6,7] and transducer-tip[8] catheters. In addition, liquid-filled feeding catheters are advantageous for intra-esophageal pressure measurements in artificially ventilated infants because the catheters are normally in situ for long term nasogastric feeding and thus conveniently accessed. Moreover, liquid-filled PVC catheters are non-traumatic[8] on insertion in comparison with the larger balloon-tip, or the relatively inflexible transducer-tip, catheters.

Although there is extensive documented frequency response characterisation of liquid-filled catheters used for intra-arterial pressure measurement,[9,10,11] there is a deficiency of such data pertaining to liquid-filled infant feeding catheters[5,12,13] since they were not manufactured for incorporation into pressure measurement devices: The high respiratory rates and wide dynamic pressure waveforms encountered during artificial infant ventilation may require flat catheter frequency responses up to 23 Hz,[6] yet it is often necessary to introduce small FG size catheters in neonates.

This study aims to quantify the suitability of commercially available polyvinyl chloride (PVC) infant nasogastric feeding catheters to measure dynamic intra-esophageal pressure. By assessing the in vitro resonance frequency characteristics

(amplitude and phase) of a range of catheter brands and French Gauge (FG) sizes we aim to provide values for the maximum respiratory rate up to which differing FG size feeding catheters may be utilised to measure intra-esophageal pressure accurately.

2.5 Materials and Methods

Infant catheter-manometer systems (CMS) employed in clinical practice to measure intra-esophageal pressure were subjected to in vitro sinusoidally oscillating pressures of varying frequency, and CMS frequency responses were determined by comparison with a reference manometer system. The CMS included 12 types of medical grade PVC catheters (three brands and four FG sizes, Table 2.1), chosen for their similar lengths, coupled to two pressure transducer-dome combinations. A Gould P10EZ pressure transducer (6.4 mm pressure sensor area) and disposable diaphragm-dome with luer lock fittings (Viggo-Spectramed Gould TA1019, Oxnard, CA) and a Gould P23XL transducer (14 mm pressure sensor area) and disposable diaphragm-dome with luer lock fittings (TA1010ND) were employed. The dome ports were fitted in-series to 4-way stopcocks (Adcock Ingram, South Africa) yielding transducer-dome-stopcock volumes of 0.6 and 0.9 ml for the transducer combinations respectively. The space between the transducer diaphragm and disposable dome diaphragm was water-filled according to manufacturer instructions and positioned at catheter-tip level.

Table 2.1. *Infant feeding catheter specifications*

Feeding Catheter	FG	OD ± Tol, mm	ID ± Tol, mm	L, cm
Portex	10	3.3 ± 0.1	2.3 ± 0.1	60
(Portex, Kent, UK)				
Adcock Ingram	10	3.3 ± 0.08	2.2 ± 0.1	50
(Sabax Division, SA)				
Ven	10	3.3 ± 0.1	2.3 ± 0.1	50
(Ven Products, SA)				
Portex	8	2.6 ± 0.08	1.8 ± 0.08	50
Adcock Ingram	8	2.6 ± 0.08	1.7 ± 0.1	50
Ven	8	2.6 ± 0.1	1.8 ± 0.1	50
Portex	6	2.0 ± 0.08	1.4 ± 0.08	50
Adcock Ingram	6	2.0 ± 0.08	1.1 ± 0.1	50
Ven	6	2.0 ± 0.1	1.2 ± 0.1	50
Adcock Ingram	5	1.7 ± 0.08	0.8 ± 0.1	50
Ven	5	1.9 ± 0.1	0.8 ± 0.1	50
Portex	4	1.3 ± 0.08	0.6 ± 0.08	50

FG, french gauge; ID, internal diameter; OD, external diameter; Tol, manufacturer specified tolerance; L, length; UK, United Kingdom; SA, South Africa.

Six samples each of the twelve different catheter types were assessed by randomly attaching their proximal female luer fittings directly to the two transducers' stopcock male luer fittings. To minimise bubble formation each catheter was flushed with carbon dioxide followed by de-ionised, degassed (by boiling) water cooled under vacuum to between 36-38 °C,[14] and the catheter distal 20 cm inserted into a laboratory designed leak-proof water chamber kept at 36-38 °C. Sinusoidal pressure waveforms between -5.5 and +10 cmH_2O (mean 2.3 cmH_2O) were generated in the chamber by means of a loudspeaker (Bose 4.5" 802, Bose Corporation, MA) powered by an 80 WRMS DC-coupled amplifier linked to a sine wave generator (Hewlett Packard 3562A, USA). A swept sine frequency response of the CMS was recorded (Fig. 2.1) using a calibrated domeless piezoresistive differential pressure transducer as a reference (Honeywell Microswitch 170PC, USA), positioned inside the chamber adjacent to the CMS catheter-tip. Unfiltered electrical outputs from the CMS and reference pressure transducer were identically pre-amplified (Hellige Servomed, Freiburg, Germany), and analyzed for phase and amplitude differences by averaging 3 repeat measurements over 10 seconds at each 1 Hz interval (Hewlett Packard Dynamic Signal Analyzer 3562A, USA). Apparatus reproducibility over the experiment was confirmed by repeating a CMS frequency response measurement of the sample of Portex FG size 6 catheters at the start and end of the experiment.

(SEE Supplemental Figures S2.A, S2.B, S2.C).

Supplemental Figure S2.A

Frequency response pressure chamber

I. 6 Ampere (continuous) power supply

II. 80 WRMS amplifier, laboratory-modified to be DC-coupled and convection air-cooled

III. 8 Ohm loudspeaker, laboratory-modified to be a leak-free cone, and ice-cooling device

IV. Back-up loudspeaker device; cold air convection-cooled

V. 16 mm acrylic (perspex) heated chamber

VI. Removable acrylic lid with sealing gasket

VII. Thermocouple chamber temperature monitor

VIII. Variable depth water slide to simulate positive airway pressure offset during frequency oscillation

IX. Reference differential pressure transducer

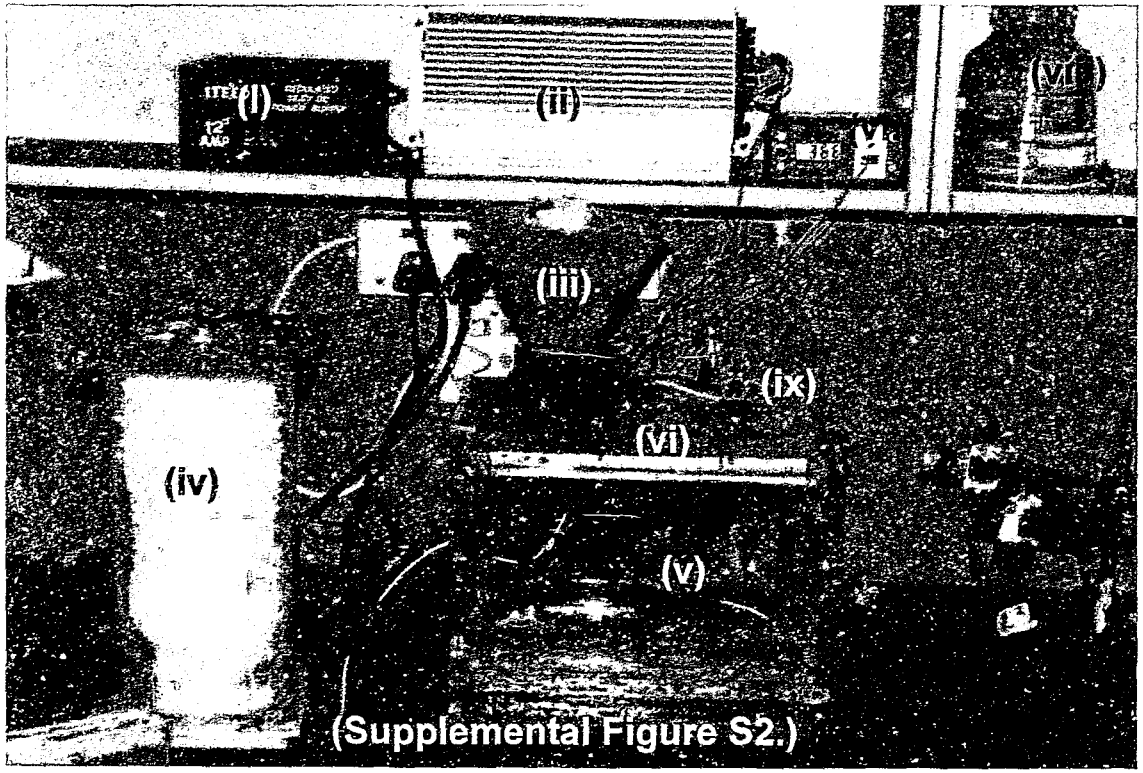

(Supplemental Figure S2.)

TOP: Supplemental Figure S2.B

Saline-filled catheters and transducers for frequency response characterisation

I. Size 10 French gauge polyvinyl chloride catheter

II. Size 4 French gauge polyvinyl chloride catheter

III. Large volume pressure transducer

IV. Small volume pressure transducer

BOTTOM: Supplemental Figure S2.C

Chamber pressure measurement and control

(i) Reference transducer and catheter under test transducers signals are (ii) preamplified, (iii) displayed on video, (iv) captured by the Hewlett Packard dynamic signal analyser, and (v) digitally stored for analysis. (vi) transducers are manually calibrated against a laboratory-made distilled-water manometer with magnified scale.

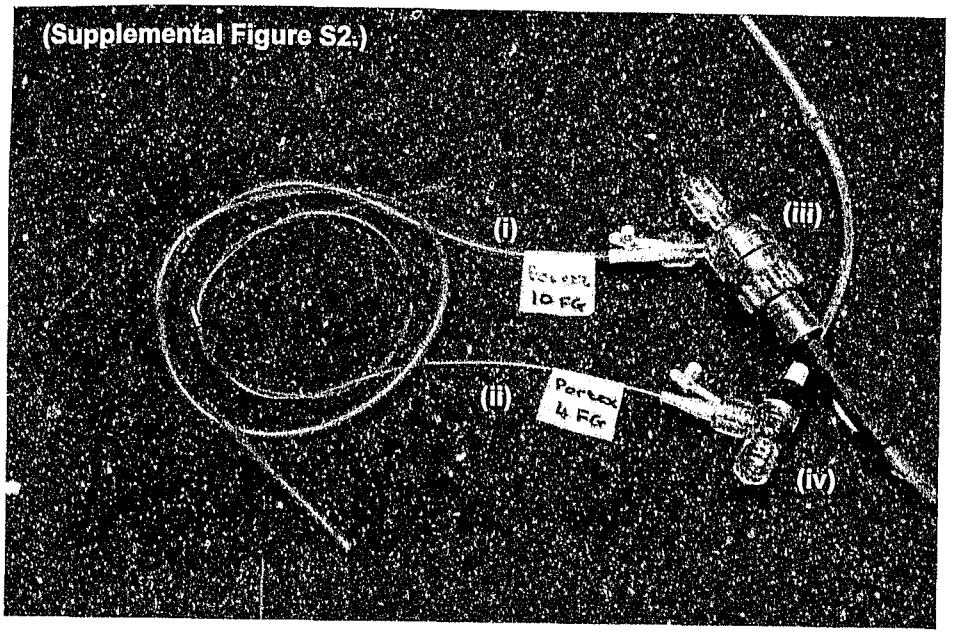
(Supplemental Figure S2.)
(i)
(ii)
(iii)
(iv)

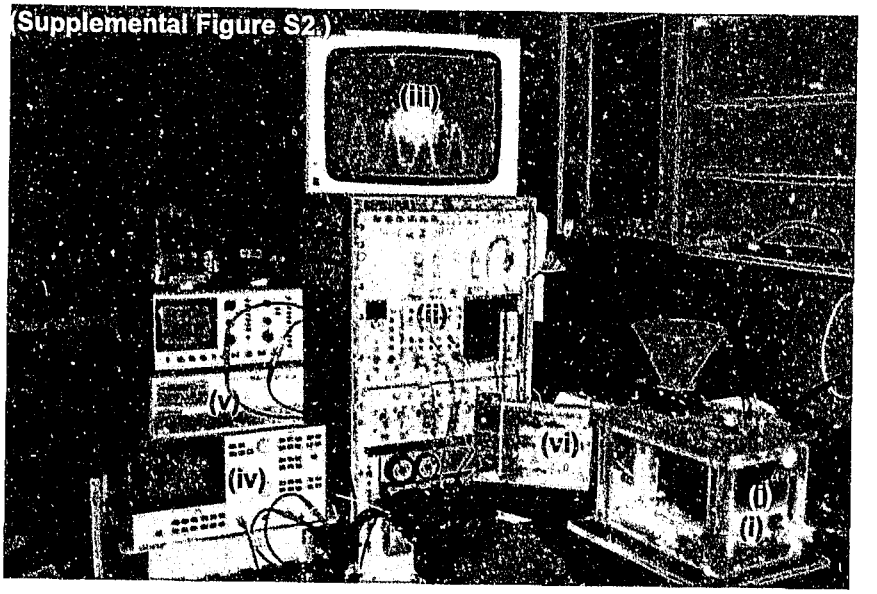
(Supplemental Figure S2.)
(iii)
(ii)
(v)
(iv)
(vi)
(i)

Frequency response measurements. Amplitude-frequency response variables relate to CMS gain or attenuation of applied pressure compared with the reference transducer over a range of applied pressure frequencies (Fig. 2.1).

Variables extracted from amplitude-frequency responses were:

F_r damped resonant frequency (frequency at maximum amplitude)

A_r/A_0 resonance amplitude ratio (maximum amplitude, A_r, divided by amplitude at 1 Hz, A_0)

F_{a5} frequency at A_0 + 5% (frequency at which the amplitude ratio = 1.05)

Phase-frequency response variables characterise the CMS temporal advancement or retardation of the applied pressure waveform over a range of frequencies; the phase-frequency response variable extracted from the recorded CMS phase-frequency response tracings was:

P_{a5} phase difference at F_{a5}

Calculated variables derived from the CMS frequency responses were:

D_c damping coefficient,

(Appendix formula 1)

F_o undamped natural resonant frequency,

(Appendix formula 2)

F_{rr} CMS maximum working respiratory rate,

(Appendix formula 3)

D_c describes CMS resistance to oscillation. F_o represents the number of oscillations per unit time that the CMS would undergo if left to oscillate undisturbed. F_{rr} predicts the maximum respiratory rate up to which an intra-esophageal CMS of measured F_o and D_c could measure an applied pressure to within ± 5% of the reference transducer.[9,15]

Figure 2.1.

Sample Portex FG size 4 catheter amplitude and phase frequency response traces. First marker circle on amplitude plot represents baseline amplitude (Y-axis, $Y_0 = A_0 =$ 1.0 Mag) and baseline frequency (X-axis, $X_0 = 1$ Hz). Second marker circle represents damped resonant frequency (X-axis, $F_r = 20$ Hz) and maximum amplitude gain (Y-axis, $A_r = 1.8$ Mag). Mag, lin ar magnitude gain over reference transducer; Hz, hertz.

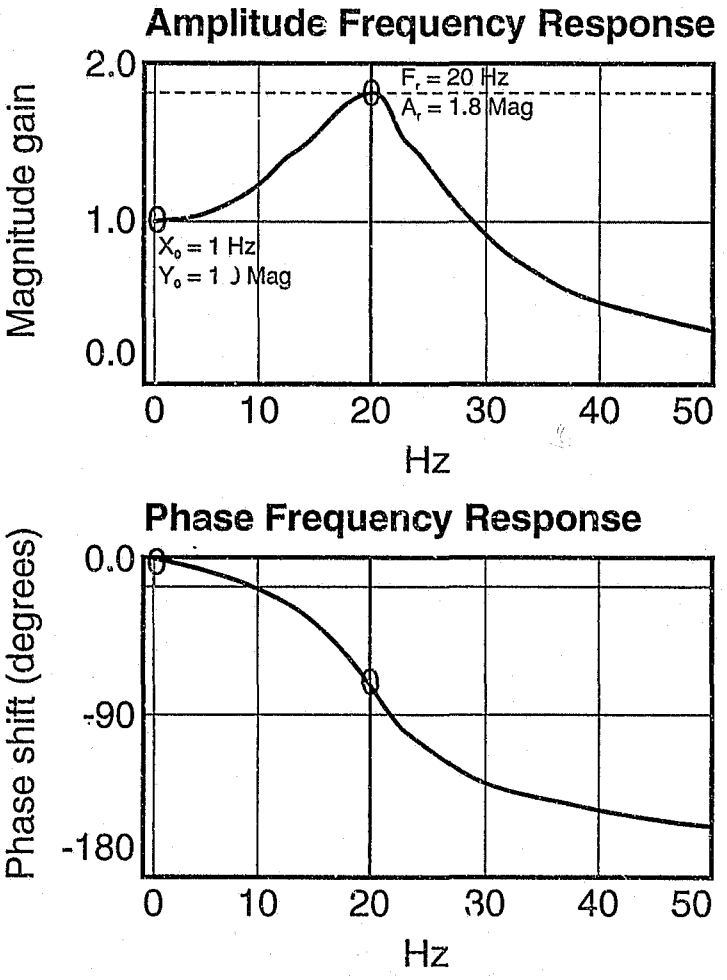
Amplitude Frequency Response
Magnitude gain
2.0
1.0
0.0
F_r = 20 Hz
A_r = 1.8 Mag
X_o = 1 Hz
Y_o = 1 Mag
0
10
20
30
40
50
Hz
Phase Frequency Response
Phase shift (degrees)
0.0
-90
-180
0
10
20
30
40
50
Hz

Statistical analysis. Between-groups multiway multivariate (7 dependent measured frequency response variables, from above) analysis of variance was performed (MANOVA F-test, Statistica™ software, Statsoft, OK) and Tukey's Significant Difference post-test correction applied to P-values < 0.05.[16] The multiway ANOVA design considers possible statistical interactions due to testing the effects of multiple catheter types (3 brands and 4 FG sizes) in addition to the effects of two different transducer types on the measured frequency response variables. Coefficient of determination (r^2) between F_{rr} and catheter diameter was calculated from the Pearson product-moment correlation. Displayed values are mean ± SD.

2.6 Results

No significant frequency response differences were found between the two transducer-dome combinations, and no significant statistical interaction between the catheters and transducers was noted. The means of 12 measured values (n = 6 catheters x two transducers) are therefore presented for each sample's variables.

The effect of catheter brand and FG on mean amplitude and phase frequency responses is illustrated in Figures 2.2 and 2.3, and on the maximum working respiratory rate is depicted in Fig. 2.4. Variables F_r, A_r, F_{a5}, P_{a5} and F_{rr} which were significantly different ($P < 0.05$) between catheter FG sizes and brands are displayed in Table 2.2. There was a trend for mean F_r, A_r, F_{a5}, and F_{rr} to decrease, and for D_c and P_{a5} to increase, with decreasing catheter FG size. Mean D_c ranged from 0.19 to 0.30.

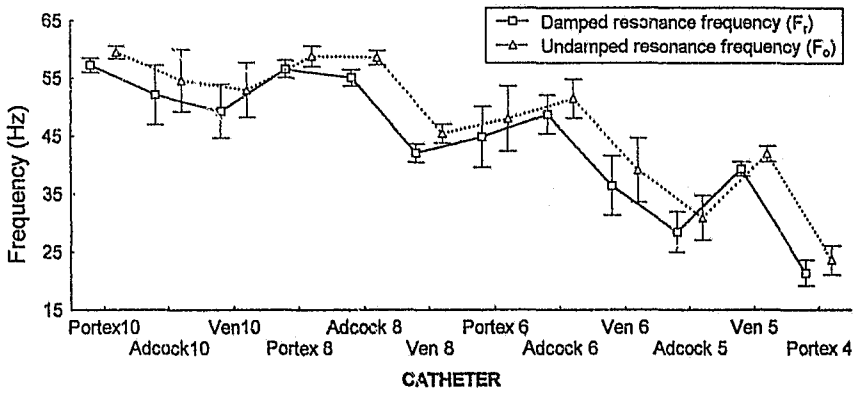
Damped resonance frequency (F_r)
Undamped resonance frequency (F_o)
Frequency (Hz)
65
55
45
35
25
15
Portex10
Adcock10
Ven10
Portex 8
Adcock 8
Ven 8
Portex 6
Adcock 6
Ven 6
Adcock 5
Ven 5
Portex 4
CATHETER

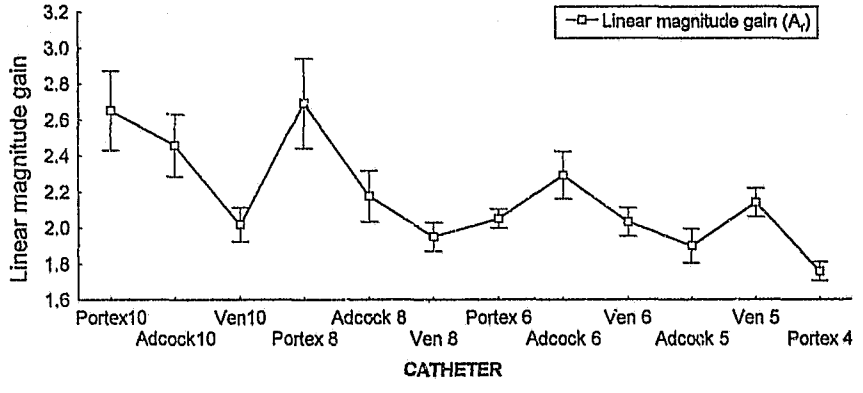
Linear magnitude gain (A_r)
Linear magnitude gain
3.2
3.0
2.8
2.6
2.4
2.2
2.0
1.8
1.6
Portex10
Adcock10
Ven10
Portex 8
Adcock 8
Ven 8
Portex 6
Adcock 6
Ven 6
Adcock 5
Ven 5
Portex 4
CATHETER

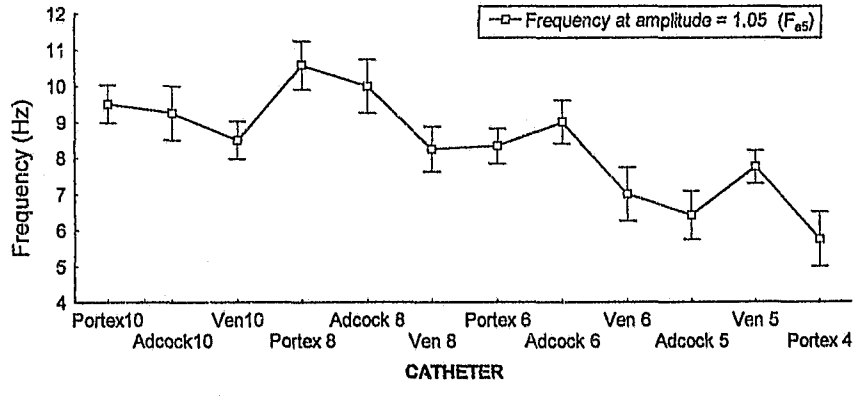
Frequency at amplitude = 1.05 (F_{a5})
Frequency (Hz)
12
11
10
9
8
7
6
5
4
Portex10
Adcock10
Ven10
Portex 8
Adcock 8
Ven 8
Portex 6
Adcock 6
Ven 6
Adcock 5
Ven 5
Portex 4
CATHETER

Figure 2.2. Catheter amplitude and phase frequency response characteristics. F_r, damped resonant frequency; F_o, undamped resonant frequency; A_r, maximum amplitude gain; F_{a5}, frequency at $A_0 + 5\%$; Catheter, catheter brand and French Gauge size.

Figure 2.3. Catheter frequency response characteristics. D_c, damping coefficient; P_{a5}, phase difference at A_0 + 5% or F_{a5}. Catheter, catheter brand and French Gauge size.

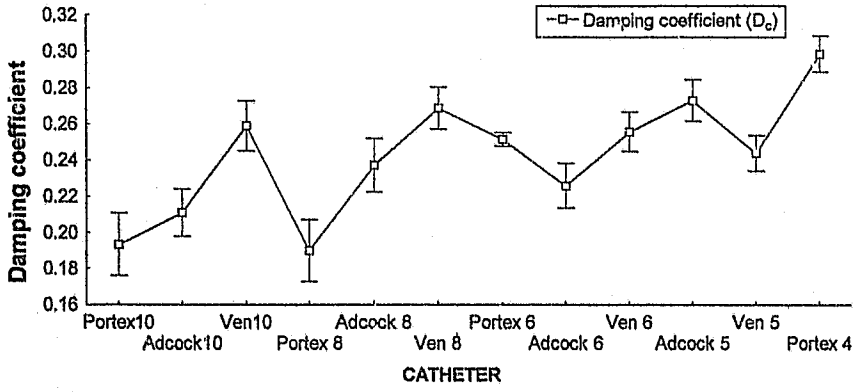
Damping coefficient (D_c)
Damping coefficient
0.32
0.30
0.28
0.26
0.24
0.22
0.20
0.18
0.16
Portex10
Adcock10
Ven10
Portex 8
Adcock 8
Ven 8
Portex 6
Adcock 6
Ven 6
Adcock 5
Ven 5
Portex 4
CATHETER

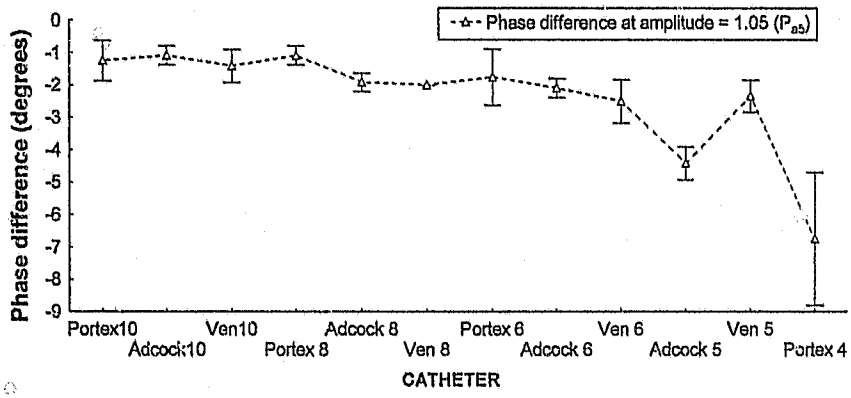
Phase difference at amplitude = 1.05 (P_{a5})
Phase difference (degrees)
0
-1
-2
-3
-4
-5
-6
-7
-8
-9
Portex10
Adcock10
Ven10
Portex 8
Adcock 8
Ven 8
Portex 6
Adcock 6
Ven 6
Adcock 5
Ven 5
Portex 4
CATHETER

Table 2.2. *Infant feeding catheter statistical summary table*

	Por10	Adc10	Ven10	Por8	Adc8	Ven8	Por6	Adc6	Ven6	Adc5	Ven5
Por10											
Adc10	ab										
Ven10	abde	be									
Por8	d	bde	abde								
Adc8	be	be	adef	be							
Ven8	abdef	abdef	af	abdef	abdef						
Por6	abdef	abdef	f	abdef	adf	-					
Adc6	abef	-	be	abdef	adf	abe	be				
Ven6	abcdef	abcdef	acdf	abcdef	adef	adf	adf	abdef			
Adc5	abcdef	abcdef	acdf	abcdef	abcdef	acdf	acdef	abcdef	acf		
Ven5	abcdef	abcdef	af	abcdef	adf	be	af	adef	-	abcdef	
Por4	abcdef	abcdef	abcdef	abcdef	abcdef	abcdef	abcdef	abcdef	abcdef	acef	abcdef

Variables a-f indicated are $P < 0.05$ between any two catheters. a, damped resonant frequency (F_r); b, maximum amplitude gain (A_r); c, phase difference at F_{a5} (P_{a5}); d, frequency at $A_0 + 5\%$ (F_{a5}); e, damping coefficient (D_c); f, maximum working respiratory rate (F_m); -, no significant difference; Por Adc Ven, Portex Adcock and Ven catheter brands and FG size.

No CMS exhibited a uniform mean frequency response above 11 Hz (F_{a5}, Fig. 2.2). Within catheter brands the F_{rr} (Fig. 2.4) of Portex and Adcock FG sizes 10 and 8 were not significantly different. The F_{rr} of the Portex FG sizes 6 and 4 and of the Adcock FG size 5 were significantly lower than their same brand larger FG sizes. Within the Ven catheter brand there was a significant decrease in F_{rr} with decreasing Ven FG sizes 10, 8 and 6. The F_{rr} was significantly lower for the Portex FG size 4 versus 6 and for the Adcock FG size 5 versus 6, but the Ven FG size 5 versus 6 was similar.

Between catheter brands there was no significant difference in F_{rr} for the Portex FG sizes 10, 8 and 6 versus the corresponding Adcock catheters, but the Ven FG sizes 8 and 6 had a significantly lower F_{rr} than the corresponding Portex and Adcock FG sizes. The F_{rr} of Portex FG size 4 was significantly lower than all other FG size catheters. The Ven FG size 5 catheter displayed a significantly greater F_{rr} than the Adcock FG size 5.

The coefficient of determination (r^2) for mean F_{rr} versus catheter inside diameter (ID) or outside diameter (OD) across all brands was 0.66 and 0.67 respectively. The within brand r^2 for mean F_{rr} versus ID of Portex, Adcock and Ven catheters was 0.90, 0.55 and 0.81 respectively. The range of F_{rr} was largest within the Ven 6 FG catheters being 31.2 to 60.2, and lowest within the Adcock 8 FG catheters being 79.5 to 84.4, breaths/min.

Figure 2.4. Catheter maximum working respiratory rate. F_{rr}, maximum working respiratory rate; Catheter, catheter brand and French Gauge size.

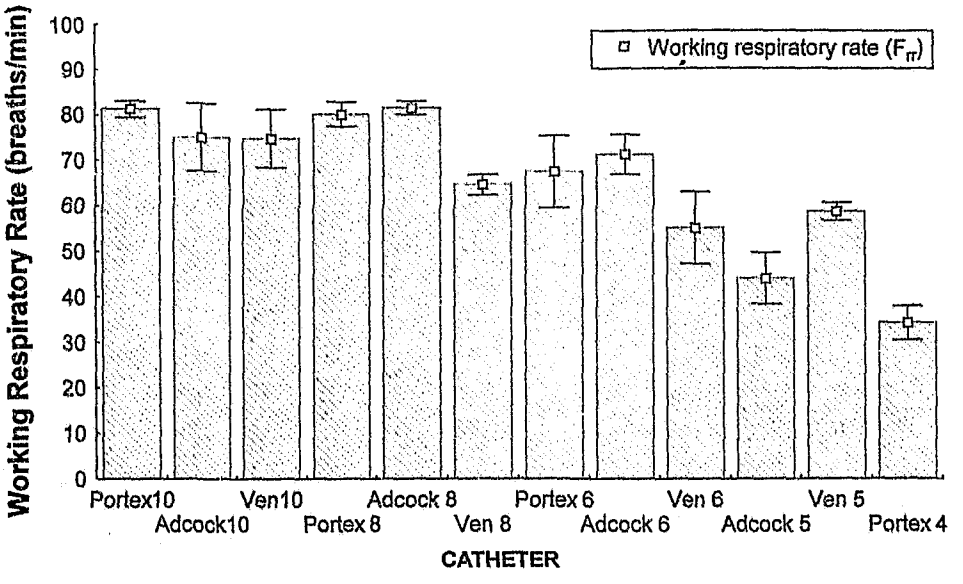
Working Respiratory Rate (breaths/min)
100
90
80
70
60
50
40
30
20
10
0
Working respiratory rate (F_{rr})
Portex10
Adcock10
Ven10
Portex 8
Adcock 8
Ven 8
Portex 6
Adcock 6
Ven 6
Adcock 5
Ven 5
Portex 4
CATHETER

2.7 Discussion

In Vitro Technique

Catheter whip and impact with the esophageal wall may affect in vivo frequency responses of in situ catheters. However, we performed in vitro frequency response analysis because use of fast flush in vivo tests, in which there is a high inertia of the external flushing liquid, has been shown to overestimate the CMS F_r,[9,10,17], thereby artefactually raising in vivo CMS working respiratory rates beyond their true values. Moreover, accurate interpretation of CMS frequency responses calculated from in vivo applied fast flush waveforms is interfered with by non-pleural pressure related superimposed esophageal waveforms such as in vivo cardiac and peristaltic waveforms.[18]

In quantifying the frequency responses we employed the swept frequency forced oscillation technique as opposed to the step response (free oscillation burst-balloon) technique. The latter, like the fast flush in vivo technique, is practically limited to underdamped CMS,[11,18] may miss subtle differences in F_o[14] and is open to potential measurement inaccuracies in the determination of the period and amplitude of the response.[18] On the other hand, the swept frequency technique employed by us is suitable for a distributed parameter system[11,18] such as liquid-filled CMS, and allows the system under test to be stimulated at equal amplitude over all frequencies, whereas the step response approach results in reducing amplitudes with increasing frequency.

We used a mean pressure offset of +2.3 cmH_2O, similar to mean intra-esophageal pressures accompanying mechanical ventilation, because this method allowed for any effects of non-linearities (amplitude and frequency-dependent) related

to dynamic CMS compliance or catheter wall hysteresis[11] to be included in the CMS frequency response measurements.

Reported effects of physiological temperatures on frequency responses in liquid-filled catheters vary from no effect[10] to significant effects caused by altered catheter wall compliance.[11,19] The compliance and compliance hysteresis of nasogastric catheter PVC is likely to be more temperature dependent than, for example, nylon or braided-polyurethane catheters used for intra-arterial pressure measurement, therefore we measured the frequency responses at primate physiological temperatures.

Catheter Frequency Responses

To our knowledge there is no formal documentation comparing the pressure-measurement frequency response characteristics of a range of differing FG sizes and brands of standard liquid-filled PVC infant nasogastric feeding catheters of matching catheter lengths: informal measurements on liquid-filled intra-esophageal catheters (usually performed with differing catheter lengths, brands and FG sizes between the researchers, and of single sample number) have demonstrated uniform frequency responses in an 8 FG 2 mm ID 38 cm long saline-filled catheter up to 10 Hz[12] and in a similar catheter to > 10 Hz,[5] while a 5 FG 1 mm ID catheter and a 6 FG catheter were also noted to be flat to 10 Hz.[5,13] Ideally CMS should have a high F_r, but a high F_r by itself may be associated with overdamping and consequent reduced CMS sensitivity at raised frequencies. Introducing damping systems to compensate for resonance in underdamped CMS is not usually practical, nor necessarily effective,[9] therefore optimal damping ($D_c = 0.71$) accompanying a high F_r is desirable in CMS.

Since both D_c and F_r can independently influence CMS performance, to facilitate

interpretation of the frequency response data obtained in our experiment, we used calculated F_{rr} as a variable which meaningfully predicts the potential of a CMS to measure intra-esophageal pressure within a 5% error limit up to a maximum calculated respiratory rate. Although mean F_{rr} did increase with larger FG catheters, it represents the accuracy with which applied pressure will be recorded assuming all of the applied pressure waveform energy is located within ten harmonics of the fundamental frequency.[9] This assumption may be incorrect when pressure cycle infant ventilators generating square pleural pressure waveforms are in use; the F_{rr} under such conditions would be reduced.

The correlation between mean F_{rr} and catheter ID or OD was similar. Therefore choosing a catheter based on either ID or OD would be similarly effective in predicting the F_{rr}. It should however be noted that FG, a term particularly applied to medical grade catheters, refers to the Charrière French scale where 1 FG unit = catheter OD of 0.33 mm, and does not necessarily reflect the ID which also depends on catheter wall thickness. Thus catheters of the same FG size can have differing ID's; for example the ID of Portex FG size 6 versus Adcock FG size 6 (Table 2.1). The Ven FG size 5 has a larger OD but the same ID compared with the corresponding Adcock FG size 5; the Ven catheter wall is thus thicker and less compliant, which may explain its superior frequency response. In addition, manufacturing tolerances on small versus large FG size catheters are similar (Table 2.1), therefore small FG catheters may have relatively larger OD tolerances. This can lead to further variability in their measured frequency response characteristics. It is therefore advisable to base catheter selection on ID rather than on OD or FG alone, although ideally values for ID and OD (or FG) should be sought: For the same catheter wall composition, a larger ID and greater wall thickness

is likely to produce a higher F_r.

The correlation between F_r and ID was different for various catheter brands, thus for a particular ID or FG size catheter there is frequency response discrepancy between different catheter makes. Resonance characteristics are dependent on CMS compliance, inertance (liquid mass), viscous resistance and catheter wall hysteresis. In practice factors which affect CMS volume displacement coefficients are gas bubbles (transparency of PVC catheters is advantageous here) which increase D_c but lower F_r,[11,16,20] catheter wall compliance,[11] leaking connections, and arrangement of stopcocks and transducer domes.[17] Manufacturing tolerances on the catheter ID or length affect F_r via catheter radius and length[14] which may partly explain the range of frequency responses found within samples from the same catheter brand and FG size noted in our experiment. These variations concur with those recorded from frequency responses of liquid-filled intravascular catheters.[10,14,21] Discrepancies between manufacturer-claimed and experimentally observed resonant frequencies of liquid-filled catheters have also been documented.[10] The quality of pressure transducer employed in the CMS directly affects resonance properties: however, transducer dome size, which has the potential to alter the liquid mass inertia and compliance of the CMS, did not affect the observed frequency responses in our experiment.

In conclusion, in vitro frequency response analysis demonstrates that, although large FG commercially available PVC liquid-filled nasogastric feeding catheters are underdamped and resonate, they have the potential to measure transmitted intra-esophageal pressures up to a maximum of 82 breaths/min within a 5% error limit. However, judging the suitability of individual feeding catheters to measure dynamic intra-esophageal pressure accurately based on FG size alone is inappropriate: The

multifactorial determination of CMS amplitude and phase frequency responses necessitates quantitative assessment of differing catheter brands and diameters prior to their utilisation.

2.8 Appendix

Equations for calculated variables:

Damping coefficient[19] (Dc) (1)

$$D_c = \sqrt{\left(\frac{1 - \sqrt{\left(1 - \left(\frac{A_o}{A_r} \right)^2 \right)}}{2} \right)}$$

Undamped natural frequency[19] (F_o) (2)

$$F_o = \frac{F_r}{\sqrt{\left(1 - 2D_c^2\right)}}$$

Maximum working respiratory rate[9,15] (F_{rr}) (3)

$$F_{rr} = \frac{(F_{a5} \times 60)}{10}$$

where F_{a5} is the frequency at which $A_r/A_0 = 1.05$; 10 refers to the Fourier series 10'th harmonic

Appendix Note:

In the author's experiment the frequency response trace was divided through by the amplitude ratio at 1 Hz (regarded as the DC response) and therefore $A_0/A_r = 1/A_r$. Equations used for undamped natural frequency (F_o) and damping coefficient (D_c) assume that the system is second order and linear.[15]

2.9 References

1. Ratjen FA, Wiesemann HG. Variability of dynamic compliance measurements in spontaneously breathing and ventilated newborn infants. Pediatr Pulmonol. 1992; 12:73-80.

2. Beardsmore CS, Helms P, Stocks J, Hatch DJ, Silverman M. Improved esophageal balloon technique for use in infants. J Appl Physiol. 1989; 49:735-742.

3. Coates AL, Stocks J, Gerhardt T. Esophageal manometry. In: Stocks J, Sly PD, Tepper RS, Morgan WJ, eds. Infant Respiratory Function Testing. John Wiley & Sons, Inc., 1996, 241-258.

4. Coates AL, Stocks J. Esophageal pressure manometry in human infants. Pediatr Pulmonol. 1991; 11:350-360.

5. Asher MI, Coates AL, Collinge JM, Milic-Emili J. Measurement of pleural pressure in neonates. J Appl Physiol. 1982; 52:491-494.

6. Maxted KJ, Shaw A, Macdonald TH. Choosing a catheter system for measuring intra-esophageal pressure. Med & Biol Eng & Comput. 1977; 15:398-401.

7. Heaf DP, Turner H, Stocks J, Helms P. The accuracy of esophageal pressure measurements in convalescent and sick intubated infants. Pediatr Pulmonol. 1986; 2:5-8.

8. Chartrand DA, Ye TH, Maarek JH, Chang HK. Measurement of pleural pressure at low and high frequencies in normal rabbits. J Appl Physiol. 1987; 63:1142-1146.

9. Hipkins SF, Rutten AJ, Runciman WB. Experimental analysis of catheter-manometer systems in vitro and in vivo. Anesthesiology. 1989; 71:893-906.

10. Rutten AJ, Nancarrow C, Isley AH, Runciman WB. An assessment of six different pulmonary artery catheters. Crit Care Med. 1987; 15:250-255.

11. Yeomanson CW, Evans DH. The frequency response of external transducer blood pressure measurement systems: a theoretical and experimental study. Clin Phys Physiol Meas. 1983; 4:435-449.

12. Coates AL, Davis GM, Vallinis P, Outerbridge EW. Liquid-filled esophageal catheter for measuring pleural pressure in preterm neonates. J Appl Physiol. 1989; 67:889-893.

13. LeSouef PN, Lopes JM, England SJ, Bryan MH, Bryan AC. Influence of chest wall distortion on esophageal pressure. J Appl Physiol. 1983; 55:353-358.

14. Shapiro GG, Krovetz LJ. Damped and undamped frequency responses of underdamped catheter manometer systems. Am Heart J. 1970; 80:226-236.

15. Fry DL. Physiologic recording of modern instruments with particular reference to pressure recording. Physiol Rev. 1960; 40:753-788.

16. Zar JH. Biostatistical Analysis. Engelwood Cliffs, N.J., Prentice-Hall, 1974:206-252.

17. Rothe CL, Kim KC. Measuring systolic arterial blood pressure; possible errors from extension tubes or disposable transducer domes. Crit Care Med. 1980; 8:683-689.

18. Gardner RM. Direct blood pressure measurement-dynamic response requirements. Anesthesiology. 1981; 54:227-236.

19. Hansen AT. The theory for elastic liquid-containing membrane manometers: Special part. Acta Physiol Scand. 1950; 19:333-343.

20. Milic-Emili J, Mead J, Turner JM, and Glauser EM. Improved technique for estimating pleural pressure from esophageal balloons. J Appl Physiol. 1964; 19:207-211.

21. Doyle DJ. Resonance properties of 85-cm and 110-cm pulmonary artery catheters. J Cardiothorac Anesth. 1990; 4:781-782.

CHAPTER 3

3 FREQUENCY RESPONSES OF INFANT AIR-BALLOON VERSUS LIQUID-FILLED CATHETERS FOR INTRA-ESOPHAGEAL PRESSURE MEASUREMENT

3.1 Linking Comments

The high frequency respiratory mechanics encountered during artificial infant ventilation may require uniform catheter frequency responses beyond those exhibited by water-filled catheters for accurate dynamic intra-esophageal pressure measurement. Published literature is sparse and divided in opinion as to which of liquid-filled versus air-filled balloon-tipped catheters are most suitable for intra-esophageal pressure measurement during high frequency respiratory mechanics, whilst a valid direct comparison between liquid-filled and air-balloon catheters has not been published.

In Chapter Three latex balloons are laboratory-manufactured to appropriate specifications for attachment to infant air-filled catheters, as would be used for intra-esophageal pressure measurement using air-balloon catheter manometers in clinical practice. The magnitude and phase frequency response performances of these infant air-balloon catheters of differing French Gauge (FG) sizes and brands are quantified and compared with those of matching water-filled catheters, using the swept sine wave apparatus developed in Chapter Two.

For practical purposes, in contrast to Chapter Two, two catheter brands (versus three in Chapter Two) and one transducer type (versus two in Chapter Two) are assessed. However, in Chapter Three a larger sample number ($n = 8$, versus $n = 6$ for Chapter Two) is tested for each catheter brand and French gauge size, and an air-balloon catheter that is available commercially at this time is included in the

analysis. Additionally, rather than re-using the data generated for liquid-filled catheter frequency responses in Chapter Two to contrast with the data collected on air-balloon catheters in Chapter Three, a new set of liquid-filled catheters' frequency responses are measured in Chapter Three. This re-measurement of liquid-filled catheters was performed in order to contrast the frequency response performances of air-balloon catheters with liquid-filled catheters in a valid fashion: the experimental conditions under which both sets were determined, the batch of catheters tested in both sets, and the analysis applied to determine the frequency response variables in both sets were identical between the liquid-filled and air-balloon catheter sets.

The findings for air-balloon catheters are translated into a "maximum respiratory rate", which is meaningful to clinicians, up to which air-balloon catheters of differing FG sizes may be utilised to measure intra-esophageal pressure appropriately, and the results contrasted with those determined for the liquid-filled catheters. [Comprehensive information is provided in Chapter Three's Abstract, Introduction and Discussion sections, which follow]:-

3.2 Summary

Amplitude and phase frequency response characteristics of infant air-balloon catheters (IABC) of differing French Gauge (FG) sizes and brands were quantified to determine their suitability for measuring dynamic intra-esophageal pressure (P_{es}) accurately. Frequency response performances of matching IABC and water-filled catheters (WFC) were also compared using the swept sine wave technique. The maximum respiratory rate within which IABCs have the potential to measure P_{es} within a 5% error limit was calculated (F_{RR}). Frequency responses of IABCs greater than FG size 5 exhibited underdamped resonant properties, while smaller FG size IABCs exhibited near-critical damping or overdamping. IABCs maintained uniform amplitude frequency responses up to 25 Hz, demonstrating the ability to measure P_{es} up to 148 breaths/min within a 5% error limit. The frequency response performance of FG size 6 IABCs was similar to that of FG size 10 IABCs. Compared with matching WFCs the frequency response performance of IABCs was significantly superior, the frequency response variability within IABC samples was lower, and IABC correlation between FG size and F_{RR} was advantageously lower than for WFCs. F_{RR} values for differing IABC brands and FG sizes are presented. We conclude that IABCs manufactured to infant-appropriate balloon specifications exhibit significantly superior frequency response characteristics compared to matching WFCs. Measurement accuracy is not improved using IABCs greater than FG size 6. Inexpensive intra-esophageal IABCs are technically suitable for the accurate measurement of dynamic P_{es} during high frequency respiratory mechanics encountered in infant artificial ventilation. **Keywords:** esophageal manometry; lung compliance; respiratory mechanics; mechanical ventilation.

3.3 Non-standard Nomenclature

ζ	Damping coefficient
A_r/A_0	Resonance amplitude ratio
CMS	Catheter Manometer System
f_{A5}	Frequency at $A_0 \pm 5\%$
f_0	Undamped (natural) resonant frequency
F_{RR}	IABC or WFC working respiratory rate
f_r	Damped resonant frequency
FG	French Gauge
IABC	Infant air-balloon catheter
Mag	Linear magnitude gain
MANOVA	Multivariate analysis of variance
P_{A5}	Phase difference at f_{A5}
P_{es}	Intra-esophageal pressure
Por	Portex catheter
PVC	Polyvinyl chloride
SA	South Africa
WFC	Water-filled catheter
WRMS	Root mean square Watts

3.4 Introduction

Pleural pressure of artificially ventilated infants is estimated by measuring dynamic intra-esophageal pressure (P_{es}) to facilitate calculation of the elastic and resistive elements of the respiratory system (1, 2). Polyvinyl chloride (PVC) infant feeding catheters, liquid-filled or air-balloon tipped (3-5) are easily inserted and well tolerated (6), and are readily available to clinicians and researchers as disposable and inexpensive alternatives to transducer-tip catheters (7-8). However, the high frequency respiratory mechanics encountered during artificial infant ventilation may require uniform catheter frequency responses up to 20 or 23 Hz (4, 8, 9), which few, if any, PVC water-filled catheters (WFCs) demonstrate (10).

Liquid-filled catheters are commonly used for intra-arterial pressure measurement, therefore extensive frequency response characterisation of these catheters exists. However, such data pertaining to infant air-balloon catheters (IABCs) used for P_{es} measurement are sparsely published (3, 4), and limited by measurements confined to one catheter FG size or to single (n = 1) catheter samples of unequal lengths or brands. Studies employing IABCs have concentrated on validating the in vivo reflection of pleural pressure by P_{es} (3, 11) and do not present quantitative data on the dynamic accuracy of differing IABC FG sizes and brands used for measuring P_{es}. Moreover, controversy exists in the literature as to the frequency responses of IABCs relative to WFCs: WFCs were qualitatively considered to have better frequency responses than IABCs (7), yet in another study IABCs were suggested to have better phase and amplitude characteristics than most WFCs (4). In the latter study catheters of FG size 6 (unspecified length) only were

tested; to our knowledge a valid direct comparison of the frequency responses of matching IABCs and WFCs has not been published.

In vivo fast flush test frequency response analysis is not applicable to IABCs, therefore this study aims to determine the in vitro frequency response characteristics (amplitude and phase) of a range of IABCs of differing French Gauge (FG) sizes and catheter brands, in order to quantify their suitability for accurate dynamic P_{es} measurements in infants, and to compare IABC frequency response performances with those of matching WFCs.

3.5 Materials and Methods

IABC laboratory manufacture

Glass rods 8.3 mm outer diameter (O.D.), attached to a rotating device, were dipped twice one hour apart into a bath containing liquid latex compound (Latex Surgical Products, South Africa) which was vacuumed to remove surface air bubbles. The latex was dried at 25 °C in air of 50% relative humidity, and manually rolled off the rods following powdering. Balloons were selected on the criteria of single wall thicknesses between 0.06 and 0.09 mm and < 25% difference between the thickest and thinnest part of the air-balloon, as determined by a micrometer screw gauge at three points along the balloon's length (3). Air-balloons were mounted on PVC feeding catheters with silicon glue and silk ties at a point 5.5 cm proximal to the catheter tip, and the IABCs leak-tested for 1 minute. Pressure-volume curves for ten samples each of FG size 10 and FG size 5 IABCs of the same catheter brand were determined as follows: Each air-balloon was evacuated by submersing it in water to the level of its silk tie, after which the IABC was attached to a 3-way stopcock and pressure transducer combination (Honeywell Microswitch 170PC, USA). Air was incrementally injected into the horizontally positioned (as in the case of supine infants) IABC using a calibrated 0.1 ml graduated syringe and the pressure recorded (3, 12).

(See Supplemental Figures S3.A, S3.B).

TOP: Supplemental Figure S3.A

Latex balloon manufacture

I. Glass rods (manufactured by glassblowers to specified dimensions) are dipped in fresh surface-vacuumed latex compound

II. The glass rods are attached to a rotation device and slowly turned in a chamber of appropriate temperature and humidity until "dry"

III. Resulting latex balloons are rolled off, characterised and selected if they fit the thickness and compliance criteria (see text).

BOTTOM: *Supplemental Figure S3.B*

Air-filled balloon-tip catheter ready for frequency response characterisation

Size 10 French gauge polyvinyl chloride catheter

I. Size 4 French gauge polyvinyl chloride catheter

II. Large volume pressure transducer

III. Small volume pressure transducer

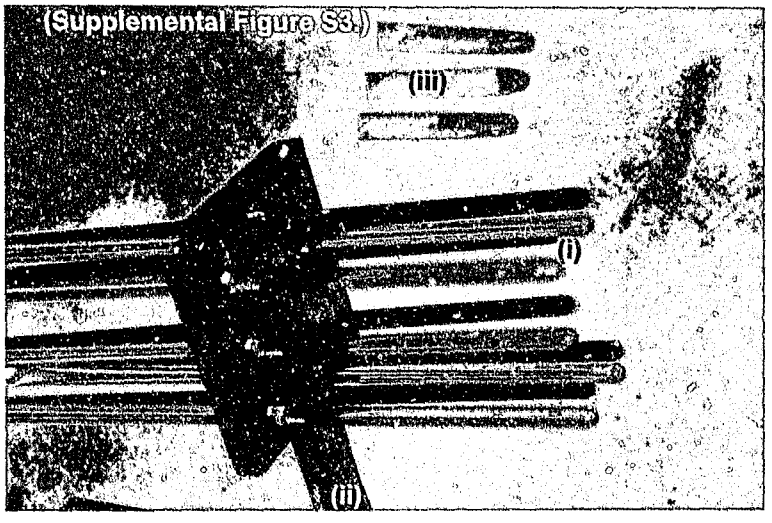
(Supplemental Figure S3.)
(iii)
(i)
(ii)

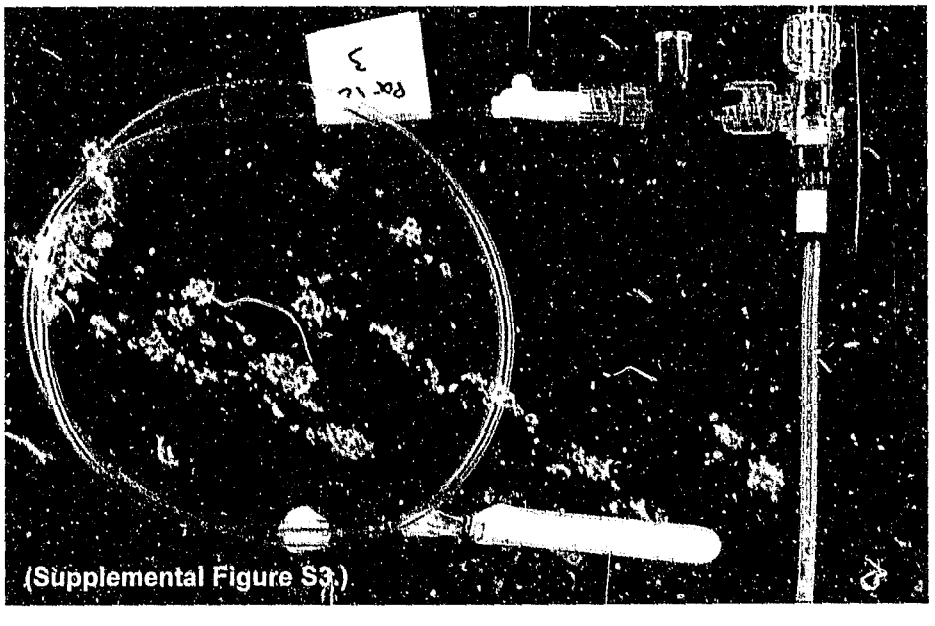
(Supplemental Figure S3.)

Table 3.1. *Infant air-balloon and water-filled catheter specifications*

Feeding Catheter	FG	OD ± Tol, mm	ID ± Tol, mm	L, cm
Portex	10	3.3 ± 0.1	2.3 ± 0.1	60
(Portex, Kent, UK)				
Ven	10	3.3 ± 0.1	2.3 ± 0.1	50
(Ven Products, SA)				
Portex	8	2.6 ± 0.08	1.8 ± 0.08	50
Ven	8	2.6 ± 0.1	1.8 ± 0.1	50
Portex	6	2.0 ± 0.08	1.4 ± 0.08	50
Ven	6	2.0 ± 0.1	1.2 ± 0.1	50
Adcock Ingram	5	1.7 ± 0.08	0.8 ± 0.1	50
(Sabax Division, SA)				
Ven	5	1.9 ± 0.1	0.8 ± 0.1	50
Portex	4	1.3 ± 0.08	0.6 ± 0.08	50
Vygon Nutrisafe (Vygon	4	1.5 ± 0.08	0.8 ± 0.08	50
Laboratories, France)				
Erich Jaegcr	8	2.7	1.5	50
(Erich Jaeger, GE)				

ID, internal diameter; OD, external diameter; Tol, manufacturer specified tolerance; L, length; UK, United Kingdom; SA, South Africa; GE, Germany

Catheter-manometer testing

Five different FG size catheters (Table 3.1), and two different brands (if available the same two brands) for each FG size catheter, chosen for their similar lengths, were coupled to a Gould P10EZ (Viggo-Spectramed Statham Gould, Oxnard, CA) pressure transducer (diaphragm area 6.4 mm, sensitivity 5 uV/V/mmHg, volume displacement 0.04 mm^3/100mmHg) and disposable diaphragm-dome with luer lock fittings (Viggo-Spectramed Gould TA1019, Oxnard, CA). The dome ports were fitted in-series to a 4-way stopcock of minimum orifice ID 2.0 mm (Adcock Ingram, South Africa) yielding a transducer-dome-stopcock volume of 0.6 ml. The space between the transducer diaphragm and disposable dome diaphragm was water-filled according to manufacturer instructions and positioned at catheter-tip level.

Matching IABCs (n = 8) and WFCs (n = 8) of differing FG sizes were assessed by randomly attaching their proximal female luer fittings directly to the transducer stopcock male luer fitting. A commercially available adult air-balloon catheter (11 cm air-balloon length, Erich Jaeger, Germany) was included in the study (Table 3.1). All IABCs were operated within their determined volume optimal working range. To minimise bubble formation each WFC was flushed with CO_2 followed by deionised and degassed (by boiling) water cooled under vacuum to 36-38 °C (13). The catheter's distal 20 cm was inserted under water into a laboratory designed leak-proof water chamber kept at 36-38 °C. Sinusoidal pressure waveforms between -5.5 and +10 cmH_2O (mean 2.3 cmH_2O) were generated in the chamber by means of an 8 Ohm loudspeaker (Bose 4.5" 802, Bose Corporation, MA, USA) powered by an 80 WRMS DC-coupled amplifier linked to a sine wave

generator (Hewlett Packard 3562A, USA). The amplifier and loudspeaker heat sinks were water-cooled and the driver diaphragm silicone-coated for water resistance. A swept-sine frequency response of the
catheter samples was recorded using a calibrated domeless piezoresistive differential pressure transducer as a reference (Honeywell Microswitch 170PC, USA), positioned inside the chamber adjacent to the IABC and WFC catheter-tips. Unfiltered electrical outputs from the catheters and reference pressure transducer were identically pre-amplified (Hellige Servomed, Freiburg, Germany), displayed oscilloscopically, and analyzed for phase and amplitude differences by averaging 3 repeat measurements over 10 s at each 1 Hz interval (Hewlett Packard Dynamic Signal Analyzer 3562A, USA). Apparatus reproducibility over the experiment was checked and confirmed by repeating frequency response measurements of the sample of Portex FG size 6 IABCs and WFCs.

Frequency response determination

The amplitude and phase responses were analysed by fitting second order curves (2 poles, no zeros) to the recorded frequency response traces (14, 15) using the curve fit function of the HP3562A analyser. Curves were fitted between 1 Hz and the frequency at which the amplitude was 1 dB down from the maximum recorded amplitude. The pole values thus obtained for the system function (Appendix equation 1) were converted to coefficients of the second order Laplace transfer function describing the curve, allowing calculation of the following variables:

f_r damped resonant frequency (frequency at maximum amplitude) [Appendix equation 4]

A_r/A_0 resonance amplitude ratio (maximum amplitude, A_r, divided by amplitude at 1 Hz, A_0) [Appendix equation 5]

f_{A5} frequency at $A_0 \pm 5\%$ (frequency at which the amplitude ratio = 1.05 or 0.95)

Amplitude frequency response variables describe IABC gain or attenuation of applied pressure compared with the reference transducer over a range of applied pressure frequencies. Phase-frequency response variables characterise the IABC CMS temporal advancement or retardation of the applied pressure waveform over a range of frequencies; the phase-frequency response variable extracted from the recorded CMS phase-frequency response tracings was:

P_{A5} phase difference at f_{A5} [Appendix equation 6]

Calculated variables derived from the frequency response recordings were:

f_0 undamped (natural) resonant frequency [Appendix equation 2]

ζ damping coefficient [Appendix equation 3]

F_{RR} IABC or WFC working respiratory rate

[Appendix equation 7]

f_0 represents the number of oscillations per unit time that the IABC exhibits if left to oscillate undisturbed. ζ describes IABC resistance to oscillation. F_{RR} predicts the maximum respiratory rate up to which an intra-esophageal IABC of given f_0 and ζ has the potential to measure an applied pressure to within ± 5% of the reference transducer (14, 16).

Statistical analysis

Between-groups one-way (independent variables; IABC or WFC types) multivariate (7 dependent measured frequency response variables, from above) analysis of variance was performed (MANOVA F-test, Statistica™ software, Statsoft, OK) and a post-analysis Tukey Significant Difference test-correction applied to significant differences (17). Coefficient of determination (r^2) between F_{RR} and catheter FG size was calculated from the Pearson product-moment correlation. All displayed values are mean ± SD, and P-values < 0.05 are regarded as statistically significant.

3.6 Results

Air-balloon pressure-volume curves

The static pressure-volume relationships of the combined 2 FG sizes of catheters (n = 20) and for each FG size separate (each group n = 10) of Portex FG sizes 10 and 5 IABC samples is illustrated in Figure 3.1. The Y-axis zero pressure mark represents the point at which the pressure in the air-balloon first became equal to atmospheric pressure with incremental air-volume additions. There was no significant difference (Student's t-test; two-tail $P > 0.05$) between the working range (region of high compliance) of air-balloons attached to Portex FG size 10 versus those attached to FG size 5 catheters (Figure 3.1, bottom traces). All our IABCs exhibited a volume working range which exceeded the required IABC specifications of < 0.4 cm H_2O pressure change across the working range (3).

Figure 3.1.

Static pressure-volume curves of infant air-balloon catheters. Upper graph is mean of combined (n = 20) FG sizes 10 and 5 catheters. Bottom traces = FG size 10 (left) and FG size 5 (right) catheters demonstrating no significant difference in their working ranges.

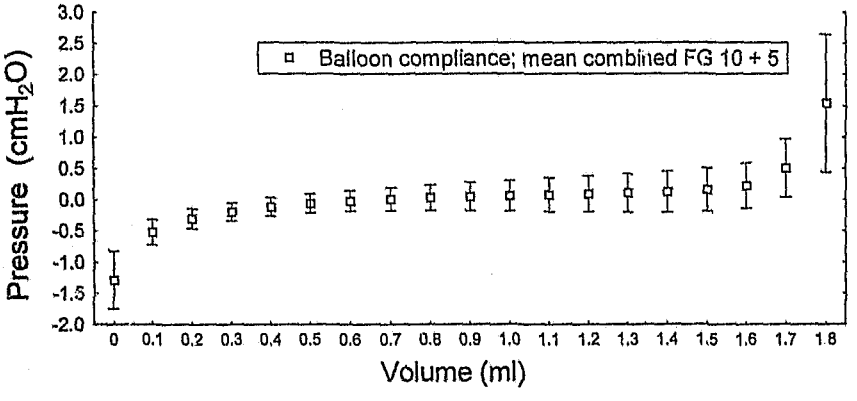
Balloon compliance; mean combined FG 10 + 5
Pressure (cmH2O)
3.0
2.5
2.0
1.5
1.0
0.5
0.0
-0.5
-1.0
-1.5
-2.0
0
0.1
0.2
0.3
0.4
0.5
0.6
0.7
0.8
0.9
1.0
1.1
1.2
1.3
1.4
1.5
1.6
1.7
1.8
Volume (ml)

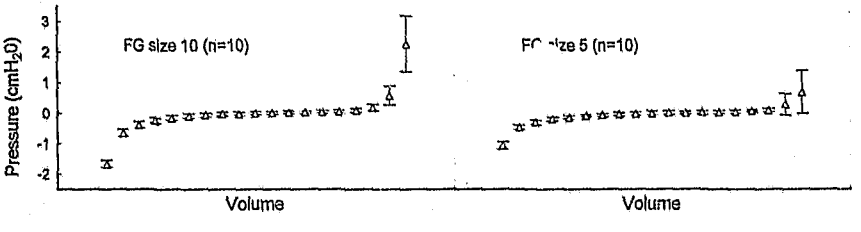
Pressure (cmH2O)
FG size 10 (n=10)
Volume
Volume

Frequency responses

Figure 3.2 illustrates typical frequency response curves recorded from a Portex FG size 6 IABC and WFC.

IABCs' f_r, ζ and A_r, and WFCs' f_r, are demonstrated in Figure 3.3. Values of ζ and A_r for WFCs have previously been published by us (10) and are therefore not presented here. Within the IABC Ven and Portex brands, f_r increased significantly with increasing catheter FG size. The f_r of all IABC FG sizes $\geq$ 6 was significantly greater than the f_r of matching FG sized WFCs (Figure 3.3, top graph). The variation about the mean f_r was less in IABCs than in the WFCs (see f_r SDs of IABCs vs WFCs in Figure 3.3, top graph).

IABC ζ significantly increased with decreasing FG size (Figure 3.3, middle graph): All IABC brands of FG size $\geq$ 6 were underdamped ($\zeta < 0.71$) and resonated. The Ven 5 FG IABCs exhibited near optimal (critical) damping ($\zeta \approx 0.71$). The Adcock FG size 5, Portex and Vygon FG size 4 IABCs were overdamped ($\zeta > 0.71$), hence their f_r values (Figure 3.3, top graph) are not presented; [for these overdamped IABC frequency response traces, damping coefficient (ζ) and attenuation of the pressure signal (A_r) at natural frequency were calculated from the curves' poles obtained with the second-order curve-fit applied to the traces]. IABC A_r (Figure 3.3, bottom graph) was proportional to f_r: The underdamped IABCs exhibited significant increases in gain ($A_r > 1.0$) with increasing FG size, whilst the overdamped smaller IABCs attenuated the applied pressure signals ($A_r < 1.0$). In contrast, all the FG sizes of WFCs were resonant and amplified the applied pressure signals ($A_r > 1.0$).

Figure 3.2.

Comparison of Portex FG size 6 IABC (solid line) versus WFC (dashed line) catheter amplitude-frequency response trace. First marker circle on IABC and WFC represents baseline amplitude (Y-axis, $Y_0 = A_0 = 1.0$) and baseline frequency (X-axis, $X_0 = 1$ Hz). Second marker circle on IABC represents damped resonant frequency (X-axis, $f_r = 68$ Hz) and maximum amplitude gain (Y-axis, $A_r = 1.7$ Mag). WFC $f_r = 43$ Hz and $A_r = 2.6$ Mag. Mag, linear gain over reference transducer.

IABC and WFC Amplitude Frequency Responses

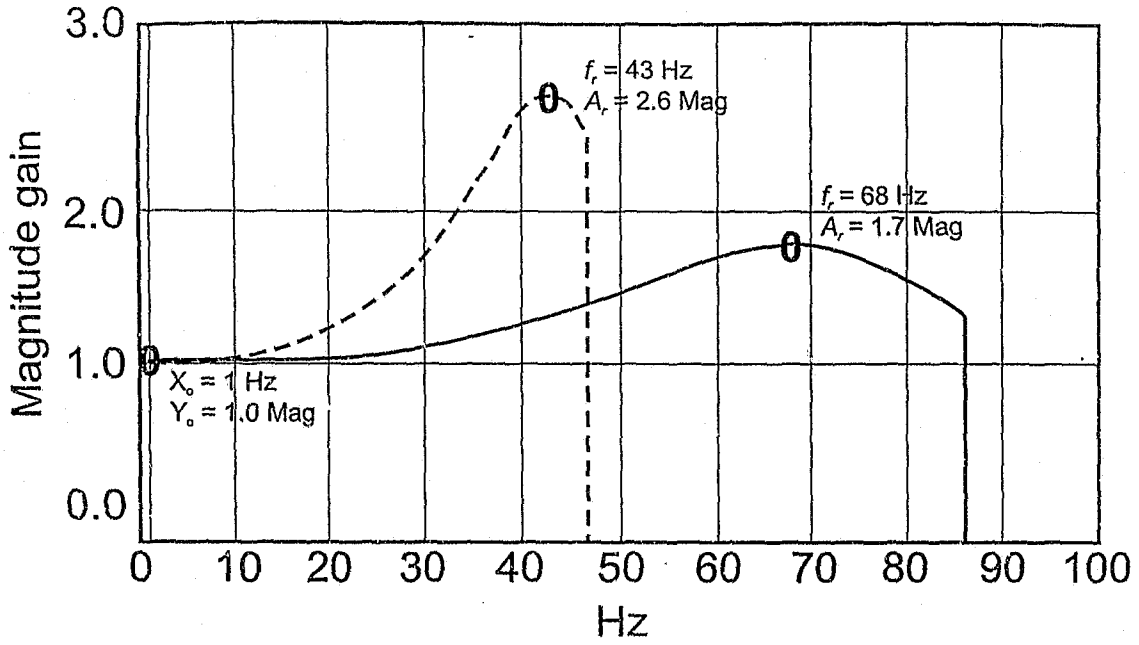

Figure 3.3.

Catheter amplitude-frequency response characteristics. X-axes set at critical damping ($z \approx 0.71$) and zero gain ($A_r = 1.0$) for z and A_r graphs respectively. X-scale break separates commercial Jaeger adult from laboratory-made IABCs. f_r, damped resonant frequency for IABCs versus WFCs; z, IABC damping coefficient (ζ); A_r, IABC amplitude gain or attenuation at f_r; Catheter, catheter brand and FG size; aPor, Portex IABC; * $P < 0.05$ for IABC vs WFC of same FG size.

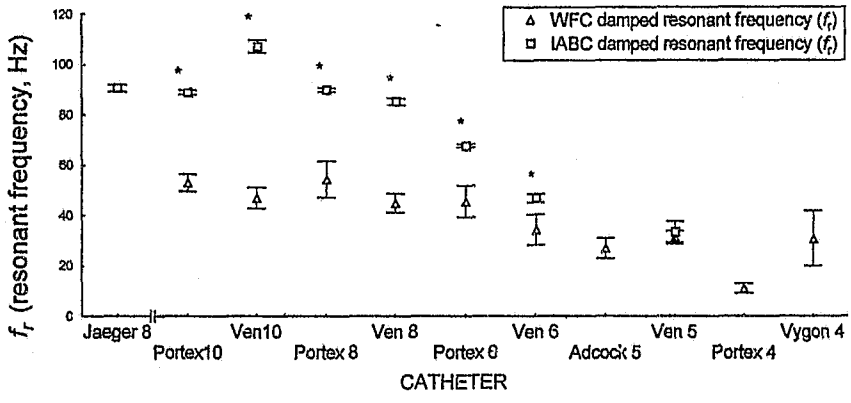
WFC damped resonant frequency (f_r)
IABC damped resonant frequency (f_r)
f_r (resonant frequency, Hz)
120
100
80
60
40
20
0
Jaeger 8
Portex10
Ven10
Portex 8
Ven 8
Portex 6
Ven 6
Adcock 5
Ven 5
Portex 4
Vygon 4
CATHETER

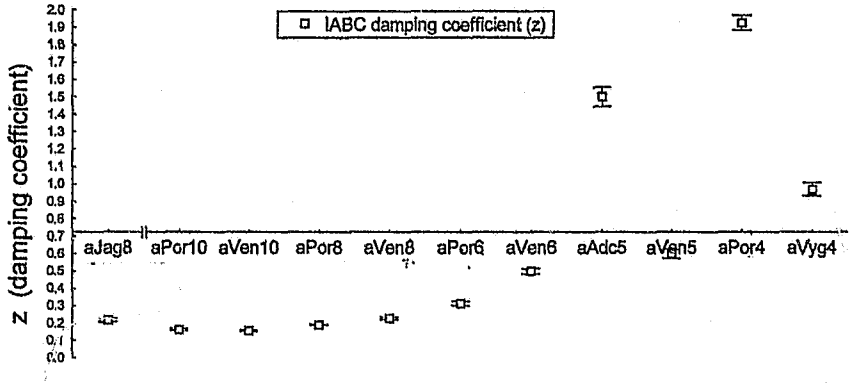
IABC damping coefficient (z)
z (damping coefficient)
2.0
1.9
1.8
1.7
1.6
1.5
1.4
1.3
1.2
1.1
1.0
0.9
0.8
0.7
0.6
0.5
0.4
0.3
0.2
0.1
0.0
aJag8
aPor10
aVen10
aPor8
aVen8
aPor6
aVen6
aAdc5
aVen5
aPor4
aVyg4

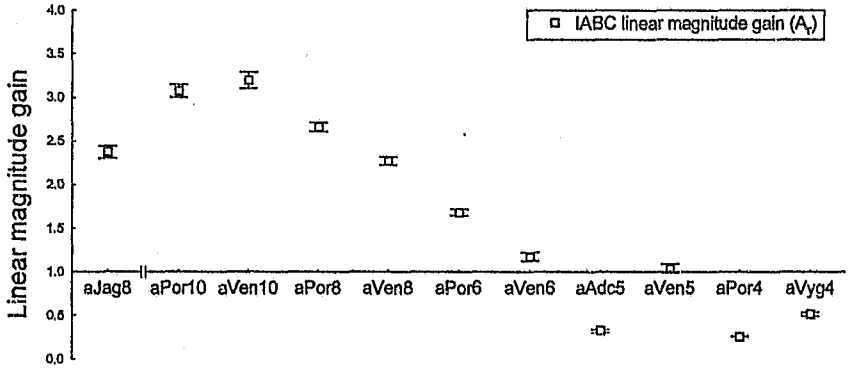
IABC linear magnitude gain (A_r)
Linear magnitude gain
4.0
3.5
3.0
2.5
2.0
1.5
1.0
0.5
0.0
aJag8
aPor10
aVen10
aPor8
aVen8
aPor6
aVen6
aAdc5
aVen5
aPor4
aVyg4

Unlike IABC f_r, the IABC f_{A5} (Figure 3.4, top graph) did not significantly increase with increasing catheter FG size ≥ 6. f_{A5} was > 18 Hz for all IABCs ≥ FG size 6. IABC phase lag at f_{A5} is illustrated in Figure 3.4, bottom graph.

Working respiratory rate

F_{RR} values for differing brands and FG sizes of IABCs are depicted in Figure 3.5, top graph. Across brands and FG sizes mean F_{RR} minimum and maximum calculated values were 20.4 ± 0.7 (Portex FG size 4) and 244.5 ± 69.8 (Ven FG size 5) breaths/min respectively. There was no significant F_{RR} difference between FG sizes 6, 8 and 10 within the same brand of Portex or Ven IABCs, nor was there any significant F_{RR} difference between these two brands for the same FG sizes 6, 8 or 10. The maximum mean F_{RR} recorded in IABCs ≥ FG size 6 was 148 breaths/min (Ven FG size 10). The overdamped IABCs (Adcock FG size 5, Portex and Vygon FG sizes 4) exhibited a significantly lower F_{RR} than all IABC FG sizes ≥ 6. The Ven FG size 5 catheters' F_{RR} was significantly greater than any other FG size catheter due to the near-critical ζ, but manifested the largest variation about mean F_{RR} due to both under and overdamped frequency responses recorded within the catheter sample.

IABC F_{RR} was significantly higher than matching FG size WFCs for all FG sizes ≥ 6, and for the Ven FG size 5 and Vygon FG size 4 catheters (Figure 3.5, bottom graph). In addition, the Portex and Ven FG size 6 IABCs exhibited a significantly higher F_{RR} than the Portex and Ven FG size 10 WFCs. The Adcock FG size 5 and Portex FG size 4 F_{RR} was similar between IABC and WFCs.

Correlation (r^2) between IABC F_{RR} and FG size, ID or OD was 0.12, 0.10 and 0.18 respectively, whereas it was 0.75, 0.82 and 0.76 for the WFCs.

IABC frequency response variables F_{RR}, ζ, A_r, and f_r which were significantly different ($P < 0.05$) between the various IABC FG sizes and brands are summarised in Table 3.2.

Figure 3.4.

IABC amplitude and phase frequency response characteristics. f_{A5}, frequency at $A_0 \pm 5\%$; P_{A5}, phase difference at $A_0 \pm 5\%$ or f_{A5}. Catheter, catheter brand and FG size; aPor, Portex IABC.

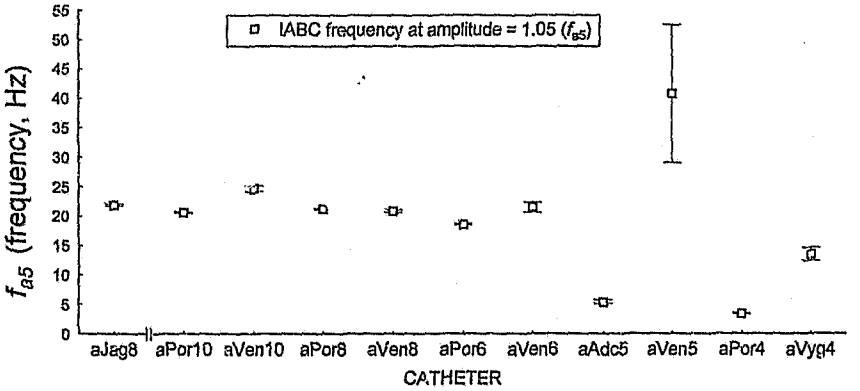
IABC frequency at amplitude = 1.05 (f_{a5})
f_{a5} (frequency, Hz)
55
50
45
40
35
30
25
20
15
10
5
0
aJag8
aPor10
aVen10
aPor8
aVen8
aPor6
aVen6
aAdc5
aVen5
aPor4
aVyg4
CATHETER

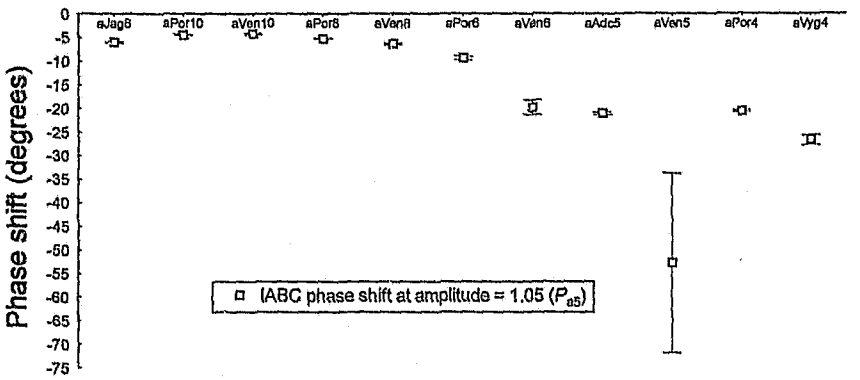
Phase shift (degrees)
0
-5
-10
-15
-20
-25
-30
-35
-40
-45
-50
-55
-60
-65
-70
-75
aJag8
aPor10
aVen10
aPor8
aVen8
aPor6
aVen6
aAdc5
aVen5
aPor4
aVyg4
IABC phase shift at amplitude = 1.05 (P_{a5})

Figure 3.5.

Working Respiratory Rate. Top bar-chart is F_{RR} of IABCs. Bottom bar-chart is mean F_{RR} difference between WFCs and IABCs. F_{RR}, working respiratory rate; Catheter, catheter brand and FG size; aPor, Portex infant air-balloon catheter; * $P < 0.05$ for infant air-balloon (IABC) vs water-filled catheter (WFC) of same FG size.

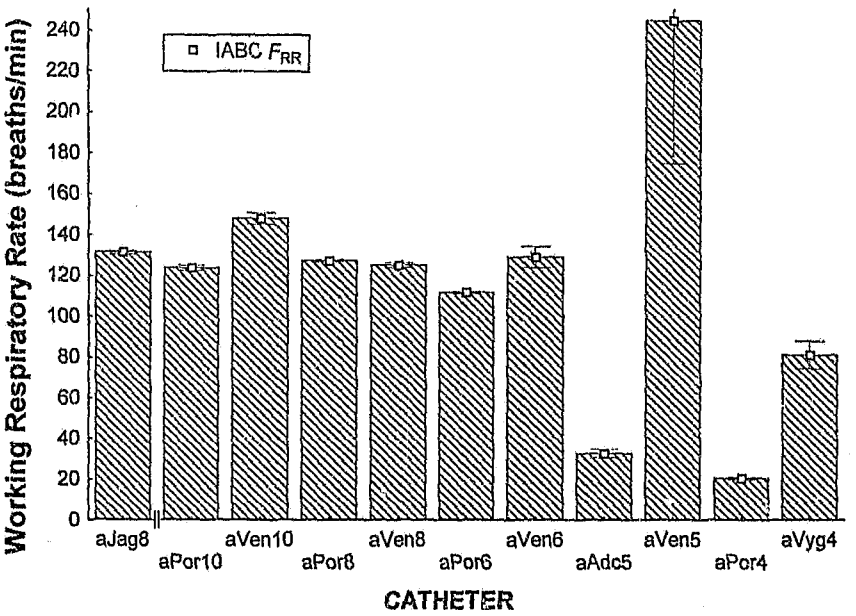
IABC F_{RR}
Working Respiratory Rate (breaths/min)
240
220
200
180
160
140
120
100
80
60
40
20
0
aJag8
aPor10
aVen10
aPor8
aVen8
aPor6
aVen6
aAdc5
aVen5
aPor4
aVyg4
CATHETER

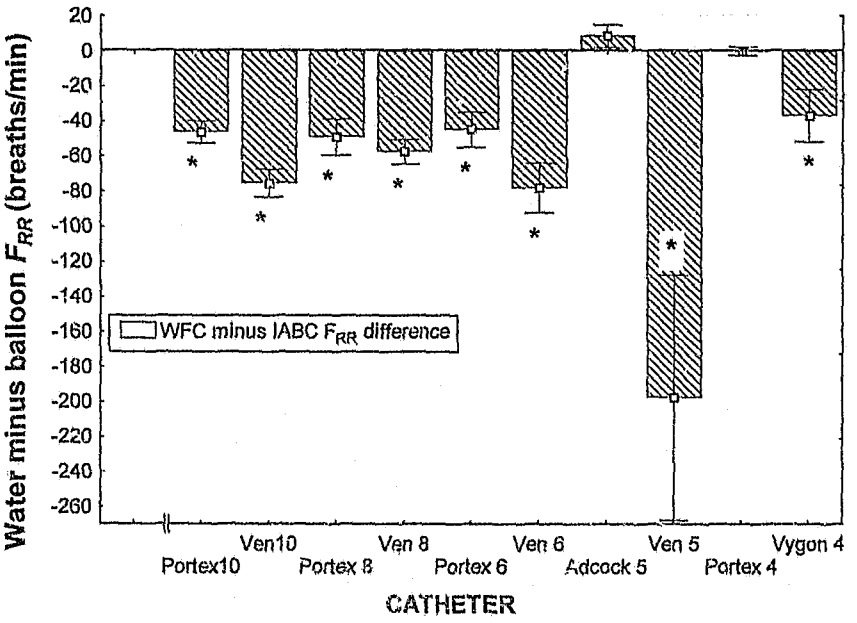
Water minus balloon F_{RR} (breaths/min)
20
0
-20
-40
-60
-80
-100
-120
-140
-160
-180
-200
-220
-240
-260
WFC minus IABC F_{RR} difference
Portex10
Ven10
Portex 8
Ven 8
Portex 6
Ven 6
Adcock 5
Ven 5
Portex 4
Vygon 4
CATHETER

Table 3.2. *Infant air-balloon catheter statistical summary table*

	Por10	Ven10	Por8	Ven8	Por6	Ven6	Adc5	Ven5	Por4	Vyg4	Jag8
Por10											
Ven10	d										
Por8	c	cd									
Ven8	bc	bcd	c								
Por6	bcd	abcd	bcd	bcd							
Ven6	bcd	bcd	bcd	bcd	bcd						
Adc5	abc	abc	abc	abc	abc	abc					
Ven5	abcd	abcd	abcd	abcd	abcd	abd	abc				
Por4	abc	abc	abc	abc	abc	abc	b	abc			
Vyg4	abc	abc	abc	abc	abc	abc	ab	abc	ab		
Jag8	bc	bcd	c	-	bcd	bcd	abc	abcd	abc	ab	

Variables a-d indicated are $P < 0.05$ between any two catheters. a, working respiratory rate (F_{RR}); b, damping coefficient (ζ); c, amplitude gain or attenuation (A_r); d, damped resonant frequency (f_r); Por Adc Ven and Jag, Portex Adcock Ven Erich-Jaeger catheter brands and FG size; -, no significant difference;

3.7 Discussion

By virtue of their construction, IABCs offer certain advantages over transducer micro-tip and WFCs (1). Transducer micro-tip catheters can exhibit absolute pressure measurement inaccuracies with changes in the temperature or fluid nature of the surrounding intra-esophageal medium (7), and they are markedly more sensitive to intra-esophageal cardiac artifacts than balloon catheters (8). WFC absolute pressure measurements are altered when the vertical distance between catheter-tip and transducer is changed, and WFCs are also sensitive to motion artifacts (9). The long IABC balloon measures mean intra-esophageal pressure over a larger portion of the lower esophagus than do WFCs or single micro-tip transducer catheters, making it more likely that the mean value of an unevenly distributed intra-thoracic pleural pressure (18-20) is recorded. IABCs are subject neither to measurement errors related to the dissipation of liquid volume around WFC tips (21), nor to worsened dynamic performance from the introduction of gas microbubbles into WFCs. The recent advent of cheap disposable pressure transducers (22) make IABCs comparatively inexpensive (8) for neonatal intensive care, and they are relatively atraumatic (4, 6) on insertion by virtue of balloon-latex and catheter PVC flexibility.

Frequency responses

The commonly performed in vivo airway occlusion test (7, 18, 23) helps to position intra-esophageal IABCs optimally by assessing the in situ intra-esophageal catheter's reflection of pleural pressure. However, this procedure does not assess the ability of IABCs to respond accurately to dynamic P_{es} changes during artificial

ventilation. Researchers employing air-balloon catheters to measure P_{es} have noted adequate frequency responses to 10 Hz, 20 Hz and 22 Hz in a FG size 6 catheter ((3, 5), (18, 24) and (25)), and to 5 Hz and 15 Hz in a FG size 8 catheter ((26, 27) and (28)). However, these studies were not aimed at formally assessing IABC frequency responses or at comparing IABCs with WFCs, and the frequency responses were reported for catheters (usually n = 1) of just one FG size and brand. Thus effects due to manufacturing tolerances within a catheter and balloon sample, and effects related to differing catheter tolerances between manufacturers for the same FG size (see Table 3.1), were excluded. Details of catheter length, wall thickness, composition, brand, balloon length, balloon diameter and latex thickness, the definition of adequate frequency response used and the method of frequency response analysis were also not provided in most of the above reports; hence the large frequency response data discrepancies for the same FG sizes noted between researchers here.

By fixing transducer type, catheter length, FG size, composition and brands between the IABC and WFC groups, the data in this report directly assesses and compares the dynamic frequency response characteristics of matching IABCs and WFCs of various FG sizes and brands. Our data suggest that IABCs, manufactured to the appropriate specifications for infants (3), offer significantly superior frequency response characteristics compared to matching WFCs. We measured f_{A5} and calculated F_{RR} as variables meaningful in clinical practice to evaluate the measurement fidelity of IABCs: The lowest f_{A5} (Figure 3.4) recorded in IABC ≥ FG size 6 was 19 Hz. Infants are commonly ventilated at high respiratory rates, and the pediatric ventilators employed may generate very steep inspiratory waveforms with high frequency harmonic contents, or be of the high-frequency-oscillatory type. Therefore, provided that the esophageal

pressure waveform's energy is located within the first 10 harmonics of the ventilator's fundamental frequency (4, 9), an IABC ≥ FG size 6 can be expected to produce a minimum F_{RR} (which predicts the potential of an IABC to measure P_{es} within a 5% error limit up to a calculated respiratory rate) of 112 breaths/min. However, under conditions of an esophageal pressure waveform's energy being located within the first 5 harmonics (1) of the fundamental frequency, our findings indicate that IABCs ≥ FG size 6 may record (to within 5% accuracy) such a waveform administered at up to 224 breaths/min.

High correlations between F_{RR} and FG size, OD or ID in the WFCs imply that choosing a larger FG size WFC extends the F_{RR}. On the other hand, the poor correlations calculated for F_{RR} versus FG size, OD or ID in IABCs can be seen as advantageous to clinicians: For the same catheter brand, FG size 6 IABCs exhibit an F_{RR} comparable with FG size 8 and 10 IABCs, and yet also exhibit a significantly better F_{RR} than FG size 10 WFCs. Thus a FG size 6 IABC offers clinicians and researchers a relatively atraumatically sized catheter with pressure measurement fidelity similar to much larger IABCs, and also exceeds the measurement fidelity of equivalent FG size 10 WFCs.

The variation of f_r within IABC catheter samples is beneficially lower than that found within matching WFC groups. Variation differences may be attributed to micro-bubbles of trapped gas in the WFCs (29-31), despite the WFC CO_2 flushing and water-degassing procedures. We noticed that WFC female luer fittings tend to trap gas-bubbles at the junction of the catheter's body and luer fitting, which in certain cases proved difficult to remove even with reverse flushing. These adverse characteristics are intensified in clinical settings where CO_2 flushing, degassing of water and reverse liquid flushing of WFCs are not possible.

We demonstrated that IABCs of FG sizes ≥ 6 are underdamped and resonate, yet IABCs of FG size 4 and 5 can be overdamped and attenuate the esophageal waveform pressure signal. The overdamped properties of small FG size IABCs are not likely to be due to occlusion of the catheter-tip eyelets by the latex balloons, nor due to partial luminal occlusion of the IABC small FG size by balloon ties, since we were able to demonstrate the overdamping effect using equivalent air-filled catheters without latex balloons attached (data not shown here). The pressure-volume coefficient (or elastance) of IABCs is determined mainly by the compressibility of the air contained in IABCs, whereas it is primarily governed by the elastic properties of the catheters and transducer-dome diaphragm combination in WFCs. The overdamping may thus be explained by the combination of a low radius, soft PVC and high compressibility of the air. In spite of the overdamped frequency characteristics of small FG size IABCs, they still possessed a F_{RR} similar to matching small FG WFCs.

Validity of Methods

We performed in vitro frequency response analysis because in vivo fast flush tests are not applicable to IABCs. An advantage of the in vitro technique is the absence of superimposed in vivo peristaltic and cardiac waveform artifacts (29). We used the swept frequency forced oscillation technique as opposed to the step response techniques (free oscillation burst-balloon, or fast flush tests) because the latter is practically limited to underdamped systems (29, 31). This would be unsuitable for the overdamped small FG size IABCs. In addition, step response techniques may miss subtle differences in f_0 (13) and are open to measurement inaccuracies in the determination of the period and amplitude of the response (29). The swept frequency

technique is suitable for a distributed parameter system (29, 31), such as that encountered with IABCs, and allows IABC stimulation at equal amplitude over all frequencies, whereas the step response approach results in diminishing amplitudes with increasing frequency.

To incorporate possible effects due to non-linearities (amplitude dependence) related to dynamic IABC compliance and catheter wall hysteresis (31), we applied an input pressure of -5 to +10 cm H_2O similar to mean P_{es} accompanying artificial ventilation. Temperature fluctuation influences frequency responses (15, 31, 32) through altering compliance or compliance hysteresis of PVC and closed-tip latex balloons, therefore the IABC and WFC frequency responses were measured at infant physiological temperatures.

We noted similar compliance curves for our laboratory-produced balloons attached to either FG size 10 or FG size 5 catheters (Figure 3.1). This suggests that, to manufacture IABCs, one size (ID 8.3 mm, length 5.5 cm) of infant latex-balloon may be adequate for attachment to differing FG sized catheters.

Conclusions

We conclude that frequency responses of IABCs greater than FG size 5 exhibit underdamped resonant traces, whereas smaller FG size IABCs may be overdamped. FG size 6 IABCs offer similar measurement accuracies to those of larger IABCs. IABCs, manufactured to infant-appropriate balloon specifications, have the potential to measure P_{es} up to 148 breaths/min within a 5% error limit. Compared to matching WFCs, IABCs have significantly superior frequency response characteristics, and lower frequency response variability within catheter samples, and are therefore more suitable

for accurate dynamic P_{es} measurements during the high-frequency respiratory mechanics commonly encountered in artificially ventilated infants.

3.8 Appendix

Equations for amplitude and phase calculations:

Poles (roots of the denominator) of the system function G(s), located from the second order curve fitted to the frequency response traces, are converted to coefficients of the standard second order Laplace transform function given by (33, 34)

$$G(s) = c/(s/a)^2 + 2\zeta(s/b) + c \qquad (1)$$

thus

Undamped natural frequency (14, 15, 33)

$$f_0 = (s/a)^{1/2} \qquad (2)$$

Damping coefficient (14, 15, 33)

$$\zeta = (s/b)/2f_0 \qquad (3)$$

Damped resonant frequency (14, 15, 33)

$$f_r = f_0(1-2\zeta^2)^{1/2} \qquad (4)$$

Maximum amplitude ratio (16)

$$A_r = 1/(1-(2\zeta^2+1)^2)^{1/2} \qquad (5)$$

Phase at A_0+5% (14)

$$P_{A5} = \tan^{-1}((2\zeta f_{A5}/f_0)/1-(f_{A5}/f_0)^2) \quad (6)$$

Working Respiratory Rate (14, 16)

$$F_{RR} = (f_{A5} \times 60)/10 \quad (7)$$

where f_{A5} is the frequency at which the amplitude ratio = 1.05 or 0.95

10 refers to the Fourier series 10'th harmonic

Appendix Note:

In this experiment the frequency response trace was divided through by the amplitude ratio at 1 Hz (regarded as the DC response) and therefore $A_0/A_r = 1/A_r$. The CMS frequency response calculations assume that the system is second order and linear (14).

3.9 References

1. Coates AL, Stocks J. Esophageal pressure manometry in human infants. Pediatr Pulmonol. 1991; 11:350-360.

2. Coates AL, Stocks J, Gerhardt T. Esophageal manometry. In: Stocks J, Sly PD, Tepper RS, Morgan WJ, eds. Infant Respiratory Function Testing. New York: John Wiley & Sons, Inc., 1996: 241-258.

3. Beardsmore CS, Helms P, Stocks J, Hatch DJ, Silverman M. Improved esophageal balloon technique for use in infants. J Appl Physiol. 1980; 49:735-742.

4. Maxted KJ, Shaw A, Macdonald TH. Choosing a catheter system for measuring intra-esophageal pressure. Med Biol Eng Comput. 1977; 15:398-401.

5. Heaf DP, Turner H, Stocks J, Helms P. The accuracy of esophageal pressure measurements in convalescent and sick intubated infants. Pediatr Pulmonol. 1986; 2:5-8.

6. Kaplan M, Galioto FM, Ruttimann UE, Hamosh P, Avery GB. Evaluation of a gastric tube with esophageal balloon for neonatal use. Am J Perinatol. 1984; 1:355-359.

7. Chartrand DA, Ye TH, Maarek JM, Chang HK. Measurement of pleural pressure at low and high frequencies in normal rabbits. J Appl Physiol. 1987; 63:1142-1146.

8. Chartrand DA, Jodoin C, Couture J. Measurement of pleural pressure with oesophageal catheter-tip micromanometer in anaesthetized humans. Can J Anaesth. 1991; 38:518-521.

9. Senterre J, Geubelle F. Measurement of endoesophageal pressure in the newborns. Biol Neonate. 1970; 16:47-53

10. Hartford CG, Rogers GG, Turner MJ. Correctly selecting a liquid-filled nasogastric infant feeding catheter to measure intra-esophageal pressure. Pediatr Pulmonol. 1997; 23:362-369.

11. Beardsmore CS, Stocks J, Silverman M. Esophageal pressure in infants at elevated lung volumes and positive airway pressure. J Appl Physiol. 1983; 55:377-382.

12. Lemen R, Benson M, Jones JG. Absolute pressure measurements with hand-dipped and manufactured esophageal balloons. J Appl Physiol. 1974; 37:600-603.

13. Shapiro GG, Krovetz LJ. Damped and undamped frequency responses of underdamped catheter manometer systems. Am Heart J. 1970; 80:226-236.

14. Fry DL. Physiologic recording of modern instruments with particular reference to pressure recording. Physiol Rev. 1960; 40:753-788.

15. Hansen AT. The theory for elastic liquid-containing membrane manometers: Special part. Acta Physiol Scand. 1950; 19:333-343.

16. Hipkins SF, Rutten AJ, Runciman WB. Experimental analysis of catheter-manometer systems in vitro and in vivo. Anesthesiology. 1989; 71:893-906.

17. Zar JH. Biostatistical Analysis. Engelwood Cliffs, NJ: Prentice-Hall, 1974: 206-252.

18. Baydur A, Behrakis PK, Zin WA, Jaeger M, Milic-Emili J. A simple method for assessing the validity of the esophageal balloon technique. Am Rev Respir Dis. 1982; 126:788-791.

19. LeSouef PN, Lopes JM, England SJ, Bryan MH, Bryan AC. Influence of chest wall distortion on esophageal pressure. J Appl Physiol. 1983; 55:353-358.

20. Ratjen FA, Wiesemann HG. Variability of dynamic compliance measurements in spontaneously breathing and ventilated newborn infants. Pediatr Pulmonol. 1992; 12:73-80.

21. Gerhardt T, Bancalari E. Chestwall compliance in full term and premature infants. Acta Paediatr Scand. 1980; 69:359.

22. Gardner RM. Accuracy and reliability of disposable pressure transducers coupled with modern pressure monitors. Crit Care Med. 1996; 24:879-882.

23. Coates AL, Davis GM, Vallinis P, Outerbridge EW. Liquid-filled esophageal catheter for measuring pleural pressure in preterm neonates. J Appl Physiol. 1989; 67:889-893.

24. Higgs BD, Behrakis PK, Bevan DR, Milic-Emili J. Measurement of pleural pressure with esophageal balloon in anaesthetized humans. Anesthesiology. 1983; 59:340-343.

25. Baydur A, Cha E, Sassoon CSH. Validation of esophageal balloon technique at different lung volumes and postures. J Appl Physiol. 1987; 65:315-321.

26. Wolfson FR, Greenspan JS, Deoras KS, Allen JL, Shaffer TH. Effect of position on mechanical interaction between rib cage and abdomen in preterm infants. J Appl Physiol. 1992; 72:1032-1038.

27. Bhutani VK, Sivieri EM, Abbasi S, Shaffer TH. Evaluation of neonatal pulmonary mechanics and energetics. Pediatr Pulmonol. 1988; 4:150-158.

28. Dechman G, Sato J, Bates JHT. Factors affecting the accuracy of esophageal balloon measurement of pleural pressure in dogs. J Appl Physiol. 1992; 72:383-388.

29. Gardner RM. Direct blood pressure measurement-dynamic response requirements. Anesthesiology. 1981; 54:227-236.

30. Milic-Emili J, Mead J, Turner JM, Glauser EM. Improved technique for estimating pleural pressure from esophageal balloons. J Appl Physiol. 1964; 19:207-211.

31. Yeomanson CW, Evans DH. The frequency response of external transducer blood pressure measurement systems: a theoretical and experimental study. Clin Phys Physiol Meas. 1983; 4:435-449.

32. Rutten AJ, Nancarrow C, Isley AH. An assessment of six different pulmonary artery catheters. Crit Care Med. 1987; 15:250-255.

33. Kuo FF. The Laplace transform; Amplitude, phase and delay. In: Network Analysis and Synthesis. John Wiley & Sons Inc. New York, 1966. 134-165,253-279.

34. Milhorn HT. Transient analysis of physical systems. In: The Application of Control Theory to Physiological Systems. WB Saunders Company, Philadelphia, 1966, 78-91.

CHAPTER 4

4 PREDICTING AIR-BALLOON AND LIQUID-FILLED CATHETER FREQUENCY RESPONSES. TESTING THE VALIDITY OF THE ASSUMPTION THAT FLUID-FILLED CATHETERS FIT A SECOND-ORDER SYSTEM.

4.1 Linking Comments

In Chapters Two and Three extensive information on the frequency response characteristics of liquid-filled and air-balloon intra-esophageal catheter manometers was collected, analysed and presented. These frequency response measurements were made using the forced oscillation swept sine-wave technique (certain advantages of this technique are discussed in Chapters Two and Three).

An alternative technique for evaluating the dynamic frequency response of catheter manometers is the square-wave step-response method, such as the in vitro burst-balloon or the in vivo fast-flush techniques (although in practice the fast-flush technique cannot be applied to air-balloon catheters). In all reported uses of square-wave step-response techniques calculations based on second-order models have been used to determine catheter-manometer characteristics. Using the swept-sine wave technique in Chapter Three, "raw" data were collected representing the true small signal frequency responses of air-balloon and liquid-filled catheters (as opposed to the predicted resonance frequencies and predicted amplitude deviations from uniformity which would be obtained using square-wave step-response techniques).

Chapter Four analyses the measured frequency response traces generated in Chapter Three to test the assumption that catheter manometer frequency responses fit a second order system: Chapter Four thus determines whether the two square-wave step-response techniques, which are alternates to the swept sine wave technique, can be used to determine in a valid fashion (within a context meaningful to clinicians) the

frequency responses of air-balloon and liquid-filled catheters, or whether the swept sine wave technique used in Chapters Two and Three should preferentially be applied. [Comprehensive information is provided in Chapter Four's Abstract, Introduction and Discussion sections, which follow]:-

4.2 Abstract

Water-filled (W-FC) and air-balloon (A-BC) catheters are favoured in clinical practice for measuring infant dynamic intra-esophageal pressure. Mathematical equations, applied to square-wave responses to predict catheter-manometer frequency responses, usually assume a second order frequency response system. We tested the validity of this assumption.

Frequency responses of differing catheter brands and sizes were determined with a sine-wave generator. Second order curves (SOFC) were fitted to original recorded curves (ORC) to calculate SOFC:ORC ratios for damped resonance frequency (f_r), maximum amplitude gain (A_r), and the frequency and phase at which amplitude gain = 1.05 (f_{A5}, P_{A5}).

SOFC.ORC ratios deviated significantly from 1.0 for f_{A5} and A_r, but not for f_r, were significantly greater in W-FCs compared to A-BCs, and increased with increasing catheter FG-size. P_{A5} of SOFCs and ORCs differed significantly.

In conclusion, A-BC and W-FC frequency responses do not adequately fit second order systems. System order should be verified experimentally prior to predicting frequency responses using the typical equations applied to square-wave response techniques. We recommend using a sine-wave generator to measure in vitro frequency responses of compliant fluid-filled catheters.

Key Words: frequency response; mathematical modelling; pressure; oesophageal manometry; lung compliance; apparatus and methods; instrumentation.

4.3 Introduction

Catheter microtip pressure transducer technology is replacing the use of fluid-filled catheters for in vivo pressure measurements. However, dynamic intra-esophageal pressure measurement, employed to estimate pleural pressure when calculating infant dynamic lung compliance, continues to be performed using fluid-filled catheters (1,2). Nasogastric water-filled catheters (W-FC) and air-balloon catheters (A-BC), by virtue of their flexibility, reduce the risk of esophageal trauma in newborns (3,4). W-FCs in situ are well tolerated by infants (4) and are commonly in use for nasogastric feeding and thus accessible to clinicians. On the other hand, transducer micro-tip catheters may drift with changes in the temperature or the fluid nature of the surrounding intra-esophageal medium (5), are markedly more sensitive to intra-esophageal cardiac artifacts than A-BCs (6), and may overestimate dynamic pleural pressures in infants (7). The A-BC balloon length is advantageous for measuring intra-esophageal pressure over a large portion of the lower esophagus, while current availability of disposable pressure transducers (8) makes the robust (9) W-FCs and A-BCs affordable manometer options.

The presence of high frequency respiratory mechanics in newborns makes formal frequency response assessment of fluid-filled catheters a necessity (10,11); this assessment may be performed using the in vitro swept sine-wave generator technique, or the in vitro (burst-balloon) or in vivo (fast-flush) square-wave response techniques. Square-wave response techniques usually invoke equations which assume catheter frequency responses are a second order system, thereby enabling prediction of the catheters' frequency response curves and the frequency up to which the catheters exhibit a near uniform response (12,13). Theory surrounding such typical equations used to analyze square-wave responses, and from there to predict underdamped liquid-

filled catheter frequency responses, is published extensively (14-20), but experimental evidence to support the assumption of an adequate second order fit, inherent to most of these equations, is sparse, and only found for certain intra-arterial liquid-filled catheters (9,21,22). The validity of assuming a second order system frequency response for liquid and gas filled Polyvinyl chloride (PVC) nasogastric feeding catheters, used to measure infant dynamic intra-esophageal pressure, is untested. Nevertheless, the square-wave response technique, typically reliant upon this assumption, is used to obtain the frequency responses of these fluid-filled nasogastric catheters (23).

This study tests quantitatively the validity of the assumption that fluid-filled nasogastric catheter frequency responses adequately fit a second order system, an assumption which is inherent to equations commonly used to predict frequency responses from square-wave response techniques.

4.4 Materials and Methods

Catheters and frequency response measurements

Data presented in this study are obtained from experiments performed by the authors to determine the frequency responses of infant air-balloon versus equivalent liquid-filled PVC feeding catheters as used to measure dynamic intra-esophageal pressure in infants (data not yet published): Infant A-BCs were laboratory manufactured by attaching suitable latex balloons (24) to PVC nasogastric catheters, and a commercially available adult A-BC (Erich Jaeger, Germany) was included in the experiment (SEE CHAPTER 3, Table 3.1).

Eight samples each of differing brands and FG (French Gauge) size A-BCs and W-FCs of similar lengths (SEE CHAPTER 3, Table 3.1), connected to a Gould P10EZ pressure transducer and disposable diaphragm dome (Viggo-Spectramed Gould TA1019, Oxnard, CA) and 4-way stopcocks, were inserted into a water-filled chamber kept at 37 °C. W-FCs were flushed with CO_2 followed by degassed water at 37 °C prior to testing (25). A-BCs were operated within their determined optimal volume working range (24). A sine-wave generator (Hewlett Packard 3562A, USA) linked to a DC-coupled amplifier and loudspeaker (Bose 4.5" 802, Bose Corporation, MA) generated sinusoidal pressure waveforms inside the chamber between -5.5 and +10 cmH_2O pressure from 1 - 100 Hz, averaged for 10 s at each 1 Hz interval. Catheter amplitude and phase-frequency responses were determined (Hewlett Packard Dynamic Signal Analyser 3562A, USA) by comparison with the output from a temperature compensated reference pressure transducer (Honeywell Microswitch 170PC, USA) located above the catheter tip.

Frequency response ratios; variables

The original recorded curves (ORC) of amplitude and phase frequency responses obtained from the sine-wave generator technique were further analysed by fitting second order system curves (2 poles, no zeros) to the ORC traces, using the curve-fit function of the HP3562A analyser. Curves were fitted between 1 Hz and the frequency at which the amplitude was 1 dB down from the maximum recorded amplitude on the ORC. The ORCs and second order fitted curves (SOFC) were then divided through by their amplitudes at 1 Hz (regarded as the DC-response).

The values of five variables (commonly quoted by researchers to describe the frequency responses of their catheter-manometer systems) were obtained from each SOFC and ORC tracing (Fig. 4.1). The SOFC:ORC ratio (for amplitude-frequency responses), and the SOFC-ORC difference (for phase-frequency responses), was determined for each variable as follows:

SOFC:ORC ratios from the amplitude-frequency response tracings;

SOFC:ORC of f_{A5}; Ratio of the SOFC and ORC tracings' frequency values at which $A = 1.05$

(A refers to the linear amplitude gain of the catheter-manometer under test over that of the reference transducer. f_{A5} is thus the frequency up to which the catheter has a near uniform amplitude-frequency response (12,17) (Figure 4.1).

SOFC:ORC of f_r; Ratio of the SOFC and ORC tracings' damped resonance frequency values (frequency at maximum amplitude gain)

SOFC:ORC of A_r; Ratio of the SOFC and ORC tracings' maximum amplitude gain values (linear gain at f_r)

SOFC-ORC phase-shift differences from the phase-frequency response tracings;

SOFC-ORC of P_{A5}; Difference between the SOFC and ORC tracings' phase-shift values at f_{A5}

SOFC-ORC of Pf_r; Difference between the SOFC and ORC tracings' phase-shift values at f_r

Figure 4.1.

Sample plot of Second Order Fitted Curve (SOFC, dashed line) versus Original Recorded Curve (ORC, solid line) for Ven FG-size 8 water-filled catheter (W-FC) amplitude-frequency response trace. First marker circle represents baseline amplitude (Y-axis, Ya = 1.0 Mag) and baseline frequency (X-axis, X = 1 Hz). Second marker circle shows frequency at which A = 1.05 Mag on the ORC trace (X-axis, $f_{A5} = X + \Delta X = 7.4$ Hz). The SOFC's f_{A5} is extended upwards relative to the ORC's f_{A5}, yielding a SOFC:ORC f_{A5} ratio of 1.5. Mag, linear gain over reference transducer; Hz, hertz.

Note that the curve-fit algorithm of the Hewlett Packard analyser fits both phase and amplitude data.

X=1 Hz ΔX=8.25 Hz
Ys=1.0 ΔYs=48.27m
M: FREQ RESP

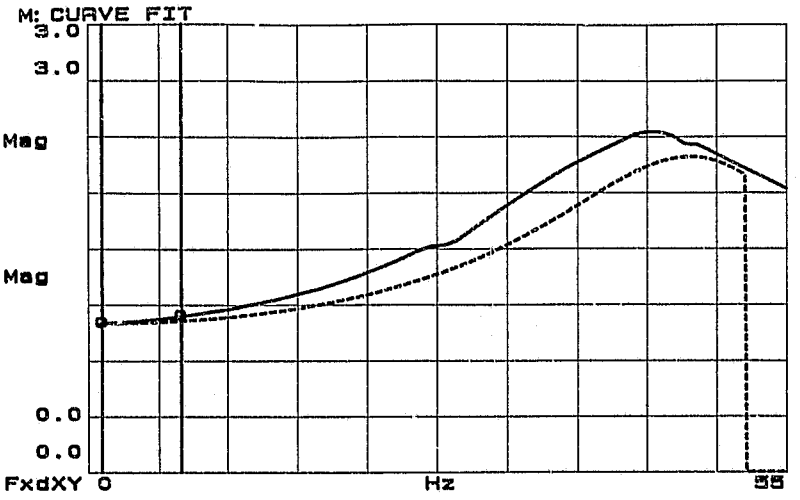

Statistical analysis

For amplitude-frequency response variables, confidence intervals (95%) for SOFC:ORC ratios were calculated (26). SOFC:ORC ratios with confidence intervals which excluded the ideal ratio of 1.0 and which additionally had mean ratios ≤ 0.95 or ≥ 1.05 were regarded as significantly different. SOFC-ORC phase-shift variables were compared using Student's two-tailed paired t-test.

Significant differences between samples of A-BC and W-FC FG-sizes and brands were determined by one-way (independent variables; A-BC or W-FC catheter types) multivariate (5 dependent SOFC:ORC amplitude or phase frequency response variables) analysis of variance (MANOVA F-test, Statistica™ software, Statsoft, OK) and a post-analysis Tukey Significant Difference test-correction applied to significant differences (27). All displayed values are mean ± SD, and P-values < 0.05 are regarded as statistically significant.

4.5 Results

SOFC:ORC ratios for the amplitude-frequency response variables are depicted in Figure 4.2. SOFCs of both A-BC and W-FC groups significantly overvalued the frequency at which the amplitude gain was 1.05 (or f_{A5}), as evidenced from the mean SOFC:ORC ratios of f_{A5} being significantly > 1.0 for all but one (wPor4) catheter sample (Figure 4.2, top graph). Between A-BC and W-FC catheter groups, for the same FG-size and brand of catheter, the SOFC of W-FC group's samples overvalued f_{A5} to a significantly greater degree than did the SOFCs of A-BC group's samples (eg., compare the ratios of wVen10 and aVen10). Within the W-FC group there was a significant decrease in the mean SOFC:ORC ratio of f_{A5} (towards the ideal ratio of 1.0) with decreasing catheter FG-size, but this decrease was less noticeable within the A-BC group. Within both A-BC and W-FC groups, for the same sample FG-sizes, the SOFC:ORC ratio of f_{A5} was unaffected by the brand of catheter tested (eg., compare the ratio of wPor10 with wVen10).

In contrast to the SOFC:ORC ratios of f_{A5} above, the SOFC:ORC ratio of f_r (Figure 4.2, middle graph) was not significantly different from the ideal ratio of 1.0 in all of the A-BC group's samples, whilst SOFCs of only a few of the W-FC group's samples significantly overvalued the f_r (to a small degree). However, SOFCs of most W-FC and A-BC group's samples significantly undervalued the amplitude magnitude at resonance frequency (A_r) as evidenced by the SOFC:ORC of A_r being significantly < 1.0 (Figure 4.2, bottom graph). This SOFC undervaluation of A_r was similar between the A-BC and W-FC groups, and in several catheter samples the magnitude of undervaluation significantly decreased with decreasing catheter FG-size in both groups. Within the A-

BC and the W-FC groups, for the same FG-size samples, the SOFC:ORC ratio of A_r was not significantly affected by the brand of catheter tested. Only one (wPor4) catheter's SOFC:ORC did not differ significantly from ideal across all three amplitude-frequency response variables.

Figure 4.2.

Second Order Fitted Curve:Original Recorded Curve (SOFC:ORC) ratios (mean ± SD) for amplitude-frequency response trace variables. Horizontal dashed line depicts ideal SOFC:ORC ratio of 1.0. X-scale break separates commercial Jaeger adult from laboratory made air-balloon catheters. SOFC:ORC of f_{A5}, SOFC:ORC ratio at the frequency at which $A = 1.05$; SOFC:ORC of f_r, SOFC:ORC ratio at damped resonance frequency; SOFC:ORC of A_r, SOFC:ORC ratio at maximum amplitude gain. Catheter, catheter brand and French Gauge size; aPor or wPor, air-balloon or water-filled Portex catheter.

* SOFC:ORC ratio significantly different from ideal 1.0 (see criteria in methods).

+ $P < 0.05$ for A-BC vs W-FC of same FG-size and brand.

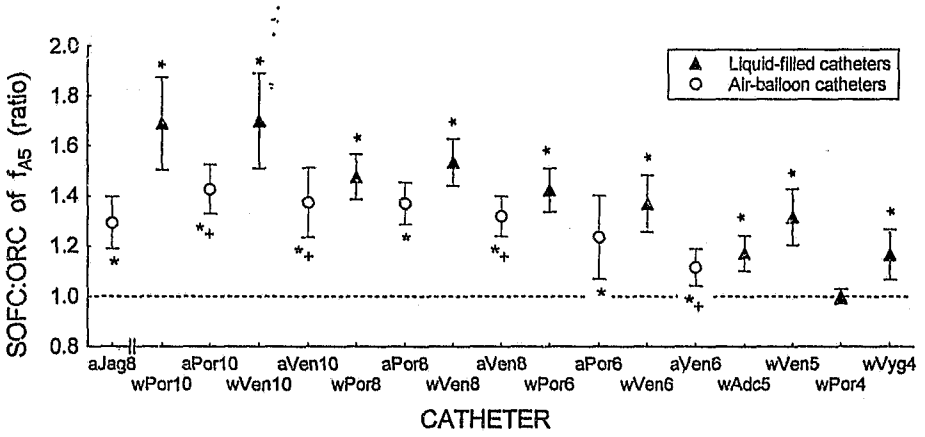
SOFC:ORC of f_{AS} (ratio)
2.0
1.8
1.6
1.4
1.2
1.0
0.8
Liquid-filled catheters
Air-balloon catheters
aJag8
aPor10
aVen10
aPor8
aVen8
aPor6
aVen6
wVen5
wVyg4
wPor10
wVen10
wPor8
wVen8
wPor6
wVen6
wAdc5
wPor4
CATHETER

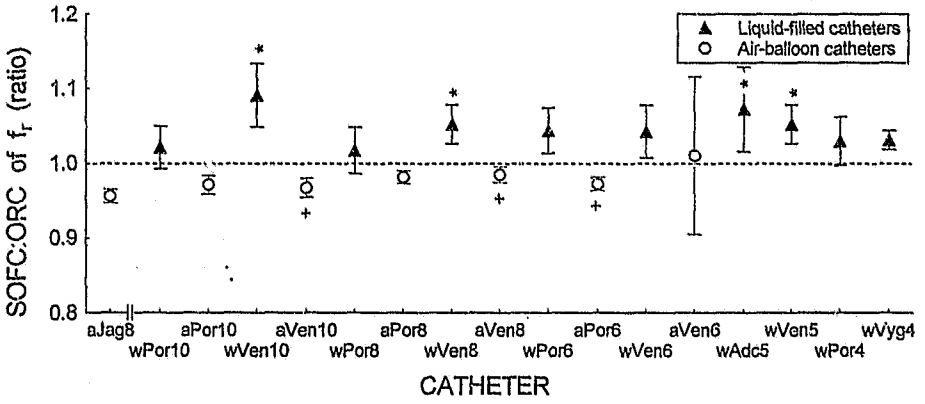
SOFC:ORC of f_r (ratio)
1.2
1.1
1.0
0.9
0.8
Liquid-filled catheters
Air-balloon catheters
aJag8
aPor10
aVen10
aPor8
aVen8
aPor6
aVen6
wVen5
wVyg4
wPor10
wVen10
wPor8
wVen8
wPor6
wVen6
wAdc5
wPor4
CATHETER

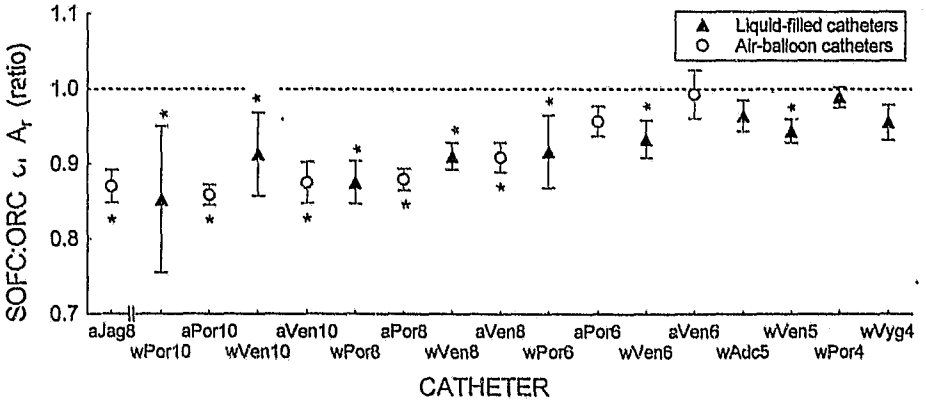
SOFC:ORC c_r A_r (ratio)
1.1
1.0
0.9
0.8
0.7
Liquid-filled catheters
Air-balloon catheters
aJag8
aPor10
aVen10
aPor8
aVen8
aPor6
aVen6
wVen5
wVyg4
wPor10
wVen10
wPor8
wVen8
wPor6
wVen6
wAdc5
wPor4
CATHETER

SOFC-ORC differences for phase-frequency response variables are depicted in Figure 4.3 (a negative phase-shift difference implies that the SOFC phase-shift is greater than the corresponding ORC phase-shift). SOFCs of A-BC and W-FC groups overvalued the phase-shift at f_{A5} (= P_{A5}) as evidenced by the SOFC-ORC phase-shift difference of P_{A5} being significant for most catheter samples (Figure 4.3, top graph). Between the A-BC and W-FC catheter groups, for the same FG-size and brand of catheter, the SOFC of all W-FC group's samples overvalued P_{A5} to a significantly greater degree than did SOFCs of the A-BC group's samples (eg., compare the SOFC-ORC phase-shift difference of wPor8 with aPor8). There was a trend, significant in several samples, for the magnitude of the phase-shift difference overvaluation by SOFCs to decrease with decreasing FG-size in the W-FC group. Within the A-BC group, for the same FG-size, the SOFC-ORC phase-shift difference of P_{A5} was unaffected by the brand of catheter tested (eg., compare the phase-shift difference of aPor8 with aVen8). However, catheter brand significantly affected the W-FC group's samples (eg., compare wPor10 with wVen10). SOFCs significantly overvalued the phase-shift difference at f_r (= Pf_r) in the W-FC group, but significantly undervalued Pf_r in the A-BC group (Figure 4.3, bottom graph).

SOFC:ORC ratios, and SOFC-ORC phase-shift differences, for the commercially available Erich-Jaeger A-BC did not differ significantly from those of our similar FG-sized laboratory manufactured A-BCs. The variance of SOFC:ORC ratios, and of the SOFC-ORC phase-shift differences, within most catheter samples was generally large (see Standard Deviation bars in Figures 4.2 and 4.3). Table 4.2 summarises the SOFC:ORC ratios', and the SOFC-ORC phase-shift differences', significant differences between differing A-BC and W-FC FG-sizes and brands.

Figure 4. 3.

Phase-shift difference (mean ± SD) between Second Order Fitted Curve and Original Recorded Curve (SOFC-ORC) for phase-frequency response trace variables. X-scale break separates commercial Jaeger adult from laboratory-made air-balloon catheter. SOFC-ORC of P_{A5}, SOFC-ORC phase-shift difference at $A = 1.05$ (or f_{A5}); SOFC-ORC of Pf_r, SOFC-ORC phase-shift difference at damped resonance frequency. Catheter, catheter brand and French Gauge size; aPor or wPor, air-balloon or water-filled Portex catheter.

* Significant SOFC-ORC phase-shift difference.

+ $P < 0.05$ for SOFC-ORC phase-shift difference between A-BC and W-FC of same FG-size and brand

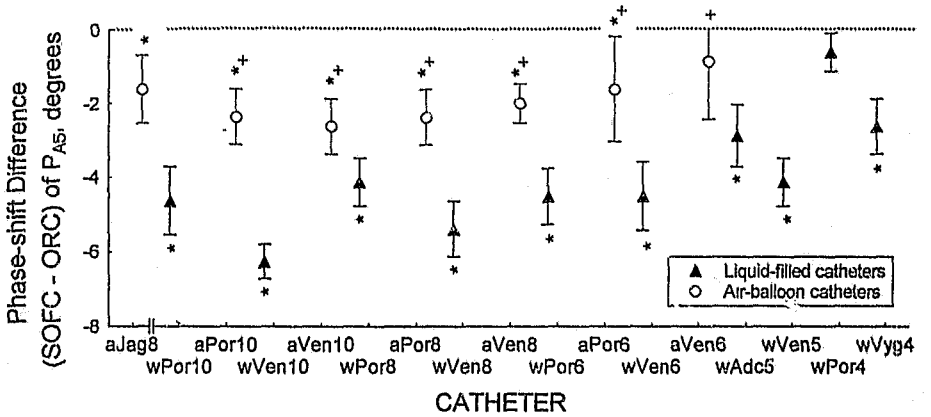
Phase-shift Difference
(SOFC - ORC) of P_{AS}, degrees
0
-2
-4
-6
-8
Liquid-filled catheters
Air-balloon catheters
aJag8
wPor10
aPor10
wVen10
aVen10
wPor8
aPor8
wVen8
aVen8
wPor6
aPor6
wVen6
aVen6
wAdc5
wVen5
wPor4
wVyg4
CATHETER

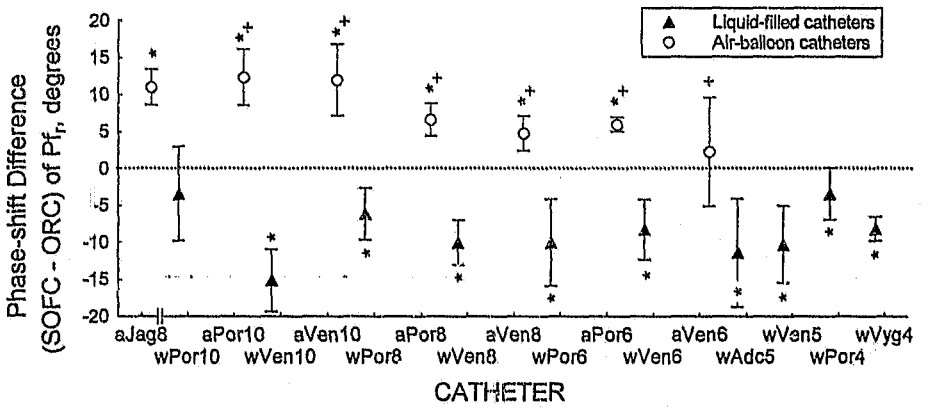
Phase-shift Difference
(SOFC - ORC) of Pf_n, degrees
20
15
10
5
0
-5
-10
-15
-20
Liquid-filled catheters
Air-balloon catheters
aJag8
wPor10
aPor10
wVen10
aVen10
wPor8
aPor8
wVen8
aVen8
wPor6
aPor6
wVen6
aVen6
wAdc5
wVen5
wPor4
wVyg4
CATHETER

Table 4.2. *SOFC:ORC Ratios; Statistical Summary Table*

Catheter	(1)	(2)	(3)	(4)	(5)	(6)	(7)	(8)	(9)	(10)	(11)	(12)	(13)	(14)	(15)	(16)	(17)
wPor10 (1)																	
aPor10 (2)	ade																
wVen10 (3)	abde	abde															
aVen10 (4)	ade	-	abde														
wPor8 (5)	a	de	abde	e													
aPor8 (6)	ade	-	abde	-	de												
wVen8 (7)	-	bde	-	bde	-	bde											
aVen8 (8)	ade	-	abde	-	de	-	abde										
wPor6 (9)	ac	bde	ad	bde	-	de	-	de									
aPor6 (10)	acde	c	abde	c	acde	c	adbd	-	bde								
wVen6 (11)	ac	bcde	ad	bde	-	de	-	de	-	bde							
aVen6 (12)	acd	ace	abcd	acde	acde	ac	acde	ac	acde	-	ade						
wAdc5 (13)	acde	abce	ad	abce	ac	bce	ad	be	ad	be	d	de					
wVen5 (14)	ac	bcde	ad	bce	c	bcde	a	bde	-	bde	-	de	-				
wPor4 (15)	acd	acde	acde	acde	acd	acde	acd	ace	acd	ae	ad	-	de	ad			
wVyg4 (16)	acd	ace	ad	ace	ac	ace	ad	e	ad	e	ad	de	-	-	d		
aJag8 (17)	ade	-	abde	-	de	-	abde	-	bde	c	bde	ce	bce	bcde	abce	bce	

SOFC, Second Order Fitted Curve; ORC, Original Recorded Curve; a, SOFC:ORC ratio of f_{A5}; b, SOFC:ORC ratio of f_r; c, SOFC:ORC ratio of A_r; d, SOFC - ORC phase-shift difference of P_{A5}; e, SOFC - ORC phase-shift difference of Pf_r; w/aPor Adc Ven Jag, water-filled/air-balloon Portex Adcock Ven Erich-Jaeger catheter brands and FG-size; Variables a-e indicated are $P < 0.05$ between any two catheters; -, no significant difference.

4.6 Discussion

The assumption that fluid-filled catheter-manometer systems adequately approximate second order systems is motivated by the advantages thereof, such as the derivation of relatively simple mathematical equations which allow prediction of catheter frequency responses from square-wave response measurement techniques: additionally, the electrical correction of incorrect information from an imperfect catheter-manometer system may be accomplished using second order system models. The square-wave response technique is used by clinicians to assess in vivo the frequency response of underdamped catheter-manometer systems in situ, as well as by researchers who do not have ready access to suitable sine-wave pressure generators. The construction of an appropriate variable-frequency sine-wave generator with a uniform pressure amplitude and waveform response at varying frequencies is difficult (9,13,28), and requires the use of a variable-temperature pressure chamber and a temperature-compensated reference transducer. Although certain researchers have experimentally validated the second order system theoretical models for the resonant behaviour of a few intra-arterial blood pressure measurement systems (21,22), and validated that of a more complex electrical transmission-line model (9), other researchers have shown quantitatively such theoretical models to not be adequate for their intra-arterial catheters (29-31). Additionally, the similarity of frequency responses obtained with square-wave response techniques compared to those obtained from the sine-wave generator technique is shown to be both adequate (32,33) and inadequate (12,31) for intra-arterial catheter-manometer systems. Extrapolating the assumption of a second order system, shown to be valid in certain fluid-filled catheter-manometers, to fluid-filled catheters of different FG-sizes, lengths and material compositions, operated under different conditions and coupled to modern pressure transducers

and domes, may be erroneous.

Our results suggest a significant deviation of the fluid-filled PVC catheter-manometers' SOFCs from the ORCs. Mathematical models, from which commonly used equations based on systems assumed to be second order are derived, state that the catheter-manometer acts as a transmission probe (based on electrical transmission line theory) in the manner of a distributed system (9,15-17). These theories, and the equations based on them, incorporate several important catheter-manometer properties influencing the theoretical frequency responses, being: compliance (catheter-manometer walls and filling-fluid); inertance (axial and radial fluid mass, and radial catheter-manometer wall inertance); viscous resistance (catheter-manometer filling fluid) and hysteresis (catheter-manometer wall hysteresis and filling fluid inelasticity). One obvious difference between fluid-filled feeding catheters used to measure intra-esophageal pressure and catheters used to measure intra-arterial pressure is the soft PVC catheter compound of the former versus the relatively rigid nylon or braided polyurethane of currently used intra-arterial catheters. Whereas wall compliance and hysteresis are validly ignored in the mathematical models applied to certain intra-arterial catheters (by assuming a tube of constant dynamic compliance, with negligible hysteresis losses directly proportional to frequency (9)), PVC nasogastric catheters are palpably compliant, and may exhibit significant dynamic energy losses through hysteresis. Moreover, in certain catheter-manometer systems compliance has been shown to be frequency dependent (21,29). The magnitude of this dependence may be influenced by catheter wall composition; PVC catheter compliance and hysteresis may not only be greater in magnitude, but also be more frequency and amplitude dependent than those of relatively rigid intra-arterial lines assumed to be linear systems (9,17,21). We have not assessed the contribution of such factors here.

Theory predicts that a gas-filled catheter-manometer system may be treated as a linear

system if the catheter radius is large enough and the frequency low enough, despite the large compressibility of the gas (17). In highly compressible fluids, such as a gas, the catheter-manometer system's compliance is principally affected by the gas compressibility in A-BCs, whereas catheter elasticity and transducer-diaphragm compliance is primarily responsible for the elastance of W-FCs. In our experiment, even though deviation from second order systems was less in A-BCs than W-FCs, we did not find an adequate second order system fit prevailing within the range of A-BC FG-sizes and lengths used in clinical practice. The SOFC:ORC ratios of our W-FCs deviated significantly more than the A-BCs even though the W-FCs filling-fluid was of lower compressibility. This may be related to the presence of gas microbubbles in the W-FCs which remained despite our efforts to reduce them. Trapped gas bubbles, which lower the catheter-manometer system elastance, remain an adverse feature of W-FCs in the clinical situation. Their formation is encouraged by the negative intra-esophageal pressures encountered physiologically; we simulated these physiologically negative pressures in vitro in this experiment using the laboratory-built sine-wave generator.

Our findings must be interpreted within the context of clinical relevance. Most physiological pressure waveforms' energy contents lie well within f_r, but not necessarily within f_{A5} of a catheter-manometer system. SOFC:ORC deviations and SOFC-ORC phase-shift differences of f_r, A_r and Pf_r are not as relevant in clinical practice as the deviations of f_{A5}. In our experiment the magnitude of SOFC:ORC amplitude-frequency response deviation is shown to be greater for f_{A5} than for f_r; this is unfavourable because deviations observed for f_r in our experiment are acceptable in clinical practice, whilst those observed at f_{A5} are relevant in clinical practice (an overestimation of the uniformity of a catheter's amplitude-frequency response is unacceptable) as well as statistically significant. Additionally, the observed magnitude of deviation is greater for W-FCs than for A-BCs; this is also unfavourable for clinicians because

the in vivo fast-flush test (square-wave response technique), which is reliant on second order system theory to predict f_{A5} (12), can currently be performed on W-FCs only and not on A-BCs in vivo, and our results suggest that assuming a second order system is less valid for W-FCs than for A-BCs.

The observed SOFC-ORC phase-shift differences are statistically significant, but relatively small in magnitude. Intra-esophageal pressure is measured to estimate dynamic lung compliance, therefore a simultaneous dynamic lung volume measurement is always recorded. The SOFC-ORC phase-shift differences may thus be relevant in clinical practice.

We noted significantly increased magnitudes of SOFC:ORC ratios with increasing catheter FG-size. Catheter elastance, which decreases with larger catheter FG-sizes (wall thickness:outer diameter ratio (13) reduces with increasing FG-size in our catheters), may have influenced this. In validating the theoretical assumptions of their mathematical models, most researchers have used only one sample of each catheter for the experimentally obtained (sine-wave generator) frequency response and compared this against the theoretical predicted response. We noted large variances in SOFC:ORC ratios within both the A-BCs' and the W-FCs' samples (n = 8 each in our experiment); large manufacturing tolerances for any particular catheter FG size may be an influencing factor here. Note however that differing catheter brands did not significantly alter the SOFC:ORC deviations for any particular FG-size catheter, and the commercially available A-BC's SOFC:ORC deviation was not significantly different from the corresponding laboratory made A-BCs.

In conclusion, A-BC and W-FC frequency responses do not adequately fit second order systems. These findings cast doubt on the validity of defining and applying second order system mathematical models to predict such catheter-manometers' frequency responses. SOFC:ORC deviations are significantly larger in W-FCs than in A-BCs, in large FG-sized

catheters, and at f_{A5} than at f_r. The system order of differing fluid-filled catheter-manometers' should be verified experimentally prior to predicting such catheters' frequency responses using the typical equations applied to square-wave response techniques. We recommend that the sine-wave generator, rather than the square-wave response technique, be used to measure in vitro frequency responses of compliant fluid-filled catheters.

4.7 References

1. Coates AL, Stocks J: Esophageal pressure manometry in human infants. *Pediatr Pulmonol* 11: 350-360, 1991.

2. Coates AL, Stocks J, Gerhardt T: Esophageal manometry. In: Stocks J, Sly PD, Tepper RS, Morgan WJ (Eds): Infant Respiratory Function Testing. John Wiley & Sons, Inc., pp 241-258, 1996.

3. Maxted KJ, Shaw A, Macdonald TH: Choosing a catheter system for measuring intra-esophageal pressure. *Med Biol Eng Comput* 15: 398-401, 1977.

4. Kaplan M, Galioto FM, Ruttimann UE, et al: Evaluation of a gastric tube with esophageal balloon for neonatal use. *Am J Perinatology* 1: 355-359, 1984.

5. Chartrand DA, Ye TH, Maarek JM, et al: Measurement of pleural pressure at low and high frequencies in normal rabbits. *J Appl Physiol* 63: 1142-1146, 1987.

6. Chartrand DA, Jodoin C, Couture J: Measurement of pleural pressure with oesophageal catheter-tip micromanometer in anaesthetized humans. *Can J Anaesth* 38: 518-21, 1991.

7. Beardsmore CS, Wong YC, Stocks J, Silverman M: Assessment of the catheter tip pressure transducer for use in infant lung function tests. *Med Biol Eng Comput* 20: 657-660, 1982.

8. Gardner RM: Accuracy and reliability of disposable pressure transducers coupled with modern pressure monitors. *Crit Care Med* 24: 879-882, 1996.

9. Yeomanson CW, Evans DH: The frequency response of external transducer blood pressure measurement systems: a theoretical and experimental study. *Clin Phys Physiol Meas* 4:435-449, 1983.

10. Hartford CG, Rogers GG, Turner MJ: Suitability of polyvinyl chloride feeding catheters in catheter manometer systems. 18th International Conference of the IEEE Engineering in Medicine and Biology Society, Amsterdam, The Netherlands, Abstract 1.1.3-1, pp 37, 1996.

11. Hartford CG, Rogers GG, Turner MJ: Correctly selecting a liquid-filled nasogastric infant feeding catheter to measure intra-esophageal pressure. *Pediatr Pulmonol* In Press, 1997.

12. Hipkins SF, Rutten AJ, Runciman WB: Experimental analysis of catheter-manometer systems in vitro and in vivo. *Anesthesiology* 71: 893-906, 1989.

13. Yanof HM, Rosen AL, McDonald NM, McDonald DA: A critical study of the response of manometers to forced oscillations. *Phys Med Biol* 8(4):407-422, 1963.

14. Frank, O: Kritik der elastischen manometer. *Z Biol* 44:445-613, 1903.

15. Hansen AT, Warburg E: The theory for elastic liquid-containing membrane manometers: General part. *Acta Physiol Scand* 19:306-332, 1950.

16. Hansen AT: The theory for elastic liquid-containing membrane manometers: Special part. *Acta Physiol Scand* 19:333-343, 1950.

17. Fry DL: Physiologic recording of modern instruments with particular reference to pressure recording. *Physiol Rev* 40:753-788, 1960.

18. Thomson WT: Forced vibration with harmonic excursion. In: Vibration Theory and Applications. New Jersey, Prentice Hall Inc., Engelwood Cliffs, pp 51-57, 1965.

19. Kuo FF: The Laplace transform; amplitude, phase and delay. In: Network Analysis and Synthesis. John Wiley & Sons Inc. New York, pp 134-165, 253-279, 1966.

20. Milhorn HT: Transient analysis of physical systems. In: The Application of Control Theory to Physiological Systems. WB Saunders Company, Philadelphia, pp 78-91, 1966.

21. Hansen AT: Experimental examinations of the theory for the elastic liquid-containing membrane manometer. In: Pressure Measurement in the Human Organism. Thesis. Copenhagen, Teknisk Forlag, *Acta Physiol Scand* 19:84-115, 1949.

22. Parnell J, Beckman EL, Peterson LH: Evaluation of pressure transducer systems. Warminster report, National Air Development Centre, NADC/MA5206 available through Defense Technical Information Centre; DTIC AD 001061, FT Belvoir, North Virginia, 1953.

23. LeSouef PN, Lopes JM, England SJ, Bryan MH, Bryan AC: Influence of chest wall distortion on oesophageal pressure. *J Appl Physiol* 55(2) 53-358, 1983.

24. Beardsmore CS, Helms P, Stocks J, et al: Improved esophageal balloon technique for use in infants. *J Appl Physiol* 49:735-742, 1980.

25. Shapiro GG, Krovetz LJ: Damped and undamped frequency responses of underdamped catheter manometer systems. *Am Heart J* 80:226-236, 1970.

26. Luus HG, Muller FO, Meyer BH: Statistical significance versus clinical relevance; methods for calculating confidence intervals. *South African Medical Journal* 76(16):681-685, 1989.

27. Zar JH: Biostatistical Analysis. Engelwood Cliffs, New Jersey, Prentice-Hall, pp 206-252, 1974.

28. Fry DL, Noble FW, Mallos AJ: An evaluation of modern pressure recording systems. *Circulation Research* 5:40-46, 1957.

29. Taylor MG: An experimental determination of the propagation of fluid oscillations in a tube with a visco-elastic wall; together with an analysis of the characteristics required in an electrical analogue.
Phys Med Biol 4:63-82, 1959.

30. Latimer KE, Latimer RD: Measurements of pressure wave transmission in liquid-filled tubes used for intravascular blood pressure recording. *Med Biol Eng* 7:143-148, 1969.

31. Billiet E, Colardyn F: Hazardous information from bedside fast-flush device test for fluid-filled pressure monitoring systems. *Angiology* 43(12):988-995, 1992.

32. Scwhid HA: Frequency response evaluation of radial artery catheter-manometer systems: sinusoidal frequency analysis versus flush method. *J Clin Monit* 4(3):181-185, 1988.

33. Sheahan NF, Tuohy B, Kirkham R et al: The fast flush test; evaluation in radial artery catheter-manometer systems. *Clin Phys Physiol Meas* 12(3):247-252, 1991.

CHAPTER 5

5 STABLE DIFFUSE ACUTE LUNG INJURY MODEL IN VERVET MONKEYS *(Cercopithecus aephiops)*.

5.1 Linking Comments

High-fidelity non-invasive estimation of dynamic intra-pleural pressure using intra-esophageal pressure measurements requires that (i) the pleural pressure wave be transmitted unchanged across the tissues between the intra-pleural and intra-esophageal spaces, and (ii) that the pressure wave be transmitted unchanged across the intra-esophageal catheter manometer systems. Chapters Two, Three and Four concentrated on the latter, characterising the suitability of intra-esophageal catheter manometer systems to transmit dynamic pressure waveforms accurately. However, to validate intra-pleural pressure estimation it is also necessary to characterise the pleuro-esophageal tissue barrier's transmission properties.

In Chapter Six the frequency response of the pleuro-esophageal tissue barrier is investigated. However, in order to record the measurements made in Chapter Six within a context meaningful to practising clinicians it was necessary to develop an animal model of human disease (acute respiratory distress syndrome) simultaneously. The vast majority of intra-esophageal measurements are made in clinical practice in this disease-state. Thus, this chapter pilots such a novel model (n = 5 animals) and describes the characteristics of this model in the subsequent animals employed (n = 12) for the measurements made in Chapter Six.

Chapter Five thus investigates whether intravenous administration of Oleic acid will induce a stable model of diffuse acute lung injury in monkeys (a novel species for modeling lung-injury in non-human primates), and quantifies the pulmonary function and histological properties of this model. [Comprehensive information is provided in Chapter Five's Abstract, Introduction and Discussion sections, which follow]:-

5.2 Abstract

Oleic acid (OA) induced acute lung injury (ALI) models are useful for studying pulmonary mechanics and gas exchange in ALI but an animal model with functional lung mechanics and thoracic phenotypic anatomy similar to humans is preferable. OA (acute lung injury group, ALIG, n=6) or saline (CTRL group, n = 6) was titrated into the central veins of anesthetized, paralysed adult monkeys breathing oxygen on positive pressure ventilation. With OA doses of 92 ± 30.3 mg/kg ALI onset occurred at 161 ± 60 min. Following ALI, arterial oxygen and dynamic and quasistatic lung compliance were significantly reduced; alveolar inflammation and edema, evidenced by lung wet:dry weight ratios and histological scores of ALI severity, were significantly increased. Ventilation requirements were significantly raised in ALIG yet gas exchange and systemic hemodynamics were suitably stable. ALIG histology revealed extensive intra-alveolar fibrin deposition. There were no significant corresponding changes in CTRL. CTRL and ALIG lung compliance values were similar to those reported for comparable healthy and respiratory distress syndrome humans respectively. In conclusion, controlled central venous administration of OA into adult monkeys breathing oxygen on positive pressure ventilation rapidly results in stable diffuse ALI characterised by decreased static and dynamic lung compliance, reduced alveolar oxygen exchange and diffuse alveolar capillary leak with fibrin deposition. The monkey OA-induced ALI model is suitable for the pathophysiological evaluation of pulmonary mechanics and gas exchange following ALI.

Keywords: oleic acid, monkeys, acute lung injury, respiratory distress syndrome, animal models of human disease.

5.3 Introduction

Acute lung injury (ALI) animal models are useful for investigating respiratory system mechanics, barotrauma and gas exchange in respiratory distress syndromes and for evaluating the effect of differing ventilation modes such as positive end expiratory pressure (PEEP) (1) or high frequency oscillatory ventilation (2) on gas exchange and the outcome of respiratory distress syndromes (RDS). Additionally, certain ALI models may be useful for evaluating exogenous surfactant therapy (3), extra-corporeal membrane oxygenation (4), and liquid lung ventilation (5).

Animal models based on premature delivery of fetuses resemble the etiology and consequences of hyaline membrane disease of the newborn, whilst other models usually resemble RDS due to other causes including neonatal pneumonias and acute RDS in adults and children (6). Demand for ALI models not effected by premature delivery of fetuses has led to several modalities being employed; instillation of endobronchial hydrochloric acid (7), surfactant inactivation with detergent (8), paraquat induced injury (9), surfactant antibodies, and the commonly used saline lung lavage and hyperoxia methods (10).

ALI models in non-human primates have been induced in baboons using hyperoxia (11), oleic acid (OA) infusion (12,13) or premature fetus delivery (14), and by premature fetus delivery in monkeys (15). Premature delivery of fetuses requires ante-natal monitoring and hysterotomy. Although OA-induced lung injury does not mimic the etiology of RDS, it is a useful model on which to study the consequences following ALI in humans (6). The phenotypic thoracic anatomy and functional pulmonary mechanics of healthy monkeys is similar to that of humans, but to the authors' knowledge a model of OA-induced ALI in monkeys has not been published.

We aim to investigate whether intravenous administration of OA will induce a stable

model of diffuse acute lung injury in adult monkeys, and to quantify the pulmonary function and histological properties of this model.

5.4 Materials and Methods

Instrumentation

University Animal Ethics Clearance (certificate 96/113/2B) was obtained prior to commencing the study and animals were humanely cared for in the University Central Animal Service. A pilot study was conducted in five animals to determine the optimal administration of OA (dose ranging, formulation, site and rate of delivery to meet ALI criteria defined below). The pilot study also determined the optimal anaesthetic regimen, paralysing agent dose and inotropic support needed to counter negative inotropy of the two anaesthetic agents, and appropriate instrumentation and monitoring for ALI. Thereafter, 12 female Vervet monkeys (*Cercopithecus Aephiops*, 3.9 ± 0.60 kg) were anesthetised (ketamine 20 mg/kg induction and ketamine 10 $mg.hr^{-1}.kg^{-1}$, sufentanyl > 30 $ug.hr^{-1}.kg^{-1}$ and adrenaline inotropic support 5 $ug.hr^{-1}.kg^{-1}$ maintenance continuous infusions), paralysed (vecuronium 10 $ug.hr^{-1}.kg^{-1}$), intubated orally (cuffed 4.5mm, Mallinkrodt, Athlone, Ireland) and mechanically ventilated supine with warm humidified 100% O_2 (FiO_2 = 1.0) using a pressure-cycle pressure-limit ventilator (Preemicare Model 105, Texas, USA).

Airway opening pressure (Paw) was measured with a piezoresistive differential pressure transducer (Honeywell Microswitch 170PC, USA). A size 7 French Gauge transducer-tip catheter (Millar Mikro-tip SPC 470, Millar Instruments, Inc., Texas, USA) was placed in the oesophagus for dynamic intra-esophageal pressure measurement (Pes)(16). The Pes catheter site was chosen according to the "paralysed airway occlusion test" in which the airway is briefly occluded and abdominal pressure applied to assess how faithfully Pes changes follow Paw changes in an isovolumic chest (17). Airway gas flow was measured with a heated Hans Rudolph 8300 screen pneumotachograph connected to a Validyne MP45 differential pressure

transducer, calibrated for in vivo inspiratory and expiratory circuit geometry against a Godart Statham 17330 wet-seal spirometer (18); *Supplemental Figure S5.A.*

Supplemental Figure S5.A.

Inspiratory and expiratory flowmeter calibration curves at in vivo Body Temperature, Pressure and Saturation (BTPS) and average expected gas compositions, for the Hans Rudolph 8300 screen pneumotachograph connected to a Validyne MP45 differential pressure transducer. The flowmeter is calibrated against a Goddart Staham 17330 wet-seal spirometer. The spirometer was calibrated against a 4 litre syringe (Cavitron PC3006). Temperature in the spirometer 100% humid gas was measured with a thermistor (Siemens M85). Constant gas flow through the flowmeter was generated using negative pressure suction across a needle valve. The inspiratory an expiratory circuit geometry used was identical to that used in vivo.

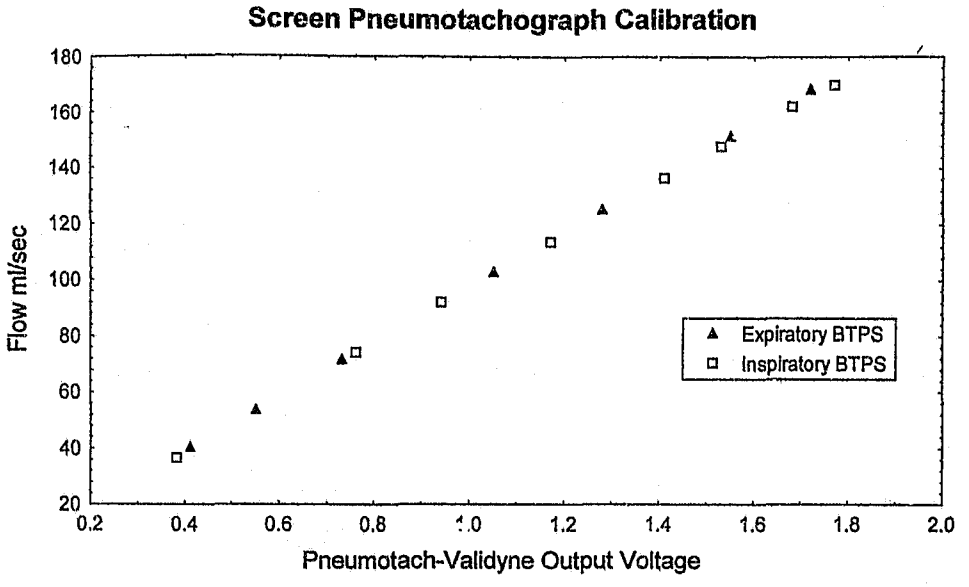
Screen Pneumotachograph Calibration
Flow ml/sec
180
160
140
120
100
80
60
40
20
0.2
0.4
0.6
0.8
1.0
1.2
1.4
1.6
1.8
2.0
Pneumotach-Validyne Output Voltage
Expiratory BTPS
Inspiratory BTPS

The right femoral artery and vein were cannulated for arterial blood pressure measurements (Statham-Gould P10, Oxnard, CA) and the injection of OA. Core body temperature was kept between 36 and 38 °C and intravenous Ringers fluid replacement administered according to suprapubic catheter urine output and central venous pressure recordings.

All pressure and flow transducer signals were pre-amplified (Hellige Servomed, Freiburg, Germany) and digitised. (Biopac MP100 and AcqKnowledge ver 3.3.2, Biopac Systems Inc., CA, USA).

Oleic acid injection

Ambient light and air protected OA (free cis-9-Octadecanoic acid, 99% pure, Sigma Chemical Company, St Louis, MO) mixed in 1 ml 0.9% saline was flushed with 5 ml 0.9% saline via the venous cannula into the central veins at the level of the right atrium. OA was administered in 2 x 25 mg/kg boluses, each 15 minutes apart, repeated hourly until ALI was produced (defined physiologically as PaO_2 < 50% of baseline value, accompanied by reduced lung compliance and increased alveolar ventilation requirement) (19,20).
(Methods Supplemental Figures S5.B, S5.C, S5.D, S5.E).

Supplemental Figure S5.B

Respiratory instrumentation and monitoring during acute lung injury.

X. Endotracheal tube

XI. In-line inspiratory oxygen temperature and humidity control

XII. Pressure cycle pressure limit ventilator (PEEP, pkPaw, RR)

XIII. Proximal airway pressure (differential pressure transducer, Paw)

XIV. Flowmeter (screen pneumotachograph connected to Validyne pressure transducer, Faw)

XV. Animal End Tidal CO_2 monitor (sidestream, rapid response, $ETCO_2$)

XVI. Plethysmographic tongue monitor (SaO_2)

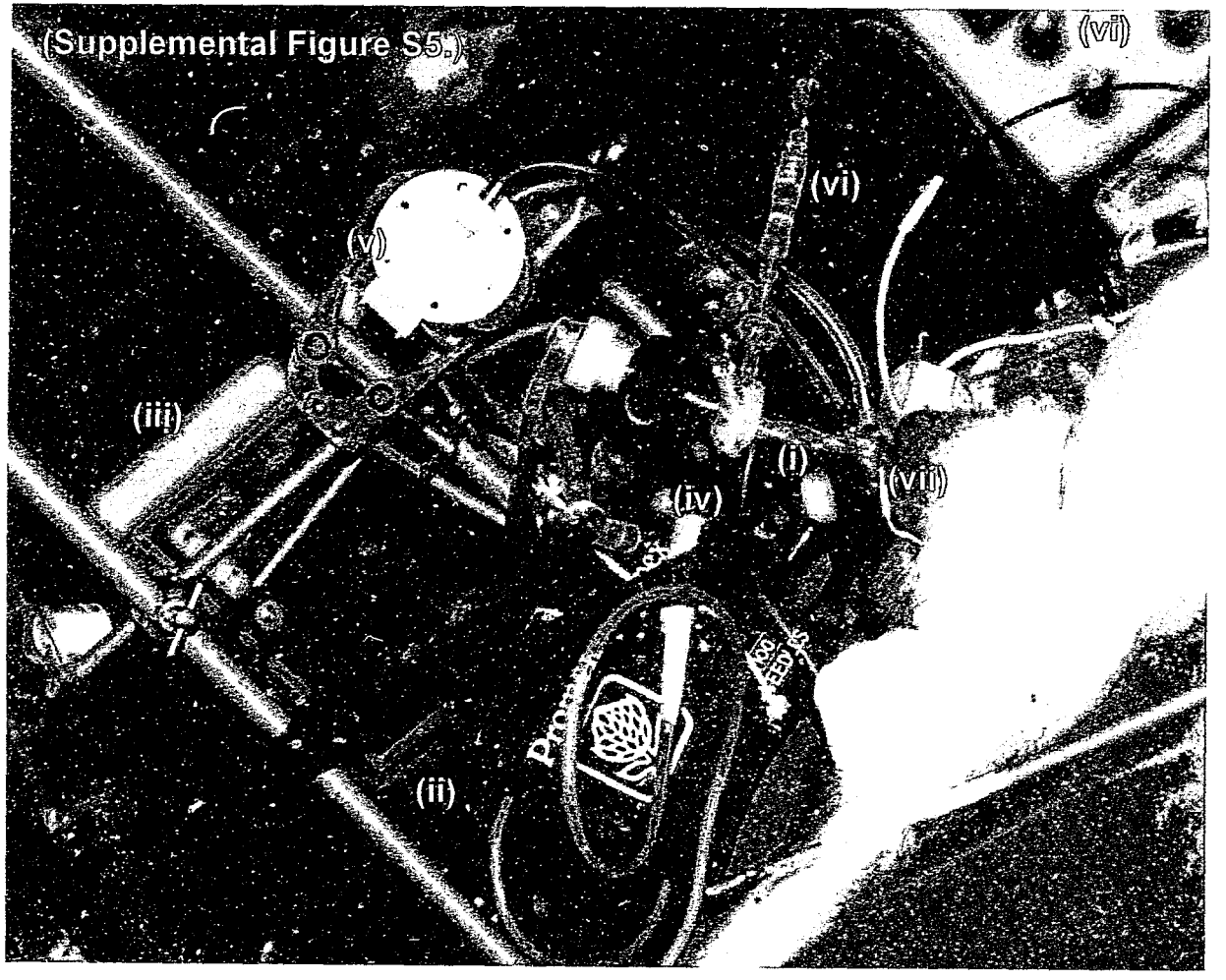
(Supplemental Figure S5.)
(vi)
(vi)
(v)
(iii)
(i)
(vii)
(iv)
(ii)

Supplemental Figure S5.C

Cardiorespiratory monitoring during acute lung injury.

I. *Intra-arterial cannula (systolic, diastolic, mean arterial pressures, PaO_2, $PaCO_2$, pH_a)*

II. *Central venous cannula (central venous pressure, maintenance fluid, anaesthetic agents infusion, oleic acid administration)*

III. *Suprapubic catheter (urine flow)*

IV. *3-lead (SL I - III) electrocardiogram (Heart rate and rhythm)*

V. *Anal thermistor (core body temperature)*

VI. *Diathermy pad as required*

VII. *Heated under-blanket*

VIII. *Transthoracic pleural pressure probe introducer (Chapter 6)*

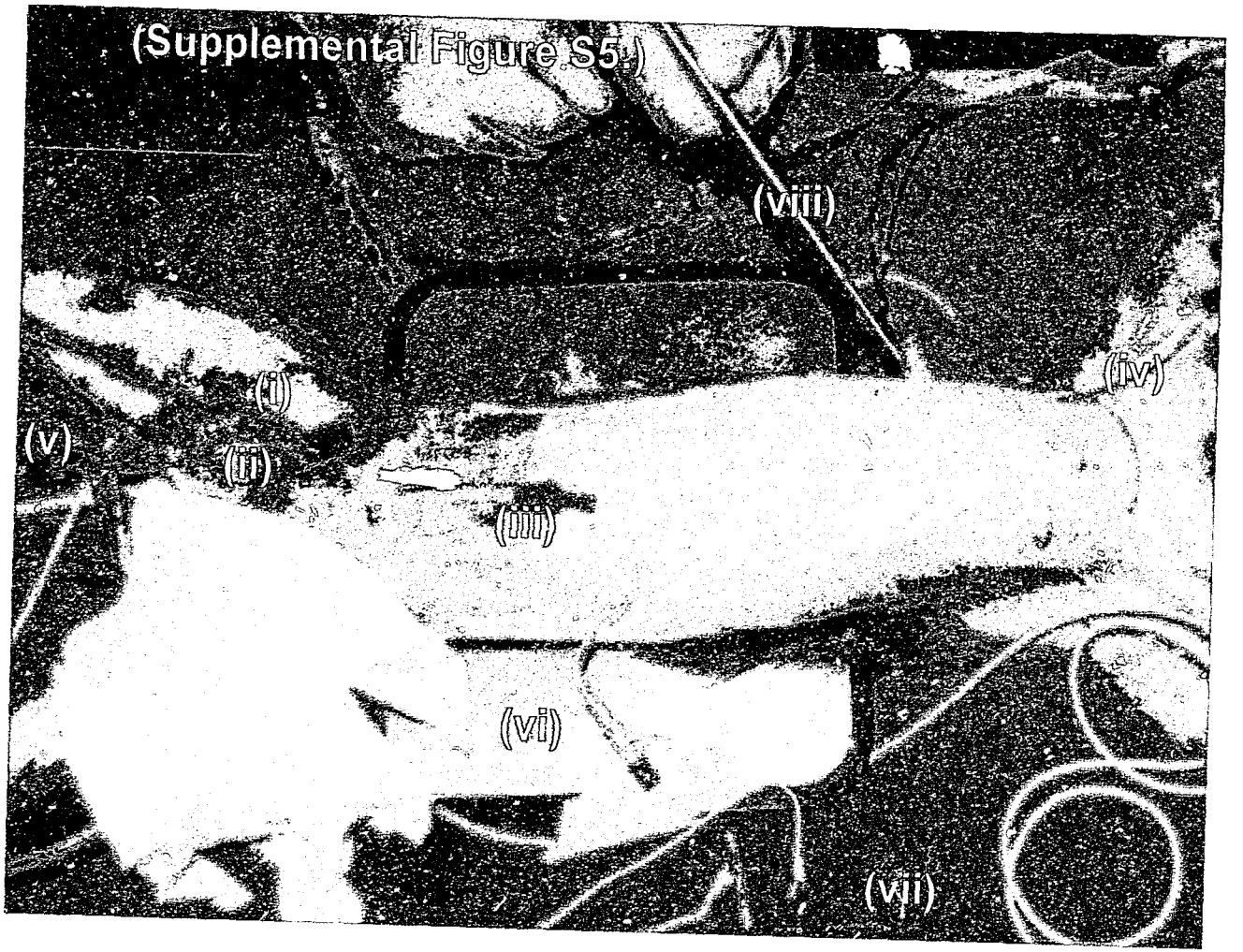
(Supplemental Figure S5.)
(viii)
(iv)
(i)
(v)
(ii)
(iii)
(vi)
(vii)

TOP. Supplemental Figure S5.D.

Dynamic data acquisition during acute lung injury.

I. ECG and pressure pre-amplifiers

II. Analog to digital acquisition card

III. Digital storage and display on computer

BOTTOM. Supplemental Figure S5.E

Acute lung injury; post-mortem macroscopic haemorrhagic edema and lung consolidation, noted in monkey Respiratory Distress Syndrome.

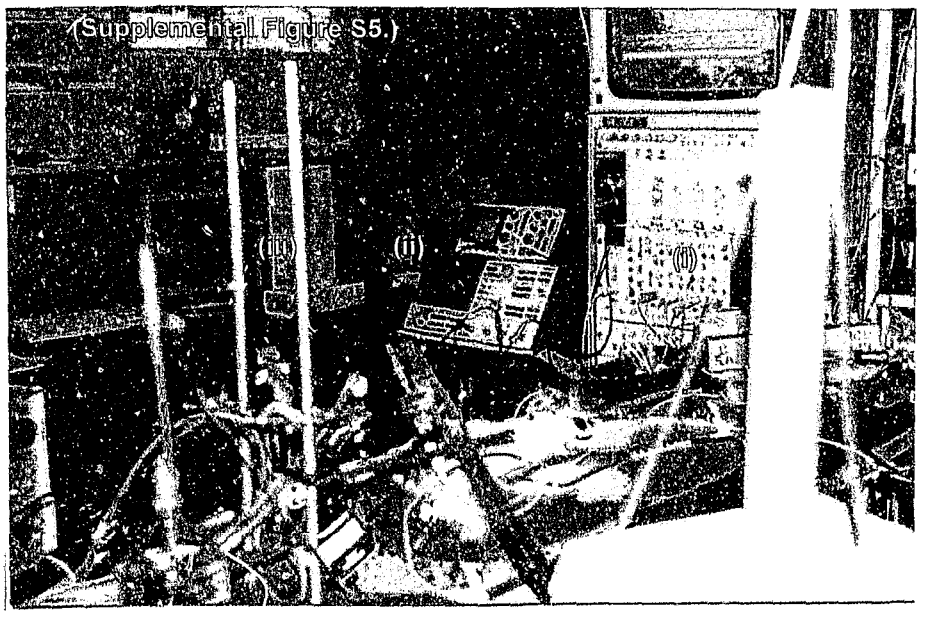
(Supplemental Figure S5.)
(i)
(ii)
(iii)

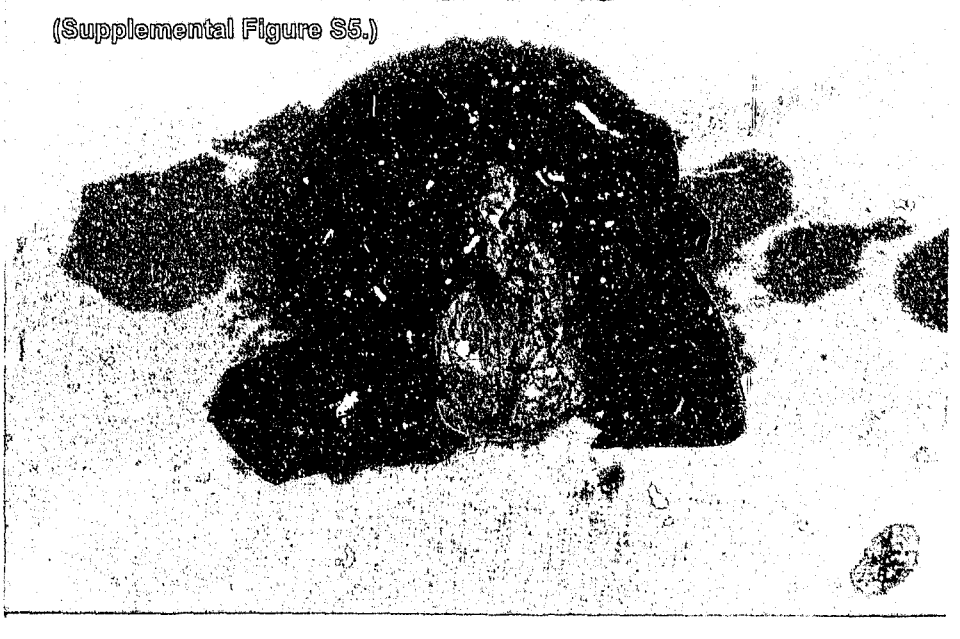
(Supplemental Figure S5.)

Ventilation variables

Measurements were made before (baseline), and approximately 2.5 and 5.5 hours after initial OA injection (acute lung injury group, ALIG, n = 6) or equivalent saline injection (control group, CTRL, n = 6). Respiratory rate (RR) and maximum Paw (Paw pk) were adjusted to achieve an arterial carbon dioxide ($PaCO_2$) of 30-40 mm Hg (calibrated Stat Profile 3, Nova biomedical, MA, USA) throughout the experiment. Once ALI criteria were met PEEP was increased in ALIG as required to optimise PaO_2 levels (but always meeting < 50% of baseline PaO_2 levels criterion). No additional systemic alkali were administered.

Dynamic total respiratory system (C_{RS}dyn) and lung ($C_L$dyn) compliance were calculated from the ratio of the average of three tidal volumes at BTPS (barometric pressure was 626 ± 1.6 mm Hg) to the average of three differences between end-inspiratory and end-expiratory Paw or transpulmonary (Paw-Pes) pressures (21,22). The percentage transmission of peak Paw pressure to Pes was determined from the end-inspiratory to end-expiratory ΔPes:ΔPaw ratio. Additionally, quasistatic deflation (at 1.6 $ml.sec^{-1}$) lung compliance ($C_L$stat) from Paw = 7 cmH_2O above functional residual capacity (FRC) down to FRC was determined (23) immediately post-mortem in the intact thorax (quasistatic deflation curves recorded in vivo were not analyzed because of the apparent variation of respiratory quotients within the animals).

Post-mortem measurements

Animals were euthanased under anesthesia with excess intravenous barbiturate and Paw held at 10 cmH_2O while the sternum was split. The lungs were removed and severed at the main stem bronchi near to each lung. Marginal sections from the anterior and posterior surfaces of the upper, middle or lingular, and lower lobes of each lung (12 sections per subject from similar locations (24)) were placed in 10% formaldehyde for haematoxylin and eosin

staining. The remaining upper, middle and lower lobes were weighed wet and dry for determination of total lung water content (24,25). Each of the twelve randomised lung sections was viewed by a pathologist (sample-blind) under a light microscope at the same magnifications (4X and 40X) between CTRL and ALIG. ALI scores were assigned according to accepted ALI scales (1,4,24) for severity of injury [0 - 3], extent of normal appearing tissue [0 - 100%, in 5% increments] and prevalence of residual intravascular red blood cells for congestion [0 - 4]. Severity was graded [0] for normal appearing lung, [1] for mild congestion, interstitial edema, with red blood cells (rbc) and/or neutrophils only occasionally in the alveolar spaces, [2] for moderate congestion and interstitial edema, with rbc's and/or neutrophils partially filling the alveolar spaces but without consolidation, and [3] for marked congestion and interstitial edema, with rbc's and/or neutrophil infiltrate nearly or completely filling the alveolar spaces (consolidation). Additionally, the presence or absence of monocyte and alveolar macrophage phagocyte invasion, invasion of alveolar septae or spaces by neutrophils, deposition of extravascular fibrin in septae or alveolar spaces, proteinaceous hyaline membranes presence and intravascular thrombus formation was recorded for each section. The mean score across each animal's 12 sections was compared between ALIG and CTRL (24).

Statistics

Significant within-group changes over time were detected using Friedman ANOVA (repeated measures) followed by identification with the Wilcoxon signed-rank test (26). The Mann-Whitney rank-sum test was used to determine significant differences between groups' data at the same time period and changes from baseline (Statistica™ software, Statsoft, OK). All displayed values are mean ± SD, and differences with P-values < 0.05 are regarded as statistically significant.

5.5 Results

The total mean dose of oleic acid necessary to produce ALI using the method defined above was 92 ± 30.3 mg/kg across ALIG. The mean delay to onset of ALI and to euthanasia (ALI remained manageable at termination of study) after initial OA injection was 161 ± 60 min and 476 ± 45 min respectively.

Ventilation, blood gases and hemodynamics

To maintain $PaCO_2$ between 30-40 mm Hg, ventilation requirements increased in ALIG following OA injection. Compared to baseline; RR, Paw pk, mean Paw and PEEP requirements within ALIG were significantly increased at 5.5 hours post OA, where there was no significant corresponding change within CTRL (Table 5.1). Arterial pH and calculated HCO_3^- decreased significantly within ALIG at 2.5 and 5.5 hours after OA injection, at which times there were no significant changes within CTRL. There was no significant change in the measured systemic hemodynamic variables within ALIG or CTRL before and after OA or saline injection (Table 5.1), however we observed that pulse rate increased and blood pressure decreased transiently for approximately fifteen minutes following OA injection and then returned to baseline.

Table 5.1. *Ventilation requirements, blood gases and hemodynamics in ALI*

	Baseline		2.5 hr post OA or S		5.5 hr post OA or S	
	CTRL	ALIG	CTRL	ALIG	CTRL	ALIG
RR	17 ± 6.6	18 ± 5.4	17 ± 7.3	20 ± 5.6	18 ± 6.8	32 ± 10.5*+
Paw pk	10 ± 1.9	12 ± 0.9	10 ± 1.1	13 ± 2.4	11 ± 1.5	18 ± 2.9 *+
PEEP	2 ± 0.4	3 ± 0.9	3 ± 0.4	4 ± 1.2	2 ± 0.6	6 ± 1.3 *+
Paw M	5.4 ± 1.07	6.2 ± 0.79	-	-	5.3 ±1.37	9.8 ± 1.44*+
$PaCO_2$	37 ± 5.4	38 ± 3.8	32 ± 3.9	40 ± 2.6	38 ± 5.0	39 ± 4.0
pH_a	7.40 ±	7.41 ±	7.44 ±	7. 28 ±	7.38 ±	7.25 ±
	0.042	0.045	0.044	0.086 *+	0.032	0.083 *+
HCO_3^-	23 ± 2.9	24 ± 2.6	22 ± 2.3	19 ± 3.1 *	22 ± 2.4	18 ± 3.9 *
HR	97 ± 18.7	100 ± 30.5	-	-	90 ± 10.1	136 ± 20.1+
SYS	120 ± 15.5	137 ± 28.1	-	-	126 ± 12.4	121 ± 15.7
DIA	56 ± 12.6	64 ± 11.0	-	-	59 ± 13.6	55 ± 12.0
MAP	82 ± 13.5	94 ± 17.8	-	-	86 ± 14.0	76 ± 9.9

RR, respiratory rate ((breaths/min); Paw pk,M, peak and mean proximal airway pressure (cmH_2O); PEEP, positive end expiratory pressure (cmH_2O); pH_a,HCO_3^-, arterial pH and calculated bicarbonate (mmol/L); HR, pulse rate (beats/min); SYS,DIA,MAP, systolic diastolic and mean arterial pressure (mmHg); PaCO2, arterial carbon dioxide partial pressure (mmHg); OA,S oleic acid or saline control. * $P < 0.05$ after vs before oleic acid within same group.+ $P < 0.05$ between ALIG and CTRL changes (Δ) from baseline.

Within ALIG, despite increasing applied alveolar ventilation (to maintain a normal $PaCO_2$), PaO_2 decreased significantly at 2.5 and 5.5 hours versus baseline. This decreased PaO_2 within ALIG was similar at 2.5 and 5.5 hrs post OA (Figure 5.1). Compared to baseline, CTRL PaO_2 did not change significantly at 2.5 or 5.5 hours post saline.

Figure 5.1.

Arterial oxygen partial pressure before, 2.5 and 5.5 hours after oleic acid injection (ALIG) versus control (CTRL). PaO_2, arterial partial pressure of oxygen; Baseline, before treatment with OA (ALIG group) or saline (CTRL). $FiO_2 = 1.0$. $^{*}P < 0.05$ compared to baseline within ALIG group. $^{+}P < 0.05$ between ALIG and CTRL changes (Δ) from baseline.

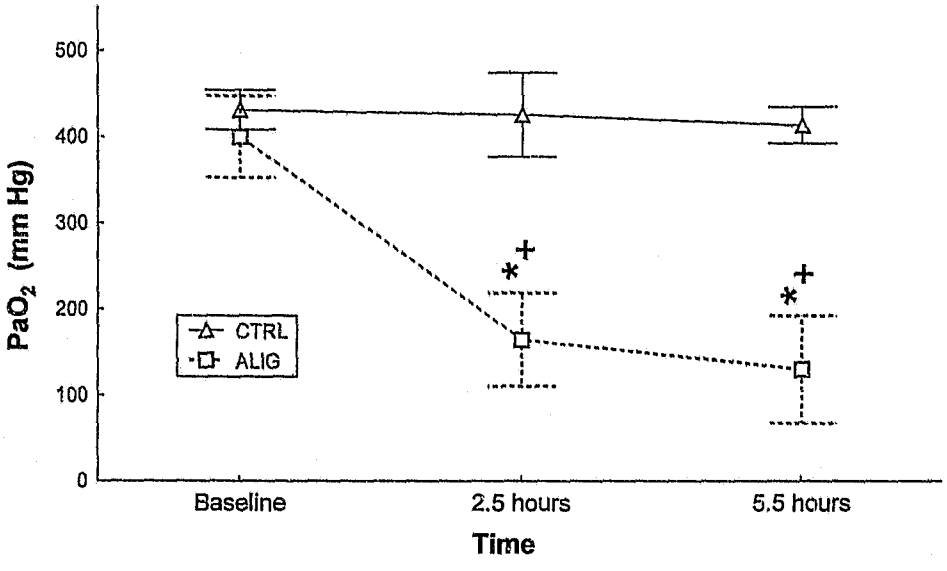
500
400
300
200
100
0
PaO2 (mm Hg)
CTRL
ALIG
*
+
*
+
Baseline
2.5 hours
5.5 hours
Time

Lung Compliance

Following OA injection, C_{RS}dyn, $C_L$dyn, $C_L$stat and ΔPes:ΔPaw ratio were all significantly reduced in ALIG versus CTRL (Table 5.2). Baseline $C_L$dyn was significantly greater than C_{RS}dyn in all animals.

Table 5.2. *Respiratory system compliance before and after oleic acid*

	Baseline		5.5 hr post OA or S	
	CTRL	ALIG	CTRL	ALIG
C_{RS}dyn ml/cm H_20/kg	1.2 ± 0.36	1.2 ± 0.25	1.4 ± 0.32	$0.8 \pm 0.19^{++*}$
$C_L$dyn ml/cm H_20/kg	3.4 ± 1.9	2.9 ± 0.66	3.1 ± 0.68	$1.1 \pm 0.35^{++*}$
ΔPes/ΔPaw %	58 ± 15	77 ± 39	53 ± 11	$35 \pm 6^{+*}$
$C_L$stat ml/cm H_20/kg			2.1 ± 0.5	$1.1 \pm 0.27^{++}$

C_{RS}, total respiratory system compliance; C_L, lung compliance; ΔPes/ΔPaw, % transmission of airway pressure to the intra-esophageal space; $C_L$stat, deflation quasistatic post-mortem lung compliance; OA,S, oleic acid or saline control. *,** $P < 0.05, 0.01$ before vs after oleic acid within same group. +,++ $P < 0.05, 0.01$ between ALIG and CTRL changes (Δ) from baseline or at same time period ($C_L$stat).

The reduction in C_{RS}dyn following OA injection in an ALIG subject is shown by illustration in Figure 5.2; after OA injection the PEEP requirement in this subject is increased and the volume-pressure curve exhibits flattening of the early inspiratory portion of the curve, typical of respiratory distress syndrome subjects.

Figure 5.2.

In vivo trans-respiratory dynamic volume-pressure curve in an ALIG subject before and 5.5 hours after oleic acid injection. C_{RS}dyn is reduced following oleic acid and the volume-pressure trace exhibits flattening of the early inspiratory portion (between the arrows) typical of respiratory distress syndromes. Compliance values are presented in Table 5.2.

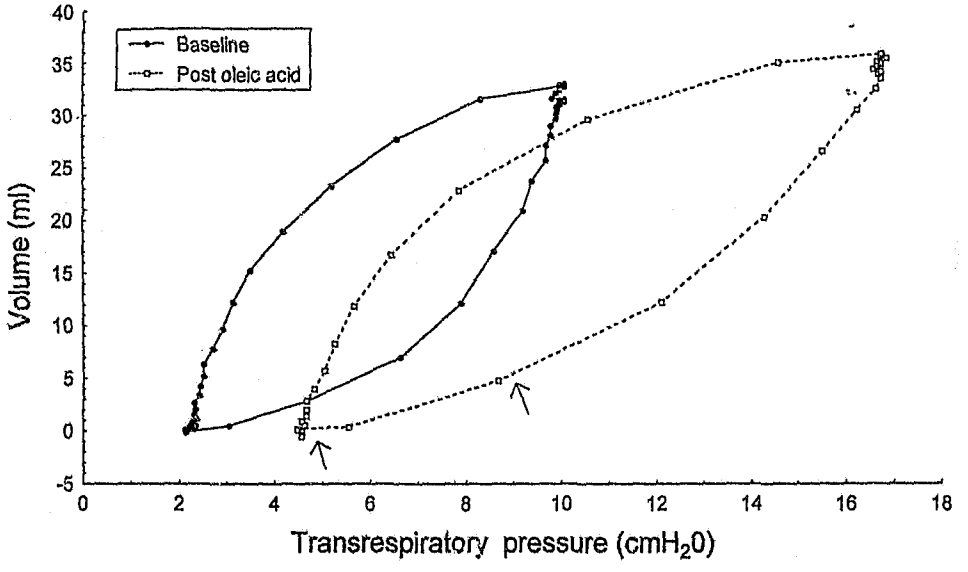
Baseline
Post oleic acid
Volume (ml)
40
35
30
25
20
15
10
5
0
-5
0
2
4
6
8
10
12
14
16
18
Transrespiratory pressure (cmH2O)

Lung water content

Combined lung lobe wet:dry weight ratios were significantly different between ALIG and CTRL (Table 5.3).

Table 5.3. *Lung water content; wet:dry weight ratios*

	CTRL wet:dry	ALIG wet:dry
All lobes combined	5.6 ± 0.22	7.2 ± 1.25 $^{+}$
Right upper lobe	5.5 ± 0.34	7.7 ± 1.41 $^{++}$
Right middle lobes	5.4 ± 0.61	7.2 ± 1.57 $^{+}$
Right lower lobe	5.9 ± 0.44	8.4 ± 2.03 $^{+}$
Left upper lobe	5.5 ± 0.44	6.6 ± 1.43
Left lingular lobe	5.4 ± 0.7	7.5 ± 1.57
Left lower lobe	5.9 ± 0.27	8.1 ± 2.10

$^{+,++}$ $P < 0.05, 0.01$ between CTRL and ALIG

However, further analysis of the right and left lobar wet:dry weight ratios revealed that the wet:dry lung weight ratios were significantly greater in ALIG versus CTRL for the right upper, middle and lower lobes, although the trend towards an increased ratio in ALIG did not reach significance for the left side of the lungs' lobes (Table 5.3). There was no significant difference in the wet:dry weight ratios between any of the lungs' lobes on the same side within ALIG or CTRL.

Lung Histology

Table 5.4 summarizes the mean lung histology scores between ALIG and CTRL. Severity of lung injury, presence of alveolar macrophage and monocytic invasion, invasion of alveolar septae and spaces by neutrophils, and extravascular intra-alveolar septal fibrin

deposition were all significantly greater in ALIG versus CTRL lungs. Normal appearing lung tissue was significantly greater in CTRL versus ALIG, and the fields examined demonstrated that the ALI was diffuse but not homogeneous. The mean presence of hyaline membranes was 7% across ALIG sections versus 0% across CTRL sections. Neither group demonstrated intravascular thrombus formation, and the prevalence of residual intravascular red blood cells in the lungs was similar between the two groups. There was no significant difference in the histology scores between the left and right lungs within CTRL or ALIG groups. Representative ALIG and CTRL lung histology is illustrated in Figures 5.3(a) and 5.3(b).

Table 5.4. *Lung histology scores*

	CTRL	ALIG
Severity (0 - 3)	0.8 ± 0.16	1.3 ± 0.24 $^{+}$
Alveolar monocytic invasion %	5 ± 5.4	73 ± 5.2 $^{++}$
Neutrophil invasion septae %	7± 8.1	80 ± 0.0 $^{++}$
Neutrophil invasion spaces %	7 ± 8.0	87 ± 10.3 $^{++}$
Extravascular fibrin septae %	3 ± 5.1	50 ± 19.0 $^{++}$
Extravascular fibrin spaces %	2 ± 4.0	8 ± 7.5
Hyaline deposition %	0	7 ± 8.1
Normal appearance tissue %	57 ± 6.3	43 ± 10.1 $^{+}$
Intravascular thrombus formation %	0	0
Residual intravascular red blood cells (0 - 4)	1.6 ± 0.15	1.5 ± 0.16

$^{+,++}$ $P < 0.05, 0.01$ between CTRL and ALIG

Figures 5.3(a) and 5.3(b)

Photomicrographs of haematoxylin and eosin stained sections of ALIG (3a.) and CTRL (3b.) lungs. ALIG lungs exhibit thickened hypercellular alveolar septae (i), and alveolar lumina are extensively infiltrated with macrophages, neutrophils (ii) and edema (iii). CTRL lungs (3b.) exhibit patent and largely acellular alveolar lumina. Mag = X40.

3a.

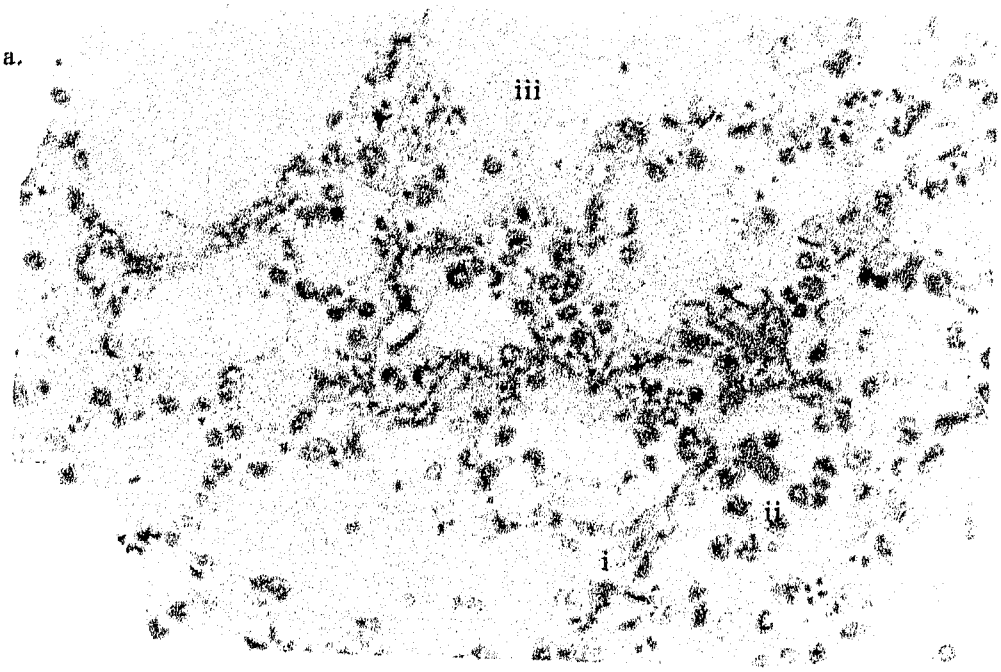

3b.

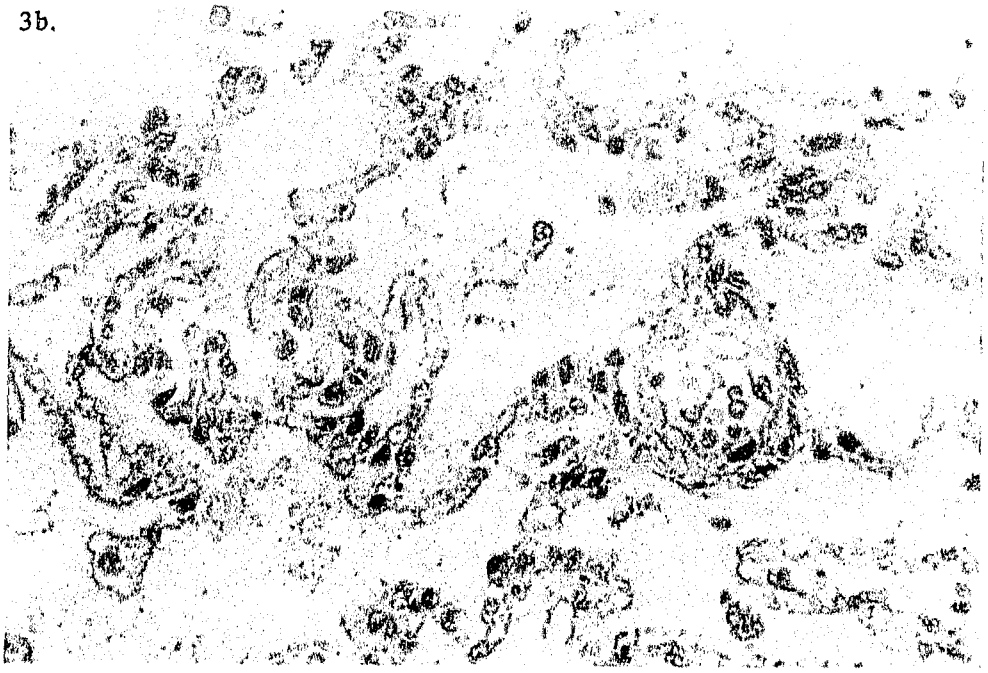

5.6 Discussion

We have shown that aliquots of OA injected into the thoracic great veins of monkeys breathing oxygen on positive pressure ventilation reliably results in stable ALI in a conveniently short period, characterised by decreased lung compliance, markedly reduced gas exchange and pulmonary edema accompanied by alveolar inflammation.

Monkey model applications

Although interpretations regarding human or animal diseases on the basis of observations obtained in animals should always be performed with caution, non-human primates are uniquely suited as animal models for complex human diseases because of their close evolutionary relationship to humans (27,28). Many experimentally relevant physiologic and genetic characteristics are shared between humans and non-human primates (27), and the respiratory system of monkeys is functionally more like that of humans than those of commonly used non-primate laboratory animals (29,30). Monkey thoracic anatomy is phenotypically similar to that of humans, and the pulmonary compliance values recorded by us before and after ALI fell within the range of those recorded for comparable normal as well as RDS humans (see below). Additionally, the stability of hemodynamic variables and blood oxygenation make the OA-induced ALI adult monkey a suitable research model for the evaluation of pulmonary mechanics and gas exchange following ALI.

Full-term and near-term monkeys' lung biochemistry and development patterns closely resemble those of humans (31,32), although surfactant composition may differ in healthy adult rhesus monkeys from that of healthy humans (33). Despite potential

differences between non-human primate and human lung biochemistry, OA-induced ALI has been demonstrated in baboons (12,34) and used as a diffuse alveolar disease model to assess oxygen therapy (13), and non-ALI monkeys have been used to investigate human infant responses to acute hypoxemia (35).

To the authors' knowledge a saline lung lavage model of ALI has not been reported in baboons or monkeys, and we were unsuccessful at producing a low compliance ALI model using repeated saline lavage in one pilot monkey subject. The saline lavage model reported in other animal classes may advantageously alter lung surfactant, but does so variably across the different animal classes, and unlike the OA model does not typically produce the primary alveolar permeability problem of many other respiratory distress syndromes (10) or pneumonias.

There are substantial staffing and cost implications for the delivery of premature fetuses where indicated for experimental ALI studies (36): specialised animal housing units and breeding programs are required with accurate knowledge of species gestation times, dates of conception (perineal skin change observations)(37), ultrasound determination of gestational age, culminating in surgical hysterotomy. There may also be a delay to the onset of experimental data collection (usually > 4 months gestation in non-human primates). ALI induced by hyperoxia requires specialised gas delivery systems and takes a few days to develop.

Oleic acid administration

Our pilot experiment established that 2 x 25 mg/kg aliquot boluses, each 15 minutes apart and repeated hourly as required (to reach PaO_2 < 50% of baseline), produced stable ALI with no OA-related mortality in the subsequent 12 pivotal animals.

The type of OA, method of mixing, dose, site of administration and rate of delivery (bolus versus infusion) (34,38) affect the outcome of OA injection (6). Accordingly, protocols for OA delivery to induce ALI vary widely between animal classes and between researchers for the same species (6), and smaller and larger doses of OA have been required.

Our mean total effective dose required was less than the 0.18 ml/kg dose used with 20% mortality in canines (39) or the 0.15 ml/kg used in canines (40). Baboons required 0.04 - 0.06 ml/kg (13) and 0.04 ml/kg (34) of OA, which is approximately half the mean accumulated dose we required. However, our mean required dose was similar to the 0.08 ml/kg used to induce ALI in pigs without mortality (41), and fell within the total dose of 0.015-0.120 ml/kg in sheep (38) and that of the 0.06-0.09 ml/kg (24) and 0.08 ml/kg (25) used for dogs.

For a similar dose administered in four aliquots, the onset to ALI in dogs was 90 min (24) versus our mean of 166 min in monkeys. We advocate the administration of OA in small aliquot boluses rather than by continuous OA infusion: Attempts to mix pure OA in infusion solutions produced variable results in our pilot experiments, even with ultrasonic mixing, and doing so may alter OA activity. Additionally, pure OA must be light and air protected prior to administration, and small aliquot injections facilitates this, yet allows the titration benefit of infusions. Slow rates of infusion may produce only minimal lung injury (34); the use of aliquot injections produced a diffuse severe ALI in our monkeys, and this technique is also successful in other animal classes (38).

Acute lung injury mechanism

OA-induced ALI is thought to be due to toxic effects on the lung capillaries, the

exact mechanism(s) of which are still unknown (6). The presence of 1.0 FiO_2 is unlikely to have exacerbated the ALI since OA injury is unaffected by O_2 in the short term in several animal models including baboons (6). However, positive pressure ventilation is likely to cause barotrauma and exacerbate OA-induced ALI (24), so we included a positive pressure ventilated CTRL group with $FiO_2 = 1.0$.

Hyaline deposition is a time dependent process (13) and rarely forms in animal models (34). Extravascular fibrin was prominent in the monkeys and is formed as part of the acute inflammatory response within damaged alveolar walls or deposited free in the alveolar spaces. Fibrin is often a component of hyaline membranes (6,12), is a marked early feature of ALI in baboons (42), and may physiologically serve to limit alveolar hemorrhage or edema.

We did not determine whether the reduced C_{RS}dyn and $C_L$dyn following OA was due to surfactant alteration. Hallmarks of RDS are alveolar leak and surfactant deficiency, but surfactant alterations may be due to changes in volume, rate of secretion, composition, the presence of inhibitors, or a combination of these (6,31). OA-induced ALI surfactant inactivation, when present, may be due to the presence of proteinaceous alveolar edema alone (6). OA is shown to inhibit bovine natural lung surfactant activity (43) and OA-induced ALI in rabbits exhibits severe alteration of surfactant function despite normal phospholipid composition and content (21). On the other hand, reduced $C_L$stat of OA-induced ALI rabbits was due to alveolar flooding rather than increased surface tension (44).

The ALIG total lung water increase is likely due to alveolar capillary leak rather than cardiac failure since pulmonary intravascular residual red blood cells were histologically similar between CTRL and ALIG, and the pulmonary edema was hemorrhagic in nature.

Alveolar capillary leak in OA injury is influenced by (i) Alveolar edema postural and gravitational dependence (24) (our animals were supine) (ii) uneven OA distribution or ventilator barotrauma causing selective lung injury, (iii) PEEP (higher in ALIG than CTRL) reducing alveolar edema (25), (iv) regional perfusion being physiologically reduced to areas affected more extensively by OA (6).

The transient increase in pulse rate observed by us during acute OA administration also occurs in pigs but was not accompanied by reduced blood pressure in pigs (41). In baboons a transient (1 - 2 min) reduction in blood pressure was accompanied by a reduced heart rate (34).

Lung compliance

The baseline CTRL and ALIG $C_L$dyn values are similar to those of human infants (45) and C_{RS}dyn or $C_L$dyn values resulting from OA fall within the ranges described for newborn infants with RDS (46) and for low birth weight infants with severe RDS (47). In our adult monkeys $C_L$dyn was larger than C_{RS}dyn suggesting that the chest wall contributes to C_{RS}dyn, similar to that of older human children (25), but unlike human newborns where the chest wall contributes only 20% of C_{RS}dyn. Smaller (0.54 kg) healthy three week old monkeys were noted to have a lower $C_L$dyn (1.02 ± 0.45 ml/cmH_2O) than our adult monkeys (35).

PEEP and RR affect dynamic compliance measurements, but $C_L$dyn frequency dependence is not reproducibly shown at under 60 breaths/min in infants (22), and the reduced C_{RS}dyn and $C_L$dyn findings in our ALI monkeys are confirmed by the significantly reduced ALI $C_L$stat measurement which is independent of PEEP and RR.

In conclusion, controlled central venous administration of OA into monkeys

breathing pure oxygen on positive pressure ventilation rapidly results in stable ALI characterised by decreased static and dynamic lung compliance, markedly reduced alveolar gas exchange and increased diffuse alveolar capillary leak accompanied by alveolar edema, polymorphonuclear infiltration and fibrin deposition. These changes are similar to those found in other animal models of OA-induced ALI, but advantageously the CTRL and ALIG monkey $C_L$dyn values are similar to comparable healthy and RDS humans respectively. The monkey OA-induced ALI model is suitable for the pathophysiological evaluation of pulmonary mechanics and gas exchange following ALI.

5.7 References

1. **Sohma, A.E., W.J. Brampton, M.S. Dunnill, et al.** 1992. Effect of ventilation with positive end-expiratory pressure on the development of lung damage in experimental acid aspiration pneumonia in the rabbit. Intensive Care Med. 19:112-117.

2. **Jackson, C.J., W.E. Truog, T.A. Standaert, et al.** 1994. Reduction in lung injury after combined surfactant and high frequency ventilation. Am. J Respir. Crit. Care Med. 150:534-9.

3. **Lewis, J.F., H.J. Jobe.** 1993. Surfactant and the Adult Respiratory Distress Syndrome. Am. Rev. Respir. Dis. 147:218-233.

4. **Dorrington, K.L., K.M. McRae, J.P. Gardaz, et al.** 1989. Randomized comparison of total extracorporeal CO2 removal with conventional mechanical ventilation in experimental hyaline membrane disease. Intensive Care Med. 15:184-191.

5. **Hirschl, R.B., A. Parent, R.Tooley, et al.** 1995. Liquid ventilation improves pulmonary function, gas exchange and lung injury in a model of respiratory failure. Annals of Surgery. (221)1:79-88.

6. **Schuster, D.P.** 1994. ARDS: Clinical lessons from the Oleic Acid Model of Acute Lung Injury. Am. J Respir. Crit. Care Med. 149:245-260.

7. **Eijking, E.P., D.S.K. Gomer, D.M.Vergeer, et al.** 1993. Surfactant treatment of respiratory failure induced by hydrochloric acid aspiration in rats. Anesthesiology. 78:1145-1151.

8. **Coker, P.J., L.A. Hernandez, K.J. Peevy, et al.** 1992. Increased sensitivity to mechanical ventilation after surfactant inactivation in young rabbit lungs. Crit. Care Med. 20(5):635-641.

9. **Shibamato, T, J.C. Parker, A.E. Taylor, et al.** 1990. Derecruitment of filtration surface area in paraquat-injured isolated dog lungs. J. Appl. Physiol. 68:1581-89.

10. **Robertson, B.** 1991. Surfactant inactivation and surfactant replacement in experimental models of ARDS. Acta Anaesth. Scand. 35(95):22-28.

11. **Huang, U.C.T., S.T. Caminiti, T.A. Fawcett, et al.** 1994. Natural surfactant and hyperoxic lung injury in primates I. Physiology and biochemistry. J. Appl. Physiol. 76(3):991-1001.

12. **Coalson, J.J., R.J. King, V.I.T. Winter, et al.** 1989. O2 and pneumonia-induced lung injury I. Pathological and morphometric studies. J. Appl. Physiol. 67(1):346-356.

13. **de los Santos, R., J. Coalson, J.R. Holcomb, et al.** 1985. Hyperoxia exposure in mechanically ventilated primates with and without previous lung injury. Exp. Lung Res. 9:255-275.

14. **Shimada, S., N.K. Raju, D. Vidyasagar, et al.** 1990. Chest radiographic course after exogenous surfactant therapy in baboons with respiratory distress syndrome. Crit. Care. Med. 18:969-73.

15. **Jackson, C.J., A.P. Mackenzie, E.Y. Chi, et al.** 1990. Mechanisms for reduced total lung capacity at birth and during hyaline membrane disease in premature newborn monkeys. Am. Rev. Respir Dis. 142:413-419.

16. **Hartford, CG, Rogers GG, van Schalkwyk J, et al.** 1997. Frequency responses of infant air-balloon versus liquid-filled catheters for intra-esophageal pressure measurement. Pediatr. Pulm. 24:353-363.

17. **Lanteri, C.J., S. Kano, P.D. Sly.** 1994. Validation of the esophageal pressure occlusion test after paralysis. Pediatr. Pulm. 17:56-62.

18. **Turner, M.J., I.M. MacLeoad, A.D. Rothberg.** 1989. The effects of temperature and composition on the viscosity of respiratory gases. J. Appl. Physiol. 67(1):472-477.

19. **Holm, B.A., S. Madeleine.** 1989. Role of pulmonary surfactant in the development and treatment of adult respiratory distress syndrome. Anesth. Analg. 69:805-818.

20. **Walti, H., M. Couchard, J.P. Relier.** 1989. Neonatal diagnosis of respiratory distress syndrome. Eur. Respir. J. 3:22a-27a.

21. **Hall, S.B., R.H. Natter, R.J. Smith, et al.** 1990. Altered function of pulmonary surfactant in fatty acid lung injury. J. Appl. Physiol. 69(3):1143-1149.

22. **Beardsmore, C.S., J. Stocks, P. Helms.** 1989. Elastic properties of the respiratory system in infants. Eur. Respir. J. 2:135s-139s.

23. **Gattinoni, L., D. Mascheroni, E. Basilico, et al.** 1987. Volume/pressure curve of total respiratory system in paralysed patients: artefacts and correction factors. Intensive Care Med. 13:19-25.

24. **Broccard, A.F., R.S. Shapiro, L.L. Schmitz, et al.** 1997. Influence of prone position on the extent and distribution of lung injury in a high tidal volume oleic acid model of acute respiratory distress syndrome. Crit. Care Med. 25:16-27.

25. **Prewitt, R.M., J. McCarthy, L.D.H. Wood.** 1981. Treatment of acute low pressure pulmonary edema in dogs. J Clin. Invest. 67:409-418.

26. **Glantz, S.A.** 1992. Alternatives to analysis of variance and the t-test based on

ranks, p 320-363. *In* Primer of Biostatistics. New York, McGraw-Hill, Inc.

27. **VandeBerg, J.L., S. Williams-Blangero.** 1996. Strategies for using nonhuman primates in genetic research on multifactorial diseases. Lab. Anim. Sci. 46(2):146-151.

28. **Harroff, H.H.** 1997. Use of animal models in pediatric research. Advances in Pediatrics. 44:453-89.

29. **Kosch, P.C., J.R. Gillepsie, J.D. Berry.** 1979. Respiratory mechanics in normal bonnet and rhesus monkeys. J. Appl. Physiol. 46(1):166-175.

30. **Wegner, C.D., A.C. Jackson, J.D. Berry, et al.** 1984. Dynamic respiratory mechanics in monkeys measured by forced oscillations. Respiration Physiology. 55:47-61.

31. **Juul, S.E., M.G. Kinsella, T.N. Wight, et al.** 1993. Alterations in nonhuman primate (M.nemestrina) lung proteoglycans during normal development and acute hyal' ~ membrane disease. Am.J Respir. Cell. Mol. Biol. 8:299-310.

32. **Hessler, J.R., G. Matinilla, B.V. Kirkpatrick, et al.** 1985. Asphyxia and hyaline membrane disease in neonatal monkeys. Am. J. of Perinatology. 2(2):101-108.

33. **Egberts, J., A. Beintema-Dubbeldam, A. de Boers.** 1987. Phosphatidylinositol and not phosphatidylglyce· ,l is the important minor phospholipid in rhesus-monkey surfactant. Biochim. Biophys. Acta. 919:90-92.

34. **Johanson, Jr., W.G., J.R. Holcomb, J.J. Coalson.** 1982. Experimental diffuse alveolar damage in baboons. Am. Rev. Respir. Dis. 126:142-151.

35. **LaFramboise, W.A., R.D. Guthrie, T.A. Standaert, et al.** 1983. Pulmonary mechanics during the ventilatory response to hypoxemia in the newborn monkey. J. Appl. Physiol.:Respirat. Environ. Exercise Physiol. 55(3):1008-1014.

36. **Jackson, C.J., S. Palmer, W.E. Truog, et al.** 1986. Surfactant quantity and composition during recovery from hyaline membrane disease. Pediatr. Res. 20:1243-1247.

37. **Meredith, K.S., R.A. DeLemos, J.J. Coalson, et al.** 1989. Role of lung injury in the pathogenesis of hyaline membrane disease in premature baboons. J. Appl. Physiol. 66(5):2150-2158.

38. **Julien, M., J.M. Hoeffel, M.R. Flick.** 1986. Oleic acid lung injury in sheep. J. Appl. Physiol. 60(2):433-440.

39. **Hofman, W.F., I.C. Ehrhardt, W.M Granger.** 1985. Sequential cardiopulmonary changes after oleic-acid induced injury in dogs. Crit Care Med. 13:22.

40. **Curtis, S.E., J.T. Peek, D.R. Kelly, et al.** 1993. Partial liquid breathing with perflubron improves arterial oxygenation in acute canine lung injury. J. Appl. Physiol. 75(6):2696-2702.

41. **Sum-Ping, S.T., T. Symreng, P. Jebson, et al.** 1991. Stable and reproducible porcine model of acute lung injury induced by oleic acid. Crit. Care Med. 3:405-408.

42. **Idell, S., K.K. James, J.J. Coalson.** 1992. Fibrinolytic activity in bronchoalveolar lavage of baboons with diffuse alveolar damage. Trends in two forms of lung injury. Crit. Care Med. 20:1431-1440.

43. **Hall, S.B., R. Zhong Lu, R. Venkitaraman, et al.** 1992. Inhibition of pulmonary surfactant by oleic acid mechanisms and characteristics. J. Appl. Physiol. 72(5):1708-1716.

44. **Grossman, R.F., J.G. Jones, J.F. Murray.** 1980. Effect of oleic acid-induced pulmonary edema on lung mechanics. J. Appl. Physiol.: Respirat. Environ. Exercise Physiol. 48(6):1045-1051.

45. **Hjalmarson, O.** 1974. Mechanics of breathing in newborn infants with pulmonary disease. Acta Paediatrica Scandanavica. 247:29,34.

46. **Teague, W.G., A. Robert, A. Darnall.** 1982. A noninvasive constant-flow method for measuring respiratory compliance in newborn infants. Crit. Care Med. 13:965-971.

47. **Thomson, A., J. Elliott, M. Silverman.** 1983. Pulmonary compliance in sick low birthweight infants. Arch. Dis. Child. 58:891-896.

CHAPTER 6

6 PRIMATE PLEURO-ESOPHAGEAL TISSUE BARRIER FREQUENCY RESPONSE AND ESOPHAGEAL PRESSURE WAVEFORM BANDWIDTH IN HEALTH AND ACUTE LUNG-INJURY

6.1 Linking Comments

High-fidelity non-invasive estimation of dynamic intra-pleural pressure using intra-esophageal pressure measurement requires that (i) the intra-pleural pressure wave be transmitted unchanged across the tissues between the intra-pleural and intra-esophageal spaces, and (ii) that the pressure wave be transmitted unchanged across the intra-esophageal catheter manometer systems.

Chapters Two, Three and Four have concentrated on the latter, characterising the suitability of intra-esophageal catheter manometer systems to transmit dynamic pressure waveforms accurately. Chapter Five developed and characterised a novel non-human primate model of human lung disease in which to investigate intra-pleural to intra-esophageal pressure wave transmission.

Chapter Six follows on Chapters Two, Three, Four and Five by investigating the in vivo pleuro-esophageal tissue frequency responses, in healthy and diseased animal-model respiratory systems. Thus Chapter Six investigates the uniformity of the pleuro-esophageal tissue barrier's amplitude frequency response (up to and beyond the (currently) relevant esophageal pressure waveform bandwidths in clinical practice), and detects the presence or absence of amplitude-dependence or lung-condition dependence of the tissue barrier, at low and high intra-pleural pressure frequencies.

Further, no data quantifying the bandwidth of dynamic intra-esophageal pressure waveforms in primates have been published. Such data are relevant for interpreting the effect of the frequency responses determined for the pleuro-esophageal tissue barrier

(Chapter Six) and the frequency responses determined for liquid-filled or air-balloon catheters transmitting the intra-esophageal waveforms (Chapters Two and Three). Thus Chapter Six goes further to quantify the dynamic response requirements of intra-esophageal manometer systems by determining the relevant bandwidth of dynamic physiological intra-esophageal waveforms, before and after lung disease. [Comprehensive information is provided in Chapter Six's Abstract, Introduction and Discussion sections, which follow]:-

6.2 Abstract

Background: Dynamic intra-esophageal pressure (Pes) is used to estimate intra-pleural pressure (Ppl) to calculate lung compliance and resistance. This study investigates the non-human primate Ppl-Pes tissue barrier frequency response and the dynamic response requirements of Pes manometer systems.

Methods: In healthy and acute lung injury (ALI) ventilated monkeys simultaneous Ppl and Pes were measured directly to determine the Ppl-Pes tissue barrier amplitude frequency response, using the swept sine wave technique. The bandwidths of physiological Pes waveforms acquired during conventional mechanical ventilation were calculated using digital low-pass signal filtering.

Results: The Ppl-Pes tissue barrier is amplitude-uniform within the bandwidth of conventional Pes waveforms in healthy and ALI lungs, and does not significantly attenuate Ppl-Pes signal transmission between 1 - 40 Hz. At Pes frequencies higher than conventional clinical regions of interest the Ppl-Pes barrier resonates significantly, is pressure amplitude dependent at low pressure offsets, and is significantly altered by ALI.

Allowing for ≤ 5% Pes waveform error, the maximum Pes bandwidth during conventional ventilation was 1.9 Hz and 3.4 Hz for physiological and extreme-case waveforms in healthy lungs, and 4.6 Hz and 8.5 Hz during ALI.

Conclusions: In monkeys the Ppl-Pes tissue barrier has a frequency response suitable for Ppl estimation during low frequency mechanical ventilation, and Pes manometers should have a uniform frequency response up to 8.5 Hz. However, the Ppl-Pes tissue barrier adversely affects the accurate estimation of dynamic Ppl at high frequencies with varied airway pressure amplitudes and offsets, such as the Ppl encountered during high frequency oscillatory ventilation.

Keywords: manometry, respiratory mechanics, lung elastance.

6.3 Non-standard Nomenclature

ALI	Acute lung injury
ALIG	Acute lung injury group (oleic acid, n =6)
AUC	Area under the curve
Ccw	Chest wall compliance
Cl	Lung compliance
Crs	Respiratory system compliance
CTRL	Control group (saline, n = 6)
EI-EE bandwidth	Pes bandwidth based on end-inspiratory to end-expiratory amplitude measurements
FFT	Fast Fourier Transform
HFOV	High frequency oscillatory ventilation
Hz	Frequency in cycles per second, Hertz
OA	Oleic acid
$PaCO_2$	Arterial carbon dioxide partial pressure
Paw	Proximal airway pressure (airway opening)
Paw offset	Proximal airway pressure offset
Paw pk	Peak proximal airway pressure
PEEP	Positive end expiratory pressure
Pes	Intra-esophageal pressure
Ppl	Intra-pleural pressure
RR	Respiratory rate
TPP	Transpulmonary pressure

6.4 Introduction

Dynamic intra-esophageal pressure (Pes) is measured to estimate intra-pleural pressure (Ppl) for the calculation of dynamic transpulmonary pressure.[1] Dynamic respiratory system compliance is given by

$$1/Crs = 1/Cl + 1/Ccw,$$

where Crs = total respiratory system compliance,

Cl = lung compliance,

Ccw = chest wall compliance.

Pes is used in clinical practice and research to separate Cl from Ccw, where Cl is calculated from

$$Cl = \Delta V/\Delta TPP$$

where ΔV = change in lung volume,

ΔTPP = change in transpulmonary pressure

and

$$\Delta TPP = \Delta(Paw - Pes)$$

where Paw = proximal airway pressure.

The accurate representation of dynamic Ppl using Pes measurements depends in part on the amplitude and phase frequency response of the intra-pleural to intra-esophageal tissue barrier (Ppl-Pes tissue barrier). This response is particularly important for the accurate construction of dynamic lung compliance loops and resistance calculations, and

for the potential measurement of dynamic Pes during high frequency oscillatory ventilation (up to 50 Hz).[2,3] One study directly compared Pes and Ppl in healthy adult dogs using a pseudo-random Paw signal with 2 Hz interval harmonics up to 20 Hz,[4] however, to our knowledge, direct Ppl and Pes comparisons to determine the amplitude and phase frequency response of the primate Ppl-Pes barrier have not been published.

Measurement of lung linear resistance and compliance also requires that the catheter manometer systems employed have a uniform frequency response and linear phase shift over the bandwidth of the signals to be measured. Frequency response characteristics of Pes catheter manometer systems employed in clinical practice have been investigated,[5-7] but suggested minimum frequency response requirements for Pes manometers are usually based on dynamic Paw waveform bandwidths, which are well described.[8] However, to our knowledge no data quantifying the bandwidth of dynamic Pes waveforms in primates have been published. Assumptions that Pes bandwidth during mechanical ventilation is the same as Paw bandwidth may be invalid since Paw frequency components transmitted to Pes may be amplified or attenuated, and cardiac motion energy (not largely apparent in Paw waveforms) is added to Ppl and Pes waveforms.

We hypothesise that the Ppl-Pes tissue barrier has a uniform amplitude frequency response within the Pes waveform bandwidth relevant to current clinical practice, and is uniform, amplitude independent and lung-condition independent at low and high frequencies. We aim to determine the amplitude and phase frequency response of the primate Ppl-Pes tissue barrier using the swept sine wave technique with simultaneous Ppl and Pes measurements in healthy mechanically ventilated monkeys and those with acute lung injury (ALI). Further, we aim to quantify the dynamic response requirements of Pes manometer systems by determining the bandwidth of physiological Pes waveforms before and after ALI.

6.5 Method

Instrumentation

Twelve female Vervet monkeys (*Cercopithecus aephiops*, 3.9 ± 0.60 kg) were anesthetised (ketamine 20 mg/kg induction and ketamine 10 $mg.hr^{-1}.kg^{-1}$, sufentanyl > 30 $ug.hr^{-1}.kg^{-1}$ and adrenaline 5 $ug.hr^{-1}.kg^{-1}$ maintenance continuous infusions), paralysed (vecuronium 10 $ug.hr^{-1}.kg^{-1}$), intubated orally (cuffed 4.5mm, Mallinkrodt, Athlone, Ireland) and mechanically ventilated supine with warm humidified 100% O_2 (FiO_2 = 1.0) using a high flow rate pressure-cycle pressure-limit ventilator (Preemicare Model 105, Texas, USA). University Animal Ethics Clearance (96/113/2B) was obtained. The right femoral vein was cannulated for injection of oleic acid (OA) to produce ALI.

Ppl and Pes catheter design and pressure measurements

Pes and Ppl catheters were adapted for dynamic pressure measurements by sealing the tips of size 7 French Gauge transducer-tip catheters (Millar Mikro-tip SPC 470, Millar Instruments, Inc., Texas, USA) into water-filled latex balloons 2 cm in length. The distal end of the Ppl transducer catheter was enclosed in a right-angled rigid perforated acrylic cylinder around which the balloon was tied: the cylinder was fashioned with a distal pointed end such that the catheter would act as an introducer during transthoracic positioning and once inserted the water-filled balloon rested parallel to the chest wall inside the pleural space. A second catheter attached to the Ppl catheter was linked to an underwater chest drain for pneumothorax deflation. The Ppl and Pes catheter balloons' water volumes were set to allow maximum balloon-catheter compliance. The suitability of the amplitude and phase frequency responses of the two resulting catheters were determined at 37 °C at differing mean pressure offsets and pressure amplitudes, using an

in vitro sine wave generator;[7] the catheter frequency responses were determined by testing the catheters against each other and against a uniform piezoresistive transducer.

With the aid of a transcutaneous cut-down to pleura and dilating trochars, the Ppl catheter was inserted transthoracically in either a cranial or caudal direction into the left or right sides of the chest (n = 3 of each side per group) at the level of the 7th intercostal space in the mid-axillary line. The in vivo Pes catheter site was chosen according to the best "paralysed airway occlusion test" in which the airway is briefly occluded and abdominal pressure applied to assess how faithfully ΔPes reproduces ΔPpl in an isovolumic chest of anesthetised paralysed subjects.[9]

(Supplemental Figures S6.A, S6.B).

TOP: Supplemental Figure S6.A

Laboratory transducer-tip probes with water-filled balloons for dynamic intra-esophageal and intra-pleural pressure monitoring.

I. Intra-esophageal probe

II. Intra-pleural probe

III. Intra-pleural probe's separate pneumothorax deflation cannula.

BOTTOM. Supplemental Figure S6.B

Transthoracic intra-pleural pressure probe in situ.

I. Probe in situ for dynamic pleural pressure measurement. The probe was introduced with a specially made trochar (see chapter 5 supplemental figure S5. photograph's (viii)).

II. A purse string suture secures the probe in place.

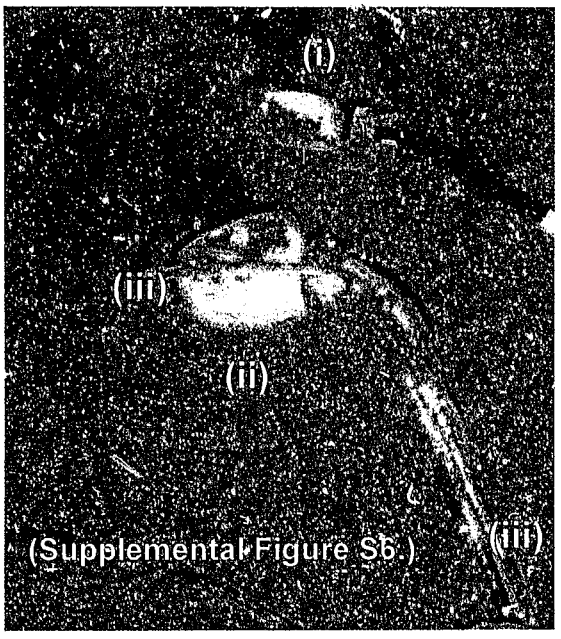
(i)
(iii)
(ii)
(Supplemental Figure S6.)
(iii)

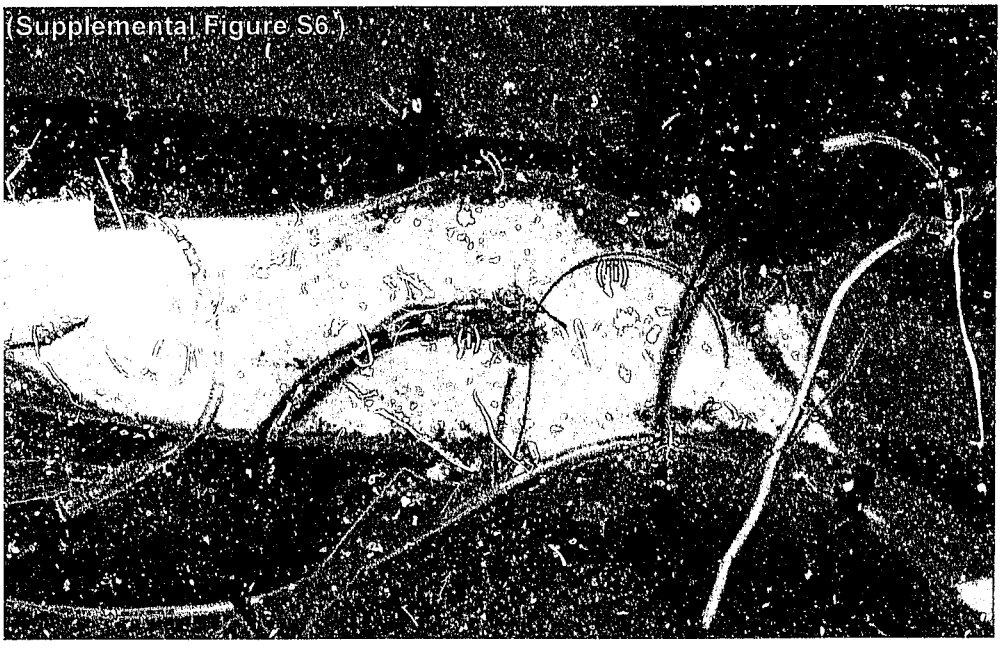
(Supplemental Figure S6.)

Airway opening pressure (Paw) was measured with a piezoresistive differential pressure transducer (Honeywell Microswitch 170PC, USA) inserted into the proximal endotracheal tube perpendicular to the gas flow direction.

All pressure transducer signals were pre-amplified using the same apparatus (Hellige Servomed, Freiburg, Germany) and digitised at 500 Hz (Biopac MP100 and AcqKnowledge ver 3.3.2, Biopac Systems Inc., CA, USA).

Ppl-Pes Tissue Barrier Frequency Response Determination

Ppl waveforms were generated by applying sinusoidal Paw waveforms using the pneumatic driver unit of a high frequency oscillatory ventilator (SensorMedics 3100A, Bilthoven, The Netherlands): To generate sine-wave rather than square-wave Paw outputs, the square-wave frequency generator of the ventilator was by-passed and the DC-coupled amplifier controlled by a separate sine-wave generator (Hewlett Packard Dynamic Signal Analyser 3562A, USA). Amplitude frequency responses of the Ppl-Pes tissue barrier were calculated by comparing the Ppl and Pes waveform signals generated between 1 Hz (taken as the DC response to which the responses were normalised) and 40 Hz. Swept-sine waves[10] were applied at 0.98 Hz intervals with 20s integration time and 90% integration threshold for each frequency interval (Hewlett Packard Dynamic Signal Analyser 3562A, USA). The dynamic signal analyser performs a high resolution Fourier transform at each measured frequency and extracts amplitude and phase information from the acquired Ppl and Pes waveform signals only at the frequency of interest thereby ignoring harmonics created by distortion. In each subject 10 swept-sine wave sequences, performed by disconnecting the standard ventilator and connecting the HFOV at 5 minutes intervals, were averaged at each of two mean Paw offsets; 1 cmH_2O and 10 cmH_2O above atmospheric pressure. These mean Paw pressure offsets were generated during the

swept-sine measurements by injecting excess oxygen into the airway and allowing the excess to bleed off under water at the appropriate depth. Frequency response traces during which esophageal peristalsis occurred were re-recorded. The acquired frequency responses were exported to a personal computer for analysis after adjustment to compensate for any non-unity gain within the Pes and Ppl measurement catheters themselves up to 40 Hz.

(Supplemental Figures S6.C, S6.D, S6.E).

TOP. Supplemental Figure S6.C

High frequency oscillation.

I. High frequency oscillator, applied to endotracheal tube

II. Variable depth water slide maintains positive airway pressure during high frequency oscillation

MIDDLE. Supplemental Figure S6.D

Sample of simultaneous intra-thoracic pressure tracings during conventional mechanical ventilation.

I. Intra-esophageal probe's pressure tracing over one mechanical breath (including cardiac motion signals)

II. Intra-pleural pressure probe's pressure tracing over one mechanical breath

BOTTOM. Supplemental Figure S6.E

Sample of intra-thoracic pressure tracings during high frequency oscillatory ventilation.

I. Proximal airway pressure tracing

II. Intra-pleural pressure probe pressure tracing

III. Intra-esophageal pressure probe pressure tracing

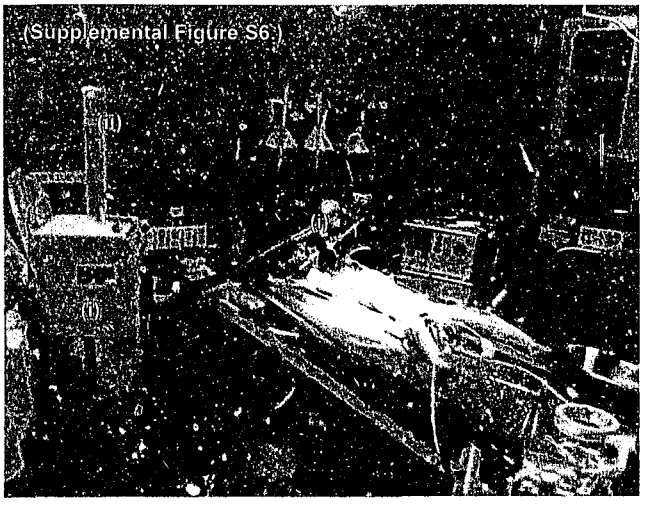
(Supplemental Figure S6.)
(i)
(i)

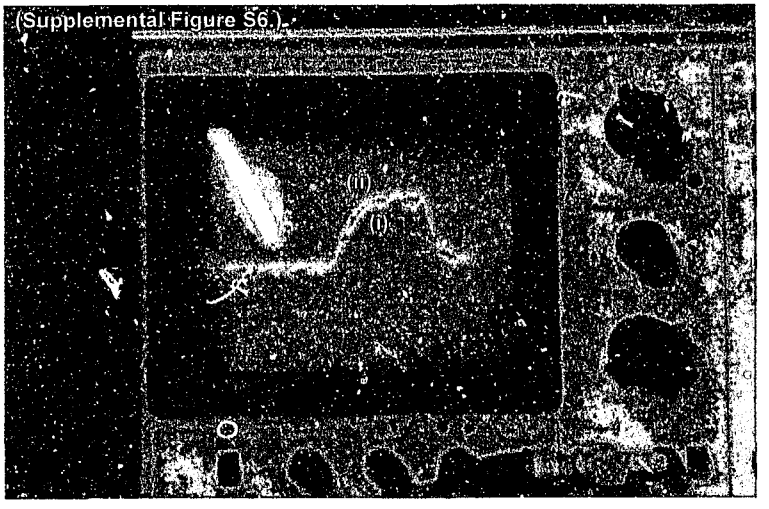
(Supplemental Figure S6.)
(ii)
(i)

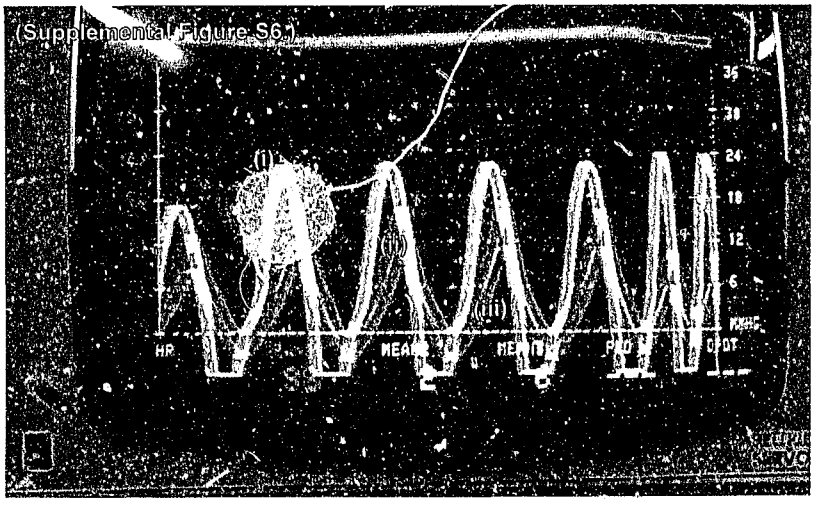
(Supplemental Figure S6.)
(i)
(ii)
36
30
24
18
12
6
HR
MEA
PVD

Frequency response measurements were recorded at two mean Paw offsets (1 or 10 cmH_2O) before and 2.5 hours after intervention (oleic acid (ALIG, n = 6) or saline (CTRL, n = 6 injection)). These measurements were recorded at a low applied Ppl amplitude (Low applied Ppl; ΔPpl waveform mean amplitudes were set to be ± 1.0 cmH_2O at 1 Hz, reducing to ± 0.5 cmH_2O at 40 Hz). At 7.5 hours after intervention the frequency response measurements were recorded at mean Paw offset of 20 cmH_2O at Low applied Ppl amplitude, and again at Paw offset of 10 cmH_2O but at a larger applied Ppl amplitude (High Ppl amplitude; ΔPpl waveform mean amplitudes were set to be ± 4.7 cmH_2O at 1 Hz, reducing to ± 1.0 cmH_2O at 40 Hz).

Pes dynamic waveform bandwidth:

Pes and Paw measurements were made in 6 subjects before (baseline, PesB and PawB) and 5.5 hours after (PesA and PawA) oleic acid injection in the acute lung injury group (ALIG, n = 6). Respiratory rate (RR) and maximum Paw (Paw pk) were adjusted to achieve an arterial carbon dioxide ($PaCO_2$) of 30-40 mmHg throughout the experiment(calibrated Stat Profile 3, Nova Biomedical, MA, USA). Physiological PesB and PawB or physiological PesA and PawA were acquired at PaCO2 = 30 - 40 mmHg. Additionally, Pes and Paw traces were acquired under extreme conditions by raising peak Paw 50% above the physiologically required peak Paw and doubling the RR simultaneously (elevated PesB and PawB or elevated PesA and PawA).

Trains of ten PesB and PesA waveform sequences, each containing ten mechanical breaths, were selected and low-pass filtered using a Blackman finite impulse response linear phase filter with minimal phase shift (AcqKnowledge ver 3.3.2, Biopac Systems Inc., CA, USA), whose response was tailored to be near -1 dB at chosen low-pass cut-off frequencies. Twelve low-pass cut-off frequencies were selected which reduced the areas under the curve (%AUC) of the Pes continuous power spectrum by pre-

determined proportions. Power spectra were determined by ensemble averaging the power spectra of ten PesB and PesA breaths. The mean value was subtracted from each ensemble and the data padded with zeros prior to fast Fourier transform (FFT) (AcqKnowledge ver 3.3.2, Biopac Systems Inc., CA, USA). 100% of Pes waveform power was assumed to be contained between 0 - 40 Hz.

The average Pes amplitude between Pes at onset of expiration to Pes at onset of inspiration over each of ten mechanical breaths was manually determined for the original trains of unfiltered Pes waveforms and compared to those of the incrementally low-pass filtered Pes waveforms. The maximum waveform amplitude error (% amplitude difference from original Pes waveform) averaged for ten breaths was determined across the 6 subjects. The Pes bandwidth up to which a Pes manometer should have a uniform amplitude frequency response to yield a ≤3% or ≤5% error when measuring the end-expiratory to end-inspiratory amplitude of physiological or extreme-case Pes waveforms was thus determined (Pes EI-EE bandwidth).

Statistical Analysis

Amplitude frequency responses in which the mean Pes/Ppl ratio deviated more than 10% from 1.0, plus the 95% confidence interval value excluded 1.0, (both conditions met), were considered by us to significantly deviate from that of uniformity.[11]

Significant within-group (within ALIG or within CTRL) changes over time were detected using Friedman anova (repeated measures) followed by identification with the Wilcoxon signed-rank test.[12] The Mann-Whitney rank-sum test was used to determine significant differences between ALIG and CTRL groups (Statistica™ software, Statsoft, OK). Frequency response graphically displayed values are mean ± SEM, all ventilation variables are mean ± SD and differences with P-values < 0.05 are regarded as statistically significant.

6.6 Results

Ppl and Pes transducer-tip balloon-tip catheters

Figure 6.1. shows the laboratory-modified Ppl and Pes catheter amplitude and phase frequency response characteristics. The catheters were tested against each other in vitro at mean pressure offsets of 1 and 10 cmH_2O, at pressure amplitudes of ± 1 cmH_2O and ± 10 cmH_2O. The y-axis scale is amplified, illustrating that the catheters' amplitude frequency responses were uniform to within 1% of each other between 1 - 40 Hz, and were suitably amplitude-linear for differing pressure amplitudes as well as varying pressure offsets. Phase differences between the two catheters were less than 0.5 degrees from 1 - 40 Hz.

Figure 6.1.

Amplitude and phase frequency responses of the water-filled balloon transducer-tip pleural (reference) and esophageal catheters, across different Paw amplitudes and Paw offsets (1 and 10 cmH2O). Ppl, intra-pleural catheter; Pes, intra-esophageal catheter; Hz, swept sine frequency in Hz; Pes/Ppl, amplitude gain of esophageal catheter over that of the reference pleural catheter; Pes - Ppl, phase difference between Pes and Ppl catheters.

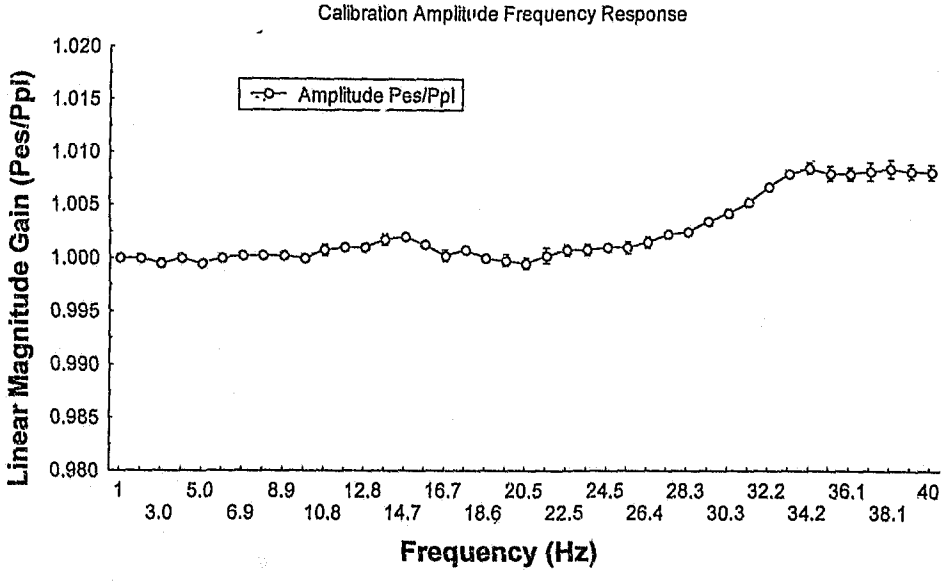
Calibration Amplitude Frequency Response
Amplitude Pes/Ppl
Linear Magnitude Gain (Pes/Ppl)
1.020
1.015
1.010
1.005
1.000
0.995
0.990
0.985
0.980
1
3.0
5.0
6.9
8.9
10.8
12.8
14.7
16.7
18.6
20.5
22.5
24.5
26.4
28.3
30.3
32.2
34.2
36.1
38.1
40
Frequency (Hz)

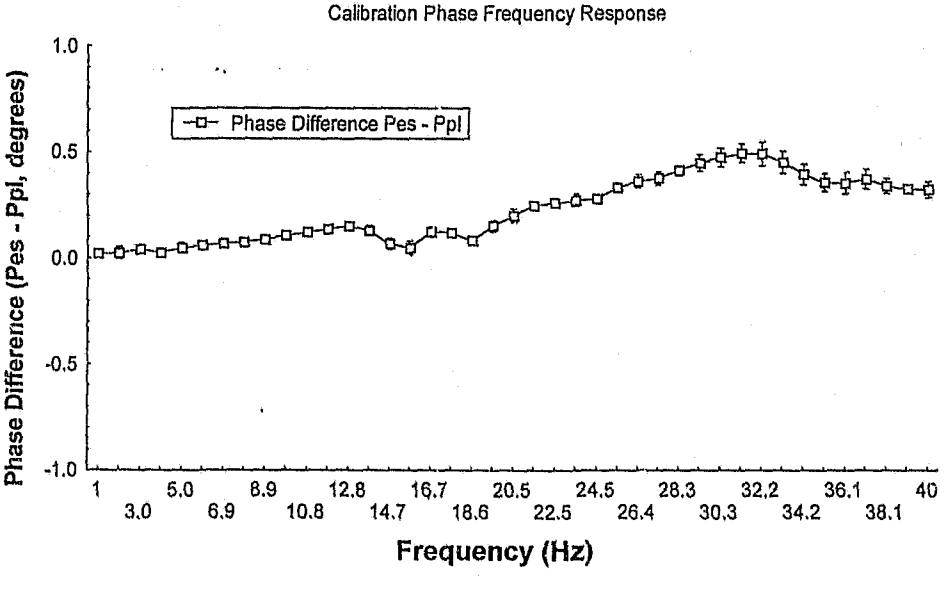
Calibration Phase Frequency Response
Phase Difference Pes - Ppl
Phase Difference (Pes - Ppl, degrees)
1.0
0.5
0.0
-0.5
-1.0
1
3.0
5.0
6.9
8.9
10.8
12.8
14.7
16.7
18.6
20.5
22.5
24.5
26.4
28.3
30.3
32.2
34.2
36.1
38.1
40
Frequency (Hz)

Pes Occlusion test in monkeys

Pes catheter insertion distance, chosen according to the optimal achievable occlusion test results, was 14.9 ± 2.67 cm from monkey canine to the tip of the catheter.

Ratios for mean area under the curve (AUC) of PesAUC/PplAUC and PawAUC/PplAUC obtained during the occlusion tests are presented in Table 6.1.

Table 6.1. *Anesthetised monkey occlusion test ratios*

Paw offset	Baseline AUC (n = 12)		Post-intervention AUC CTRL (n = 6)		Post-intervention AUC ALIG (n = 6)	
	Pes/Ppl	Paw/Ppl	Pes/Ppl	Paw/Ppl	Pes/Ppl	Paw/Ppl
1 cmH_2O	0.94 ± 0.067	0.95 ± 0.108	0.90 ± 0.126	0.94 ± 0.061	0.95 ± 0.092	0.90 ± 0.082
10 cmH_2O	0.90 ± 0.080	0.96 ± 0.065	0.90 ± 0.148	0.97 ± 0.163	0.96 ± 0.059	0.92 ± 0.077

AUC, ratio of two pressure waveform AUC values; Paw offset, airway pressure offset during occlusion test; Pes/Ppl, AUC ratio of esophageal to pleural pressure during occlusion test; Paw/Ppl, AUC ratio of airway to pleural pressure during occlusion test; CTRL, control group receiving saline; ALIG, acute lung injury group receiving oleic acid.

There were no significant differences in the occlusion test AUC ratios within or between ALIG and CTRL, before and after saline or oleic acid injection, at 1 or 10 cmH_2O Paw offsets. During the occlusion tests both Pes and Paw mean AUC pressures were lower than Ppl, by similar amounts. Mean Pes/Ppl AUC ratios were > 0.90 in all groups, however the variation about the mean was large (see SD's in Table 6.1). For Pes/Ppl AUC ratios, 8 and 9 out of 12 baseline subjects' fell between 0.90 - 1.10 when Paw offsets were 1 and 10 cmH_2O respectively; for Pes/Paw AUC ratios, 8 and 8 out of 12 baseline subjects' ratios fell between 0.90 - 1.10 when Paw offsets were 1 and 10 cmH_2O respectively. For

Pes/Paw AUC ratios, 4 and 7 out of the 12 baseline subjects' ratios fell between 0.95 - 1.05 when Paw offsets were 1 and 10 cmH_2O respectively.

Ppl-Pes tissue barrier frequency response

Figure 6.2. is a sample tracing of the Paw, Ppl and Pes waveforms obtained using the modified HFOV oscillator unit switching from 3 Hz (on the left) to 4 Hz (on the right) of the tracing.

Figure 6.2.

Sample tracings of Paw, Ppl and Pes sinusoidal waveforms obtained using the modified driver switching from 3 Hz on the left to 4 Hz on the right in one monkey. Paw, airway opening pressure; Ppl, intra-pleural pressure; Pes, intra-esophageal pressure.

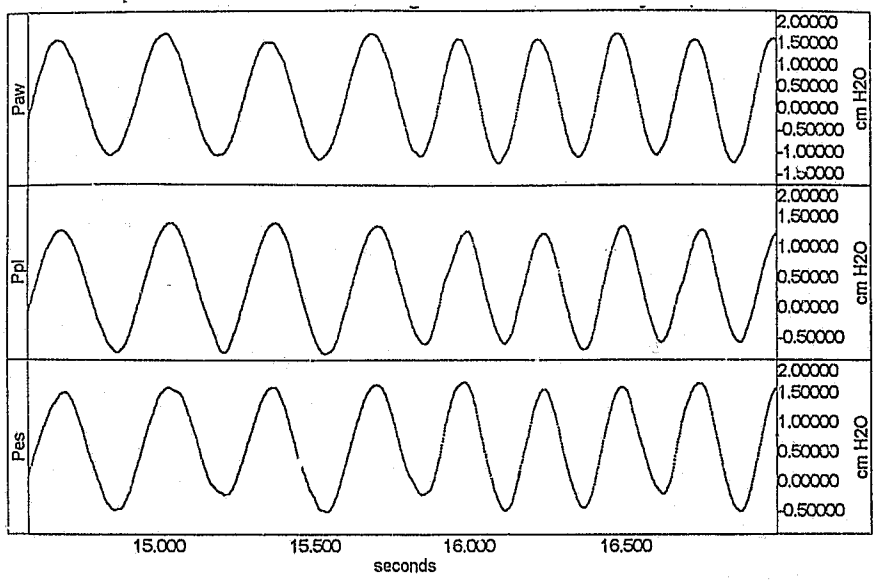
Paw
2.00000
1.50000
1.00000
0.50000
0.00000
-0.50000
-1.00000
-1.50000
cm H2O
Ppl
2.00000
1.50000
1.00000
0.50000
0.00000
-0.50000
cm H2O
Pes
2.00000
1.50000
1.00000
0.50000
0.00000
-0.50000
cm H2O
15.000
15.500
16.000
16.500
seconds

The Low Ppl amplitudes were similar before and after acute lung injury and between ALIG and CTRL, and the High Ppl amplitudes were similar between ALIG and CTRL: Mean combined (n = 12) CTRL and ALIG Ppl waveform amplitudes were ± 1.0 cmH_2O reducing to ± 0.5 cmH_2O from 1 to 40 Hz for the low applied Ppl amplitude sequences (Low Ppl amplitude; see methods), and ± 4.7 cmH_2O reducing to ± 1.0 cmH_2O from 1 to 40 Hz for the high applied Ppl amplitude sequences (High Ppl amplitude; see methods).

There were no significant differences between the ALIG (n = 6) and CTRL (n = 6) monkeys' amplitude frequency responses at Baseline: Figure 6.3. depicts the swept-sine amplitude frequency response from 1 - 40 Hz at Baseline in the combined (n = 12) ALIG and CTRL subjects, for Paw offset = 1 cmH_2O and 10 cmH_2O. The Ppl-Pes tissue barrier amplitude frequency response was uniform from
1 - 40 Hz when Paw offset = 10cmH_2O. However, the 95% confidence interval lower limit of the response was greater than unity and the mean response greater than 1.10 at frequencies above 14.7 Hz when Paw offset = 1 cmH_2O. From 20.5 - 40 Hz the swept sine amplitude frequency response with Paw offset = 1cmH_2O was significantly greater than when Paw offset = 10cmH_2O (higher lung volume, figure 6.3).

Figure 6.3.

Baseline Ppl-Pes tissue barrier amplitude frequency responses at low and high mean airway pressure offsets. Pes/Ppl, amplitude gain of esophageal pressure over intra-pleural pressure; Hz, swept-sine frequency in cycles/sec; Paw, airway opening pressure. *,** $P < 0.05,0.01$ amplitude gain significantly different for Paw offset of 10 cmH_2O versus 1 cmH_2O; + amplitude response deviates significantly from uniformity (see criteria in methods).

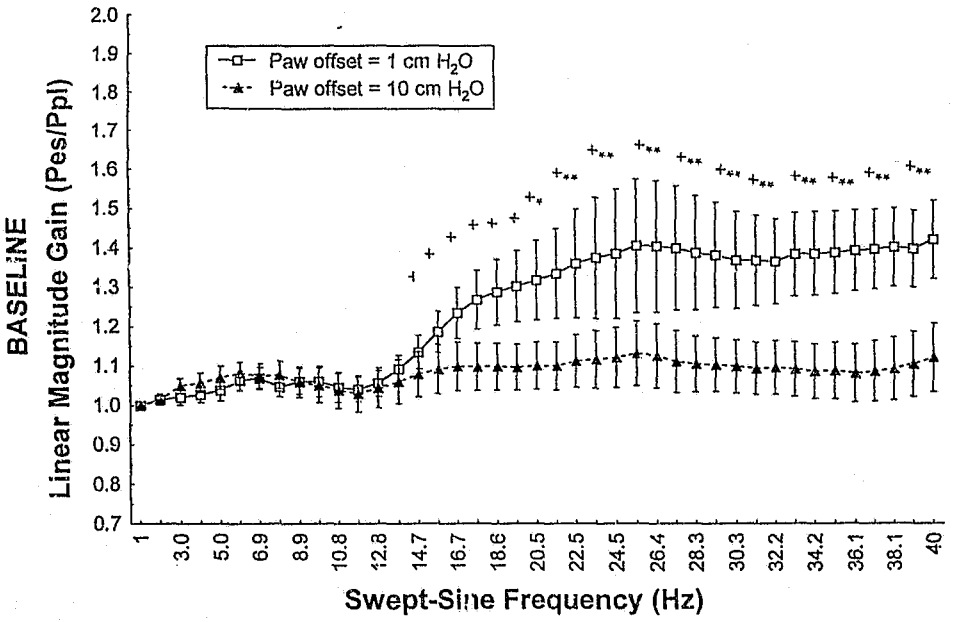
BASELINE
Linear Magnitude Gain (Pes/Ppl)
Paw offset = 1 cm H2O
Paw offset = 10 cm H2O
2.0
1.9
1.8
1.7
1.6
1.5
1.4
1.3
1.2
1.1
1.0
0.9
0.8
0.7
1
3.0
5.0
6.9
8.9
10.8
12.8
14.7
16.7
18.6
20.5
22.5
24.5
26.4
28.3
30.3
32.2
34.2
36.1
38.1
40
Swept-Sine Frequency (Hz)

After control saline injection the CTRL subjects (n = 6) retained amplitude frequency response characteristics similar to the baseline values shown in Figure 6.3. The amplitude frequency response was uniform between 1 and 40 Hz at Paw offset of 10 cmH_2O, and the amplitude gain was significantly greater at Paw offset of 1 cmH_2O compared to Paw offset of 10 cmH_2O between 19 - 35 and 38 - 40 Hz. However, unlike CTRL, the amplitude frequency response characteristics of the ALI group (n = 6) changed following acute lung injury (figure 6.4): at Paw offset of 1 cmH_2O the amplitude response was now uniform from 1 - 40 Hz (whereas before lung injury it was significantly raised, see baseline figure 6.3), and at Paw offset of 10 cmH_2O the response of ALIG was significantly raised from 13.7 - 15.7 Hz and from 26.4 - 32.2 Hz (whereas before lung injury it was uniform from 1 - 40 Hz, see baseline figure 6.3). Within ALIG the amplitude response was significantly different between Paw offset of 1 cmH_2O versus Paw offset of 10 cmH_2O from 3.0 - 5.9 Hz, 8.9 - 14.7 Hz and at 30.3 Hz (figure 6.4).

Figure 6.4.

Ppl-Pes tissue barrier amplitude frequency responses at low and high mean airway pressure offsets following acute lung injury (ALIG). Pes/Ppl, amplitude gain of esophageal pressure over intra-pleural pressure; Hz, swept-sine frequency in cycles/sec; Paw, airway opening pressure. $^{*}P < 0.05$ amplitude gain significantly different for Paw offset of 10 cmH_2O versus 1 cmH_2O; $^{+}$amplitude response deviates significantly from uniformity (see criteria in methods).

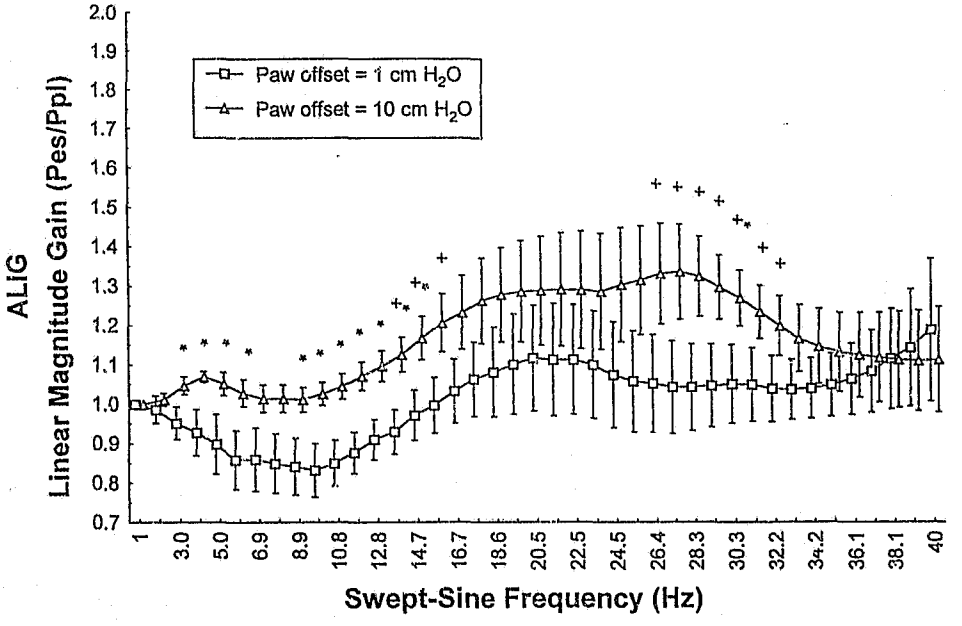
ALIG
Linear Magnitude Gain (Pes/Ppl)
Paw offset = 1 cm H2O
Paw offset = 10 cm H2O
2.0
1.9
1.8
1.7
1.6
1.5
1.4
1.3
1.2
1.1
1.0
0.9
0.8
0.7
1
3.0
5.0
6.9
8.9
10.8
12.8
14.7
16.7
18.6
20.5
22.5
24.5
26.4
28.3
30.3
32.2
34.2
36.1
38.1
40
Swept-Sine Frequency (Hz)

At Paw offset of 20 cmH_2O CTRL amplitude frequency response was uniform from 1 - 40 Hz (similar to CTRL baseline at Paw offset of 10 cmH_2O from figure 6.3, and to CTRL following saline injection at Paw offset of 10 cmH_2O), while the ALIG amplitude response continued to deviate from uniformity between 4.0 - 5.0 Hz and 30.3 - 36.1 Hz (resembling the ALIG amplitude response at Paw offset of 10 cmH_2O from figure 6.4 which deviated from uniformity after acute lung injury).

At Paw offset of 10 cmH_2O but with High Ppl amplitude CTRL was uniform between 1 - 40 Hz (similar to the baseline
figure 6.3 and post-saline CTRL responses at Paw offset of 10 cmH_2O with Low Ppl amplitude), while ALIG significantly deviated from uniformity between 23.5 - 31.3 Hz (similar to the ALIG response at Paw offset of 10 cmH_2O with Low Ppl amplitude from figure 6.4).

Under any of the conditions tested no traces exhibited significant damping of the amplitude frequency response. Ppl-Pes tissue barrier phase differences were small, and the amplitude gain at Baseline exhibited in figure 6.3 was not accompanied by a significant phase difference: minimum to maximum phase differences were -11 to +26 degrees across all frequencies and lung conditions tested.

Pes waveform EI-EE bandwidth

The physiological Paw and Pes waveforms, as measured before (physiological PawB and PesB) and after lung injury (physiological PawA and PesA) used for Pes EI-EE bandwidth determination are characterised in Table 6.2. "Extreme-case" pressures were generated by increasing the Paw by 50% and doubling the RR of the PawB and PesB waveforms characterised in Table 6.2 (yielding elevated PawB and PesB and elevated PawA and PesA).

Table 6.2 *Physiological ventilation characteristics for Pes EI-EE bandwidth determination*

	Before ALI		5.5 hr after ALI	
	PawB	PesB	PawA	PesA
RR	19 ± 4.9		33 ± 10.7	
Paw pk	12 ± 0.9	7 ± 2.4	18 ± 2.9	8.3 ± 2.0
PEEP	3 ± 1.0	1 ± 1.9	5.5 ± 1.3	3 ± 1.2
Paw M	6 ± 0.8	3 ± 2.2	10 ± 1.3	5 ± 1.5

RR, respiratory rate; Paw pk,M, peak and mean proximal airway pressure in cmH_2O; PEEP, positive end expiratory pressure; ALI oleic-acid induced acute lung injury; PawB,PawA, physiological mean proximal airway pressure at baseline and in ALI; PesB,PesA, physiological mean intra-esophageal pressure at baseline and in ALI. Values are those required for PaCO2 of 30 - 40 mmHg.

The mean % delivery of dynamic Paw to Pes, defined by Pes AUC/Paw AUC for 10 respiratory cycle ensembles was 64 ± 7% and 62 ± 8.7% for physiological PesB/PawB and elevated PesB/PawB respectively. Following ALI, % delivery values were reduced to 41 ± 6.3 and 43 ± 7.7 for physiological PesA/PesA and elevated PesA/PawA respectively. Thus ALI reduces the % delivery of Paw to Pes, but doubling the RR simultaneously and raising the Paw above that required for physiological PaCO2 did not significantly affect the % delivery of Paw to Pes, before or after ALI. Note that PesB and PesA values include Pes derived from cardiac pressure oscillations in the chest.

The response of the linear phase finite impulse response low-pass filter applied to the Pes waveforms for chosen cut-off frequencies of 1 and 2 Hz is demonstrated in figures 6.5a and 6.5b.

Figures 6.5a and 6.5b

Low-pass filter response curves for cut-off frequencies of

1 Hz (5a) and 2 Hz (5b) respectively. Hz, frequency in Hertz; dbV, logarithmic attenuation of waveform frequency content in Decibels.

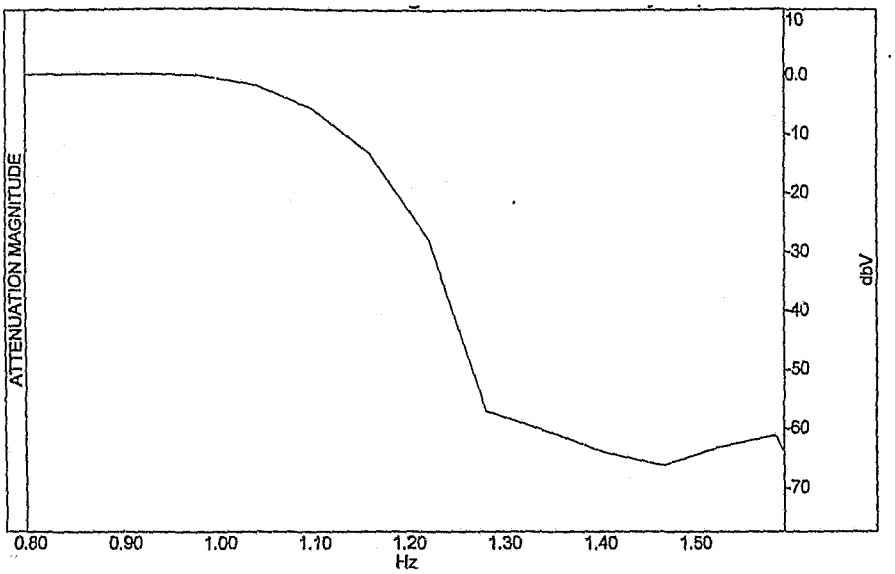
ATTENUATION MAGNITUDE
10
0.0
-10
-20
-30
-40
-50
-60
-70
dbV
0.80
0.90
1.00
1.10
1.20
1.30
1.40
1.50
Hz

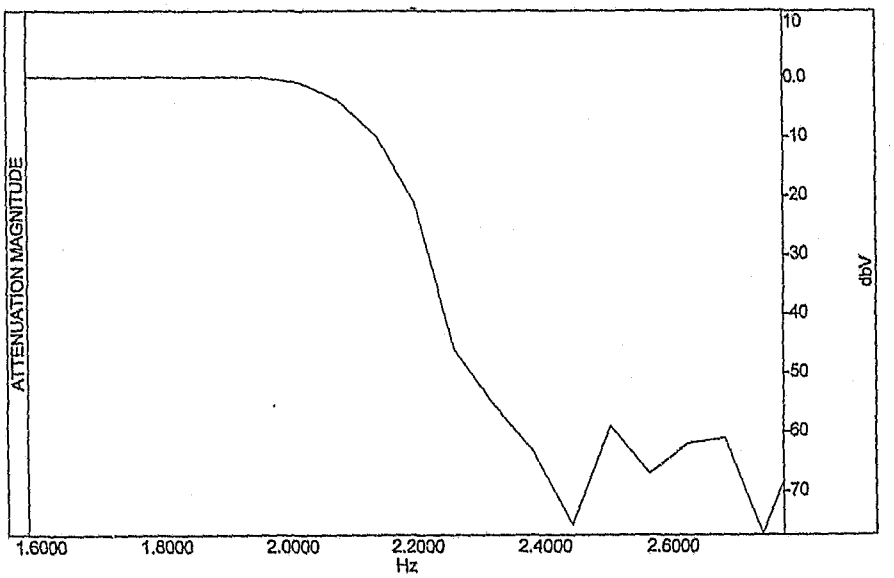
ATTENUATION MAGNITUDE
10
0.0
-10
-20
-30
-40
-50
-60
-70
dbV
1.6000
1.8000
2.0000
2.2000
2.4000
2.6000
Hz

The effect of low-pass filtering physiological PesB waveforms is shown by example in Figure 6.6. The Pes fundamental frequency is 0.34 Hz (20 breaths/min). Incrementally low-pass filtering the Pes waveforms between the third and fourth (1.2 Hz) and the second and third (0.8 Hz) harmonic frequencies leads to erosion of the sharp edges of the waveforms with consequent errors in the end-inspiratory to end-expiratory waveform amplitudes. Small cardiac motion signals are present in the Pes waveforms and to a lesser degree in the Paw waveforms (cardiac motion signals were also present in the dynamic Ppl tracings).

Figure 6.6

Illustration of low-pass filtering effect on Pes waveforms. Paw, Original proximal airway pressure waveform; Pes, original and two filtered (low-pass cut-off frequencies 1.8 and 0.8 Hz respectively) intra-esophageal physiological pressure waveforms at baseline. Over-damped Pes acquisitions result in gradual erosion of Pes waveform shape.

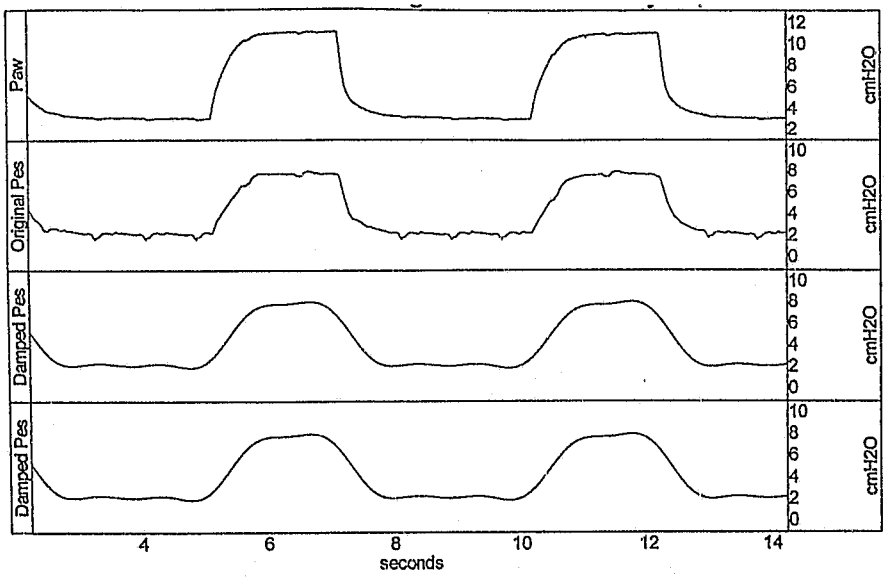
Paw
Original Pes
Damped Pes
Damped Pes
cmH2O
cmH2O
cmH2O
cmH2O
12
10
8
6
4
2
10
8
6
4
2
0
10
8
6
4
2
0
10
8
6
4
2
0
4
6
8
10
12
14
seconds

Assuming that 100% of Pes waveform energy lies between 0 - 40 Hz, the mean (n = 6 subjects) frequencies at which the power in the Pes waves is 78 - 90% of the total power are shown in Figure 6.7, for the physiological and elevated PesB and PesA waveforms. It is seen that on average, across all the lung conditions tested, up to 90% of Pes waveform power is found below 8.0 Hz and up to 78% of waveform power in the Pes energy spectra is contained below 3.4 Hz.

Figure 6.7

Pes power spectrum's frequency value as a function of Pes waveform energy content, assuming 100% of waveform energy content lies between 0- 40 Hz. AUC, % energy above 0 Hz remaining under the power spectrum curve relative to that between 0 - 40 Hz (100%). Hz, average frequency recorded for the particular % AUC value. PesB, PesA, mean intra-esophageal pressure waveforms at baseline and after ALI, at physiological ($PaCO_2$ = 30 - 40 mm Hg) or artificially elevated airway pressures.

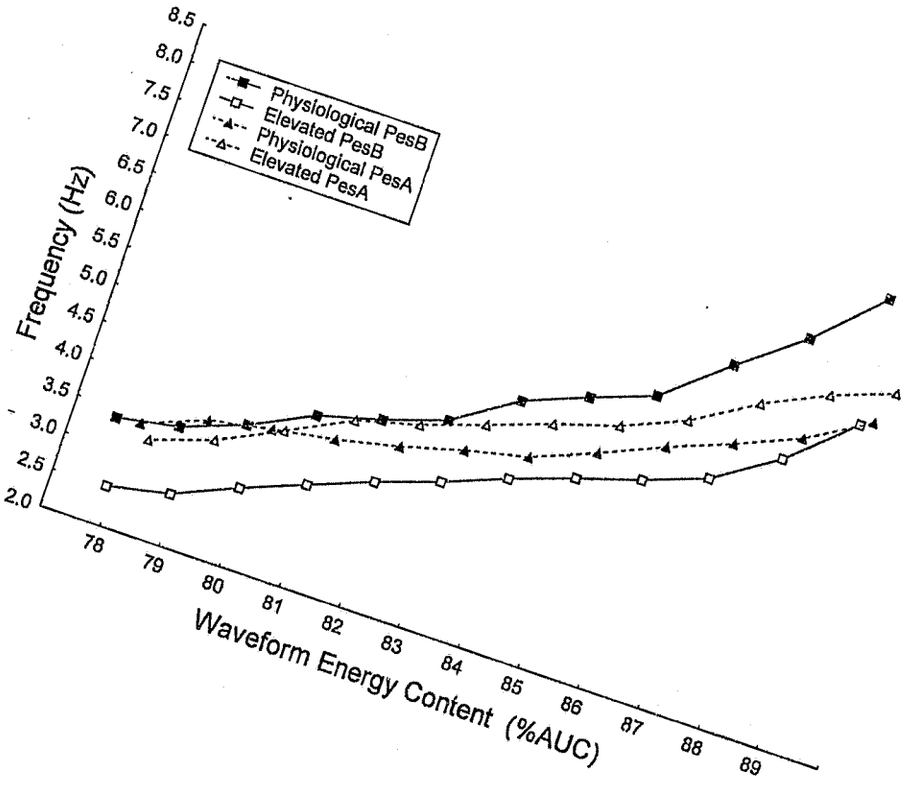
Physiological PesB
Elevated PesB
Physiological PesA
Elevated PesA
Frequency (Hz)
8.5
8.0
7.5
7.0
6.5
6.0
5.5
5.0
4.5
4.0
3.5
3.0
2.5
2.0
78
79
80
81
82
83
84
85
86
87
88
89
Waveform Energy Content (%AUC)

Figure 6.8 shows the maximum Pes waveform error (defined in methods section) associated with reduced waveform energy contents produced by low-pass filtering the Pes waveforms, in healthy (figure 6.8a) and ALI (figure 6.8b) lungs. With increasing attenuation of Pes waveform energy content the waveform error increases. The maximum waveform error for Pes waveforms with residual waveform energy contents less than 90% AUC trended towards being larger for the elevated PesB waveforms than for the physiological PesB waveforms in healthy ventilated monkeys (see waveform % error values for elevated PesB versus physiological PesB, figure 6.8a). The maximum waveform error (and the 95% upper confidence interval error values) for Pes waveforms with residual waveform energy contents just below 90% AUC were larger for PesA waveforms (following ALI) than for PesB waveforms (at baseline) (see figure 6.8b physiological PesA versus figure 6.8a physiological PesB).

In Pes waveforms across all subjects' Pes the highest cut-off frequency value (largest waveform EI-EE bandwidth) which yielded a > 5% waveform error was 1.9 Hz, 3.4 Hz, 4.6 Hz and 8.5 Hz for the physiological PesB, elevated PesB, physiological PesA and elevated PesA waveforms respectively. Corresponding values for the highest cut-off frequency which yielded a waveform error of > 3% were 2.1 Hz, 4.9 Hz, 6.0 Hz, and 8.5 Hz.

Figures 6.8a and 6.8b

Pes waveform error as a function of reducing Pes waveform energies after low-pass filtering before (8a) and after (8b) ALI. Waveform error (%) is the maximum value for the end-inspiratory onset to end-expiratory onset amplitude error, following low-pass filtering at chosen cut-off frequencies defined from reducing waveform energy contents (reducing % AUC). max Hz, highest Pes waveform frequency (largest waveform EI-EE bandwidth) found at maximum waveform errors > 5% or > 3%; ALI, acute lung injury; PesB, PesA, mean intra-esophageal pressure waveforms at baseline (top graph) and in ALI (bottom graph), at physiological ($PaCO_2$ = 30 - 40 mm Hg) or artificially elevated airway pressures.

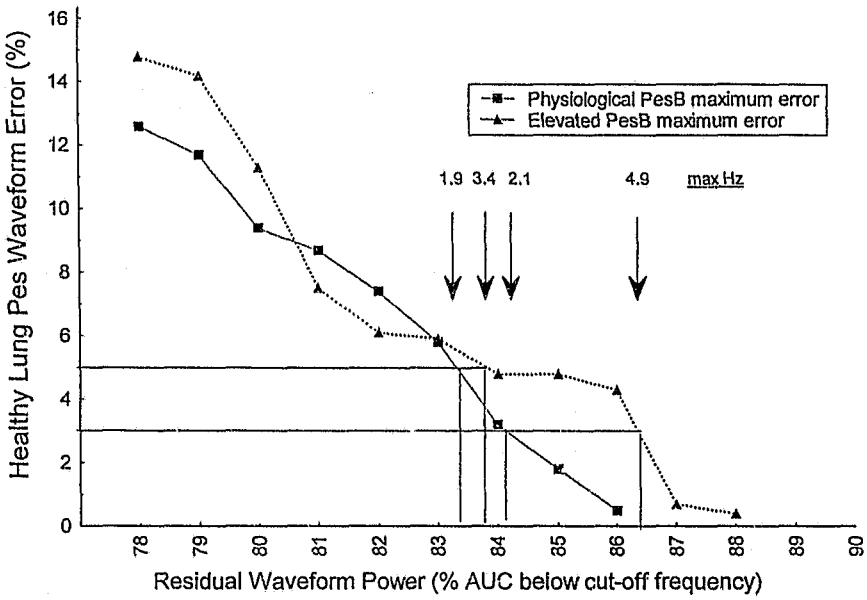
Healthy Lung Pes Waveform Error (%)
Residual Waveform Power (% AUC below cut-off frequency)
Physiological PesB maximum error
Elevated PesB maximum error
1.9 3.4 2.1
4.9
max Hz

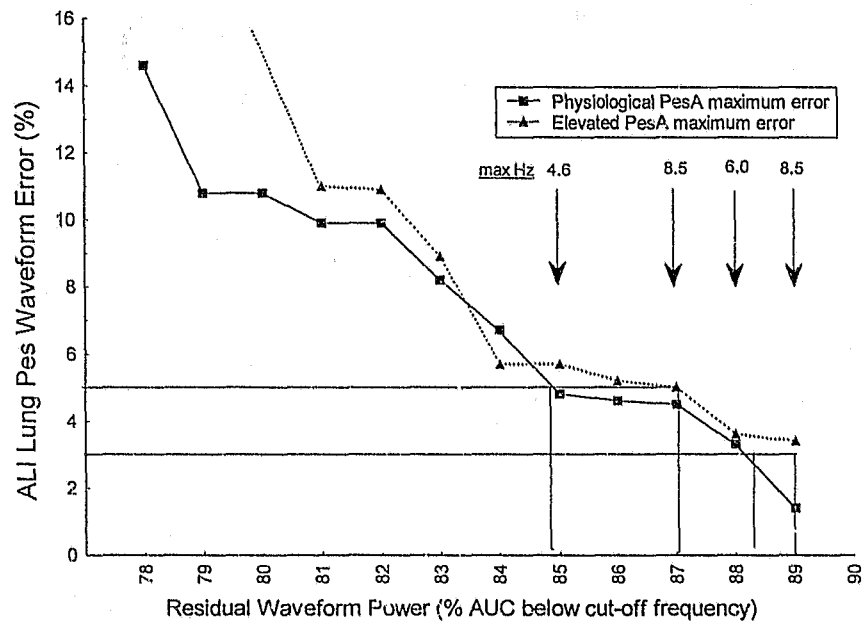
ALI Lung Pes Waveform Error (%)
Residual Waveform Power (% AUC below cut-off frequency)
Physiological PesA maximum error
Elevated PesA maximum error
max Hz 4.6
8.5
6.0
8.5

6.7 Discussion

Ppl and Pes transducer-tip balloon-tip catheters

The Ppl and Pes catheters were designed to exhibit a uniform frequency response up to 40 Hz whilst allowing for pressure measurement over a larger representative volume than an isolated transducer-tip[2] catheter can do. They are thus comparable to the air-balloon catheters used in clinical practice to measure dynamic Pes, but have a lower volume-displacement coefficient (being water-filled) and wider dynamic range suitable for assessing the Ppl-Pes tissue barrier at high frequencies. The catheter frequency responses were also shown to be pressure amplitude independent (amplitude-linear, figure 6.1) at differing applied amplitudes as well as mean pressure offsets, hence changes in the in vivo amplitude frequency responses traces are likely to be due to the Ppl-Pes tissue barrier rather than arising from the measurement systems themselves. Note however that one limitation of all direct Ppl measurements is that the devices themselves may change local Ppl to varying degrees.[1]

Ppl-Pes tissue barrier frequency responses

Concerns pertaining to Pes measurements are raised through findings such as the lung volume dependence and Paw-dependence of Pes changes in infants[13] and adults,[14] and the frequency-dependence and Paw-dependence of lung compliance values in healthy adult monkeys.[15] The mechanical properties of the esophageal wall and surrounding structures are a potential cause of signal alteration when estimating dynamic Ppl from Pes.[16] Using direct simultaneous Ppl and Pes measurements we have demonstrated that the Ppl-Pes amplitude frequency response of the Ppl-Pes tissue barrier is uniform within the EI-EE bandwidth (i.e. up to 8.5 Hz) of physiological Pes waveforms

measured in anesthetised mechanically ventilated primates, in health and acute lung injury. The barrier does not significantly attenuate Ppl-Pes signal transmission between 1 - 40 Hz. However, at higher frequencies in this range the Ppl-Pes frequency response resonates significantly, is amplitude dependent, and is significantly altered in the presence of lung pathology. These findings have implications for the accurate estimation of dynamic Ppl at high frequencies and varied Paw offsets, such as are commonly encountered during HFOV.[2,3]

The frequency response of the Ppl-Pes barrier was assessed by us using simultaneous direct Ppl and Pes measurements. Characterizing Ppl-Pes signal transmission using models of the respiratory system, as opposed to direct measurements, is constrained by inherent assumptions. One direct comparison of measured Ppl and Pes in 5 anesthetised and paralysed dogs was performed using validated Pes and Ppl catheters;[4] the amplitude frequency response did not deviate by > 10% from unity between 2 - 20 Hz, and no amplitude dependence was observed by varying the mean Paw offset. This study differs from ours in that it was performed in upright dogs (vs supine primates), through a tracheotomy (vs endotracheal tube), using a pseudorandom Paw signal with a measurement resolution of 2 Hz between 2 - 20 Hz (vs a 10-average repeated swept sine wave technique at 1 Hz intervals up to 40 Hz), applied to healthy lungs only (vs healthy and ALI lungs), and the Pes catheter was placed above the heart in all their subjects to avoid cardiac motion interference (rather than according to the occlusion test used in clinical practice). In rabbits there was slight attenuation of Pes measured at discrete frequencies of 30, 40 and 50 Hz compared to Ppl measured via a chest drain.[17] One study in humans has demonstrated systematic amplitude and phase differences between Pes and Paw during airway occlusion: using a pseudorandom pressure signal applied to the chest rather than down the airway in healthy adult humans,

Pes/Paw amplitude was uniform from 2 - 32 Hz only if the cheeks were supported, and Pes led Paw by 21 degrees at 32 Hz. With unsupported cheeks the Pes/Paw amplitude response resonated significantly at 32 Hz. However, Ppl could not be measured directly in this study.[3]

Assessing the amplitude dependence of the Ppl-Pes barrier's frequency response by varying the Paw amplitudes as well as varying the Paw pressure offsets has become important with the advent of HFOV modes which make extensive use of high Paw offsets with variable applied Paw amplitudes at up to 50Hz. Moreover, in lung pathologies requiring conventional artificial ventilation, PEEP requirements are often considerably raised.

Alterations in the Ppl-Pes tissue barrier frequency response seen after induction of ALI could be due to changing lung conditions in ALI affecting Ppl-Pes transmission, or possibly due to reduced amplitudes in the Ppl waveforms during the ALI swept-sine runs (low lung compliance reduces Paw transmission to Ppl space): In the latter case if the system is amplitude non-linear then the frequency response could change due to the differing amplitudes of the applied oscillatory pressure rather than due to other changes in Ppl-Pes transmission conditions. However, in our subjects the Ppl signal's amplitude was continuously fed back to the oscillator's signal generator such that Paw amplitudes were automatically adjusted to produce consistent Ppl amplitude power spectra before and after intervention. Thus the alterations in the Ppl-Pes tissue barrier frequency response seen after induction of ALI are likely to be related to ALI changes in the respiratory system's condition rather than due to amplitude non-linearity in the Ppl-Pes system itself. Perceived changes in respiratory system condition can also result from partial or complete isolation of the Ppl or Pes catheters. This is also unlikely since across subjects we inserted the Ppl catheter into both the left or the right sides of the chest, in caudal or cranial directions, and

the Ppl, Pes and Paw occlusion test results before and after ALI were similar (Table 6.1). The generation of negative pressures in the airways during oscillation, which occurred when mean Paw offset was 1 cmH_2O, may have altered the Ppl-Pes tissue barrier frequency responses. Inaccuracy of Pes measurements has been attributed to chest wall distortion producing uneven pleural pressure distribution.[18] This is an unlikely contributing factor though, since from Figure 6.3 the Ppl-Pes tissue barrier frequency responses at low frequencies did not depend on mean Paw (and thus on negative proximal Paw) in our animals.

When Paw pressure offsets were switched from 1 to 10 cmH_2O the Ppl-Pes tissue barrier frequency response changed, in CTRL and ALIG (though the 1 or 10 cmH_2O Paw offsets at which the Ppl-Pes gain occured is different in ALIG versus CTRL). Such a change is not seen when the Paw pressure offsets were switched from 10 to 20 cmH_2O. Additionally, increasing applied Ppl amplitude at a Paw offset of 10 cmH_2O did not significantly change the Ppl-Pes amplitude responses within ALIG or CTRL. However, to avoid the risk of Paw negative pressure trauma we did not test the effect of a larger Ppl amplitude when the Paw offset was 1 cmH_2O. The amplitude dependence lies at lower Paw pressures (1 to 10 cmH_2O). These findings suggest that in conditions in which PEEP or mean Paw are higher (such as occur during HFOV modes) it may be possible to correct the Pes waveform output using an esophageal transfer function to compensate for the Ppl-Pes tissue barrier gain(found during ALI at 10 and 20 cmH_2O Paw offsets) since the Ppl-Pes frequency response exhibited a linear amplitude gain based on the 10 and 20 cmH_2O Paw offsets.

Pes waveform EI-EE bandwidth Extensive literature exists on the bandwidth of cardiovascular pressure waveforms[19] but there is a paucity of literature pertaining to

respiratory system pressure waveforms: Suggested minimum dynamic response requirements for respiratory system pressure measurement apparatus vary from up to the 5'th or 10'th harmonic frequency of the pressure waveform,[20] to 6 Hz and 20 Hz for 3% and 1% Paw errors respectively,[8] and up to 23 Hz.[21] In healthy intubated adult humans, FFT of Pes showed no significant harmonics above 5 Hz[22] but no criteria or methods were detailed for this paper's subsection and no waveform errors were quantified.

The bandwidth of respiratory system pressure waveforms is influenced by the calculation methods applied such as the type of transform used for frequency content analysis, characteristics of the filters implemented and the criteria for waveform error chosen. A universal methodology to determine waveform bandwidth cannot be applied to pressures of different origins since the clinical acquisition equipment and clinical application of those waveforms differ.

We chose to analyse the waveform frequency contents of Pes waveforms associated with ventilation parameters which resulted in adequate ventilation (normal PaCO2), in the healthy and ALI lungs. Additionally, to obtain "extreme case" Pes EI-EE bandwidths,[19] we then elevated peak Paw by 50% (and doubled RR in the event that this too affects energy transmission to the intra-esophageal space) above the physiological ventilation parameters. Accordingly, our Pes EI-EE bandwidths represent the maximum likely EI-EE bandwidths of a range of Pes waveforms encountered in ventilated healthy and ALI monkeys.

The larger maximum EI-EE bandwidths (figure 6.8)noted in the supra-physiological (elevated) PesB and PesA waveforms, compared to the physiological PesB and PesA waveforms, are likely to be due to increased energy content found at higher frequencies in some of the elevated Pes waveforms, where the artificially elevated Paw results in sharper inspiratory and expiratory limbs. The larger Pes EI-EE bandwidths noted following ALI

(PesA) compared to healthy baseline lungs (PesB) may be due to increased energy content found at higher frequencies in some of the PesA waveforms due to the higher Paw values required for ALI (Table 6.2), or due to the ALI condition itself altering the transmission of waveform frequency components to the esophageal space. The latter is likely to play a lesser role since transmission of Paw to Pes was reduced in ALI, and the frequency response of the pleuro-esophageal tissue barrier was uniform up to the determined EI-EE bandwidths before and after ALI.

In the frequency domain the continuous Fourier transform of a single transformed Pes waveform is a continuous spectrum to which the pressure measurement system must respond. A Fourier series of a waveform period T and an FFT of a waveform of finite duration T both comprise harmonics at intervals of 1/T. Therefore the amplitude and frequencies of the harmonics of a periodic waveform depend on T which can be arbitrarily selected (if a train of waveforms is transformed the amplitude in between the harmonics of the frequency domain approaches zero as the number of breaths selected increases). Thus we expressed EI-EE bandwidth as the effective frequency span (in Hz) of the relevant Pes waveform energy content, rather than as the number of harmonics above the fundamental Pes frequency.[19,20]

In determining Pes bandwidth, options are to truncate the original waveform's Fourier series terms above the desired cut-off frequency in the frequency-domain and re-synthesise the waveforms (inverse FFT),[19] or to operate on the original waveform with a filter of known response.[8] The former is a more radical approach which completely removes the waveform higher harmonics above the cut-off frequency and preserves all of the energy below the cut-off frequency, resulting in a filter unrealisable in current clinical practice which has undesirable time-domain characteristics. Thus we chose to apply to the Pes waveforms a linear phase low-pass filter whose response (figure 6.5) approximates

that of an appropriately low-pass filtered underdamped catheter manometer system adjusted by an investigator to be critically damped with no resonance near to the recommended bandwidth. This is the preferred pressure measurement system set-up for routine clinical conditions.[19]

We based Pes waveform error on the Pes amplitude difference between end-inspiration and end-expiration, since these are commonly used points of reference for lung compliance calculations in clinical settings. However, end-inspiratory to end-expiratory amplitude can be identified from the first points of zero flow following an inspiratory and expiratory breath, or alternatively from the onset of expiration to the onset of inspiration (easily identified from the Paw trace).[23] With a suitable Pes manometer these two techniques will make little difference to the resultant Pes end-inspiratory to end-expiratory amplitude values. However, as the shape (sharp edges) of Pes waveforms is eroded by the use of inappropriate (overdamped) catheter manometer systems, the Pes waveform begins to assume the shape of a pure sine wave at the Pes fundamental harmonic frequency (see figure 6.6). The method of identification of end-inspiratory to end-expiratory amplitude then affects estimates of Pes values. Thus we chose the onset of expiration to the onset of inspiration as the criterion for waveform error since this offered a "worst-case" scenario (largest waveform amplitude error and hence widest waveform EI-EE bandwidth).

This technique also discloses the magnitude of error which could be introduced into the end-inspiratory and end-expiratory traces of dynamic lung pressure-volume loops: As the end-inspiratory and end-expiratory Pes values are artefactually reduced and increased respectively by an inappropriately damped Pes catheter, the lung pressure-volume loop is artefactually distorted. Using peak amplitude, or end-inspiratory to end-expiratory amplitude based on the first points of zero gas flow, as opposed the method we chose,

reduces the calculated Pes waveform error and thus plays down the potential distorting effect on dynamic lung compliance loops. Note that the actual effect of Pes waveform errors on ΔTPP, and thus on dynamic lung compliance, is also dependent on the Paw value, since Cl = $\Delta V/\Delta$(Paw-Pes) and as Paw becomes larger the magnitude of the dynamic Cl error introduced by the Pes waveform error may be altered.

Pes Occlusion test in monkeys

The mean catheter distance to optimum Pes position in our monkeys (14.9 cm from canine, 3.9 kg subjects) is similar to that reported for healthy term infants (15.4 cm from nose tip in 3.5 kg subjects).[24] We used a modified form (for anesthetised paralysed subjects)[9] of the occlusion test widely employed by clinicians[1,20] to site the Pes catheter. The test assumes that; pressure is distributed evenly between Paw, Ppl and Pes compartments in an isovolumic chest; alveolar transmission of pressure to Paw is instantaneous; the esophageal wall has an adequate frequency response, and that locally measured Pes is similar to average Ppl.[2]

Where Ppl is not measured, the suggested optimal occlusion test value, based on the slope of the plot of Pes versus Paw is 0.95 - 1.05.[1,20] This figure depends on the lung condition and animal model[1] and is not always achieved, particularly in sick and preterm infants where as few as 8%[25] and 75%[18] of Pes/Paw occlusion test ratios have been reported to fall between 0.90 - 1.10, and only 33% fell within 0.95 - 1.05.[26] On the other hand Pes/Paw was reported to lie between 0.9 - 1.1 in 100% of preterm subjects.[27] Direct Ppl measurements in 4 rabbits yielded Pes to be 70 - 95% of Ppl during spontaneous respiration.[28]

We reported Pes/Paw AUC ratios rather than the slope of the line fitted to the X-Y plot of Paw and Pes. The regression technique assumes that changes in Paw

instantaneously affect Pes and the dynamics play no part at all. The AUC technique uses only the low frequency components of the signal and is insensitive to the frequency response of the Paw-Pes tissue barrier. Unless values are reported for the continuous X-Y plots as opposed to the average slope of the X-Y plot (line of identity), both techniques will average out pressure amplitude information and the X-Y technique is more complex to perform. While our mean occlusion test AUC ratios across monkeys superficially appear satisfactory (Table 6.1), approximately 75% and 50% of the individual monkeys' occlusion test Pes/Paw AUC ratios were between 0.90 - 1.10 and 0.95 - 1.05 respectively at baseline. These figures represent the optimal Pes/Paw occlusion test ratios achievable in the supine, intubated, anesthetised, and paralysed monkeys. The results are similar to those for paralysed dogs in which 71% of subjects lay between 0.90 and 1.10.[9]

Since we directly measured Ppl, occlusion test AUC results are presented as the ratios of Paw/Ppl and Pes/Ppl (Table 6.1), rather than as Pes/Paw, to show that if both Paw and Pes are similarly lower than Ppl during the occlusion test (as is the case in our subjects mean values), then the occlusion test, which is ordinarily based on attaining a Pes/Paw ratio of 1.0, can yield a false impression that Pes adequately reflects Ppl.

The occlusion test ratios did not change significantly with differing Paw offsets or after ALI despite the amplitude frequency responses doing so at the same Pes site. The occlusion test is a relatively static procedure and does not necessarily test Pes/Paw over all the amplitudes applied during mechanical ventilation (the effect of differing Paw mean offsets are however reported for our occlusion test ratios in Table 6.1). It is an isovolumic test and in anesthetised paralysed subjects the test pressure is applied in the reverse direction to conventional ventilation.

Conclusion

Direct simultaneous Ppl and Pes measurement reveals that the Ppl-Pes tissue barrier has a uniform amplitude frequency response within the EI-EE bandwidth of conventional Pes waveforms in healthy and ALI lungs, and does not significantly attenuate Ppl-Pes signal transmission between 1 - 40 Hz. At Pes frequencies higher than conventional clinical regions of interest the Ppl-Pes barrier resonates significantly, is pressure amplitude dependent at low pressure offsets, and is significantly altered by ALI.

Allowing for ≤ 5% Pes waveform error, the maximum Pes EI-EE bandwidth during conventional ventilation is
1.9 Hz and 3.4 Hz for physiological and extreme-case waveforms in healthy lungs, and 4.6 Hz and 8.5 Hz during acute lung injury. For a ≤ 3% waveform error maximum Pes EI-EE bandwidth is 8.5 Hz.

In Vervet monkeys the Ppl-Pes tissue barrier has a frequency response suitable for Ppl estimation during low frequency mechanical ventilation, and Pes manometers should have a uniform frequency response up to 8.5 Hz. However, the Ppl-Pes tissue barrier adversely affects the accurate estimation of dynamic Ppl at high frequencies with varied airway pressure amplitudes and offsets, such as the Ppl encountered during HFOV. These findings may facilitate improving the accuracy of pulmonary function studies in high frequency respiratory mechanics.

6.8 References

1. Coates AL, Stocks J: Esophageal pressure manometry in human infants. Pediatr Pulmonol 1991; 11:350-360

2. Chartrand DA, Ye TH, Maarek JM, Chang HK: Measurement of pleural pressure at low and high frequencies in normal rabbits. J Appl Physiol 1987; 63:1142-1146

3. Peslin R, Navajas D, Rotger M, Farre R: Validity of the esophageal balloon technique at high frequencies. J Appl Physiol 1993; 74(3):1039-44

4. Nagels J, Landser FJ, van de Linden L, Clement J, van Woestijne KP: Mechanical properties of lungs and chest wall during spontaneous breathing. J. Appl. Physiol *1980;* 49:408-416

5. Hartford CG, van Schalkwyk J, Turner MJ, Rogers GG: Application of curve fitting to air-balloon and liquid-filled catheter frequency response traces. IEEE Engineering in Medicine and Biology 1997; 16:27-33

6. Hartford CG, Rogers GG, Turner MJ: Correctly selecting a fluid-filled nasogastric infant feeding catheter to measure intra-esophageal pressure. Pediatr Pulmonol 1997; 23:362-9

7. Hartford CG, Rogers GG, van Schalkwyk J, Turner MJ: Frequency responses of infant air-balloon versus liquid-filled catheters for intra-esophageal pressure measurement. Pediatr Pulm 1997; 24:353-9

8. Turner MJ, Davies VA, Ravel TJL: Bandwidths of respiratory gas flow and pressure waveforms in mechanically ventilated infants. Physiological Measurement 1983; 14:419-431

9. Lanteri CJ, Kano S, Sly PD: Validation of the esophageal pressure occlusion test after paralysis. Pediatr Pulm 1994; 17:56-62

10. Hipkins SF, Rutten AJ, Runciman WB: Experimental analysis of catheter-manometer systems in vitro and in vivo. ANESTHESIOLOGY 1989; 71:893-906

11. Luus HG, Muller FO, Meyer BH: Statistical significance versus clinical relevance; methods for calculating confidence intervals. South African Medical Journal 1989; 76(16):681-685

12. Glantz SA. Confidence intervals, Alternatives to analysis of variance and the t-test based on ranks. In: Primer of Biostatistics. New York, McGraw-Hill, Inc., 1992, pp 188-217, 320-63.

13. Beardsmore CS, Stocks J, Silverman M: Esophageal pressure in infants at elevated lung volumes and positive airway pressure. J Appl Physiol 1983; 55:377-382

14. Baydur A, Cha E, Sassoon CSH: Validation of esophageal balloon technique at different lung volumes and postures. J Appl Physiol 1987; 65:315-321

15. Wegner CD, Jackson AC, Berry JD, Gillepsie JR: Dynamic respiratory mechanics in monkeys measured by forced oscillations. Respiration Physiology 1984; 55:47-61

16. Dechman G, Sato J, Bates JHT: Factors affecting the accuracy of esophageal balloon measurement of pleural pressure in dogs. J Appl Physiol 1992; 72:383-388

17. Kaplan M, Galioto FM, Ruttimann UE, Hamosh P, Avery GB: Evaluation of a gastric tube with esophageal balloon for neonatal use. Am J Perinatology 1:355-359, 1984

18. LeSouef PN, JM Lopes, SJ England, HM Bryan, CA Bryan: Influence of chest wall distortion on esophageal pressure. J Appl Physiol 1983; 55:353-358

19. Paulsen AW: Implications for clinical monitoring of intra-arterial blood pressure based on the frequency content of worst-case pressure waveforms. Biomedical Instrumentation and Technology 1993; May:217-234

20. Stocks J, Sly PD, Tepper RS, Morgan WJ: Infant Respiratory Function Testing. New York, U.S.A., Wiley-Liss, Inc., 1996.

21. Maxted KJ, Shaw A, Macdonald TH: Choosing a catheter system for measuring intra-esophageal pressure. Med Biol Eng Comput 1977; 15:398-401

22. Chartrand DA, Jodoin C, Couture J: Measurement of pleural pressure with oesophageal catheter-tip micromanometer in anaesthetized humans. Can J Anaesth 1991; 38:518-21

23. Ahrens TS: Effects of mechanical ventilation on hemodynamic waveforms. Crit Care Nurse Clin North America 1991; 3(4):629-639

24. Asher MI, Coates AL, Collinge JM, Milic-Emili J: Measurement of pleural pressure in neonates. J Appl Physiol 1982; 52:491-494

25. Thomson A, Elliott J, Silverman M: Pulmonary compliance in sick low birthweight infants. Arch Dis Child 1983; 58:891-896

26. Heaf DP, Turner H, Stocks J, Helms P: The accuracy of esophageal pressure measurements in convalescent and sick intubated infants. Pediatr Pulmonol 1986; 2:5-8

27. Coates AL, Davis GM, Vallinis P, Outerbridge EW: Liquid-filled esophageal catheter for measuring pleural pressure in preterm neonates. J Appl Physiol 1989; 67:889-893

28. Deen L, Porcelijn T: Oesophageal pressure measurement in rabbits and human infants using and air-filled balloon system. Br J Anaesth 1976; 48:521-526

7 THESIS CONCLUSION

7.1 Recap of Rationale and Objectives

Inappropriate mechanical ventilation adversely affects gas exchange, haemodynamics, and lung barotrauma. For clinicians to select optimal mechanical ventilator settings, adequate quantitative information about the respiratory system is required on which to base sound clinical judgements. Pulmonary function measurements in sick patients include the determination of dynamic respiratory system compliance: measuring dynamic intra-esophageal pressure (Pes) to estimate pleural pressure (Ppl) is gaining popularity amongst researchers and clinicians as part of the pulmonary function work-up of infants, particularly for the calculation of the elastic and resistive elements of the respiratory system.

For reasons outlined in Chapter One, traditional fluid-filled (liquid or gas) catheter manometer systems are likely to continue to be made use of extensively to estimate Ppl in clinical practice during high frequency respiratory mechanics, such as occurs during conventional infant ventilation and high frequency ventilation modes. The use of micro-tip pressure transducer catheters to estimate Ppl is not yet validated. Polyvinyl chloride infant feeding catheters, liquid-filled or air-balloon tipped, are easily inserted and well tolerated, and are readily available to clinicians and researchers as disposable and inexpensive alternatives to transducer-tip catheters.

High-fidelity non-invasive estimation of dynamic Ppl by using Pes measurements requires that the Ppl waveform be transmitted unchanged across the tissues between the intra-pleural and intra-esophageal spaces, and that the Pes waveform be transmitted unchanged across the Pes catheter manometer systems. These two requirements were the subjects of investigation in this thesis.

In this thesis: the suitability of Pes catheter manometer systems used in clinical practice to transmit dynamic pressure waveforms accurately was characterised quantitatively; the validity of the assumption that fluid-filled catheter frequency responses fit a second-order system was tested; a new species model of non-human primate acute respiratory distress syndrome was developed; the transmission properties of the in vivo pleuro-esophageal tissue barrier were investigated in health and lung disease at low and high frequencies; and the relevant bandwidth of dynamic physiological intra-esophageal pressure waveforms was determined.

7.2 Conclusions From the Data

When employed in catheter manometer systems, liquid-filled Polyvinyl chloride feeding catheters are underdamped, resonate and exhibit a uniform mean frequency response up to 11 Hz. The maximum respiratory rate within which they have the potential to measure dynamic intra-esophageal pressure within a 5% error limit (F_{RR}) is 82 breaths/min. Significant accuracy differences exist between catheter French Gauge sizes and between catheters of similar diameters but differing brands. Correlation (r^2)between catheter inner diameter and F_{RR} is 0.66 across brands. F_{RR} values for differing catheter FG sizes and brands are presented. It is concluded that liquid-filled feeding catheters are suitable for

estimating pleural pressures in subjects mechanically ventilated without sharp inspiratory waveforms or high respiratory rates. However, judging the suitability of individual feeding catheters to measure dynamic intra-esophageal pressure accurately based on FG size alone is inappropriate: The multi factorial determination of amplitude and phase frequency responses necessitates quantitative assessment of differing catheter brands and diameters prior to their utilisation.

Infant air-balloon catheters greater than FG size 5 exhibit underdamped resonant properties, while smaller FG size air-balloon catheters exhibit near-critical damping or overdamping. Assuming a second order system, air-balloon catheters maintain uniform amplitude frequency responses up to 25 Hz, demonstrating the ability to measure F_{RR} up to 148 breaths/min. The frequency response performance of FG size 6 air-balloon catheters is similar to that of larger air-balloon catheters. It is concluded that, compared to matching liquid-filled catheters, air-balloon catheters made to infant-appropriate specifications have significantly superior frequency response characteristics, lower frequency response variability within catheter samples, and are more suitable for accurate dynamic intra-esophageal pressure measurements during high-frequency respiratory mechanics.

The frequency responses of fluid-filled Polyvinyl chloride catheters in catheter manometer systems do not adequately fit second order systems. Deviations of fit are significantly larger in liquid-filled than in air-balloon catheters, in large FG-sized catheters, and at the early departures from uniformity in the amplitude-frequency response tracing rather than at the resonance frequency point. These findings cast doubt on the validity of defining and applying second order mathematical models to predict such catheter-manometers'

frequency responses, and therefore applying fast-flush or burst-balloon step-response techniques is inappropriate. It is concluded that the system order of differing fluid-filled catheter-manometers should be verified experimentally prior to predicting such catheters' frequency responses. It is recommended that the sine-wave generator technique, rather than the square-wave step-response techniques, be used to measure the frequency responses of compliant fluid-filled catheters in vitro.

Controlled central venous administration of Oleic-acid into monkeys breathing pure oxygen on positive pressure ventilation rapidly results in stable Acute Lung Injury characterised by decreased static and dynamic lung compliance, markedly reduced alveolar gas exchange and increased diffuse alveolar capillary leak accompanied by alveolar edema, polymorphonuclear infiltration and fibrin deposition. These changes are similar to those found in other animal models of Oleic-acid lung injury, but advantageously the healthy and sick monkey lung compliance values recorded are similar to comparable healthy and sick humans. It is concluded that the model is suitable for the pathophysiological evaluation of pulmonary mechanics and gas exchange in acute lung injury.

Direct simultaneous Ppl and Pes measurement reveals that the Ppl-Pes tissue barrier has a uniform amplitude frequency response within the bandwidth of conventional Pes waveforms in healthy and diseased lungs, and does not significantly attenuate Ppl-Pes signal transmission between 1 - 40 Hz. However, at Pes frequencies higher than conventional clinical regions of interest the Ppl-Pes barrier resonates significantly, is pressure amplitude dependent at low pressure offsets, and is significantly altered by lung disease.

Allowing for ≤ 5% Pes waveform error, the maximum relevant Pes waveform bandwidth during conventional ventilation is 1.9 Hz and 3.4 Hz for physiological and extreme-case waveforms in healthy lungs, and 4.6 Hz and 8.5 Hz during acute lung injury.

Thus in non-human primates the Ppl-Pes tissue barrier has a frequency response suitable for Ppl estimation during low frequency mechanical ventilation, and Pes manometers should have a uniform frequency response up to 8.5 Hz. However, the Ppl-Pes tissue barrier, in health and acute lung injury, adversely affects the accurate estimation of dynamic Ppl at high frequencies with varied airway pressure amplitudes and offsets: Ppl is estimated under such conditions during conventional infant mechanical ventilation and during High Frequency Ventilation.

These findings advance the accuracy of pulmonary function studies in high frequency respiratory mechanics, such as conventional infant mechanical ventilation or High Frequency Ventilation.

7.3 Explanation of Potential Study Limitations

There are, of course, potential limitations and assumptions inherent to the studies of this thesis. Individual assumptions and limitations of the studies have been presented under the relevant Chapters' Discussion and Appendix sections.

Linearity

The findings in Chapters Two and Three are constrained by the assumption that the systems under test are amplitude linear, and the fact that the measurements were performed in vitro, which excludes potential altera. ns due to the effect of the esophageal wall and surrounding liquid media on the catheter tips themselves. It should be noted, however, that a technique for in vivo frequency response characterisation of air-balloon catheters does not exist in any event, and that the in vivo fast-flush tests applicable to liquid-filled catheters are also constrained by the second order system assumption, which assumption was invalidated in Chapter Four. Further, the maximum working respiratory rate values presented in Chapters Two and Three assume that the significant energy of oesophageal pressure waveforms is located within the first ten harmonics of the waveforms: this assumption was validated in this thesis for non-human primates in Chapter Six.

Animal models of human disease

Extrapolating the conclusions made in Chapters Five and Six to humans would require the assumption that non-human primate anatomy, physiology, pathophysiology and respiratory mechanics are similar to those found in humans: consideration of the similarity between non-human and human primates is given in Chapter Five's Discussion section.

Intra-thoracic pressure distribution

In Chapter Six the characterisation of the pleuro-esophageal tissue barrier's transmission properties could be dependent on the anatomical situation of the pressure measurement catheters, and it is assumed that the intra-pleural and intra-esophageal catheters are measuring and estimating respectively the mean intra-pleural pressure across the entire intra-pleural space. Note however that the intra-esophageal catheter's position was therefore deliberately chosen according to the occlusion test criteria accepted in clinical practice, and the results obtained are thus from sites relevant to clinical practice. Additionally, the Ppl manometer was inserted in a variety of directions and chest-sides to allow as broad a coverage of Ppl in relation to Pes as possible.

Potential for airways collapse with negative Paw oscillation

In the discussion section of Chapter Six the potential for negative Paw to cause airways collapse during the swept-sine wave runs, and thereby the potential to contribute to the resonance observed at Paw offset of 1 cmH_2O, is acknowledged. However, this is asserted to be an unlikely cause of the observed resonance. Further comment justifying the latter conclusion is appropriate here:

During the swept-sine wave runs Ppl was the reference pressure monitored and controlled. To this end Paw was also monitored and controlled, but only in order to generate $\triangle$1 cmH_2O Ppl (the Ppl signal amplitude was monitored in real-time and the proximal Paw adjusted accordingly via a feedback setup to the High Frequency Ventilator's amplifier). Thus proximal Paw was varied to control Ppl.

At 1 cmH_2O proximal Paw offset, Paw did fall below atmospheric pressure during the swept-sine frequency runs. At 10 cmH_2O proximal Paw offset accompanied by the High Ppl setting (generating large Ppl amplitudes) proximal Paw also went negative during the swept-sine frequency runs. Thus in these two cases there was potential for airways collapse.

However, at 10 cmH_2O proximal Paw offset accompanied by the Low Ppl setting Paw did not go negative during the swept sine frequency runs. Additionally, at 20 cmH_2O proximal Paw offset accompanied by the Low Ppl setting, Paw did not go negative during the swept sine frequency runs. Thus in these two cases there was no potential for airways collapse.

In all recordings the mean proximal Paw was always positive, but it is possible that the negative components of the oscillatory pressures generated in the chest may have produced alterations in the Ppl-Pes barrier in the recordings made at 1 cmH_2O proximal Paw offset, or at 10 cmH_2O proximal Paw offset accompanied by the High Ppl setting (large Paw offset but with large applied Ppl amplitudes). The following points have bearing on this possibility:-

1. The magnitude of the negative pressures generated in the upper airways distal to the 4.5mm oral endotracheal tube in the animals cannot be ascertained (since distal tracheal pressure was not monitored in this experiment). However, a large proportion of the negative proximal Paw is normally lost across the endotracheal tube in vitro, and is therefore dissipated above the collapsible airways. The ratio of distal tracheal pressure to proximal Paw during high frequency ventilation is dependent on the applied frequency, size and length of the endotracheal tube. Distal tracheal pressure/proximal Paw is < 0.1 from 15 Hz upwards in humans; and thus at high frequencies

concomitant with an applied Paw offset no negative pressure is transmitted to the airways in humans.

2. In those swept-sine runs in which the proximal Paw troughs were negative, the Paw and Ppl tracings themselves do not demonstrate distortion of the sine waves with increasing Paw sinusoidal amplitude. Increasing distortion of the Paw or Ppl tracings would be expected if the airways were collapsing with increasingly applied negative pressures (proximal airway pressure would not be transmitted to the smaller airways beyond the points of collapse). Note that the frequency response analyser employed evaluates only the fundamental component of the Ppl and Pes waveforms in this thesis' studies.

3. If negative pressure was causing any airways collapse, this would have occurred predominantly at the lower applied frequencies since (i) the transmission of any pressure fluctuations from the proximal airway down to collapsible airways should be strongly attenuated at higher frequencies (because of the distributed compliance and inertance of the airways), and (ii) airway walls have inertia and therefore resist transient collapse better at high frequencies than at low. From Figure 3 of Chapter 6 (the Baseline Ppl-Pes frequency response) it is seen that Ppl-Pes tissue barrier frequency responses at low frequencies did NOT depend on mean Paw (and thus not on negative Paw) in this study.

4. The proximal Paw amplitude (RMS) does not significantly correlate with the resulting Ppl-Pes amplitude frequency response curves.

5. If airways collapse was playing a major role in causing the resonance recorded in the CTRL group at 1 cm H_2O Paw offset (where airways collapse could have occurred with negative Paw pressures), it does not explain why the ALIG group did not similarly resonate at 1 cmH_2O Paw offset following ALI (where there was equal potential for negative proximal Paw and airways collapse) or further why the ALIG group did demonstrate resonance at 10 cmH_2O Paw offset following ALI (in spite of there being no potential for airways collapse during these recordings), or

why the ALIG group also exhibited resonance at 20 cmH_2O Paw offset following ALI (where again there was no potential for airways collapse).

6. The CTRL animals did not show signs of damage from repeated airways collapse, which, given the number of swept sine runs we performed on each subject, would be likely if the airways were significantly collapsing regularly during the applied negative oscillatory Paw.

The potential for cyclical negative pressure in the upper airways to alter the transmission of pressure between the intra-pleural and intra-oesophgeal spaces is not known. If there is such an effect, it still represents a form of amplitude dependence. Note also that large negative intra-thoracic pressures are found in exercising and acute respiratory distress syndrome patients, although the pressures here are applied to the outside of the airways.

Thus, in the experiments of Chapter 6, and only in those instances in which oscillatory proximal Paw was negative, it is highly unlikely that short intervals of negative proximal Paw pressure influenced the observed Ppl-Pes tissue barrier behaviour.

7.4 Suggestions For Future Research

Suggestions for continuing research, beyond the undertakings of this thesis, are:-

- Evaluate pressure amplitude-linearity, and the effect of temperature and catheter radius of curvature on the frequency responses of compliant fluid-filled catheters, since the softer PVC compound and latex could be affected by these factors.

- Formally assess whether intra-arterial pressure measurement catheters' frequency responses adequately fit a second order system, since published literature on this

topic is sparse and conflicting (see Chapter Four). This may become less important if liquid-filled intra-arterial catheters are replaced by micro-tip transducer catheters in clinical practice.

- Cardiac pressure waveforms superimposed on intra-esophageal pressure traces are frequently referred to in published literature as "cardiac motion artefact", and are largely ignored or filtered out. The direct pleural pressure waveforms recorded in Chapter Six suggest that this notion should be challenged by determining the relative contribution of cardiac motion to intra-pleural pressure, and thus to the continuous lung compliance values derivable from dynamic lung volume-pressure tracings.

- Using the methodology described in this thesis, bandwidth analysis should be extended to human intra-esophageal waveforms acquired during mechanical ventilation for clinical disease and recovery from disease, to corroborate human waveform bandwidths with the non-human primate findings presented in this thesis.

- In recent years the application of alternative methods for estimating the power spectral density of signals (including Wavelet transforms applied to biological signals) is increasing in popularity. Certain of these transforms can be applied to assess the bandwidths of intra-esophageal pressure waveforms and the results contrasted with the bandwidths determined using the conventional fast Fourier transform analysis presented in this thesis.

8 BIBLIOGRAPHY

References to the thesis text are presented at the end of each of Chapters 1 through 6.

The following additional sources were consulted for this thesis but are not cited in the thesis text and are therefore not listed in the reference sections behind each chapter.

Abbasi S, Bhutani VK, Gerdes JS. Long-term pulmonary consequences of respiratory distress syndrome in preterm infants treated with exogenous surfactant. J Pediatr 1993;122(3):446-52.

Abbasi S, Bhutani VK, Spitzer AR, Fox WW. Pulmonary mechanics in preterm neonates with respiratory failure treated with high-frequency oscillatory ventilation compared with conventional mechanical ventilation. Pediatrics 1991;87(4):487-93.

Adams JA. Monitoring respiration in the neonate. Neonatal Intensive Care 1992;5(1):10-3.

Adams JA, Osiovich H, Goldberg RN, Suguihara C, Bancalari E. Hemodynamic effects of continuous negative extrathoracic pressure and continuous positive airway pressure in piglets with normal lungs. Biol Neonate 1992;62(2-3):69-75.

Adams JA, Zabaleta IA, Stroh D, Sackner MA. Measurement of breath amplitudes: comparison of three noninvasive respiratory monitors to integrated pneumotachograph. Pediatr Pulmonol 1993;16(4):254-8.

Agostoni E, D'Angelo E. Pleural liquid pressure. J Appl Physiol 1991;71(2):393-403.

Allen JL, Greenspan JS, Deoras KS, Keklikian E, Wolfson MR, Shaffer TH. Interaction between chest wall motion and lung mechanics in normal infants and infants with bronchopulmonary dysplasia. Pediatr Pulmonol 1991;11(1):37-43.

Andre P, Bal dit Sollier C, Bonneau M, Gnaud G, Hainaud P, Assam K, Drouet L. Which experimental model to choose to study arterial thrombosis and evaluate potentially useful therapeutics. Haemostasis 1996;26(S4):55-69.

Andreasson B, Lindroth M, Svenningsen NW, Drefeldt B, Jonsson GI, Niklason L, Jonson B. Measurement of ventilation and respiratory mechanics during continuous positive airway pressure (CPAP) treatment in infants. Acta Paediatr Scand 1989;78(2):194-204.

Ank AW, TenHave-Opbroek, Plopper CG. Morphogenetic and functional activity of type II cells in early fetal rhesus monkey lungs. The Anatomical Record 1992;23:93-104.

Argiras EP, Blakeley CR, Dunnill MS, Otremski S, Sykes MK. High PEEP decreases hyaline membrane formation in surfactant deficient lungs. Br J Anaesth 1987;59:1278-1285.

Athanasiou KA, Agarwal A, Muffoletto A, Dzida FJ, Constantinides G, Clem M. Biomechanical properties of hip cartilage in experimental animal models. Clinical Orthopaedics and Related Research 1995;316:254-266.

Avery ME, Mead J. Surface properties in relation to atelectasis and hyaline membrane disease. AMA Journal of Diseases of Children 1959;97:517-523.

Ballot DE, Rothberg AD, Davies VA. The late administration of surfactant. S Afr Med J 1995;85(7):644-6.

Ballot DE, Rothberg AD, Davies VA. The selection of infants for surfactant replacement therapy under conditions of limited financial resources. S Afr Med J 1995;85(7):640-3.

Bancalari A, Gerhardt T, Bancalari E, Suguihara C, Hehre D, Reifenberg L, Goldberg RN. Gas trapping with high-frequency ventilation: jet versus oscillatory ventilation. J Pediatr 1987;110(4):617-22.

Bancalari E, Gerhardt T. Bronchopulmonary dysplasia. Pediatr Clin North Am 1986;33(1):1-23.

Baraldi E, Filippone M. Passive respiratory mechanics to assess lung function in infants. Monaldi Arch Chest Dis 1994;49(1):83-5.

Baraldi E, Filippone M, Trevisanuto D, Zanardo V, Zacchello F. Pulmonary function until two years of life in infants with bronchopulmonary dysplasia. Am J Respir Crit Care Med 1997;155(1):149-55.

Baraldi E, Pettenazzo A, Filippone M, Magagnin GP, Saia OS, Zacchello F. Rapid improvement of static compliance after surfactant treatment in preterm infants with respiratory distress syndrome. Pediatr Pulmonol 1993;15(3):157-62.

Barrington KJ, Finer NN. Care of near term infants with respiratory failure. BMJ 1997;315:1215-8.

Bates JH, Sly PD, Okubo S. General method for describing and extrapolating monotonic transients and its application to respiratory mechanics. Med Biol Eng Comput 1987;25(2):131-5.

Bates JH, Decramer M, Zin WA, Harf A, Milic-Emili J, Chang HK. Respiratory resistance with histamine challenge by single-breath and forced oscillation methods. Appl Physiol 1986;61(3):873-80.

Bates JH, Milic-Emili J. Influence of the viscoelastic properties of the respiratory system on the energetically optimum breathing frequency. Ann Biomed Eng 1993;21(5):489-99.

Beardsmore CS, Godfrey S, Shani N, Maayan C, Bar-Yishay E. Airway resistance measurements throughout the respiratory cycle in infants. Respiration 1986;49(2):81-93.

Beardsmore CS, Stocks J, Silverman M. Problems in measurement of thoracic gas volume in infancy. J Appl Physiol 1982;52(4):995-9.

Belaguid A, Marchal F, Mazurek H, Hascoet JM, Peslin R. Low-frequency vs. high-frequency respiratory mechanics after methacholine challenge in artificially ventilated rabbits. Pediatr Pulmonol 1993;16(5):297-302.

Belshe RB, Richardson LS, London WT, Sly DL, Lorfeld JH, Camargo E, Prevar DA, Chanock RM. Experimental respiratory syncytial virus infection of four species of primates. J Medical Virology 1977;1:157-162.

Benameur M, Goldman MD, Ecoffey C, Gaultier C. Ventilation and thoracoabdominal asynchrony during halothane anesthesia in infants. J Appl Physiol 1993;74(4):1591-6.

Bennett FM, Tenney SM. Comparative mechanics of mammalian respiratory system. Respiration Physiology 1982;49:131-140.

Beydon L, Svantesson C, Brauer K, Lemaire F, Jonson B.
Respiratory mechanics in patients ventilated for critical lung disease. Eur Respir J 1996;9(2):262-73.

Bhutani VK, Abbasi S, Sivieri EM. Continuous skeletal muscle paralysis: effect on neonatal pulmonary mechanics. Pediatrics 1988;81(3):419-22.

Bhutani VK, Abbasi S. Long-term pulmonary consequences in survivors with bronchopulmonary dysplasia. Clin Perinatol 1992;19(3):649-71.

Bhutani VK, Abbasi S. Relative likelihood of bronchopulmonary dysplasia based on pulmonary mechanics measured in preterm neonates during the first week of life J Pediatr 1992;120(4):605-13.

Bhutani VK, Abbasi S, Long WA, Gerdes JS. Pulmonary mechanics and energetics in preterm infants who had respiratory distress syndrome treated with synthetic surfactant. J Pediatr 1992;120(S2):18-24.

Bhutani VK, Shaffer TH, Abbasi S, Spitzer AR, Fox WW. Effect of high-frequency jet ventilation on preterm and rabbit tracheal mechanics. Pediatr Pulmonol 1986;2(6):327-31.

Bijaoui E, Tuck SA, Remmers JE, Bates JHT. *Estimating respiratory mechanics in the presence of flow limitation.* J Appl Physiol 1999;86(1):418-26.

Bolliger C, Fourie P, Coetzee A. The effect of prostaglandin E1 on acute pulmonary artery hypertension during oleic acid-induced respiratory dysfunction. Chest 1991;99(6):1501-6.

Borisov AB. Regeneration of skeletal and cardiac muscle in mammals: do non primate models resemble *human pathology? Wound Reg Reg* 1999;7:26-35.

Bose CL, Manne DN, D'Ercole AJ, Lawson EE. Delayed fetal pulmonary maturation in a rabbit model of the diabetic pregnancy. J Clin Invest 1980;60:220-226.

Bose CL, Richardson P, Wood B, Gonzalez F, King J. Phospholipids in tracheal effluent from infants with severe respiratory distress syndrome. American Journal of Perinatology 1984;1(3):208-213.

Bourbon JR, Farrell PM. Fetal lung development in the diabetic pregnancy. Peadiatric Research 1985;19(3):253-267.

Brown K, Sly PD, Milic-Emili J, Bates JH. Evaluation of the flow-volume loop as an intra-operative monitor of respiratory mechanics in infants. Pediatr Pulmonol 1989;6(1):8-13.

Bruce MC, Schuyler M, Martin RJ, Starcher BC, Tomashefski JF Jr, Wedig KE.
Risk factors for the degradation of lung elastic fibers in the ventilated neonate. Implications for impaired lung development in bronchopulmonary dysplasia. Am Rev Respir Dis 1992;146(1):204-12.

Byford LJ, Finkler JH, Froese AB. Lung volume recruitment during high-frequency oscillation in atelectasis-prone rabbits. J Appl Physiol 1988;64(4)1607-1614.

Cantor NL. Can healthcare providers obtain judicial intervention against surrogates who demand medically inappropriate life support for incompetent patients. Crit Care Med 1996;24:883-887.

Casals C, Herrera L, Miguel E, Garcia-Barreno P, Municio AM. Comparison between intra- and extracellular surfactant in respiratory distress induces by oleic acid. Biochimica et Biophysica Acta 1989;1003:201-203.

Castile R, Mead J, Jackson A, Wohl ME, Stokes D. Effects of posture on flow-volume curve configuration in normal humans. J Appl Physiol 1982;53(5):1175-83.

Chartrand DA, Maarek JM, Ye TH, Chang HK. Lung and chest wall mechanics in rabbits during high-frequency body-surface oscillation. J Appl Physiol 1990;68(4):1722-6.

Challis RE, Kitney RI. The frequency transforms and their inter-relationships. Med & Biol Eng and Comput 1991;29:1-17.

Cheney FW, Bishop MJ, Chi EY, Eisenstein BL. Effect of regional alveolar hypoxia on permeability pulmonary edema formation in dogs. J Appl Physiol 1987;62(4):1690-1697.

Christman BW, Lefferts PL, Blair IA, Snapper JR. Effect of platelet-activating factor receptor antagonism on endotoxin-induced lung dysfunction in awake sheep. Am Rev Respir Dis 1990;142:1272-1278.

Chu JS, Dawson P, Klaus M, Sweet AY. Lung compliance and lung volume measured concurrently in normal full-term and premature infants. Pediatrics 1964:525-532.

Clarke J, Silverman M. Infant lung function and tidal breathing patterns. Pediatr Pulmonol 1995;20(3):135-6.

Claure N, Gerhardt T, Hummler H, Everett R, Bancalari E. Computer-controlled minute ventilation in preterm infants undergoing mechanical ventilation. J Pediatr 1997;131(6):910-3.

Clinton CW, Van Heerden PV, Roux A. Postoperative hypoxaemia--its causes and prevention. S Afr J Surg 1992;30(3):95-9.

Coates AL. Chronic lung disease in infants - long-term pulmonary sequelae. Pediatr Pulmonol 1997;S16:40-2.

Coates AL, Desmond KJ, Demizio D, Allen P, Beaudry PH. Sources of error in flow-volume curves. Effect of expired volume measured at the mouth vs that measured in a body plethysmograph. Chest 1988;94(5):976-82.

Coates AL, Desmond K, Willis D, Nogrady MB. Oxygen therapy and long-term pulmonary outcome of respiratory distress syndrome in newborns. Am J Dis Child 1982;136(10):892-5.

Coates AL, Fletcher ME, Dundas I, Stocks J. The single breath test in neonates: does pressurization of the pneumotachograph make a difference? Pediatr Pulmonol 1995;19(5):299-306.

Coates AL, Peslin R, Rodenstein D, Stocks J. Measurement of lung volumes by plethysmography. Eur Respir J 1997;10(6):1415-27.

Coates AL, Vallinis P, Mullahoo K, Seddon P, Davis GM.
Pulmonary impedance as an index of severity and mechanisms of neonatal lung disease. Pediatr Pulmonol 1994;17(1):41-9.

Coetzee A, Rousseau H, Lahner D. Acute pulmonary hypertension and right ventricular failure in adult respiratory distress syndrome. S Afr Med J 1996;86(S3):C147-51.

Coetzee A, Rossouw J.The adult respiratory distress syndrome. S Afr Med J 1981;5 60;(10):377-8.

Cook CD, Sutherland JM, Segal S, Cherry RB, Mead J, McIlroy MB, Smith CA. Studies of respiratory physiology in the newborn infant. III Measurements of mechanics of respiration. J Clin Invest 1957;36:440-48.

Cooper PA, Simchowitz ID, Sandler DL, Rothberg AD, Davies VA, Wainer S.
Prevalence of hyaline membrane disease in black and white low-birth-weight infants. S Afr Med J 1994;84(1):23-5.

Cooper PA, Saloojee H, Bolton KD, Mokhachane M. Survival of low-birth-weight infants at Baragwanath Hospital--1950-1996. S Afr Med J 1999;89(11):1179-81.

Cooper PA, Sandler DL. Outcome of very low birth weight infants at 12 to 18 months of age in Soweto, South Africa. Pediatrics 1997;99(4):537-44.

Cooper PA, Simchowitz ID, Sandler DL, Rothberg AD, Davies VA, Wainer S.
Prevalence of hyaline membrane disease in black and white low-birth-weight infants. S Afr Med J 1994;84(1):23-5.

Corbridge TC, Wood LDH, Crawford GP, Chudoba MJ, Yanos J, Sznajder JI. Adverse effects of large tidal volume and low PEEP in canine acid aspiration. Am Rev Respir Dis 1990;142:311-315.

Cordero L, Tallman RD, Wasielweski R, Nissen C. Comparison of conventional and high-frequency ventilation in piglets after lung lavage. Pediatr Pulmonol 1989;6:158-163.

Da Silva WJ, Abbasi S, Pereira G, Bhutani VK. Role of positive end-expiratory pressure changes on functional residual capacity in surfactant treated preterm infants. Pediatr Pulmonol 1994;18(2):89-92.

Dalmeida RE. Why we need spirometry in the ICU (Abstract). 11th World Congress of Anaesthesiologists, Sydney, March 1996. Hospital Supples 1997;Nov:16-24.

Davey BL, Bates JH. Regional lung impedance from forced oscillations through alveolar capsules. Respir Physiol 1993;91(2-3):165-82.

Davies VA, Ballot DE, Rothberg AD. The cost and effectiveness of surfactant replacement therapy at Johannesburg Hospital, November 1991-December 1992. S Afr Med J 1995;85(7):646-9.

Davis GM, Coates AL, Dalle D, Bureau MA. Measurement of pulmonary mechanics in the newborn lamb: a comparison of three techniques. J Appl Physiol 1988;64(3):972-981.

Davis GM, Coates AL, Dalle D, Bureau MA. Measurement of pulmonary mechanics in the newborn lamb: a comparison of three techniques. J Appl Physiol 1988;64(3):972-81.

Davis GM, Coates AL, Papageorgiou A, Bureau MA. Direct measurement of static chest wall compliance in animal and human r eonates. J Appl Physiol 1988;65(3):1093-8.

Davis GM, Lands LC. Measurement of infant pulmonary mechanics: comparative analysis of techniques. Pediatr Pulmonol 1997;23(2):105-13.

Davies VA, Rothberg AD, Cooper PA, Brown CA. Johannesburg Hospital neonatal statistics--1983. S Afr Med J 1985 13;67(15):594-6.

Deakers TW, Reynolds G, Stretton M, Newth CJ. Cuffed endotracheal tubes in pediatric intensive care. J Pediatr 1994;125(1):57-62.

Dechman G, Lauzon AM, Bates JH. Mechanical behaviour of the canine respiratory system at very low lung volumes. Respir Physiol 1994;95(2):119-29.

Dechman GS, Chartrand DA, Ruiz-Neto PP, Bates JH. The effect of changing end-expiratory pressure on respiratory system mechanics in open- and closed-chest anesthetized, paralyzed patients. Anesth Analg 1995;81(2):279-86.

Dechman G, Sato J, Bates JH. Effect of pleural effusion on respiratory mechanics, and the influence of deep inflation, in dogs. Eur Respir J 1993;6(2):219-24.

De Los Santos R, Seidenfeld JJ, Anzueto A, Collins JF, Coalson JJ, Johanson WG, Peters JR and JI. One hundred percent oxygen lung injury in adult baboons. Am Rev Respir Dis 1987;136:657-661.

Deoras KS, Greenspan JS, Wolfson MR, Keklikian EN, Shaffer TH, Allen JL.
Effects of inspiratory resistive loading on chest wall motion and ventilation: differences between preterm and full-term infants. Pediatr Res 1992;32(5):589-94.

Desager KN, Buhr W, Willemen M, van Bever HP, de Backer W, Vermeire PA, Landser FJ. Measurement of total respiratory impedance in infants by the forced oscillation technique. J Appl Physiol 1991;71(2):770-6.

Desager KN, Cauberghs M, Van de Woestijne KP. Two-point calibration procedure of the forced oscillation technique. Med Biol Eng Comput 1997;35(6):752-6.

De Winter JP, Egberts J, Merth IT, Peerdeman A, van Bel F, Bakker GC, Quanjer PH. Biochemical lung maturity, static respiratory compliance, and pulmonary gas transfer in intubated preterm infants with and without respiratory distress syndrome. Pediatr Pulmonol 1995;20(3):152-9.

De Winter JP, Merth IT, van Bel F, Egberts J, Brand R, Quanjer PH. Changes of respiratory system mechanics in ventilated lungs of preterm infants with two different schedules of surfactant treatment. Pediatr Res 1994;35(5):541-9.

Dorrington K., McRae K, Bellhouse BJ. Extracorporeal CO2 removal (ECCO2R) improves oxygenation in a lung lavage model of acute respiratory failure. Trans Am Soc Artif Intern Organs 1987;XXXIII;574-578.

Dorrington KL, Radcliffe FM. Effect of a single inflation of the lungs on oxygenation during total extracorporeal carbon dioxide removal in experimental repiratory distress syndrome. Intensive Care Med 1991;17:469-474.

Ducharme FM, Davis GM, Ducharme GR. Pediatric reference values for respiratory resistance measured by forced oscillation. Chest 1998;113(5):1322-8.

Dueck R, Wagner PD, West JB. Effects of positive end-expiratory pressure on gas exchange in dogs with normal and edematous lungs. Anesthesiology 1977;47:359-366.

Dundas I, Beardsmore C, Wellman T, Stocks J. A collaborative study of infant respiratory function testing. Eur Respir J 1998;12(4):944-53.

Dundas I, Dezateux CA, Fletcher ME, Jackson EA, Stocks J. Comparison of single-breath and plethysmographic measurements of resistance in infancy. Am J Respir Crit Care Med 1995;151(5):1451-8.

Eijking EP, Gommers D, Kullander J, de Buijzer E, Beukenholdt RW, Lachmann B. Different surfactant treatment strategies for respiratory failure induced by hydrochloric acid aspiration in rats. Oxygen Transport to Tissue 1992;XIV;349-355.

El-Azab J, Steward PB. The difference in effect of predosing with antiallergic compounds between the rat PCA model and the monkey asthma model. Int. Archs Allergy appl. Immun. 1997;55;343-349.

Enhorning G. Pulsating bubble technique for evaluating pulmonary surfactant. J Appl Physiol 1977;43(2):198-203.

Ennema JJ, Kobayashi T, Robertson B, Curstedt T. Inactivation of exogenous surfactant in experimental respiratory failure induced by hyperoxia. Acta Anaesthesiol Scand 1988;32:665-671.

Fanconi S, Kraemer R, Weber J, Tschaeppeler H, Pfenninger J. Long-term sequelae in children surviving adult respiratory distress syndrome. J Pediatr 1985;106(2):218-22.

Fisher JT, Mortola JP. Statics of the respiratory system in newborn mammals. Respiratory Physiology 1980;41:155-172.

Fletcher ME, Dezateux CA, Stocks J. Respiratory compliance in infants--a preliminary evaluation of the multiple interrupter technique. Pediatr Pulmonol 1992;14(2):118-25.

Fletcher PR, Epstein RA. Frequency dependence of dead space during high-frequency ventilation in rhesus monkeys. Respir Physiol 1988;73(1):125-32.

Fletcher ME, Ewert M, Stack C, Hatch DJ, Stocks J. Influence of tidal volume on respiratory compliance in anesthetized infants and young children. J Appl Physiol 1990;68(3):1127-33.

Fletcher ME, Stack C, Ewart M, Davies CJ, Ridley S, Hatch DJ, Stocks J. Respiratory compliance during sedation, anesthesia, and paralysis in infants and young children. J Appl Physiol 1991;70(5):1977-82.

Fletcher ME, Stocks J, Ridley S, Braude N, Yates AP, Hatch DJ. Total respiratory compliance during anaesthesia in infants and young children. Br J Anaesth 1989;63(3):266-75.

Fort PF, Farmer C, Westerman J, Johannigman J, Beninati W, Dolan S, Derdak S. High-frequency oscillatory ventilation for adult respiratory distress syndrome; a pilot study. Crit Care Med 1997;25(6):937-47.

Freezer NJ, Nicolai T, Sly PD. Effect of volume history on measurements of respiratory mechanics using the interrupter technique. Pediatr Res 1993;33(3):261-6.

Freezer NJ, Sly PD. Predictive value of measurements of respiratory mechanics in preterm infants with HMD. Pediatr Pulmonol 1993;16(2):116-23.

Frey U, Schibler A, Kraemer R. Pressure oscillations after flow interruption in relation to lung mechanics. Respir Physiol 1995;102(2-3):225-37.

Frey U, Silverman M, Kraemer R, Jackson AC. High-frequency respiratory input impedance measurements in infants assessed by the high speed interrupter technique. Eur Respir J 1998;12(1):148-58.

Frey U, Silverman M, Kraemer R, Jackson AC. High-frequency respiratory impedance measured by forced-oscillation technique in infants. Am J Respir Crit Care Med 1998;158(2):363-70.

Frey U, Suki B, Kraemer R, Jackson AC. Human respiratory input impedance between 32 and 800 Hz, measured by interrupter technique and forced oscillations. J Appl Physiol 1997;82(3):1018-23.

Fridman EP, Popova VN. Species of the genus papio (cercopithecidae) as subjects of biomedical research: I. Biological basis of experiments on baboons. J Med Primatol 1988;17:291-307.

Friedman EP, Popova VN. Species of the genus papio (cercopithecidae, primates) as subjects of biomedical research: II. quantitative characteristics of contemporary use of baboon species in medical and biological investigations. J Med Primatol 1988;17:309-318.

Ganesan S, Lai-Fook, SJ. Alveolar liquid pressure measured in the intact rabbit chest by micropuncture. J Appl Physiol 1993;75(4):1525-1528.

Gappa M, Costeloe K, Southall DP, Rabbette PS, Stocks J. Effect of continuous negative extrathoracic pressure on respiratory mechanics and timing in infants recovering from neonatal respiratory distress syndrome. Pediatr Res 1994;36(3):364-72.

Gappa M, Rabbette PS, Costeloe KL, Stocks J. Assessment of passive respiratory compliance in healthy preterm infants: a critical evaluation.
Pediatr Pulmonol 1993;15(5):304-11.

Gaultier C, Fletcher ME, Beardsmore C, England S, Motoyama E. Respiratory function measurements in infants: measurement conditions. Working group of the European Respiratory Society and the American Thoracic Society. Eur Respir J 1995;8(6):1057-66.

Gauthier R, Beyaert C, Feillet F, Peslin R, Monin P, Marchal F. Respiratory oscillation mechanics in infants with bronchiolitis during mechanical ventilation. Pediatr Pulmonol 1998;25(1):18-31.

Geddes LA. Medical Device Accidents. CRC Press, Boston, 1998.

Geddes LA. Respiration. In: The Biomedical Engineering Handbook. Bronzino JD (Ed), CRC Press Inc. and IEEE Press, 1996.

Gerhardt T, Bancalari E. Components of effective elastance and their maturational changes in human newborns. J Appl Physiol 1982;53(3):766-9.

Gerhardt T, Hehre D, Feller R, Reifenberg L, Bancalari E. Pulmonary mechanics in normal infants and young children during first 5 years of life. Pediatr Pulmonol 1987;3(5):309-16.

Gerhardt T, Reifenberg L, Duara S, Bancalari E. Comparison of dynamic and static measurements of respiratory mechanics in infants. J Pediatr 1989;114(1):120-5.

Gerhardt T, Reifenberg L, Goldberg RN, Bancalari E. Pulmonary function in preterm infants whose lungs were ventilated conventionally or by high-frequency oscillation. J Pediatr 1989;115(1):121-6.

Gerhardt TO, Bancalari E. Measurement and monitoring of pulmonary function. Clin Perinatol 1991;18(3):581-609.

Giannobile WV, Finkelman RD, Lynch SE. Comparison of canine and non-human primate animal models for periodontal regenerative therapy: results followign a single administration of PDGF/IGF-I. J Periodontol 1994;65:1158-1168.

Gibson GJ. Clinical Tests of Respiratory Function. Raven Press, New York, 1984.

Goerke J. Lung Surfactant. Biochimica et Biophysica Acta 1974;344:241-261.

Greenough A, Morley CJ. Oesophageal pressure measurements in ventilated preterm babies. Archives of Disease in Childhood 1982;57:851-855.

Gresham GA, Howard AN. Cardiovascular diseases. Primates in Med 1969;3:1-8.

Godfrey S. On pulmonary functions in survivors of neonatal respiratory distress. Pediatr Pulmonol 1988;5(1):60-1.

Godfrey S, Bar-Yishay E, Arad I, Landau LI, Taussig LM. Flow-volume curves in infants with lung disease. Pediatrics 1983;72(4):517-22.

Gonzalez A, Tortorolo L, Gerhardt T, Rojas M, Everett R, Bancalari E. Intrasubject variability of repeated pulmonary function measurements in preterm ventilated infants. Pediatr Pulmonol 1996;21(1):35-41.

Greenspan JS, Abbasi S, Bhutani VK. Sequential changes in pulmonary mechanics in the very low birth weight (less than or equal to 1000 grams) infant. J Pediatr 1988;113(4):732-7.

Hall SB, Bermel MS, Ko YT, Palmer HJ, Enhorning G, Notter RH. Approximations in the measurement of surface tension on the oscillating bubble surfactometer. J Appl Physiol 1993;75(1):468-477.

Hammer J, Newth CJ. Effort and volume dependence of forced-deflation flow-volume relationships in intubated infants. J Appl Physiol 1996;80(1):345-50.

Hammer J, Newth CJ. Infant lung function testing in the intensive care unit. Intensive Care Med 1995;21(9):744-52.

Hammer J, Newth CJ. Influence of endotracheal tube diameter on forced deflation flow-volume curves in rhesus monkeys. Eur Respir J 1997;10(8):1870-3.

Hammer J, Sivan Y, Deakers TW, Newth CJ. Flow limitation in anesthetized rhesus monkeys: a comparison of rapid thoracoabdominal compression and forced deflation techniques. Pediatr Res 1996;39(3):539-46.

Hampton F, Beardsmore CS, Morgan W, Williams A, Taussig L, Thompson JR.
A scoring system for lung function tests in infants. Pediatr Pulmonol 1992;14(3):149-55.

Hanrahan JP, Tager IB, Castile RG, Segal MR, Weiss ST, Speizer FE. Pulmonary function measures in healthy infants. Variability and size correction. Am Rev Respir Dis 1990;141(5):1127-35.

Hansen AT. Pressure measurement in the human organism. Acta Physiologica Scandinavica 1949;19(S68):S7-227.

Haouzi P, Marchal F, Crance JP, Monin P, Vert P. Respiratory mechanics in spontaneously breathing term and preterm neonates. Biol Neonate 1991;60(6):350-60.

Heaf D P, Turner H, Stocks J, Helms P. Comparison of the occlusion and inflation techniques for measuring total respiratory compliance in sick, intubated infants. pediatr pulmonol 1987;3:78-82.

Helms P, Beardsmore CS, Stocks J. Absolute intraesophageal pressure at functional residual capacity in frequency. J Appl Physiol 1981;51(2):270-5.

Hernandez LA, Coker PJ, May S, Thompson AL, Parker JC. Mechanical ventilation increases microvascular permeability in oleic acid-injured lungs. J Appl Physiol 1990;69(6):2057-2061.

Hibbert ME, Lannigan A, Landau LI, Phelan PD. Lung function values from a longitudinal study of healthy children and adolescents. Pediatr Pulmonol 1989;7(2):101-9.

Hjalmarson O. Mechanics of breathing in newborn infants with pulmonary disease. Acta Paediatrica Scandanavica 1974;S247:S5-65.

Hirai T, McKeown KA, Gomes RF, Bates JH. Effects of lung volume on lung and chest wall mechanics in rats. J Appl Physiol 1999;86(1):16-21.

Hodson WA, Luchtel DL, Kessler DL, Murphy J, Palmer S, Truog WE, Standaert TA. The immature monkey as a model for studies of bronchopulmonary dysplasia. J Pediatrics 1979;95(5):895-904.

Hummler H, Gerhardt T, Gonzalez A, Claure N, Everett R, Bancalari E. Influence of different methods of synchronized mechanical ventilation on ventilation, gas exchange, patient effort, and blood pressure fluctuations in premature neonates. Pediatr Pulmonol 1996;22(5):305-13.

Idell S, Kumar A, Koenig KB, Coalson JJ. Pathways of fibrin turnover in lavage of premature baboons with hyperoxic lung injury. Am J Respir Crit Car Med 1994;149:767-75.

Ingenito EP, Mark L, Davison B. Effects of acute lung injury on dynamic tissue properties. J Appl Physiol 1994;77(6):2689-2697.

Innes JA, DeCort SC, Kox W, Guz A. Within-breath modulation of left ventricular function during normal breathing and positive-pressure ventilation in man. J Physiology 1993;460:487-502.

Jackson JC, Clark JG, Standaert TA, Truog WE, Murphy JH, Juul SE, Chi EY, Hodson WA. Collagen synthesis during lung development and during hyaline membrane disease in the nonhuman primate. Am Rev Respir Dis 1990;141:846-853.

Jackson E, Stocks J, Pilgrim L, Dundas I, Dezateux C. A critical assessment of uncalibrated respiratory inductance plethysmography (respitrace) for the measurement of tidal breathing parameters in newborns and infants. Pediatr Pulmonol 1995;20(2):119-24.

Jackson EA, Coates AL, Gappa M, Stocks J. In vitro assessment of infant pulmonary function equipment. Pediatr Pulmonol 1995;19(4):205-13.

Jackson JC, Chi EY, Wilson CB, Truog WE, Chuan Teh, E, Hodson WA. Sequence of inflammatory cell migration into lung during recovery from hyaline membrane disease in premature newborn monkeys. Am Rev Respir Dis 1987;135:937-940.

Jackson JC, Palmer S, Wilson CB, Standaert TA, Truog WE, Murphy JH, Hodson WA. Postnatal changes in lung phospholipids and alveolar macrophages in term newborn monkeys. Respiration Physiology 1988;73:289-300.

Jackson JC, Standaert TA, Truog WE, Murphy JH, Palmer S, Chi EY, Woodrum DE, Watchko JF, Hodson WA. Changes in lung volume and deflation stability in hyaline membrane disease. J Appl Physiol 1985;59(6):1783-1789.

Jackson JC, Truog WE, Standaert TA, Juul SE, Murphy JH, Chi EY, Mackenzie AP, Hodson WA. Effect of high-frequency ventilation on the development of alveolar edema in premature monkeys at risk for hyaline membrane disease. Am Rev Respir Dis 1991;143:865-871.

Jacob SV, Coates AL, Lands LC, MacNeish CF, Riley SP, Hornby L, Outerbridge EW, Davis GM, Williams RL. Long-term pulmonary sequelae of severe bronchopulmonary dysplasia. J Pediatr 1998;133(2):193-200.

Jacobs RF, Wilson CB, Palmer S, Springmeyer SC, Henderson WR, Glover DM, Kessler Jnr DL, Murphy JH, Hughes JP, Van Belle G, Chi EY, Hodson WA. Factors related to the appearance of alveolar macrophages in the developing lung. Am Rev Respir Dis 1985;131:548-553.

Jobe A. Protein leaks and surfactant dysfunction in the pathogenesis of respiratory distress syndrome. Eur Respir J 1989;2(S3):27-32.

Jobe AH. Pulmonary surfactant therapy. Drug Therapy 1993;328(12):861-868.

Johnson WC, John MD, Tyson E, Wayne Mitzner MD, Beck JC, Andressen B, William T, London DVM, Villar, Jose. Amniotic fluid prolactin and fetal lung maturation. Am J Obstet Gynecol 1985;153;372-80.

Jonson B. Ventilation patterns, surfactant and lung injury. Biol Neonate 1997;71(S1):13-7.

Jonson B, Beydon L, Brauer K, Mansson C, Valind S, Grytzell H.
Mechanics of respiratory system in healthy anesthetized humans with emphasis on viscoelastic properties. J Appl Physiol 1993;75(1):132-40.

Jonson B, Lachmann B, Fletcher R. Monitoring of physiological parameters during high frequency ventilation (HFV). Acta Anaesthesiol Scand 1989;S90:165-9.

Jonson B, Lachmann B. Setting and monitoring of high-frequency jet ventilation in severe respiratory distress syndrome. Crit Care Med 1989;17(10):1020-4.

Jonson B, Richard JC, Straus C, Mancebo J, Lemaire F, Brochard L. Pressure-volume curves and compliance in acute lung injury: evidence of recruitment above the lower inflection point. Am J Respir Crit Care Med 1999;159(4):1172-8.

Jonson B, Svantesson C. Elastic pressure-volume curves: what information do they convey? Thorax 1999;54(1):82-7.

Juul SE, Kinsella MG, Jackson C, Truog WE, Standaert TA, Hodson WA. Changes in hyaluron deposition during early respiratory distress syndrome in premature monkeys. Pediatr Res 1994;35:238-243.

Kaditis AG, Motoyama EK, Seki I, Gronert BJ, Venkataraman ST, Milic-Emili J, Zin WA. Flow and volume dependence of respiratory mechanics in anesthetized children. Pediatr Res 1999;46(4):419-28.

Kano S, Lanteri CJ, Duncan AW, Sly PD. Influence of nonlinearities on estimates of respiratory mechanics using multilinear regression analysis. J Appl Physiol 1994;77(3):1185-97.

Kano S, Lanteri CJ, Pemberton PJ, Lesouef PN, Sly PD. Fast versus slow ventilation for neonates. Am Rev Respir Dis 1993;148(3):578-84.

Kawano T, Mori S, Cybulsky M, Burger R, Ballin A, Cutz E, Bryan AC. Effect of granulocyte depletion in a ventilated surfactant-depleted lung. J Appl Physiol 1987;62(1):27-33.

King RJ, Coalson JJ, deLemos RA, Gerstmann DR, Seidner SR. Surfactant protein-A deficiency in a primate model of bronchopulmonary dysplasia. Am J Respir Crit Care Med 1995;151:1989-1997.

Kleinman B. Understanding natural frequency and damping and how they relate to the measurement of blood pressure. J Clin Monit 1989;5:137-147.

Kobayashi T, Ganzuka M, Taniguchi J, Nitta K, Murakami S. Lung lavage and surfactant replacement for hydrochloric acid aspiration in rabbits. Acta Anaesthesiol Scand 1990;34:216-221.

Kondo T, Matsumoto I, Lanteri CJ, Sly PD. Respiratory mechanics during mechanical ventilation: a model study on the effects of leak around a tracheal tube. Pediatr Pulmonol 1997;24(6):423-8.

Korcarz CE, Padrid PA, Shroff SG, Weinert L, Lang R . Doppler echocardiographic reference values for healthy rhesus monkeys under ketamine hydrochloride sedation. J Med Primatol 1997;26:287-298.

Kosch PC, Gillespie JR, Berry JD. Flow-volume curves and total pulmonary resistance in normal bonnet and rhesus monkeys. J Appl Physiol Respirat Environ Exercise Physiol 1979;46(1):176-183.

Kraemer R. Assessment of lung function in infants and young children with lung disease. Eur J Pediatr 1995;154(S9):13-7.

Krishnan V. Linear Systems Properties. CRC Press, New York, 1998.

Kuo FF. Amplitude phase and delay. In: Network Analysis and Synthesis. John Wiley and Sons, New York, 2nd edition, 1962:224-39.

Lachmann B, Jonson B, Lindroth M, Robertson B. Modes of artificial ventilation in severe respiratory distress syndrome. Lung function and morphology in rabbits after wash-out of alveolar surfactant. Crit Care Med 1982;10(11):724-32.

Lachmann B, Schairer W, Hafner M, Armbruster S, Jonson B. Volume-controlled ventilation with superimposed high frequency ventilation during expiration in healthy and surfactant-depleted pig lungs. Acta Anaesthesiol Scand 1989;S90:117-9.

LaFramboise WA, Tuck RE, Woodrum DE, Guthrie RD. Maturation of eupneic respiration in the neonatal monkey. Respiration 1984;18(10):943-948.

Lai-Fook SJ, Rodarte JR. Pleural pre sure distribution and its relationship to lung volume and interstitial pressure. J Appl Physiol 1991;70(3):: 37-978.

Lambert M, van Golde G, Batenburg JJ, Robertson B. The pulmonary surfactant system. NIPS 1994;9:13-21.

Lansing R, Savelle J. Chest surface recording of diaphragm potentials in man. Electroencephalography and clinical neurophysiology 1980;72:59-68.

Lanteri CJ, Kano S, Duncan AW, Sly PD. Changes in respiratory mechanics in children undergoing cardiopulmonary bypass. Am J Respir Crit Care Med 1995;152(6):1893-900.

Lanteri CJ, Kano S, Nicolai T, Sly PD. Measurement of dynamic respiratory mechanics in neonatal and pediatric intensive care: the multiple linear regression technique. Pediatr Pulmonol 1995;19(1):29-45.

Lanteri CJ, Petak F, Gurrin L, Sly PD. Influence of inertance on respiratory mechanics measurements in mechanically ventilated puppies. Pediatr Pulmonol 1999;28(2):130-8.

Lanteri CJ, Sly PD. Changes in respiratory mechanics with age. J Appl Physiol 1993;74(1):369-78.

Lachman B, Jonson B, Lindroth M, Robertson B. Modes of artificial ventilation in severe respiratory distress syndrome. Lung function and morphology in rabbits after wash-out of alveolar surfactant. Crit Care Med 1982;10(11):724-32.

Lachmann B, Robertson B, Vogel J. In Vivo Lung lavage as an experimental model of the respiratory distress syndrome. Acta anaesth. Scand 1980;24:231-236.

Lachmann B, Schairer W, Hafner M, Armbruster S, Jonson B. Volume-controlled ventilation with superimposed high frequency ventilation during expiration in healthy and surfactant-depleted pig lungs. Acta Anaesthesiol Scand 1989;33(S90):117-119.

Latimer KE. The transmission of sound waves in liquid-filled catheter tubes used for intravascular blood-pressure recording. Med & Biol Eng 1968;6:29-42.

Latimer RD, Latimer KE. Continuous flushing systems. Anaesthesia 1974;29:307-317.

Lauzon AM, Dechman G, Bates JH. On the use of the alveolar capsule technique to study bronchoconstriction. Respir Physiol 1995;99(1):139-46.

Le Souef PN. Validity of methods used to test airway responsiveness in children. Lancet. 1992 23;339(8804):1282-4.

Le Souef PN, Hughes DM, Landau LI. Shape of forced expiratory flow-volume curves in infants. Am Rev Respir Dis 1988;138(3):590-7.

Le Souef PN, Hughes DM, Landau LI. Effect of compression pressure on forced expiratory flow in infants. J Appl Physiol 1986;61(5):1639-46.

Le Souef PN, Landau LI. Validity of forced expiratory flow volume loops in neonates. Arch Dis Child 1988;63(4):460-1.

Lindroth M, Svenningsen NW, Ahlstrom H, Jonson B. Evaluation of mechanical ventilation in newborn infants. II. Pulmonary and neuro-developmental sequelae in relation to original diagnosis Acta Paediatr Scand 1980;69(2):151-8.

Liu CT. Comparison of cardiorenal functions between women and female rhesus macaques. Am J Vet Res 1997;38(9):1439-1442.

Liu CT, DeLauter RD. Pulmonary functions in conscious and anesthetized rhesus macaques. Am J Vet Res 1997;38(11):1843-1848.

Li JKJ, Van Brummelen AGW, Noordergraaf A. Fluid-filled blood pressure measurement systems. J Appl Physiol 1976;40(5):839-43.

Luyt S, Coetzee A, Lahner D, Jansen J. Nitric oxide has little effect on acute pulmonary hypertension and right ventricular function during acute respiratory distress syndrome. S Afr Med J 1997;87(S5):639-42.

Maeta H, Vidyasagar D, Raju T, Bhat R, Matsuda H. Response to bovine surfactant (surfactant TA) in two different HMD models (lambs and baboons). Eur J Pediatr 1988;147:162-167.

Maksym GN, Bates JH. A distributed nonlinear model of lung tissue elasticity. J Appl Physiol 1997;82(1):32-41.

Malcolm JD, Elliott CD. Interfacial tension from height and diameter of a single sessile drop or captive bubble. The Canadian Journal of Chemical Engineering 1980;58:151-153.

Mallol J, Willet K, Burton P, Sly PD. Influence of duration of occlusion time on respiratory mechanics measured with the single-breath technique in infants. Pediatr Pulmonol 1994;17(4):250-7.

Malmkvist G, Fletcher R, Drefeldt B, Jonson B, Luhrs C, Mori N. Deadspace during high frequency jet ventilation: the effects of frequency, inspiratory time and entrainment. Clin Physiol 1985;5(S3):143-6.

Mammel MC, Boros SJ, Bing DR, Holloman KK, Connett JR. Determining optimum inspiratory time during intermittent positive pressure ventilation in surfactant-depleted cats. Pediatric Pulmonology 1989;7:223-229.

Mankikian B, LeMaire F, Benito S, Brun-Buisson C, Harf A, Maillot J P, Becker J. A new device for measurement of pulmonary pressure-volume curves in patients on mechanical ventilation. Critical Care Medicine 1983;11(11):897-901.

Marchal F, Bouaziz N, Baeyert C, Gallina C, Duvivier C, Peslin R. Separation of airway and tissue properties by transfer respiratory impedance and thoracic gas volume in reversible airway obstruction. Eur Respir J 1996;9(2):253-61.

Marchal F, Crance JP. Measurement of ventilatory system compliance in infants and young children. Respir Physiol 1987;68(3):311-8.

Marchal F, Haouzi P, Gallina C, Crance JP. Measurement of ventilatory system resistance in infants and young children. Respir Physiol 1988;73(2):201-9.

Marchal F, Haouzi P, Peslin R, Duvivier C, Gallina C. Mechanical properties of the upper airway wall in children and their influence on respiratory impedance measurements. Pediatr Pulmonol 1992;13(1):28-33.

Marchal F, Peslin R, Duvivier C, Gallina C, Crance JP. Measurement of ventilatory mechanical impedance in infants using a head pressure generator. Pediatr Pulmonol 1989;7(4):209-16.

Marchal F, Peslin R, Duvivier C, Gallina C, Crance JP. Mechanics of the ventilatory system in sedated infants: forced oscillations versus single-breath method. Pediatr Pulmonol 1988;5(1):19-26.

Marks JD, Schapera A, Kraemer RW, Katz JA. Pressure and flow limitations of anesthesia ventilators. Anesthesiology 1989;71(3):403-8.

Marson OH. Mechanics of breathing in newborn infants with pulmonary disease. Acta Paediatrica Scandinavica 1974;S247:1160-1164.

Martin RJ. Neonatal surfactant therapy - where do we go from here? J Pediatr 1991;118(4):555-6.

Martino MA, Hubbard GB, Butler TM, Hilliard JK. Clinical disease associated with simian agent 8 infection in the baboon. American Association for Laboratory Animal Science 1988;48(1):18-22.

Masters IB, Vance J, Hills BA. Surfactant abnormalities in ALTE and SIDS. Archives of Disease in Childhood 1994;71:501-505.

Mauderly JL. Effect of age on pulmonary structure and function of immature and adult animals and man. Federation Proc 1979;38:173-177.

Mead J, McIlroy MB, Selverstone NJ, Kriete BC. Measurement of intraesophageal pressure. J Appl Physiol 1979;7:491-495.

Mercurio MR, Fiascone JM, Lima DM, Jacobs HC. Surface tension and pulmonary compliance in premature rabbits. J Appl Physiol 1989;66(5):2039-2044

Merth IT, de Winter JP, Zonderland HM, Borsboom GJ, Quanjer PH. Pulmonary function in infants with neonatal chronic lung disease with or without hyaline membrane disease at birth. Eur Respir J 1997;10(7):1606-13.

Merth IT, Quanjer PH. Respiratory system compliance assessed by the multiple occlusion and weighted spirometer method in non-intubated healthy newborns. Pediatr Pulmonol 1990;8(4):273-9.

Merth IT, Verschragen GJ, Olievier IC, De Winter PJ, Quanjer PH. Water-sealed spirometer for measurements in newborns and infants. J Appl Physiol 1993;74(1):470-5.

Milhorn HT. The application of frequency analysis methods to technological and physiological systems. In: The Application of Control Theory to Physiological Systems. WB Saunders Company, Philadelphia, 1996:167-76.

Milic-Emili J, Robatto FM, Bates JH. Respiratory mechanics in anaesthesia. Br J Anaesth 1990;65(1):4-12.

Miller DR, Aufdermorte TB, Fox WC, Waldrop TC, Mealey BL, Brunsvold MA. Periodontitis in the baboon: a potential model for human disease. J Periodon Res 1995;30;404-409.

Milner AD, Hull D, Hatch DJ, Cogswell JJ. A new method for measuring static compliance in infants and young children. Clinical Science 1972;43:689-694.

Milner AD, Saunders RA, Hopkin IE. Relationship of intra-oesophageal pressure to mouth pressure during the measurement of thoracic gas volume in the newborn. Biol Neonate 1978;33:314-19.

Mishima M, Balassy Z, Bates JH. Assessment of local lung impedance by the alveolar capsule oscillator in dogs: a model analysis. J Appl Physiol 1996;80(4):1165-72.

Mitzner W, Johnson JWC, Beck J, London W, Sly PD. Influence of betamethasone on the development of mechanical properties in the fetal rhesus monkey lung. Am Rev Respir Dis 1982;125:233-38.

Mitzner W, Johnson WC, Scott R, London WT, Palmer AE. Effect of betamethasone on pressure-volume relationship of fetal rhesus monkey lung. J Appl Physiol Respirat Environ Exercise Physiol 1979;47(2):377-82.

Moawad H, Ismail MA, River P. Use of the drop volume of amniotic fluid in predicting fetal lung maturity. The Journal of Reproductive Medicine 1991;36(6):425-428.

Montero Matamala A, Vidal Lopez F, Aguilar Sanchez J L, Donoso Bach L. Percutaneous anterior approach to the coeliac plexus using ultrasound. Br J Anaesth 1989;62:637-640.

Morgan WJ, Geller DE, Tepper RS, Taussig LM. Partial expiratory flow-volume curves in infants and young children. Pediatr Pulmonol 1988;5(4):232-43.

Mosekilde EM, Mouritsen OG (Eds). Modelling the Dynamics of Biological Systems, Springer-Verlag, Berlin, 1994.

Mutoh T, Lamm WJE, Embree LJ, Hildebrandt J, Albert RK. Abdominal distension alters regional pleural pressures and chest wall mechanics in pigs in vivo. J Appl Physiol 1991;70(6):2611-2618.

Naulty CM, Horn S, Conry J, Avery GB. Improved lung compliance after ligation of patent ductus arteriosus in hyaline membrane disease. Brief Clinical and Laboratory Observations 1978;93(4):682-685.

Navajas D, Maksym GN, Bates JH. Dynamic viscoelastic nonlinearity of lung parenchymal tissue. J Appl Physiol 1995;79(1):348-56.

Nemoto T, Hatzakis GE, Thorpe CW, Olivenstein R, Dial S, Bates JH. Automatic control of pressure support mechanical ventilation using fuzzy logic. Am J Respir Crit Care Med 1999;160(2):550-6.

Newth CJ, Amsler B, Anderson GP, Morley J. The effects of varying inflation and deflation pressures on the maximal expiratory deflation flow-volume relationship in anesthetized rhesus monkeys. Am Rev Respir Dis 1991;144(4):807-13.

Newth CJ, Hammer J. Pulmonary function in ventilated infants with bronchiolitis. Pediatr Pulmonol 1998;26(6):438-41.

Newth CJ, Stretton M, Deakers TW, Hammer J. Assessment of pulmonary function in the early phase of ARDS in pediatric patients. Pediatr Pulmonol 1997;23(3):169-75.

Niblett DJ, Sandhar BK, Dunnill MS, Sykes MK. Comparison of the effects of high frequency oscillation and controlled mechanical ventilation on hyaline membrane formation in a rabbit model of the neonatal respiratory distress syndrome. Br J Anaesth 1989;62:628-636.

Nicolai T, Lanteri C, Freezer N, Sly PD. Non-invasive determination of alveolar pressure during mechanical ventilation. Eur Respir J 1991;4(10):1275-83.

Nicolai T, Lanteri CJ, Sly PD. Frequency dependence of elastance and resistance in ventilated children with and without the chest opened. Eur Respir J 1993;6(9):1340-6.

Nicolai T, Lanteri CJ, Sly PD. Inherent coupling of elastic and dissipative behaviour of the lung through a viscoelastic time constant. J Appl Physiol 1993;74(5):2358-64.

Nicolai T, Lanteri C, Freezer N, Sly PD. Non-invasive determination of alveolar pressure during mechanical ventilation. Eur Respir J 1991;4(10):1275-83.

Nieman GF, Goyette D, Paskanik A, Brendenberg C. Surfactant displacement by plasma lavage results in pulmonary edema. Surgery 1990;107:677-683.

Nikischin W, Gerhardt T, Everett R, Bancalari E. A new method to analyze lung compliance when pressure-volume relationship is nonlinear. Am J Respir Crit Care Med 1998;158(4):1052-60.

Numa AH, Hammer J, Newth CJ. Effect of prone and supine positions on functional residual capacity, oxygenation, and respiratory mechanics in ventilated infants and children. Am J Respir Crit Care Med 1997;156(4):1185-9.

Numa AH, Newth CJ. Assessment of lung function in the intensive care unit. Pediatr Pulmonol 1995;19(2):118-28.

O'Connor GT. Cancer: a general review. Primates in Med 1969;3:9-22.

Olinsky A, Bryan AC, Bryan MH. A simple method of measuring total respiratory system compliance in newborn infants. S Afr Med J 1976;50:128-130.

O'Neil RM, Ashack RJ, Goodman FR. A comparative study of the respiratory responses to bronchoactive agents in rhesus and cynomolgus monkeys. Journal of Pharmacological Methods 1981;5:267-273.

O'Neil RM, Goodman FR. Respiratory responses to ascaris antigen in rhesus and cynomolgus monkeys. J Allergy Clin Immunol 1981;67(3):229-236.

Painter MJ. Animal models of perinatal asphyxia: contributions, contradictions, clinical relevance. Seminars in Pediatric Neurology 1995;2(1):37-56.

Papastamelos C, Panitch HB, England SE, Allen JL. Developmental changes in chest wall compliance in infancy and early childhood. J Appl Physiol 1995;78(1):179-84.

Parat S, Moriette G, Delaperche MF, Escourrou P, Denjean A, Gaultier C. Long-term pulmonary functional outcome of bronchopulmonary dysplasia and premature birth. Pediatr Pulmonol 1995;20(5):289-96.

Pare PD, Boucher R, Michoud M-C, Hogg JC. Static lung mechanics of intact and excised rhesus monkey lungs and lobes. J Appl Physiol Respirat Environ Exercise Physiol 1978;44(4):547-552.

Pare PD, Michoud M-C, Hogg C. Lung mechanics following antigen challenge of ascaris suum-sensitive rhesus monkeys. J Appl Physiol 1976;41(5):668-676.

Perelman RH, Engle M J, Kemnitz J W, Kotas RV, Farrell PM. Biochemical and physiological development of fetal rhesus lung. J Appl Physiol Respirat Environ Exercise Physiol 1982;53(1):230-235.

Perez Arellano JL, Barrios Gonzalez MN, Dominguez TM, Sanchez Benitez de Soto ML, Jimenez Lopez A. Experimental models of hypersensitivity pneumonitis. J Invest Allergy Clin Immunol 1992;2(4):218-228.

Peslin R, Marchal F, Chone C. Viscoelastic properties of rabbit lung during growth. Respir Physiol 1991;86(2):189-98.

Petak F, Hall GL, Sly PD. Repeated measurements of airway and parenchymal mechanics in rats by using low-frequency oscillations. J Appl Physiol 1998;84(5):1680-6.

Petak F, Hayden MJ, Hantos Z, Sly PD. Volume dependence of respiratory impedance in infants. Am J Respir Crit Care Med 1997;156(4):1172-7.

Peterson BT, Brooks JA, Zack AG. Use of microwave oven for determination of postmortem water volume of lungs. J Appl Physiol Respirat Environ Exercise Physiol 1982;52(6):1661-1663.

Petit JM, Milic-Emili G. Measurement of endoesophageal pressure. J Appl Physiol 1958;13(3):481-485.

Pfaff JK, Morgan WJ. Pulmonary function in infants and children. Pediatr Clin North Am 1994;41(2):401-23.

Plantadosi CA, Fracica PJ, Duhaylongsod FG, Huang Y-C T, Welty-Wolf KE, Crapo JD, Young SL. Artificial surfactant attenuates hyperoxic lung injury in primates. II. Morphometric analysis. J Appl Physiol 1995;78(5):1823-1831.

Poets CF, Arning A, Bernhard W, Acevedo C, von der Hardt H. Active surfactant in pharyngeal aspirates of term neonates: lipid biochemistry and surface tension function. Eur J Clin Invest 1997;27(4):293-8.

Pokora TJ, Mammel MC, Thompson TR, Ebert J, Boros SJ. Measurement of esophageal pressure in newborn infants using an esophageal balloon gastric catheter. Crit Care Med 1982;10(8):522-525.

Polgar G. Pulmonary function tests in children. J Pediatr 1979;95(1):168-70.

Polgar G, Weng TR. The functional development of the respiratory system from the period of gestation to adulthood. Am Rev Respir Dis 1979;120(3):625-95.

Popper H, Juettner F, Pinter J. The gastric juice aspiration syndrome (mendelson syndrome). Aspects of pathogenesis and treatment in the pig. Virchows Arch (Pathol Anat) 1986;409:105-117.

Preuss JM, Hall GL, Sly PD. Repeat measurement of respiratory mechanics using the forced oscillation technique in non-paralysed rats. Pulm Pharmacol Ther 1999;12(3):173-83.

Putz G, Goerke J, Schurch S, Clements JA. Evaluation of pressure-driven captive bubble surfactometer. J Appl Physiol 1994;76(4):1417-1424.

Putz G, Goerke J, Taeusch W, Clements JA. Comparison of captive and pulsating bubble surfactometers with use of lung surfactants. J Appl Physiol 1994;76(4):1425-1431.

Quanjer PH, Sly PD, Stocks J. Respiratory function measurements in infants: symbols, abbreviations and units. Eur Respir J 1995;8(6):1039-56.

Quanjer PH, Sly PD, Stocks J. Uniform symbols, abbreviations, and units in pediatric pulmonary function testing. Pediatr Pulmonol 1997;24(1):2-11.

Quanjer PH, Stocks J, Polgar G, Wise M, Karlberg J, Borsboom G. Compilation of reference values for lung function measurements in children. Eur Respir J 1989;S4:184-261.

Reiterer F, Sivieri E, Abbasi S, Bhutani VK. Evaluation of pulmonary functions during pressure-limited manual ventilation in preterm neonates. Pediatr Pulmonol 1993;15(2):117-21.

Ring A. Monitoring the surface tension of lipid membranes by a bubble method. Pflugers Arch 1992;420:264-268.

Robatto FM, Romero PV, Fredberg JJ, Ludwig MS. Contribution of quasi-static tissue hysteresis to the dynamic alveolar pressure-volume loop. J Appl Physiol 1991;70(2):708-714.

Rodriguez RJ, Martin RJ. Exogenous surfactant therapy in newborns. Respir Care Clin N Am 1999;5(4):595-616.

Roske K, Foitzik B, Wauer RR, Schmalisch G. Accuracy of volume measurements in mechanically ventilated newborns: a comparative study of commercial devices. J Clin Monit Comput 1998;14(6):413-20.

Rothberg AD, Bibby BD, Herman AA, Cooper PA. Analysis of neonatal and infant mortality data for the white population of the Witwatersrand. S Afr Med J 1984; 22-29;66(25):941-4.

Rothberg AD, Maisels MJ. Changes in mean esophageal pressure during early recovery in mechanically-ventilated neonates - evidence for airway-closure and gas-trapping? Pediatr Res 1981;15(12):1468-72.

Rothberg AD, Maisels MJ, Bagnato S, Murphy J, Gifford K, McKinley K, Palmer EA, Vannucci RC. Outcome for survivors of mechanical ventilation weighing less than 1,250 gm at birth. J Pediatr 1981;98(1):106-11.

Roze JC, Darmaun D, Gaultier C. Oxygen consumption in infants with bronchopulmonary dysplasia. Pediatr Pulmonol 1997;S16:172-3.

Russel G, Dinwiddie R. Measurement of intrathoracic pressure in the newborn. Paediatric Research Society 1973;48:325.

Russel G, Dinwiddie R. Measurement of intrathoracic pressure in the newborn. Paediatric Research Society 1973;48:325.

Sandhar BK, Niblett DJ, Argiras EP, Dunhill MS, Sykes MK. Effects of positive end-expiratory pressure on hyaline membrane formation in a rabbit model of the neonatal respiratory distress syndrome. Intensive Care Med 1988;14:538-546.

Schraufstatter I, Revak SD, Cochrane CG. Biochemical factors in pulmonary inflammatory disease. Inflammation and Wound repair. Federation Proceedings 1984;43(13):2806-2811.

Schroter RC. Quantitative comparisons of mammalian lung pressure volume curves. Respiration Physiology 1980;42:101-107.

Schussler TF, Gottfried SB, Bates JH. A model of the spontaneously breathing patient: applications to intrinsic PEEP and work of breathing. J Appl Physiol 1997;82(5):1694-703.

Schulze A, Gerhardt T, Musante G, Schaller P, Claure N, Everett R, Gomez-Marin O, Bancalari E. Proportional assist ventilation in low birth weight infants with acute respiratory disease: A comparison to assist/control and conventional mechanical ventilation. J Pediatr 1999;135(3):339-44.

Schulze A, Suguihara C, Gerhardt T, Schaller P, Claure N, Everett R, Bancalari E. Effects of respiratory mechanical unloading on thoracoabdominal motion in meconium-injured piglets and rabbits. Pediatr Res 1998;43(2):191-7.

Schurch S, Bachofen H, Goerke J, Green F. Surface properties of rat pulmonary surfactant studied with the captive bubble method: adsorption, hysteresis, stability. Biochimica et Biophysica Acta 1992;1103:127-136.

Schurch S, Bachofen H, Goerke J, Possmayer F. A captive bubble method reproduces the in situ behaviour of lung surfactant monolayers. J Appl Physiol 1989;67(6):2389-2396.

Schurch S, Possmayer F, Cheng S, Cockshutt A M. Pulmonary SP-A enhances adsorption and appears to induce surface sorting of lipid extract surfactant. Am J Physiol (Lung Cell Mol Physiol) 1992;263(7):L210-L218.

Schurch S, Schurch D, Curstedt T, Robertson B. Surface activity of lipid extract surfactant in relation to film area compression and collapse. J Appl Physiol 1994;77(2):974-986.

Seagrave JC, Mauderly JL. Lovelace Respiratory Research Institute Annual Symposium: Validity of animal models of human respiratory diseases. Lab Anim Sci 1999;49:7-9.

Seddon PC, Davis GM, Coates AL. Do tidal expiratory flow patterns reflect lung mechanics in infants? Am J Respir Crit Care Med 1996;153(4):1248-52.

Servillo G, Svantesson C, Beydon L, Roupie E, Brochard L, Lemaire F, Jonson B. Pressure-volume curves in acute respiratory failure: automated low flow inflation versus occlusion. Am J Respir Crit Care Med 1997;155(5):1629-33.

Shulman DL, Bar-Yishay E, Godfrey S. Respiratory mechanics and intrinsic PEEP during ketamine and halothane anesthesia in young children. Anesth Analg 1988;67(7):656-62.

Shulman DL, Goodman A, Bar-Yishay E, Godfrey S. Comparison of the single breath and volume recruitment techniques in the measurement of total respiratory compliance in anesthetized infants and children. Anesthesiology 1989;70(6):921-7.

Silva Neto G, Gerhardt T, Claure N, Duara S, Bancalari E. Effect of chestwall distortion on the measurement of pulmonary mechanics in preterm infants. Pediatr Pulmonol 1995;20(1):34-9.

Silva Neto G, Gerhardt TO, Claure N, Duara S, Bancalari E. Influence of chest wall distortion and esophageal catheter position on esophageal manometry in preterm infants. Pediatr Res 1995;37(5):617-22.

Sivan Y, Deakers TW, Newth CJ. Effect of positive end-expiratory pressure on respiratory compliance in children with acute respiratory failure. Pediatr Pulmonol 1991;11(2):103-7.

Sivan Y, Mor C, al-Jundi S, Newth CJ. Adult respiratory distress syndrome in severely neutropenic children. Pediatr Pulmonol 1990;8(2):104-8.

Slutsky AS, Sonarf SM, Brown R, Ingram Jnr RH. The effect of oleic acid-induced pulmonary edema on pulmonary and chest wall mechanics in dogs. Am Rev Respir Dis 1980;121:91-97.

Sly PD. A computer-model analysis of the influence of the upper airway on passive flow-volume loops in infants. Pediatr Pulmonol 1989;6(2):86-90.

Sly PD, Brown KA, Bates JH, Spier S, Milic-Emili J. Noninvasive determination of respiratory mechanics during mechanical ventilation of neonates: a review of current and future techniques. Pediatr Pulmonol 1988;4(1):39-47.

Sly PD, Hayden MJ, Petak F, Hantos Z. Measurement of low-frequency respiratory impedance in infants. Am J Respir Crit Care Med 1996;154(1):161-6.

Sly PD, Lanteri CJ, Kelly JH, Meretoja O. Disturbance in respiratory mechanics with extreme truncal flexion during anaesthesia in children. Anaesth Intensive Care 1991;19(2):220-4.

Sly PD, Robertson CF. A review of pulmonary function testing in children. J Asthma 1990;27(3):137-47.

Smith J, Pieper CH, Kirsten GF, Maree D, van Zyl J, Pretorius M-L. High-frequency oscillatory ventilation-rescue treatment for infants with severe respiratory failure. In: Hospital Supplies 1998;30-39.

Smith RJ. Signal waveforms. In: Circuits Devices and Systems. John Wiley and Sons, New York, 3rd edition, 61-86.

Southall DP, Samuels MP, Poets CF. Neonatal respiratory distress syndrome. Arch Dis Child 1993;S69(3):330.

Springer C, Vilozni D, Bar-Yishay E, Avital A, Noviski N, Godfrey S. Comparison of airway resistance and total respiratory system resistance in infants. Am Rev Respir Dis 1993;148(4):1008-12.

Staub NC. Mechanical properties in breathing: dynamics. In: Basic Respiratory Physiology. Churchill Livingstone, New York, 1991:81-104.

Stick S, Turner D, LeSouef P. Transmission of pressure across the chest wall during the rapid thoracic compression technique in infants. J Appl Physiol 1994;76(4):1411-1416.

Stocks J. Lung function testing in infants. Pediatr Pulmonol 1999;S18:14-20.

Stocks J. Recent advances in the assessment of lung function in infants. Pneumologie 1991;45(11):881-6.

Stocks J. Respiratory function testing in early childhood: where have we come from and where are we going? Pediatr Pulmonol 1999;S18:24-8.

Stocks J. Respiratory physiology during early life. Monaldi Arch Chest Dis 1999;54(4):358-64.

Stocks J, Beardsmore C. Flow resistance in infancy. Eur Respir J 1989;S4:144-149.

Stocks J, Beardsmore C, Helms P. Infant lung function: measurement conditions and equipment. Eur Respir J 1989;S4:123-129.

Stocks J, Jackson E. Comparison of dynamic and passive respiratory mechanics in ventilated newborn infants. Pediatr Pulmonol 1996;22(4):280-2.

Stocks J, Nothen U, Sutherland P, Hatch D, Helms P. Improved accuracy of the occlusion technique for assessing total respiratory Compliance in infants. Pediatr Pulmonol 1987;3(2):71-7.

Stocks J, Quanjer PH. Reference values for residual volume, functional residual capacity and total lung capacity. ATS workshop on lung volume measurements. official statement of the european respiratory society. Eur Respir J 1995;8(3):492-506.

Stocks J, Thomson A, Silverman M. The numerical analysis of pressure-flow curves in infancy. Pediatr Pulmonol 1985;1(1):19-26.

Stocks J, Thomson A, Wong C, Silverman M. Pressure-flow curves in infancy. Pediatr Pulmonol 1985;1(1):32-9.

Strohmaier W, Redl H, Schlag G. Studies of the potential role of a semisynthetic surfactant preparation in an experimental aspiration trauma in rabbits. Experimental lung research 1990;16:101-110.

Suki B, Bates JHT. A nonlinear viscoelastic model of lung tissue mechanics. J Appl Physiol 1991;71(3):826-833.

Suki B, Davey BL, Sato J, Bates JH. A model of transient oscillatory pressure-flow relationships of canine airways. Ann Biomed Eng 1995;23(5):682-90.

Svantesson C, John J, Taskar V, Evander E, Jonson B. Respiratory mechanics in rabbits ventilated with different tidal volumes. Respir Physiol 1996;106(3):307-16.

Svantesson C, Sigurdsson S, Larsson A, Jonson B. Effects of recruitment of collapsed lung units on the elastic pressure-volume relationship in anaesthetised healthy adults. Acta Anaesthesiol Scand 1998;42(10):1149-56.

Tepper RS, Gunst SJ, Doerschuk CM, Shen X, Bray W. Effect of transpulmonary pressure on airway closure in immature and mature rabbits. J Appl Physiol 1995;78(2):505-12.

Tepper RS, Morgan WJ, Cota K, Wright A, Taussig LM. Physiologic growth and development of the lung during the first year of life. Am Rev Respir Dis 1986;134(3):513-9.

Tepper RS, Pagtakhan RD, Taussig LM. Noninvasive determination of total respiratory system compliance in infants by the weighted-spirometer method. Am Rev Respir Dis 1984;130(3):461-6.

Thomson AH, Beardsmore CS, Silverman M. The total compliance of the respiratory system during the first year of life. Bull Eur Physiopathol Respir 1985;21(5):411-6.

Thomson A, Elliott J, Silverman M. Compliance in sick pre-term babies: How reliable is the measurement of oesophageal pressure? Abstracts from the meeting of the neonatal society. Biol Neonate 1983;43:297-301.

Thomson WT. Forced vibration with harmonic excitation. In: Vibration Theory and Applications. New Jersey, Prentice Hall Inc., Engelwood Cliffs, 51-6.

Trindade O, Goldberg RN, Bancalari E, Dickstein P, Ellison J, Gerhardt T. Conventional vs high-frequency jet ventilation in a piglet model of meconium aspiration: comparison of pulmonary and hemodynamic effects. J Pediatr 1985;107(1):115-20.

Truog WE, Jackson JC, Standaert TA, Juul SE, Murphy JH, Hodson WA, Henderson WR. Acute changes in vasoactive lipid mediators in experimental hyaline membrane disease. Respiration Physiology 1992;90:363-375.

Truog WE, Kessler DL, Palmer S, Murphy J, Woodrum DE, Hodson WA. Differential effect of sex in experimental hyaline membrane disease in newborn monkeys. Am Rev Respir Dis 1981;124:435-439.

Truog WE, Standaert TA, Murphy J, Palmer S, Woodrum DE, Hodson WA. Effect of high-frequency oscillation on gas exchange and pulmonary phospholipids in experimental hyaline membrane disease. Am Rev Respir Dis 1983;127:585-589.

Tsuno K, Prato P, Kolobow T. Acute lung injury from mechanical ventilation at moderately high airway pressures. J Appl Physiol 1990;69(3):956-961.

Turner DJ, Lanteri CJ, LeSouef PN, Sly PD. Pressure transmission across the respiratory system at raised lung volumes in infants. J Appl Physiol 1994;77(2):1015-20.

Turner DJ, Morgan SE, Landau LI, LeSouef PN. Methodological aspects of flow-volume studies in infants. Pediatr Pulmonol 1990;8(4):289-93.

Turner DJ, Stick SM, Lesouef KL, Sly PD, Lesouef PN. A new technique to generate and assess forced expiration from raised lung volume in infants. Am J Respir Crit Care Med 1995;151(5):1441-50.

Turner MJ, MacLeod IM, Rothberg AD. Effect of airway inertance on linear regression estimates of resistance and compliance in mechanically ventilated infants: a computer model study. Pediatr Pulmonol 1991;11(2):147-52.

Turner MJ, MacLeod IM, Rothberg AD. Lumped parameter approximation for the prediction of the dynamic response of the fleisch pneumotachograph. Med Biol Eng Comput 1988;26(4):443-8.

Turner MJ, MacLeod IM, Rothberg AD. Measurement of respiratory mechanics in a mechanically ventilated infant lung simulator: effects of variations in the frequency response of the flow measurement system. Med Biol Eng Comput 1994;32(1):49-54.

Uzawa T, Ashbaugh DG. Continuous positive-pressure breathing in acute hemorrhagic pulmonary edema. J Appl Physiol 1969;26(4):427-432.

Vaitukaitis JL. Animal models of human disease for the 21st Century. Laboratory Animal Science 1998;48(6):652-565.

Vallinis P, Retfalvi S, Davis GM, Coates AL. A simplified method for determining the frequency response of pneumotachographs used in infants. Pediatr Pulmonol 1993;16(2):109-15.

Van de Woestijne KP. The forced oscillation technique in intubated, mechanically-ventilated patients. Eur Respir J 1993;6(6):767-9.

Van Noord JA, Van de Woestijne KP, Demedts M. Clinical applications and modelling of forced oscillation mechanics of the respiratory system. Eur Respir J 1991;4(2):247-8.

Vilstrup CT, Bjorklund LJ, Larsson A, Lachmann B, Werner O. Functional residual capacity and ventilation homogeneity in mechanically ventilated small neonates. J Appl Physiol 1992;73(1):276-283.

Von Wichert P, Joseph K, Muller B, Franck WM. Bronchoalveolar lavage quantitation of intraalveolar fluid. Am Rev Respir Dis 1993;147:148-152.

Walker JS. Fast Fourier Transforms. Krantz SG (Ed). CRC Press, New York, 2nd edition, 1996.

Walsh GP, Tan EV, Dela Cruz EC, Abalos RM, Villahermosa LG, Young LJ, Cellona RV, Nazareno JB, Horwitz MA. The Philippine cynomolgus monkey (Macaca fasicularis) provides a new nonhuman primate model of tuberculosis that resembles human disease. Nature Medicine 1996;2(4):430-437.

Warburg E. A method of determining the undamped natural frequency and the damping in over-damped and slightly underdamped systems of one degree of freedom by means of a square-wave impact. Determination of Frequency and Damping 1949:344-349.

Wegner CD, Jackson AC, Gillespie JR. Linear-Lumped-Parameter modelling of pulmonary impedance in monkeys. Annals of Biomedical Engineering 1986;14:401-415.

West JB. Respiratory Physiology - The Essentials. Tracy TM (Ed), Williams and Wilkins, Baltimore, 1985.

Whitsett JA, Nogee LM, Weaver TE, Horowitz AD. Human surfactant protein B: structure, function, regulation, and genetic disease. Physiological Reviews 1995;75(4):749-759.

Whitford WG, Sherman RE. Sweating responses in the rhesus monkey (Macaca Mulatta). Comp Biochem Physiol 1976;53a:337-341.

Wong YC, Beardsmore CS, Silverman M. Pulmonary sequelae of neonatal respiratory distress in very low birthweight infants: a clinical and physiological study. Arch Dis Child 1982;57(6):418-24.

Woodrum DE, Standaert TA, Mayock DE, Guthrie RD. Hypoxic ventilatory response in the newborn monkey. Pediatr Res 1981;15:367-370.

Wilen R, Naftolin F. Age, weight and weight gain in the individual pubertal female rhesus monkey (macaca mulatta). Biology of Reproduction 1976;15:356-360.

Zapletal A. Lung elasticity in children and adolescents. Eur Respir J 1989;2(S4):S140-143.

Zelter M, Escudier BJ, Hoeffel JM, Murray JF. Effects of aerosolized artificial surfactant on repeated oleic acid injury in sheep. Am Rev Respir Dis 1990;141:1014-1019.

9 APPENDICES

9.1 Paper Reprint Copy From Thesis Chapter 2

C.G. Hartford, G.G. Rogers, M.J. Turner

Correctly selecting a fluid-filled nasogastric infant feeding catheter to measure intra-esophageal pressure. ***Pediatric Pulmonology***. 1997;23:362-9.

9.2 Paper Reprint Copy From Thesis Chapter 3

C.G. Hartford, G.G. Rogers, Jv Schalkwyk, M.J. Turner

Frequency responses of infant air-balloon versus liquid-filled catheters for intra-esophageal pressure measurement. ***Pediatric Pulmonology.*** 1997;Nov;24:353-363.

9.3 Paper Reprint Copy From Thesis Chapter 4

C.G. Hartford, Jv Schalkwyk, GG Rogers, M.J. Turner

Predicting air-balloon and liquid-filled catheter frequency responses. Testing the validity of the assumption that fluid-filled catheters fit a second-order system. ***IEEE Engineering in Medicine and Biology***. 1997;May/June:27-33.

9.4 Paper Arising From Thesis Chapter 5

Thesis Chapter Five's paper is under review: The manuscript under review is identical in content to the text presented in Thesis Chapter Five.

C.G. Hartford, Jv Schalkwyk, GG Rogers, M.J. Turner

Stable diffuse acute lung injury model in vervet monkeys (*(Cercopithecus aephiops*). Under review in 2000.

9.5 Paper Reprint Copy From Thesis Chapter 6

For publication purposes, Thesis Chapter Six was shortened following review at the request of the journal's editor. The shorter version was accepted for publication and is presented here. [Figures 1, 2, 3, 4 and 5 of the shortened published version presented in this appendix are Figures 3, 4, 6, 7 and 8 presented in Chapter Six].

C.G. Hartford, Jv Schalkwyk, GG Rogers, M.J. Turner

Primate pleuro-esophageal tissue barrier frequency response and esophageal pressure waveform bandwidth in health and acute lung-injury. ***Anesthesiology.*** 2000;Feb;92(2):550-558.

9.6 Scholar Prizes Attained in Relation to Research Presented From Thesis

- CHAPTERS 2-4

  Institute of Electrical and Electronic Engineers (IEEE) Engineering in Medicine and Biology Society (EMBS) Student Whitaker Competition First Place Prize Winner, Amsterdam, 1996.

- CHAPTERS 5-6:

  Institute of Electrical and Electronic Engineers Engineering in Medicine and Biology Society IEEE Region 8 Finalist (student represented Europe, Africa and the Middle East in the finals), Hong Kong, 1998.

THE INSTITUTE OF ELECTRICAL AND ELECTRONICS ENGINEERS, INC.

EMB

ENGINEERING IN MEDICINE AND BIOLOGY SOCIETY

recognizes

Craig Hartford

Open Competition Finalist

in the

EMBS
Whitaker Foundation
Student Paper Competition

1996

Gregory Lapin, Ph.D.
Chair, Student Activities Committee

Susan M. Blanchard, Ph.D.
President

ENGINEERING IN MEDICINE
AND BIOLOGY SOCIETY

IS HONORED TO RECOGNIZE

Craig Hartford

1st Place

1996

EMBS
Whitaker Foundation
Student Paper Competition

THE INSTITUTE OF ELECTRICAL AND ELECTRONICS ENGINEERS, INC.

THE INSTITUTE OF ELECTRICAL AND ELECTRONICS ENGINEERS, INC.

EMB

ENGINEERING IN MEDICINE AND BIOLOGY SOCIETY

recognizes

CRAIG G. HARTFORD

as the

REGION 8 FINALIST

In the
1998

EMBS
Student Paper Competition

R. Kearney, President
EMB Society

S. Wright, Chair
Student Activities Committee

Pediatric Pulmonology 23:362–369 (1997)

Diagnostic and Therapeutic Methods

Correctly Selecting a Liquid-Filled Nasogastric Infant Feeding Catheter to Measure Intraesophageal Pressure

C.G. Hartford, MB, BCh, MSc,[1]* G.G. Rogers, PhD,[1] and M.J. Turner, PhD[2]

Summary. Polyvinyl chloride (PVC) nasogastric feeding catheters are used clinically to measure intraesophageal pressure as an estimate of pleural pressure for calculating lung compliance in infants. The accuracy of pressure measurement of 4 French gauge (FG) catheter sizes and three brands of liquid-filled catheter manometer systems (CMS) was evaluated by determining their resonance-frequency amplitude and phase properties. All CMS were underdamped and resonated. No CMS exhibited a uniform mean frequency response above 11 Hz. The maximum respiratory rate (F_{rr}) within which CMS could potentially measure dynamic intraesophageal pressure within a 5% error limit was determined (F_{rr}): the highest mean F_{rr} recorded reliably in large-diameter catheters was 82 breaths/min. Significant CMS differences in accuracy existed between catheter FG sizes and between catheters of similar diameters but differing brands. Correlation (r^2) between catheter inner diameter and CMS F_{rr} was 0.66 across brands. In conclusion, intraesophageal PVC liquid-filled feeding catheters are suitable for estimating pleural pressures in subjects mechanically ventilated without sharp inspiratory waveforms or high respiratory rates. Quantitative frequency response characterization of different nasogastric catheter brands and different diameters is mandatory prior to their utilization. Pediatr. Pulmonol. 1997; 23:362–369.

Key words: lung compliance; pleural pressure; esophageal manometry; respiratory mechanics; feeding catheters; mechanical ventilation.

INTRODUCTION

Measurements of dynamic intraesophageal pressure to estimate pleural pressure are used by researchers and clinicians to evaluate pulmonary function of infants, particularly for the calculation of the elastic and resistive elements of the respiratory system.[1–3] Commercial nasogastric liquid-filled feeding catheters are easily inserted and well tolerated[4,5] and are readily available to clinicians as disposable and inexpensive alternatives to balloon[2,6,7] or transducer-tip[8] catheters. In addition, liquid-filled feeding catheters are advantageous for intraesophageal pressure measurements in mechanically ventilated infants because the catheters are normally in situ for long-term nasogastric feeding. Moreover, liquid-filled PVC catheters are nontraumatic on insertion, in comparison with the larger balloon-tip or the relatively inflexible transducer-tip catheters.[8]

Although there is extensive documented frequency response characterization of liquid-filled catheters used for intra-arterial pressure measurement,[9–11] there are insufficient data for liquid-filled infant feeding catheters[5,12,13] since they were not manufactured for incorporation into pressure measurement devices: the high respiratory rates and wide dynamic pressure waveforms encountered during mechanical infant ventilation may require flat catheter frequency responses up to 23 Hz, yet it is often necessary to introduce small FG size catheters in neonates.[6]

[1]Department of Physiology, University of the Witwatersrand, Johannesburg, South Africa.

[2]Department of Electrical Engineering, University of the Witwatersrand, Johannesburg, South Africa.

Contract grant sponsor: the South African Foundation for Research and Development; Contract grant sponsor: Medical Research Council; Contract grant sponsor: Iris Ellen; Contract grant sponsor: H.E. Griffin; Contract grant sponsor: University of the Witwatersrand and Medical Faculty Research Council; Contract grant sponsor: The Boots Company, SA.

*Correspondence to: Dr. C.G. Hartford, Department of Physiology, University of the Witwatersrand Medical School, 7 York Road, Parktown, Johannesburg, 2193, South Africa.

Received 2 August 1996; accepted 24 December 1996.

TABLE 1—Infant Feeding Catheter Specifications[1]

Feeding catheter	FG	OD ± Tol (mm)	ID ± Tol (mm)	L (cm)
Portex (Portex, Kent, UK)	10	3.3 ± 0.1	2.3 ± 0.1	60
Adcock Ingram (Sabax Division, SA)	10	3.3 ± 0.08	2.2 ± 0.1	50
Ven (Ven Products, SA)	10	3.3 ± 0.1	2.3 ± 0.1	50
Portex	8	2.6 ± 0.08	1.8 ± 0.08	50
Adcock Ingram	8	2.6 ± 0.08	1.7 ± 0.1	50
Ven	8	2.6 ± 0.1	1.8 ± 0.1	50
Portex	6	2.0 ± 0.08	1.4 ± 0.08	50
Adcock Ingram	6	2.0 ± 0.08	1.1 ± 0.1	50
Ven	6	2.0 ± 0.1	1.2 ± 0.1	50
Adcock Ingram	5	1.7 ± 0.08	0.8 ± 0.1	50
Ven	5	1.9 ± 0.1	0.8 ± 0.1	50
Portex	4	1.3 ± 0.08	0.6 ± 0.08	50

[1]Tol, manufacturer-specified tolerance; L, length.

This study aims to quantify the suitability of commercially available PVC infant nasogastric feeding catheters to measure dynamic intraesophageal pressure. By assessing the in vitro resonance frequency characteristics (amplitude and phase) of a range of catheter brands and FG sizes, we have provided values for the maximum respiratory rate up to which differing FG size feeding catheters may be utilized to measure intraesophageal pressure accurately.

MATERIALS AND METHODS

Infant CMSs clinically employed to measure intraesophageal pressure were subjected to in vitro sinusoidally oscillating pressures of varying frequency. CMSs frequency responses were determined by comparison with a reference manometer system. The CMS included 12 types of medical grade PVC catheters (three brands and four FG sizes; Table 1), chosen for their similar lengths, coupled to two pressure transducer-dome combinations. A Gould P10EZ pressure transducer (6.4 mm pressure sensor area), with a disposable diaphragm-dome and luer lock fittings (Viggo-Spectramed Gould TA1019, Oxnard, CA), and a Gould P23XL transducer (14 mm pressure sensor area), with a disposable diaphragm-dome and luer lock fittings (TA1010ND), were used in conjunction with the various catheters. The dome ports were fitted in-series to four-way stopcocks (Adcock Ingram, South Africa) yielding transducer-dome-stopcock volumes of 0.6 and 0.9 ml for the transducer combinations, respectively. The space between the transducer diaphragm and the disposable dome diaphragm was water filled according to the manufacturer's instructions and positioned at the catheter-tip level.

Six samples each of the 12 different catheter types were assessed by randomly attaching their proximal female luer fittings directly to the two transducers' stopcock male luer fittings. To minimize bubble formation, each catheter was flushed with carbon dioxide followed by deionized, degassed (by boiling) water cooled under vacuum to between 36° and 38°C.[14] The distal 20 cm of the catheter was inserted into a laboratory-designed leakproof water chamber kept at 36°–38°C. Sinusoidal pressure waveforms between −5.5 and +10 cmH_2O (mean, 2.3 cmH_2O) were generated in the chamber by means of a loudspeaker (Bose 4.5″ 802, Bose Corporation, MA), powered by an 80 WRMS DC-coupled amplifier linked to a sine wave generator (Hewlett Packard 3562A, USA). A swept sine frequency response of the CMS was recorded (Fig. 1) using a calibrated domeless piezoresistive differential pressure transducer as a reference (Honeywell Microswitch 170PC, USA), positioned inside the chamber adjacent to the CMS catheter tip. Unfiltered electrical outputs from the CMS and reference pressure transducer were identically preamplified (Hellige Servomed, Freiburg, Germany), and analyzed for phase and amplitude differences by averaging three repeat measurements over 10 seconds at each 1 Hz interval (Hewlett Packard Dynamic Signal Analyzer 3562A). Apparatus reproducibility over the experiment was confirmed by repeating a CMS frequency response measurement of the sample of Portex FG size 6 catheters at the start and end of the experiment.

Abbreviations

A_r/A_0	Resonance amplitude ratio
Ade	Adcock Ingram catheter
CMS	Catheter manometer system
D_c	Damping coefficient
F_{a5}	Frequency at A_0 + 5%
F_0	Undamped natural resonant frequency
F_r	Damped resonant frequency
F_{rr}	Maximum working respiratory rate
FG	French gauge
ID	Inside diameter
Mag	Linear magnitude gain
MANOVA	Multivariate analysis of variance
OD	Outside diameter
P_{a5}	Phase difference at F_{a5}
Por	Portex catheter
PVC	Polyvinyl chloride
WRMS	Root mean square Watts

Frequency Response Measurements

Amplitude-frequency response variables relate to CMS gain or attenuation of applied pressure compared with the reference transducer over a range of applied pressure frequencies (Fig. 1). Variables extracted from amplitude-frequency responses were:

F_r damped resonant frequency (frequency at maximum amplitude);

A_r/A_0 resonance amplitude ratio (maxium amplitude, A_r, divided by amplitude at 1 Hz, A_0);

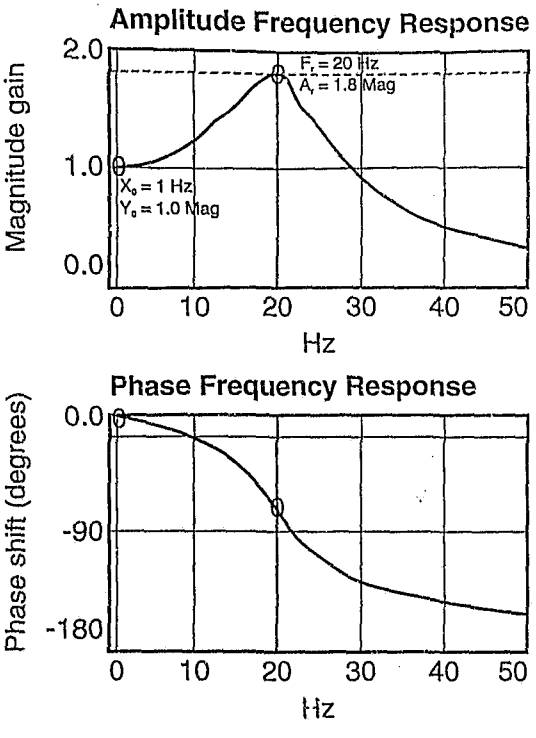

Fig. 1. Sample Portex FG size 4 catheter amplitude and phase frequency response traces. First marker circle on amplitude plot represents baseline amplitude (Y-axis, $Y_0 = A_0 = 1.0$ Mag) and baseline frequency (X-axis, $X_0 = 1$ Hz). Second marker circle represents damped resonant frequency (X-axis, $F_r = 20$ Hz) and maximum amplitude gain (Y-axis, $A_r = 1.8$ Mag). Mag, linear magnitude gain over reference transducer; Hz, Hertz.

F_{a5} frequency at $A_0 + 5\%$ (frequency at which the amplitude ratio = 1.05).

Phase-frequency response variables characterize the CMS temporal advancement or retardation of the applied pressure waveform over a range of frequencies; the phase-frequency response variable extracted from the recorded CMS phase-frequency response tracings was:

P_{a5} phase difference at F_{a5}.

Calculated variables derived from the CMS frequency responses were:

D_c damping coefficient (Appendix formula 1);
F_o undamped natural resonant frequency (Appendix formula 2);
F_{rr} CMS maximum working respiratory rate (Appendix formula 3).

D_c describes CMS resistance to oscillation. F_o represents the number of oscillations per unit time that the CMS would undergo if left to oscillate undisturbed. F_{rr} predicts the maximum respiratory rate up to which an intraesophageal CMS of measured F_o and D_c will potentially measure an applied pressure to within ±5% of the reference transducer.[9,15]

Statistical Analysis

Between-groups multiway multivariate (7 dependent measured frequency response variables, from above), analysis of variance was performed (MANOVA F-test, Statistica® software, Statsoft, OK) and Tukey's Significant Difference post-test correction applied to P-values < 0.05.[16] The multiway ANOVA design considers possible statistical interactions due to testing the effects of multiple catheter types (3 brands and 4 FG sizes) in addition to the effects of two different transducer types on the measured frequency response variables. Coefficient of determination (r^2) between F_{rr} and catheter diameter was calculated from the Pearson product-moment correlation. Displayed values are mean ± SD.

RESULTS

No significant frequency response differences were found between the two transducer-dome combinations, and no significant statistical interaction between the catheters and transducers was noted. The means of 12 measured values ($n = 6$ catheters × two transducers) are therefore presented for each sample's variables.

The effect of catheter brand and FG on mean amplitude and phase frequency responses is illustrated in Figures 2 and 3; the effect of catheter brand and FG on the maximum working respiratory rate is depicted in Figure 4. Variables F_r, A_r, F_{a5}, P_{a5}, and F_{rr}, which were significantly different ($P < 0.05$) between catheter FG sizes and brands, are displayed in Table 2. There was a trend for mean F_r, A_r, F_{a5}, and F_{rr} to decrease, and for D_c and P_{a5} to increase with decreasing catheter FG size. Mean D_c ranged from 0.19 to 0.30.

No CMS exhibited a uniform mean frequency response above 11 Hz (F_{a5}; Fig. 2). Within catheter brands the F_{rr} (Fig. 4) of Portex and Adcock FG sizes 10 and 8 were not significantly different. The F_{rr} of the Portex FG sizes 6 and 4 and of the Adcock FG size 5 were significantly lower than their same-brand larger FG sizes. Within the Ven catheter brand there was a significant decrease in F_{rr} with decreasing Ven FG sizes 10, 8, and 6. The F_{rr} was significantly lower for the Portex FG size 4 versus 6, and for the Adcock FG size 5 versus 6, but the Ven FG size 5 versus 6 was similar.

Between catheter brands there was no significant difference in F_{rr} for the Portex FG sizes 10, 8, and 6 versus the corresponding Adcock catheters, but the Ven FG sizes 8 and 6 had a significantly lower F_{rr} than the corresponding Portex and Adcock FG sizes. The F_{rr} of Portex FG size 4 was significantly lower than all other FG

TABLE 2—Infant Feeding Catheter Statistical Summary Table[1]

	Por10	Adc10	Ven10	Por8	Adc8	Ven8	Por6	Adc6	Ven6	Adc5	Ven5
Por10	ab										
Ven10	abde	be									
Por8	d	bde	abde								
Adc8	be	be	adef	be							
Ven8	abdef	abdef	af	abdef	abdef						
Por6	abdef	abdef	f	abdef	adf	–					
Adc6	abef	–	be	abdef	adf	abe	be				
Ven6	abcdef	abcdef	acdf	abcdef	adef	adf	adf	abdef			
Adc5	abcdef	abcdef	acdf	abcdef	abcdef	acdf	acdef	abcdef	acf		
Ven5	abcdef	abcdef	af	abcdef	adf	be	af	adef	–	abcdef	
Por4	abcdef	abcdef	abcdef	abcdef	abcdef	abcdef	abcdef	abcdef	abcdef	acef	abcdef

[1]Variables a–f indicated are $P < 0.05$ between any two catheters. a, damped resonant frequency (F_r); b, maximum amplitude gain (A_r); c, phase difference at F_{a5} (P_{a5}); d, frequency at $A_0 + 5\%$ (F_{a5}); e, damping coefficient (D_c); f, working respiratory rate (F_{rr}); –, no significant difference; Por, Adc, Ven: Portex, Adcock, and Ven catheter brands and FG size.

size catheters. The Ven FG size 5 catheter displayed a significantly greater F_{rr} than the Adcock FG size 5.

The coefficient of determination (r^2) for mean F_{rr} versus catheter ID or OD across all brands was 0.66 and 0.67, respectively. The within-brand r^2 for mean F_{rr} versus ID of Portex, Adcock, and Ven catheters was 0.90, 0.55, and 0.81, respectively. The range of F_{rr} was largest within the Ven 6 FG catheters (31.2–60.2 breaths/min) and lowest within the Adcock 8 FG catheters (79.5–84.4 breaths/min).

DISCUSSION

In Vitro Technique

Catheter whip and impact with the esophageal wall may affect in vivo frequency responses of in situ catheters. However, we performed in vitro frequency response analysis because use of fast flush in vivo tests has been shown to overestimate the CMS F_r, possibly due to the high mass inertia of external flushing liquid, thereby artifactually raising in vivo CMS working respiratory rates beyond their true values.[9,10,17] Moreover, accurate interpretation of CMS frequency responses calculated from in vivo applied fast flush waveforms is interfered with by non-pleural pressure-related superimposed esophageal waveforms such as in vivo cardiac and peristaltic waveforms.[18]

In quantifying the frequency responses, we employed the swept frequency forced oscillation technique as opposed to the step response (free oscillation burst-balloon) technique. The latter, like the fast flush in vivo technique, is practically limited to underdamped CMS,[11,18] may miss subtle differences in F_o,[14] and is open to potential measurement inaccuracies in the determination of the period and amplitude of the response.[18] On the other hand, the swept frequency technique employed by us is suitable for a distributed parameter system such as liquid-filled CMS and allows the system under test to be stimulated at equal amplitude over all frequencies, whereas the step response approach results in reducing amplitudes with increasing frequency.[11,18]

We used a mean pressure offset of +2.3 cmH_2O, similar to mean intraesophageal pressures accompanying mechanical ventilation, because this method allowed for any effects of nonlinearities (amplitude dependent) related to dynamic CMS compliance or catheter wall hysteresis to be included in the CMS frequency response measurements.[11]

Reported effects of physiological temperatures on frequency responses in liquid-filled catheters vary from no effect[10] to significant effects caused by altered catheter wall compliance.[11,19] The compliance and compliance hysteresis of nasogastric catheter PVC are likely to be more temperature dependent than, for example, nylon or braided-polyurethane catheters used for intra-arterial pressure measurement; therefore, we measured the frequency responses at primate physiological temperatures.

Catheter Frequency Responses

To our knowledge there is no formal documentation comparing the pressure measurement frequency response characteristics of a range of differing FG sizes and brands of standard liquid-filled PVC infant nasogastric feeding catheters of matching catheter lengths: informal measurements on liquid-filled intraesophageal catheters (usually performed with differing catheter lengths, brands, and FG sizes between the researchers and of single sample number) have demonstrated uniform frequency responses in an 8 FG 2 mm ID 38 cm long saline-filled catheter up to 10 Hz[12] and in a similar catheter to > 10 Hz;[5] a 5 FG 1 mm ID catheter and a 6 FG catheter were also noted to be flat to 10 Hz.[5,13] Ideally CMSs should have a high F_r, but a high F_r by itself may be associated with overdamping and consequent reduced CMSs sensitivity at raised frequencies. Introducing damping systems to compensate for resonance in underdamped CMSs is not usually practical, nor necessarily effective; therefore optimal damping ($D_c = 0.71$) accompanying a high F_r is desirable in CMSs.[9]

Since both D_c and F_r can independently influence

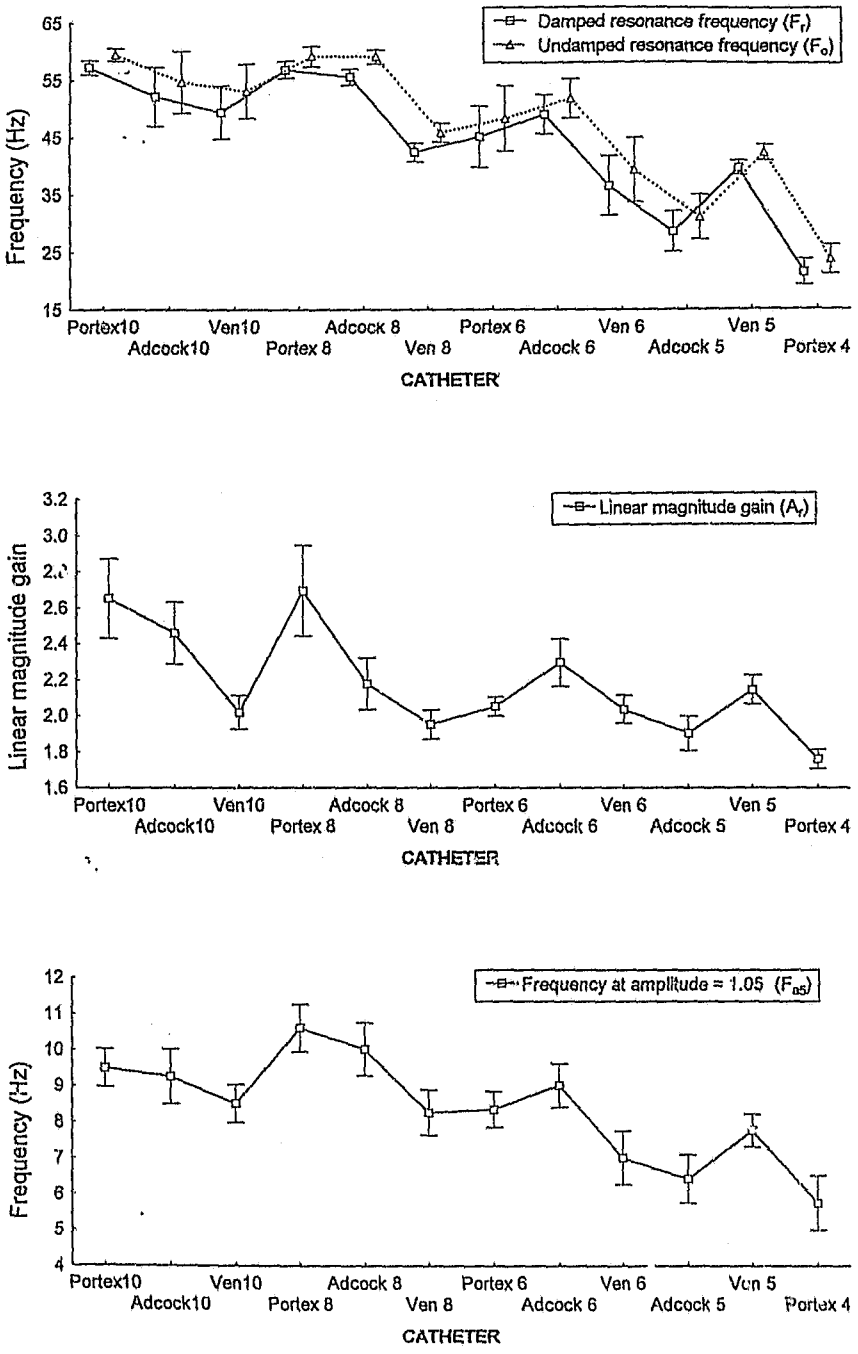

Fig. 2. Catheter amplitude and phase frequency response characteristics. F_r, damped resonant frequency; F_o, undamped resonant frequency; A_r, maximum amplitude gain; F_{a5}, frequency at A_g + 5%; Catheter, catheter brand and French gauge size.

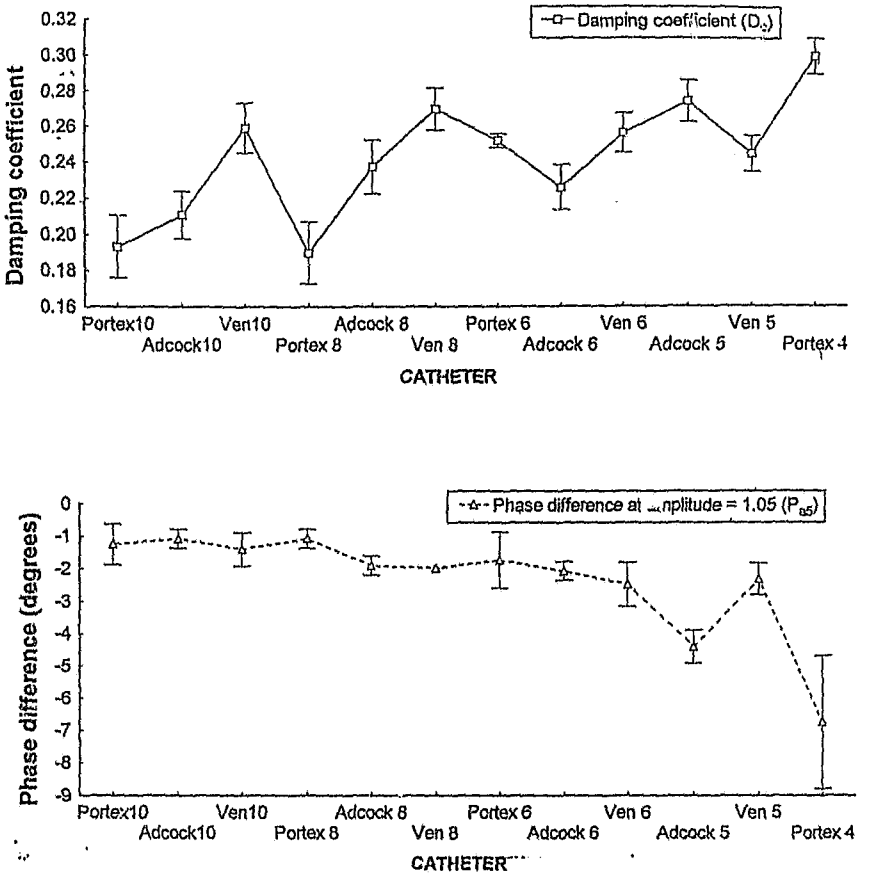

Fig. 3. Catheter frequency response characteristics. D_c, damping coefficient; P_{a5}, phase difference at A_0 + 5% or F_{a5}. Cathet catheter brand and French gauge size.

CMS performance and facilitate interpretation of the frequency response data obtained in our experiment, we used calculated F_{rr} as a variable that meaningfully predicts the potential of a CMS to measure intraesophageal pressure within a 5% error limit up to a maximum calculated respiratory rate. Although mean F_{rr} did increase with larger FG catheters, it represents the accuracy with which applied pressure will be recorded, assuming all of the applied pressure waveform energy is located within ten harmonics of the fundamental frequency.[9] This assumption may be incorrect when pressure cycled infant ventilators generating square pleural pressure waveforms are in use; the F_{rr} under such conditions would be reduced.

The correlation between mean F_{rr} and catheter ID or OD was similar. Therefore, choosing a catheter based on either ID or OD would be similarly effective in predicting the F_{rr}. It should, however, be noted that FG, a term particularly applied to medical grade catheters, refers the Charrière French scale, where 1 FG unit = cathe OD of 0.33 mm, and does not necessarily reflect the I which also depends on catheter wall thickness. Th catheters of the same FG size can have differing IDs; example, see the ID of Portex FG size 6 versus Adc FG size 6 in Table 1. The Ven FG size 5 has a larger (but the same ID compared with the corresponding A cock FG size 5; the Ven catheter wall is thus thicker a less compliant, which may explain its superior freque response. In addition, manufacturing tolerances on sn versus large FG size catheters are similar (Table therefore, small FG catheters may have relatively lar OD tolerances. This can lead to further variability in th measured frequency response characteristics. It is, the fore, advisable to base catheter selection on ID rat than on OD or FG alone, although ideally values for and OD (or FG) should be sought. For the same cath

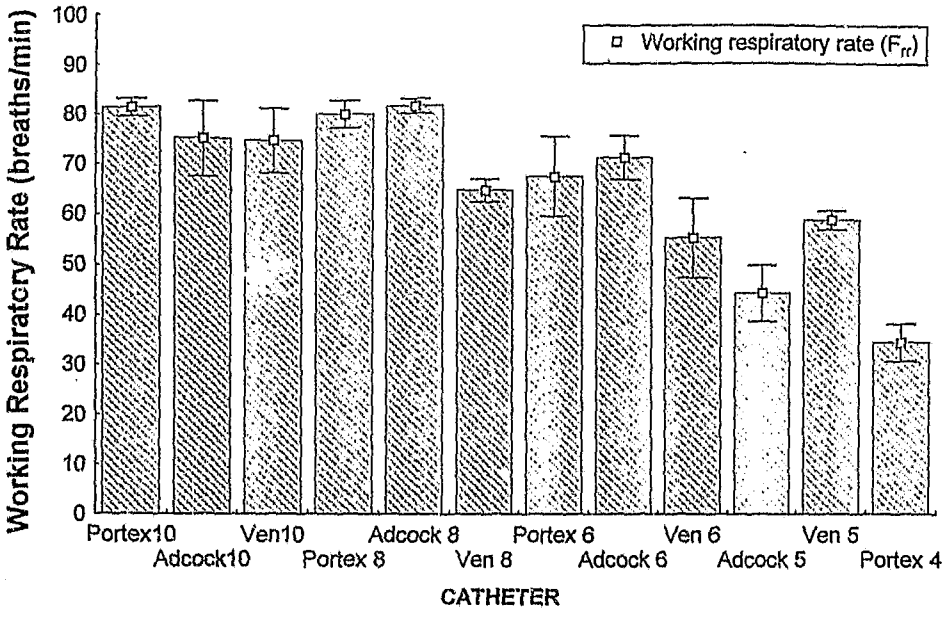

Fig. 4. Catheter maximum working respiratory rate. F_{rr}, maximum working respiratory rate; Catheter, catheter brand and French gauge size.

wall composition, a larger ID and greater wall thickness is likely to produce a higher F_r.

The correlation between F_{rr} and ID was different for various catheter brands; thus for a particular ID or FG size catheter there is frequency response discrepancy between different catheter makes. Resonance characteristics are dependent on CMS compliance, inertance (liquid mass), viscous resistance, and catheter wall hysteresis. In practice, factors that affect CMS volume displacement coefficients are gas bubbles (transparency of PVC catheters is advantageous here), which increase D_c but lower F_r,[11,18,20] catheter wall compliance,[11] leaky connections, and arrangement of stopcocks and transducer domes.[17] Manufacturing tolerances on the catheter ID or length affect F_r via catheter radius and length, which may partly explain the range of frequency responses found within samples from the same catheter brand and FG size noted in our experiment.[14] These variations concur with those recorded from frequency responses of liquid-filled intravascular catheters.[10,14,21] Discrepancies between manufacturer-claimed and experimentally observed resonant frequencies of liquid-filled catheters have also been documented.[10] The quality of pressure transducers employed in the CMS directly affects resonance properties; however, transducer dome size, which potentially alters the liquid mass inertia and compliance of the CMS, did not affect the observed frequency responses in our experiment.

In conclusion, in vitro frequency response analysis demonstrates that, although large FG commercially available PVC liquid-filled nasogastric feeding catheters are underdamped and resonate, they can potentially measure transmitted intraesophageal pressures up to a maximum of 82 breaths/min within a 5% error limit. However, judging the suitability of individual feeding catheters to measure dynamic intraesophageal pressure accurately based on FG size alone is inappropriate; the multifactorial determination of CMS amplitude and phase frequency responses necessitates quantitative assessment of different catheter brands and diameters prior to their utilization.

APPENDIX: EQUATIONS FOR CALCULATED VARIABLES

Damping coefficient[19] (Dc):

$$D_c = \sqrt{\left(\frac{1 - \sqrt{\left(1 - \left(\frac{A_w}{A_r}\right)^2\right)}}{2}\right)}, \qquad (1)$$

Undamped natural frequency[19] (F_n):

$$F_n = \frac{F_r}{\sqrt{(1 - 2D_c^2)}}, \qquad (2)$$

Maximum working respiratory rate[9,15] (F_{rr}):

$$F_{rr} = \frac{(F_{a5} \times 60)}{10} \quad (3)$$

where F_{a5} is the frequency at which $A_r/A_0 = 1.05$; 10 refers to the Fourier series 10th harmonic.

In the authors' experiment the frequency response trace was divided through by the amplitude ratio at 1 Hz (regarded as the DC response) and therefore $A_0/A_r = 1/A_r$.

Equations used for undamped natural frequency (F_o) and damping coefficient (D_c) assume that the system is second order and linear.[15]

REFERENCES

1. Ratjen FA, Wiesemann HG. Variability of dynamic compliance measurements in spontaneously breathing and ventilated newborn infants. Pediatr Pulmonol. 1992; 12:73–80.
2. Beardsmore CS, Helms P, Stocks J, Hatch DJ, Silverman M. Improved esophageal balloon technique for use in infants. J Appl Physiol. 1989; 49:735–742.
3. Coates AL, Stocks J, Gerhardt T. Esophageal manometry. In: Stocks J, Sly PD, Tepper RS, Morgan WJ, eds. Infant Respiratory Function Testing. New York: John Wiley & Sons, 1996:241–258.
4. Coates AL, Stocks J. Esophageal pressure manometry in human infants. Pediatr Pulmonol. 1991; 11:350–360.
5. Asher MI, Coates AL, Collinge JM, Milic-Emili J. Measurement of pleural pressure in neonates. J Appl Physiol. 1982; 52:491–494.
6. Maxted KJ, Shaw A, Macdonald TH. Choosing a catheter system for measuring intra-esophageal pressure. Med Biol Eng Comput. 1977; 15:398–401.
7. Heaf DP, Turner H, Stocks J, Helms P. The accuracy of esophageal pressure measurements in convalescent and sick intubated infants. Pediatr Pulmonol. 1986; 2:5–8.
8. Chartrand DA, Ye TH, Maarek JH, Chang HK. Measurement of pleural pressure at low and high frequencies in normal rabbits. J Appl Physiol. 1987; 63:1142–1146.
9. Hipkins SF, Rutten AJ, Runciman WB. Experimental analysis of catheter-manometer systems in vitro and in vivo. Anesthesiology. 1989; 71:893–906.
10. Rutten AJ, Nancarrow C, Isley AH, Runciman WB. An assessment of six different pulmonary artery catheters. Crit Care Med. 1987; 15:250–255.
11. Yeomanson CW, Evans DH. The frequency response of external transducer blood pressure measurement systems: a theoretical and experimental study. Clin Phys Physiol Meas. 1983; 4:435–449.
12. Coates AL, Davis GM, Vallinis P, Outerbridge EW. Liquid-filled esophageal catheter for measuring pleural pressure in preterm neonates. J Appl Physiol. 1989; 67:889–893.
13. LeSouëf PN, Lopes JM, England SJ, Bryan MH, Bryan AC. Influence of chest wall distortion on esophageal pressure. J Appl Physiol. 1983; 55:353–358.
14. Shapiro GG, Krovetz LJ. Damped and undamped frequency responses of underdamped catheter manometer systems. Am Heart J. 1970; 80:226–236.
15. Fry DL. Physiologic recording of modern instruments with particular reference to pressure recording. Physiol Rev. 1960; 40: 753–788.
16. Zar JH. Biostatistical Analysis. Engelwood Cliffs, NJ: Prentice-Hall, 1974:206–252.
17. Rothe CL, Kim KC. Measuring systolic arterial blood pressure; possible errors from extension tubes or disposable transducer domes. Crit Care Med. 1980; 8:683–689.
18. Gardner RM. Direct blood pressure measurement-dynamic response requirements. Anesthesiology. 1981; 54:227–236.
19. Hansen AT. The theory for elastic liquid-containing membrane manometers: Special part. Acta Physiol Scand. 1949; 19:333–343.
20. Milic-Emili J, Mead J, Turner JM, Glauser EM. Improved technique for estimating pleural pressure from esophageal balloons. J Appl Physiol. 1964; 19:207–211.
21. Doyle DJ. Resonance properties of 85-cm and 110-cm pulmonary artery catheters. J Cardiothorac Anesth. 1990; 4:781–782.

Pediatric Pulmonology 24:353–363 (1997)

Diagnostic and Therapeutic Methods

Frequency Responses of Infant Air-Balloon Versus Liquid-Filled Catheters for Intra-Esophageal Pressure Measurement

Craig G. Hartford, MB, BCh, MSc Med,[1]* Martin J. Turner, MSc Eng, PhD,[2] Johan M. van Schalkwyk, MB, BCh, FCP(SA),[3] and Geoffrey G. Rogers, MSc, PhD[1]

Summary. Amplitude and phase frequency response characteristics of infant air-balloon catheters (IABC) of differing French gauge (FG) sizes and brands were quantified to determine their suitability for measuring dynamic intra-esophageal pressure (P_{es}) accurately. Frequency response performances of matching IABC and water-filled catheters (WFC) were also compared using the swept sine wave technique. The maximum respiratory rate within which IABCs could potentially measure P_{es} within a 5% error limit was calculated (F_{RR}).

Frequency responses of IABCs greater than FG size 5 exhibited underdamped resonant properties, while smaller FG size IABCs exhibited near-critical damping or overdamping. IABCs maintained uniform amplitude frequency responses up to 25 Hz, demonstrating the ability to measure P_{es} potentially up to 148 breaths/min within a 5% error limit. The frequency response performance of FG size 6 IABCs was similar to that of FG size 10 IABCs. Compared with matching WFCs, the frequency response performance of IABCs was significantly superior, the frequency response variability within IABC samples was lower, and IABC correlation between FG size and F_{RR} was advantageously lower than for WFCs. F_{RR} values for differing IABC brands and FG sizes are presented. We conclude that IABCs manufactured to infant-appropriate balloon specifications exhibit significantly superior frequency response characteristics compared with matching WFCs. Measurement accuracy is not improved using IABCs greater than FG size 6. Inexpensive intra-esophageal IABCs are technically suitable for the accurate measurement of dynamic P_{es} during high-frequency respiratory mechanics encountered during infant artificial ventilation. Pediatr. Pulmonol. 1997; 24:353–363.

Key words: esophageal manometry; lung compliance; respiratory mechanics; mechanical ventilation.

INTRODUCTION

Pleural pressure of artificially ventilated infants is estimated by measuring dynamic P_{es} to facilitate calculation of the elastic and resistive elements of the respiratory system.[1,2] PVC infant feeding catheters, liquid-filled or air-balloon tipped,[3–5] are easily inserted and well tolerated[6] and are readily available to clinicians and researchers as disposable and inexpensive alternatives to transducer-tip catheters.[7,8] However, the high-frequency respiratory mechanics encountered during artificial infant ventilation may require uniform catheter frequency responses up to 20 or 23 Hz,[4,8,9] which few, if any, PVC WFCs demonstrate.[10]

Liquid-filled catheters are commonly used for intra-arterial pressure measurement; therefore extensive fre-

Contract grant sponsors: the South African, Medical Research Council, Levenberg Bequest, University of the Witwatersrand and Medical Faculty Research Council grants.

[1]Department of Physiology, University of the Witwatersrand Medical School, Johannesburg, South Africa.

[2]Department of Electrical Engineering, University of the Witwatersrand Medical School, Johannesburg, South Africa.

[3]Department of Anesthetics, Johannesburg Hospital, University of the Witwatersrand Medical School, Johannesburg, South Africa.

*Correspondence to: Dr. C.G. Hartford, Department of Physiology, University of the Witwatersrand Medical School, 7 York Road, Parktown, Johannesburg, 2193, South Africa.

Received 13 March 1997; accepted 30 June 1997.

quency response characterization of these catheters exists. However, data pertaining to IABCs used for P_{es} measurement are sparse[3,4] and are limited by measurements confined to one catheter FG size or to single (n = 1) catheter samples of unequal lengths or brands. Studies employing IABCs have concentrated on validating the in vivo reflection of pleural pressure by P_{es}[3,11] and do not present quantitative data on the dynamic accuracy of differing IABC FG sizes and brands used for measuring P_{es}. Moreover, controversy exists in the literature as to the frequency responses of IABCs relative to WFCs: WFCs were qualitatively considered to have better frequency responses than IABCs,[7] yet in another study IABCs were reported to have better phase and amplitude characteristics than most WFCs.[4] In the latter study catheters of FG size 6 (unspecified length) only were tested; to our knowledge a valid direct comparison of the frequency responses of matching IABCs and WFCs has not been published.

In vivo fast flush test frequency response analysis is not applicable to IABCs; therefore this study aims to determine the in vitro frequency response characteristics (amplitude and phase) of a range of IABCs of differing FG sizes and catheter brands, to quantify their suitability for accurate dynamic P_{es} measurements in infants and to compare IABC frequency response performances with those of matching WFCs.

MATERIALS AND METHODS

IABC Laboratory Manufacture

Glass rods of 8.3 mm OD, attached to a rotating device, were dipped twice 1 h apart into a bath containing liquid latex compound (Latex Surgical Products, South Africa) which was vacuumed to remove surface air bubbles. The latex was dried at 25°C in air of 50% relative humidity and manually rolled off the rods following powdering. Balloons were selected on the criteria of single wall thicknesses between 0.06 and 0.09 mm and <25% difference between the thickest and thinnest part of the air-balloon, as determined by a micrometer screw gauge at three points along the balloon's length.[3] Air-balloons were mounted on PVC feeding catheters with silicon glue and silk ties at a point 5.5 cm proximal to the catheter tip and the IABCs leak-tested for 1 min. Pressure-volume curves for ten samples each of FG size 10 and FG size 5 IABCs of the same catheter brand were determined as follows: Each air-balloon was evacuated by submersing it in water to the level of its silk tie, after which the IABC was attached to a three-way stopcock and pressure transducer combination (Honeywell Microswitch 170PC, USA). Air was incrementally injected into the horizontally positioned (as in the case of supine infants) IABC using a calibrated 0.1 mL graduated syringe and the pressure recorded.[3,12]

TABLE 1—Infant Air-Balloon and Water-Filled Catheter Specifications[1]

Feeding catheter	FG	OD ± Tol (mm)	ID ± Tol (mm)	L (cm)
Portex (Portex, Kent, UK)	10	3.3 ± 0.1	2.3 ± 0.1	60
Ven (Ven Products, SA)	10	3.3 ± 0.1	2.3 ± 0.1	50
Portex	8	2.6 ± 0.08	1.8 ± 0.08	50
Ven	8	2.6 ± 0.1	1.8 ± 0.1	50
Portex	6	2.0 ± 0.08	1.4 ± 0.08	50
Ven	6	2.0 ± 0.1	1.2 ± 0.1	50
Adcock Ingram (Sabax Division, SA)	5	1.7 ± 0.08	0.8 ± 0.1	50
Ven	5	1.9 ± 0.1	0.8 ± 0.1	50
Portex	4	1.3 ± 0.08	0.6 ± 0.08	50
Vygon Nutrisafe (Vygon Laboratories, France)	4	1.5 ± 0.08	0.8 ± 0.08	50
Erich Jaeger (Erich Jaeger, GE)	8	2.7	1.5	50

[1]ID, internal diameter; OD, external diameter; Tol, manufacturer specified tolerance; L, length; UK, United Kingdom; SA, South Africa; GE, Germany.

Abbreviations

ζ	Damping coefficient
A_r/A_0	Resonance amplitude ratio
CMS	Catheter Manometer System
f_{A5}	Frequency at A_0 ± 5%
f_0	Undamped (natural) resonant frequency
F_{RR}	IABC or WFC working respiratory rate
f_r	Damped resonant frequency
FG	French gauge
IABC	Infant air-balloon catheter
Mag	Linear magnitude gain
MANOVA	Multivariate analysis of variance
P_{A5}	Phase difference at f_{A5}
P_{es}	Intra-esophageal pressure
Por	Portex catheter
PVC	Polyvinyl chloride
SA	South Africa
WFC	Water-filled catheter
WRMS	Root mean square Watts

Catheter-Manometer Testing

Five different FG size catheters (Table 1), and two different brands (the same two brands if available) for each FG size catheter, chosen for their similar lengths, were coupled to a Gould P10EZ (Viggo-Spectramed Statham Gould, Oxnard, CA) pressure transducer (diaphragm area 6.4 mm; sensitivity 5 uV/V/mmHg; volume displacement 0.04 mm^3/100 mmHg) and disposable diaphragm-dome with Luer lock fittings (Viggo-Spectramed Gould TA1019, Oxnard, CA). The dome ports were fitted in series to a four-way stopcock of minimum orifice ID 2.0 mm (Adcock Ingram, South Africa) yielding a transducer-dome-stopcock volume of 0.6 mL. The space between the transducer diaphragm and disposable dome diaphragm was water-filled according to the manufacturer's instructions and positioned at catheter-tip level.

Matching IABCs (n = 8) and WFCs (n = 8) of differing FG sizes were assessed by randomly attaching their proximal female Luer fittings directly to the transducer stopcock male Luer fitting. A commercially available adult air-balloon catheter (11 cm air-balloon length; Erich Jaeger, Germany) was included in the study (Table 1). All IABCs were operated within their determined volume optimal working range (balloon air volume = 1 ml). To minimize bubble formation each WFC was flushed with CO_2 followed by deionized and degassed (by boiling) water cooled under vacuum to 36–38°C.[13] The catheter's distal 20 cm was inserted under water into a laboratory designed leak-proof water chamber kept at 36–38°C. Sinusoidal pressure waveforms between −5.5 and +10 cmH_2O (mean 2.3 cmH_2O) were generated in the chamber by means of an 8 Ohm loudspeaker (Bose 4.5" 802; Bose Corporation, USA) powered by an 80 WRMS DC-coupled amplifier linked to a sine wave generator (Hewlett Packard 3562A, USA). The amplifier and loudspeaker heat sinks were water-cooled and the driver diaphragm silicone-coated for water resistance. A swept-sine frequency response of the catheter samples was recorded using a calibrated domeless piezoresistive differential pressure transducer as a reference (Honeywell Microswitch 170PC, USA), positioned inside the chamber adjacent to the IABC and WFC catheter-tips. Unfiltered electrical outputs from the catheters and reference pressure transducer were identically pre-amplified (Hellige Servomed, Freiburg, Germany), displayed oscilloscopically, and analyzed for phase and amplitude differences by averaging three repeat measurements over 10 s at each 1 Hz interval (Hewlett Packard Dynamic Signal Analyzer 3562A, USA). Apparatus reproducibility over the experiment was checked and confirmed by repeating frequency response measurements of the sample of Portex FG size 6 IABCs and WFCs.

Frequency Response Determination

The amplitude and phase responses were analyzed by fitting second-order curves (two poles, no zeros) to the recorded frequency response traces[14,15] using the curve fit function of the HP3562A analyzer. Curves were fitted between 1 Hz and the frequency at which the amplitude was 1 dB down from the maximum recorded amplitude. The pole values thus obtained for the system function (Appendix Eq. 1) were converted to coefficients of the second-order Laplace transfer function describing the curve, allowing calculation of the following variables:

- f_r damped resonant frequency (frequency at maximum amplitude; Appendix, Eq. 4);
- A_r/A_0 resonance amplitude ratio (maximum amplitude, A_r, divided by amplitude at 1 Hz, A_0; Appendix, Eq. 5);
- f_{A5} frequency at $A_0 \pm 5\%$ (frequency at which the amplitude ratio = 1.05 or 0.95).

Amplitude frequency response variables describe IABC gain or attenuation of applied pressure compared with the reference transducer over a range of applied pressure frequencies. Phase-frequency response variables characterize the IABC CMS temporal advancement or retardation of the applied pressure waveform over a range of frequencies; the phase-frequency response variable extracted from the recorded CMS phase-frequency response tracings was:

- P_{A5} phase difference at f_{A5} (Appendix, Eq. 6).

Calculated variables derived from the frequency response recordings were:

- f_0 undamped (natural) resonant frequency (Appendix, Eq. 2);
- ζ damping coefficient (Appendix, Eq. 3);
- F_{RR} IABC or WFC working respiratory rate (Appendix, Eq. 7).

f_o represents the number of oscillations per unit time that the IABC exhibits if left to oscillate undisturbed. ζ describes IABC resistance to oscillation. F_{RR} predicts the maximum respiratory rate up to which an intra-esophageal IABC of given f_o and ζ can potentially measure an applied pressure to within ±5% of the reference transducer.[14,16]

Statistical Analysis

Between-groups one-way (independent variables; IABC or WFC types) multivariate (seven dependent measured frequency response variables, from above) analysis of variance was performed (MANOVA F-test, Statistica™ software, Statsoft, USA) and a post-analysis Tukey significant difference test-correction applied to significant differences.[17] Coefficient of determination (r^2) between F_{RR} and catheter FG size was calculated from the Pearson product-moment correlation. All displayed values are mean ± SD, and P values <0.05 are regarded as statistically significant.

RESULTS

Air-Balloon Pressure-Volume Curves

The static pressure-volume relationships of the combined two FG sizes of catheters (n = 20) and for each FG size separate (each group, n = 10) of Portex FG sizes 10 and 5 IABC samples are illustrated in Figure 1. The Y-axis zero pressure mark represents the point at which the pressure in the air-balloon first became equal to atmospheric pressure with incremental air-volume additions. There was no significant difference (Student's t-test; two-tailed $P > 0.05$) between the working range (region of high compliance) of air-balloons attached to

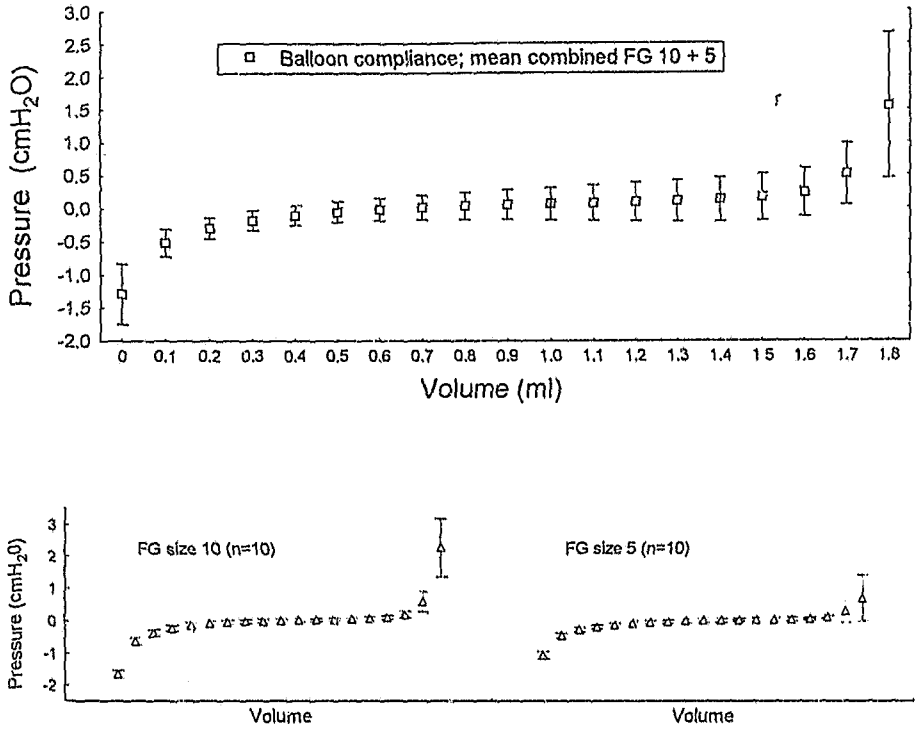

Fig. 1. Static pressure-volume curves of infant air-balloon catheters. Upper graph is mean of combined ($n \approx 20$) FG sizes 10 and 5 catheters. Bottom traces, FG size 10 (left) and FG size 5 (right) catheters demonstrating no significant difference in their working ranges.

Portex FG size 10 versus those attached to FG size 5 catheters (Fig. 1, bottom traces). All our IABCs exhibited a volume working range that exceeded the required IABC specifications of <0.4 cm H_2O pressure change across the working range.[3]

Frequency Responses

Figure 2 illustrates typical frequency response curves recorded from a Portex FG size 6 IABC and WFC.

IABCs f_r, ζ, and A_r and WFCs f_r are demonstrated in Figure 3. Values of ζ and A_r for WFCs have been previously published[10] and are therefore not presented here. Within the IABC Ven and Portex brands, f_r increased significantly with increasing catheter FG size. The f_r of all IABC FG sizes ≥6 was significantly greater than the f_r of matching FG sized WFCs (Fig. 3, top graph). The variation about the mean f_r was less in IABCs than in the WFCs (see f_r SDs of IABCs vs. WFCs in Fig. 3, top graph).

IABC ζ significantly increased with decreasing FG size (Fig. 3, middle graph). All IABC brands of FG size ≥6 were underdamped ($\zeta < 0.71$) and resonated. The Ven 5 FG IABCs exhibited near optimal (critical) damping ($\zeta = 0.71$). The Adcock FG size 5, Portex, and Vygon FG size 4 IABCs were overdamped ($\zeta > 0.71$); hence their f_r values (Fig. 3, top graph) are not presented [for these overdamped IABC frequency response traces, damping coefficient (ζ) and attenuation of the pressure signal (A_r) at natural frequency were calculated from the curves' poles obtained with the second-order curve-fit applied to the traces].

IABC A_r (Fig. 3, bottom graph) was proportional to f_r. The underdamped IABCs exhibited significant increases in gain ($A_r > 1.0$) with increasing FG size, while the overdamped smaller IABCs attenuated the applied pressure signals ($A_r < 1.0$). In contrast, all the FG sizes of WFCs were resonant and amplified the applied pressure signals ($A_r > 1.0$).

Unlike IABC f_r, the IABC $f_{\Lambda 5}$ (Fig. 4, top graph) did not significantly increase with increasing catheter FG size ≥6. $f_{\Lambda 5}$ was >18 Hz for all IABCs ≥FG size 6. IABC phase lag at $f_{\Lambda 5}$ is illustrated in Figure 4, bottom graph.

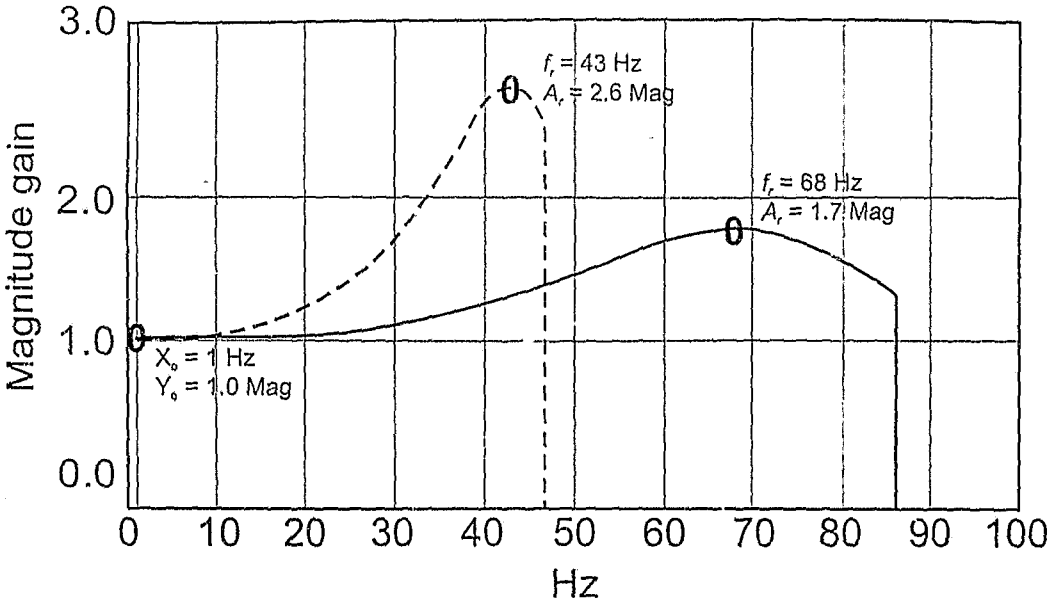

Fig. 2. Comparison of Portex FG size 6 IABC (solid line) versus WFC (dashed line) catheter amplitude-frequency response trace. First marker circle on IABC and WFC represents baseline amplitude (Y-axis, $Y_o = A_o = 1.0$) and baseline frequency (X-axis, $X_o = 1$ Hz). Second marker circle on IABC represents damped resonant frequency (X-axis, $f_r = 68$ Hz) and maximum amplitude gain (Y-axis, $A_r = 1.7$ Mag). WFC $f_r = 43$ Hz and $A_r = 2.6$ Mag. Mag, linear gain over reference transducer.

Working Respiratory Rate

F_{RR} values for differing brands and FG sizes of IABCs are depicted in Figure 5, top graph: Across brands and FG sizes mean F_{RR} minimum and maximum calculated values were 20.4 ± 0.7 (Portex FG size 4) and 244.5 ± 69.8 (Ven FG size 5) breaths/min, respectively. There was no significant F_{RR} difference between FG sizes 6, 8, and 10 within the same brand of Portex or Ven IABCs, nor was there any significant F_{RR} difference between these two brands for the same FG sizes 6, 8, or 10. The maximum mean F_{RR} recorded in IABCs ≥FG size 6 was 148 breaths/min (Ven FG size 10). The overdamped IABCs (Adcock FG size 5, Portex, and Vygon FG sizes 4) exhibited a significantly lower F_{RR} than all IABC FG sizes ≥6. The Ven FG size 5 catheter F_{RR} was significantly greater than any other FG size catheter due to the near critical ζ, but it manifested the largest variation about mean F_{RR} due to both under- and overdamped frequency responses recorded within the catheter sample.

IABC F_{RR} was significantly higher than matching FG size WFCs for all FG sizes ≥6, and for the Ven FG size 5 and Vygon FG size 4 catheters (Fig. 5, bottom graph). In addition, the Portex and Ven FG size 6 IABCs exhibited a significantly higher F_{RR} than the Portex and Ven FG size 10 WFCs. The Adcock FG size 5 and Portex FG size 4 F_{RR} was similar between IABC and WFCs.

Correlation (r^2) between IABC F_{RR} and FG size, ID, or OD was 0.12, 0.10, and 0.18, respectively, whereas it was 0.75, 0.82, and 0.76, respectively, for the WFCs.

IABC frequency response variables F_{RR}, ζ, A_r, and f_r that were significantly different ($P < 0.05$) between the various IABC FG sizes and brands are summarized in Table 2.

DISCUSSION

By virtue of their construction, IABCs offer certain advantages over transducer micro-tip and WFCs.[1] Transducer micro-tip catheters can exhibit absolute pressure measurement inaccuracies with changes in the temperature or fluid nature of the surrounding intra-esophageal medium,[7] and they are markedly more sensitive to intra-esophageal cardiac artifacts than balloon catheters.[8] WFC absolute pressure measurements are altered when the vertical distance between catheter-tip and transducer is changed, and WFCs are also sensitive to motion artifacts.[9] The long IABC balloon measures mean intra-esophageal pressure over a larger portion of the lower esophagus than do WFCs or single micro-tip transducer catheters, making it more likely that the mean value of an unevenly distributed intra-thoracic pleural pressure[18–20] is recorded. IABCs are subject neither to measurement

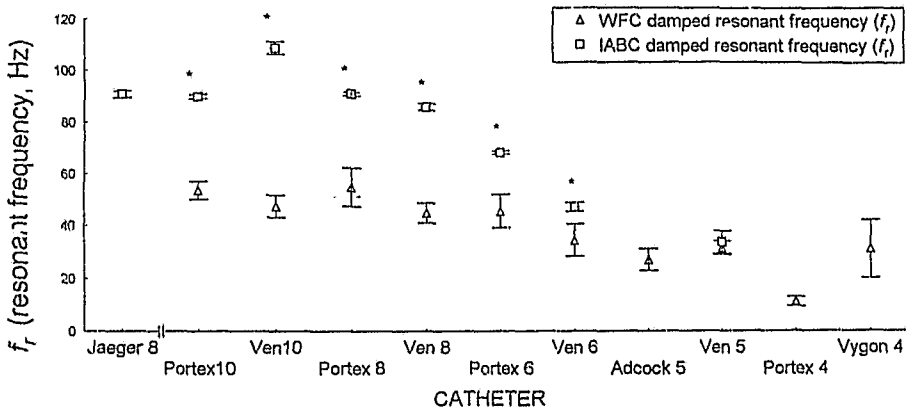

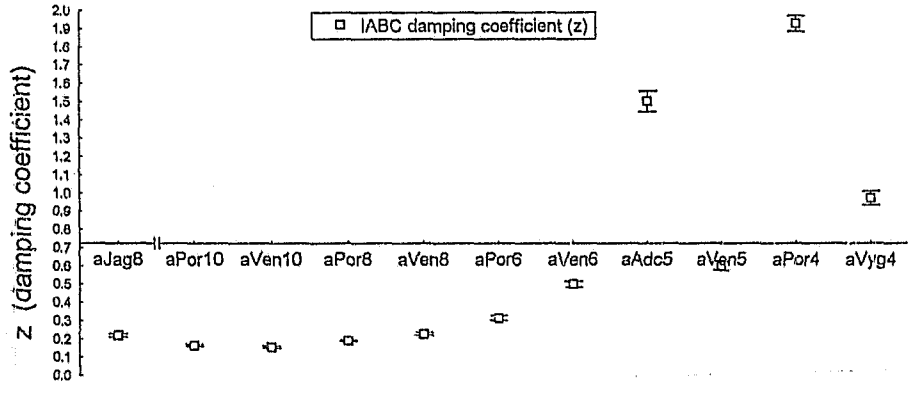

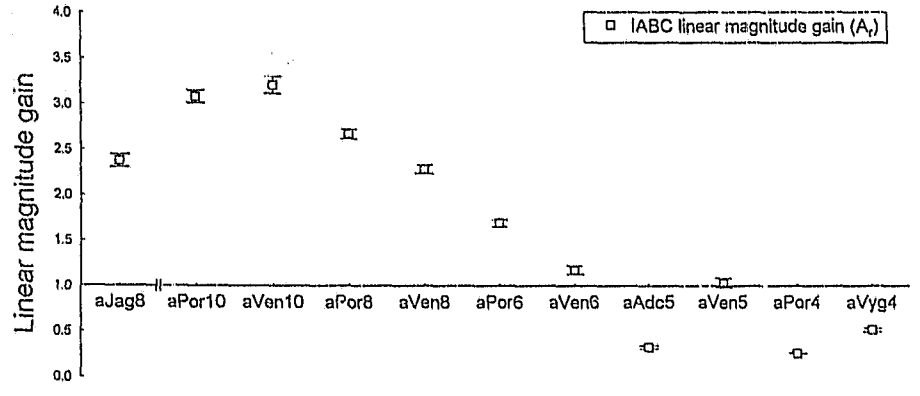

Fig. 3. Catheter amplitude-frequency response characteristics. X-axes set at critical damping ($z = 0.71$) and zero gain ($A_r = 1.0$) for z and A_r graphs, respectively. X-scale break separates commercial Jaeger adult from laboratory-made IABCs. f_r, damped resonant frequency for IABCs versus WFCs; z, IABC damping coefficient (ζ); A_r, IABC amplitude gain or attenuation at f_r; Catheter, catheter brand and FG size; aPor, Portex IABC; *, $P < 0.05$ for IABC vs. WFC of same FG size.

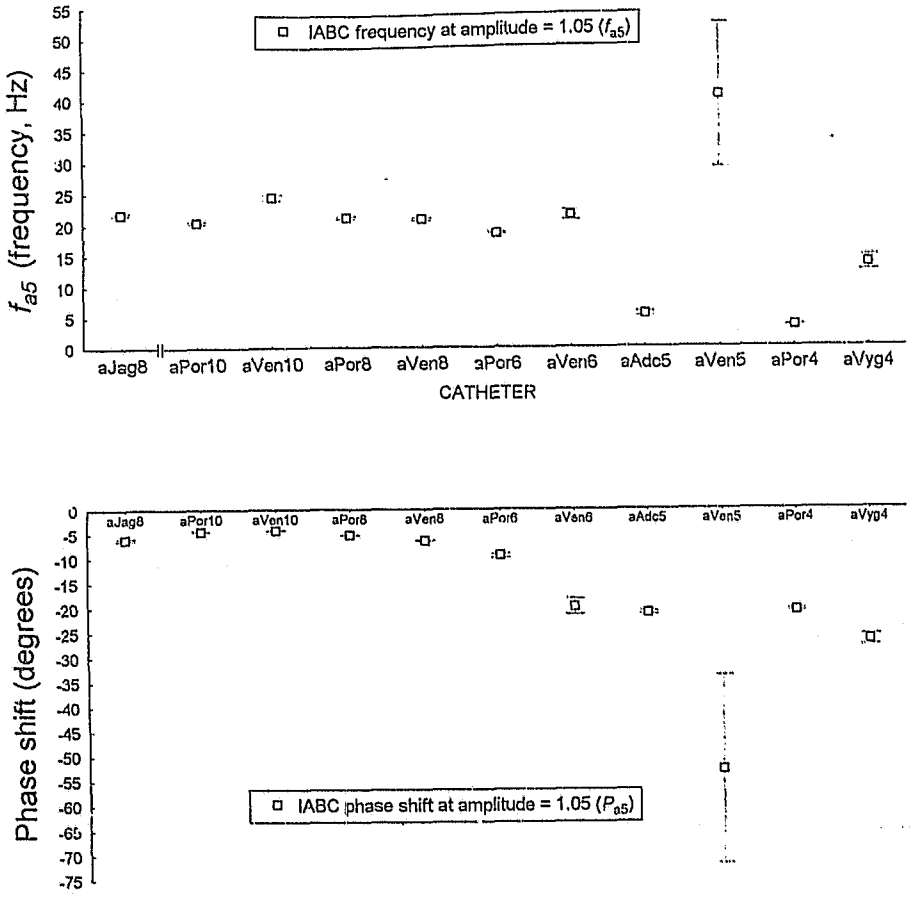

Fig. 4. IABC amplitude and phase frequency response characteristics. f_{A5}, frequency at $A_o \pm 5\%$; P_{A5}, phase difference at $A_o \pm 5\%$ or f_{A5}. Catheter, catheter brand and FG size; aPor, Portex IABC.

errors related to the dissipation of liquid volume around WFC tips[21] nor to worsened dynamic performance from the introduction of gas microbubbles into WFCs. The recent advent of cheap disposable pressure transducers[22] make IABCs comparatively inexpensive[8] for neonatal intensive care, and they are relatively atraumatic[4,6] on insertion by virtue of balloon-latex and catheter PVC flexibility.

Frequency Responses

The commonly performed in vivo airway occlusion test[17,18,23] helps to position intra-esophageal IABCs optimally by assessing the in situ intra-esophageal catheter's reflection of pleural pressure. However, this procedure does not assess the ability of IABCs to respond accurately to dynamic P_{es} changes during artificial ventilation. Researchers employing air-balloon catheters to measure P_{es} have noted adequate frequency responses to 10,[3,5] 20,[18,24] and 22 Hz[25] in a FG size 6 catheter and to 5[26,27] and 15 Hz[28] in an FG size 8 catheter. However, these studies were not aimed at formally assessing IABC frequency responses or at comparing IABCs with WFCs, and the frequency responses were reported for catheters (usually n = 1) of just one FG size and brand. Thus effects due to manufacturing tolerances within a catheter and balloon sample, and effects related to differing catheter tolerances between manufacturers for the same FG size (Table 1) were excluded. Details of catheter length, wall thickness, composition, brand, balloon length, balloon diameter and latex thickness, the definition of adequate frequency response used, and the method of frequency response analysis were also not provided in most of the above reports; hence the large frequency response

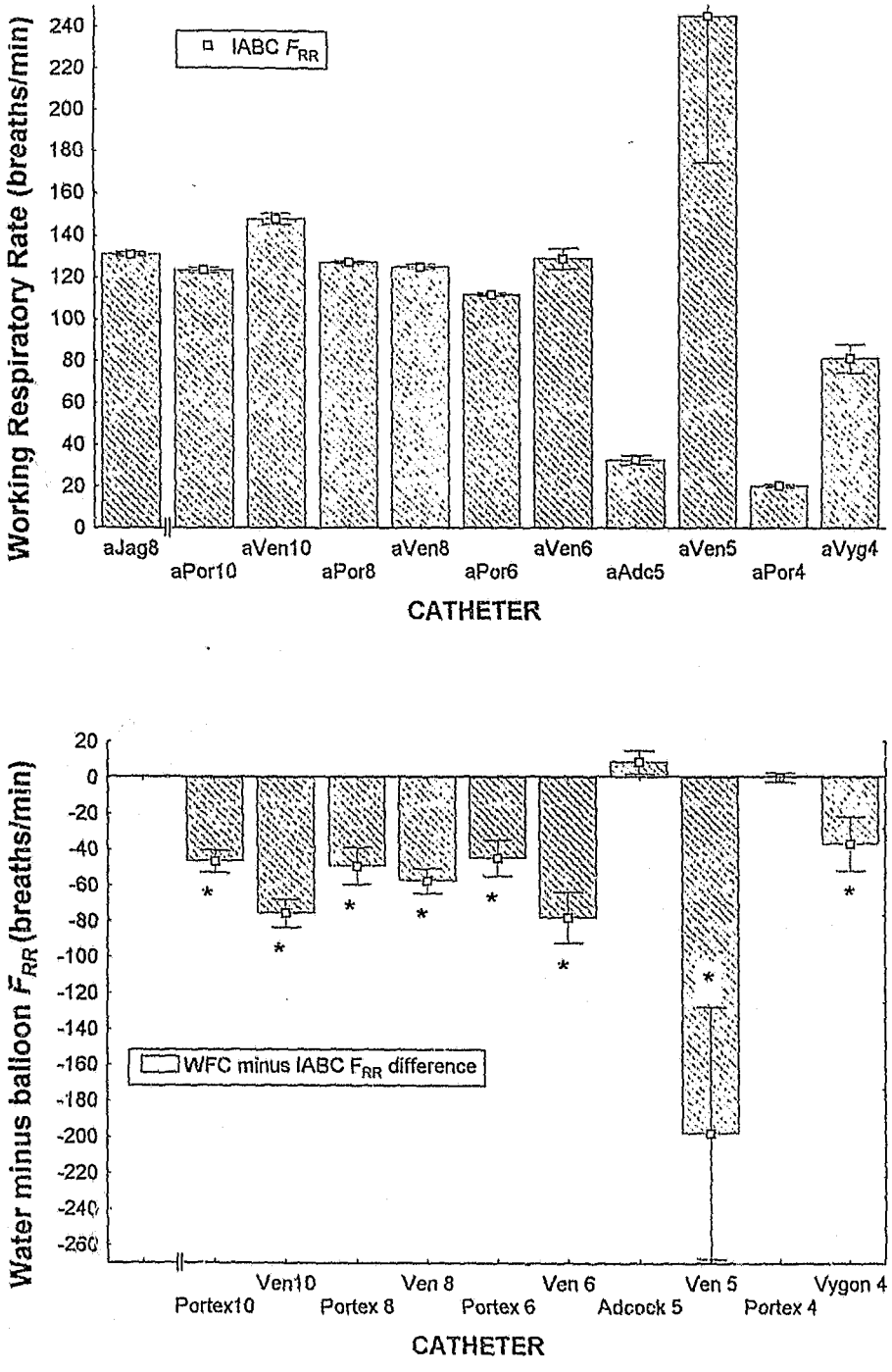

Fig. 5. Working respiratory rate. Top bar-chart is F_{RR} of IABCs. Bottom bar-chart is mean F_{RR} difference between WFCs and IABCs. F_{RR}, working respiratory rate; Catheter, catheter brand and FG size; aPor, Portex infant air-balloon catheter; *, $P < 0.05$ for infant air-balloon (IABC) vs. water-filled catheter (WFC) of same FG size.

TABLE 2—Infant Air-Balloon Catheter Statistical Summary Table[1]

	Por10	Ven10	Por8	Ven8	Por6	Ven6	Adc5	Ven5	Por4	Vyg4	Jag8
Por10											
Ven10	d										
Por8	c	cd									
Ven8	bc	bcd	c								
Por6	bcd	abcd	bcd	bcd							
Ven6	bcd	bcd	bcd	bcd	bcd						
Adc5	abc	abc	abc	abc	abc	abc					
Ven5	abcd	abcd	abcd	abcd	abcd	abd	abc				
Por4	abc	abc	abc	abc	abc	abc	b	abc			
Vyg4	abc	abc	abc	abc	abc	abc	ab	abc	ab		
Jag8	bc	bcd	c	–	bcd	bcd	abc	abcd	abc	ab	

[1]Variable a–d indicated are $P < 0.05$ between any two catheters. a, working respiratory rate (F_{RR}); b, damping coefficient (ζ); c, amplitude gain or attenuation (A_r); d, damped resonant frequency (f_r); Por, Adc, Ven, and Jag, Portex, Adcock, Ven, Erich-Jaeger catheter brands and FG size; –, no significant difference.

data discrepancies for the same FG sizes noted between researchers here.

By fixing transducer type, catheter length, FG size, composition, and brands between the IABC and WFC groups, the data in this report directly assess and compare the dynamic frequency response characteristics of matching IABCs and WFCs of various FG sizes and brands. Our data suggest that IABCs, manufactured to the appropriate specifications for infants[3] offer significantly superior frequency response characteristics compared with matching WFCs. We measured f_{A5} and calculated F_{RR} as clinically meaningful variables to evaluate the measurement fidelity of IABCs: The lowest f_{A5} (Fig. 4) recorded in IABC ≥FG size 6 was 19 Hz. Infants are commonly ventilated at high respiratory rates, and the pediatric ventilators employed may generate very steep inspiratory waveforms with high-frequency harmonic contents, or be of the high-frequency-oscillatory type. Therefore, provided that the esophageal pressure waveform's energy is located within the first ten harmonics of the ventilator's fundamental frequency,[4,9] an IABC ≥FG size 6 can be expected to produce a minimum F_{RR} (which predicts the potential of an IABC to measure P_{es} within a 5% error limit up to a calculated respiratory rate) of 112 breaths/min. However, under conditions of an esophageal pressure waveform's energy being located within the first 5 harmonics[1] of the fundamental frequency, our findings indicate that IABCs ≥FG size 6 may record (to within 5% accuracy) such a waveform administered at up to 224 breaths/min.

High correlations between F_{RR} and FG size, OD, or ID in the WFCs imply that choosing a larger FG size WFC extends the F_{RR}. On the other hand, the poor correlations calculated for F_{RR} versus FG size, OD, or ID in IABCs can be seen as advantageous to clinicians: For the same catheter brand, FG size 6 IABCs exhibit an F_{RR} comparable to FG size 8 and 10 IABCs, and yet also exhibit a significantly better F_{RR} than FG size 10 WFCs. Thus an FG size 6 IABC offers clinicians and researchers a relatively atraumatically sized catheter with pressure measurement fidelity similar to much larger IABCs and also exceeds the measurement fidelity of equivalent FG size 10 WFCs.

The variation of f_r within IABC catheter samples is fortunately lower than that found within matching WFC groups. Variation differences may be attributed to microbubbles of trapped gas in the WFCs,[29–31] despite the WFC CO_2 flushing and water-degassing procedures. We noticed that WFC female Luer fittings tend to trap gas bubbles at the junction of the catheter's body and Luer fitting, which in certain cases proved difficult to remove even with reverse flushing. These adverse characteristics are intensified in clinical settings in which CO_2 flushing, degassing of water, and reverse liquid flushing of WFCs are not possible.

We demonstrated that IABCs of FG sizes ≥6 are underdamped and resonate, yet IABCs of FG size 4 and 5 can be overdamped and attenuate the esophageal waveform pressure signal. The overdamped properties of small FG size IABCs are not likely to be due to occlusion of the catheter-tip eyelets by the latex balloons, nor to partial luminal occlusion of the IABC small FG size by balloon ties, since we were able to demonstrate the overdamping effect using equivalent air-filled catheters without latex balloons attached (data not shown here). The pressure-volume coefficient (or elastance) of IABCs is determined mainly by the compressibility of the air contained in IABCs, whereas it is primarily governed by the elastic properties of the catheters and transducer-dome diaphragm combination in WFCs. The overdamping may thus be explained by the combination of a low radius, soft PVC, and high compressibility of the air. In spite of the overdamped frequency characteristics of small FG size IABCs, they still possessed an F_{RR} similar to matching small FG WFCs.

Validity of Methods

We performed in vitro frequency response analysis because in vivo fast flush tests are not applicable to

IABCs. An advantage of the in vitro technique is the absence of superimposed in vivo peristaltic and cardiac waveform artifacts.[29] We used the swept frequency forced oscillation technique as opposed to the step response techniques (free oscillation burst-balloon, or fast flush tests) because the latter is practically limited to underdamped systems.[29,31] This would not be suitable for the overdamped small FG size IABCs. In addition, step response techniques may miss subtle differences in f_0[13] and are open to measurement inaccuracies in the determination of the period and amplitude of the response.[29] The swept frequency technique is suitable for a distributed parameter system,[29,31] such as that encountered with IABCs, and allows IABC stimulation at equal amplitude over all frequencies, whereas the step response approach results in diminishing amplitudes with increasing frequency.

To incorporate possible effects due to non-linearities (amplitude dependency) related to dynamic IABC compliance and catheter wall hysteresis,[31] we applied an input pressure of −5 to +10 cmH_2O similar to mean P_{es} accompanying artificial ventilation. Temperature fluctuation influences frequency responses[15,31,32] through altering compliance or compliance hysteresis of PVC and closed-tip latex balloons; therefore the IABC and WFC frequency responses were measured at infant physiological temperatures.

We noted similar compliance curves for our laboratory-produced balloons attached to either FG size 10 or FG size 5 catheters (Fig. 1). This suggests that, to manufacture IABCs, one size (ID 8.3 mm, length 5.5 cm) of infant latex-balloon may be adequate for attachment to differing FG sized catheters.

We conclude that frequency responses of IABCs greater than FG size 5 exhibit underdamped resonant traces, whereas smaller FG size IABCs may be overdamped. FG size 6 IABCs offer similar measurement accuracies to those of larger IABCs. IABCs, manufactured to infant-appropriate balloon specifications, can potentially measure P_{es} up to 148 breaths/min within a 5% error limit. Compared with matching WFCs, IABCs have significantly superior frequency response characteristics and lower frequency response variability within catheter samples and are therefore more suitable for accurate dynamic P_{es} measurements during the high-frequency respiratory mechanics commonly encountered in artificially ventilated infants.

APPENDIX

Equations for Amplitude and Phase Calculations

Poles (roots of the denominator) of the system function G(s), located from the second-order curve fitted to the frequency response traces, are converted to coefficients of the standard second-order Laplace transform function given by[33,34]

$$G(s) = c/(s/a)^2 + 2\zeta(s/b) + c \quad (1)$$

thus

Undamped natural frequency[14,15,33]

$$f_0 = (s/a)^{1/2} \quad (2)$$

Damping coefficient[14,15,33]

$$\zeta = (s/b)/2f_0 \quad (3)$$

Damped resonant frequency[14,15,33]

$$f_r = f_0(1 - 2\zeta^2)^{1/2} \quad (4)$$

Maximum amplitude ratio[16]

$$A_r = 1/(1 - (2\zeta^2 + 1)^2)^{1/2} \quad (5)$$

Phase at $A_0 + 5\%$[14]

$$P_{A5} = \tan^{-1}((2\zeta \pm f_{A5}/f_0)/1 - (f_{A5}/f_0)^2) \quad (6)$$

Working respiratory rate[14,16]

$$F_{RR} = (f_{A5} \times 60)/10 \quad (7)$$

where f_{A5} is the frequency at which the amplitude ratio = 1.05 or 0.95 and 10 refers to the Fourier series 10th harmonic.

Appendix Note

In this experiment the frequency response trace was divided through by the amplitude ratio at 1 Hz (regarded as the DC response) and therefore $A_o/A_r = 1/A_r$. The CMS frequency response calculations assume that the system is second order and linear.[14]

ACKNOWLEDGMENTS

Catheter donations: Erich-Jaeger, Selwyn Sher ElectroMed, S.A.; Portex, the Boots Company S.A. and Portex, U.K.; Ven, Ven Products, S.A.; Vygon, Art Medical Equipment, S.A.; Sabax, Adcock Ingram, S.A.

REFERENCES

1. Coates AL, Stocks J. Esophageal pressure manometry in human infants. Pediatr Pulmonol, 1991; 11:350–360.
2. Coates AL, Stocks J, Gerhardt T. Esophage[illegible] manometry. In:

Stocks J, Sly PD, Tepper RS, Morgan WJ, eds. Infant Respiratory Function Testing. New York: John Wiley & Sons, 1996:241–258.
3. Beardsmore CS, Helms P, Stocks J, Hatch DJ, Silverman M. Improved esophageal balloon technique for use in infants. J Appl Physiol. 1980; 49:735–742.
4. Maxted KJ, Shaw A, Macdonald TH. Choosing a catheter system for measuring intra-esophageal pressure. Med Biol Eng Comput. 1977; 15:398–401.
5. Heaf DP, Turner H, Stocks J, Helms P. The accuracy of esophageal pressure measurements in convalescent and sick intubated infants. Pediatr Pulmonol. 1986; 2:5–8.
6. Kaplan M, Galioto FM, Ruttimann UE, Hamosh P, Avery GB. Evaluation of a gastric tube with esophageal balloon for neonatal use. Am J Perinatol. 1984; 1:355–359.
7. Chartrand DA, Ye TH, Maarek JM, Chang HK. Measurement of pleural pressure at low and high frequencies in normal rabbits. J Appl Physiol. 1987; 63:1142–1146.
8. Chartrand DA, Jodoin C, Couture J. Measurement of pleural pressure with oesophageal catheter-tip micromanometer in anaesthetized humans. Can J Anaesth. 1991; 38:518–521.
9. Senterre J, Geubelle F. Measurement of endoesophageal pressure in the newborns. Biol Neonate. 1970; 16:47–53.
10. Hartford CG, Rogers GG, Turner MJ. Correctly selecting a liquid-filled nasogastric infant feeding catheter to measure intraesophageal pressure. Pediatr Pulmonol. 1997; 23:362–369.
11. Beardsmore CS, Stocks J, Silverman M. Esophageal pressure in infants at elevated lung volumes and positive airway pressure. J Appl Physiol. 1983; 55:377–382.
12. Lemen R, Benson M, Jones JG. Absolute pressure measurements with hand-dipped and manufactured esophageal balloons. J Appl Physiol. 1974; 37:600–603.
13. Shapiro GG, Krovetz LJ. Damped and undamped frequency responses of underdamped catheter manometer systems. Am Heart J. 1970; 80:226–236.
14. Fry DL. Physiologic recording of modern instruments with particular reference to pressure recording. Physiol Rev. 1960; 40: 753–788.
15. Hansen AT. The theory for elastic liquid-containing membrane manometers; Special part. Acta Physiol Scand. 1950; 19:333–343.
16. Hipkins SF, Rutten AJ, Runciman WB. Experimental analysis of catheter-manometer systems in vitro and in vivo. Anesthesiology. 1989; 71:893–906.
17. Zar JH. Biostatistical Analysis. Englewood Cliffs, NJ: Prentice-Hall, 1974:206–252.
18. Baydur A, Behrakis PK, Zin WA, Jaeger M, Milic-Emili J. A simple method for assessing the validity of the esophageal balloon technique. Am Rev Respir Dis. 1982; 126:788–791.
19. LeSouef PN, Lopes JM, England SJ, Bryan MH, Bryan AC. Influence of chest wall distortion on esophageal pressure. J Appl Physiol. 1983; 55:353–358.
20. Ratjen FA, Wiesemann HG. Variability of dynamic compliance measurements in spontaneously breathing and ventilated newborn infants. Pediatr Pulmonol. 1992; 12:73–80.
21. Gerhardt T, Bancalari E. Chestwall compliance in full term and premature infants. Acta Paediatr Scand. 1980; 69:359.
22. Gardner RM. Accuracy and reliability of disposable pressure transducers coupled with modern pressure monitors. Crit Care Med. 1996; 24:879–882.
23. Coates AL, Davis GM, Vallinis P, Outerbridge EW. Liquid-filled esophageal catheter for measuring pleural pressure in preterm neonates. J Appl Physiol. 1989; 67:889–893.
24. Higgs BD, Behrakis PK, Bevan DR, Milic-Emili J. Measurement of pleural pressure with esophageal balloon in anaesthetized humans. Anesthesiology. 1983; 59:340–343.
25. Baydur A, Cha E, Sassoon CSH. Validation of esophageal balloon technique at different lung volumes and postures. J Appl Physiol. 1987; 65:315–321.
26. Wolfson FR, Greenspan JS, Deoras KS, Allen JL, Shaffer TH. Effect of position on mechanical interaction between rib cage and abdomen in preterm infants. J Appl Physiol. 1992; 72:1032–1038.
27. Bhutani VK, Sivieri EM, Abbasi S, Shaffer TH. Evaluation of neonatal pulmonary mechanics and energetics. Pediatr Pulmonol. 1988; 4:150–158.
28. Dechman G, Sato J, Bates JHT. Factors affecting the accuracy of esophageal balloon measurement of pleural pressure in dogs. J Appl Physiol. 1992; 72:383–388.
29. Gardner RM. Direct blood pressure measurement-dynamic response requirements. Anesthesiology. 1981; 54:227–236.
30. Milic-Emili J, Mead J, Turner JM, Glauser EM. Improved technique for estimating pleural pressure from esophageal balloons. J Appl Physiol. 1964; 19:207–211.
31. Yeomanson CW, Evans DH. The frequency response of external transducer blood pressure measurement systems: A theoretical and experimental study. Clin Phys Physiol Meas. 1983; 4:435–449.
32. Rutten AJ, Nancarrow C, Isley AH. An assessment of six different pulmonary artery catheters. Crit Care Med. 1987; 15:250–255.
33. Kuo FF. The Laplace transform: Amplitude, phase and delay. In: Network Analysis and Synthesis. New York: John Wiley & Sons. 1966:134–165, 253–279.
34. Milhorn HT. Transient analysis of physical systems. In: The Application of Control Theory to Physiological Systems. Philadelphia: WB Saunders, 1966:78–91.

Predicting Air-Balloon and Water-Filled Infant Catheter Frequency Responses

Testing the Validity of the Assumption that Fluid-Filled Catheters Fit a Second-Order System

Catheter microtip pressure-transducer technology is replacing the use of fluid-filled catheters for *in vivo* pressure measurements. However, dynamic intra-esophageal pressure measurement, employed to estimate pleural pressure when calculating infant dynamic lung compliance, continues to be performed using fluid-filled catheters [1, 2]. Nasogastric water-filled catheters (W-FC) and air-balloon catheters (A-BC), by virtue of their flexibility, reduce the risk of esophageal trauma in newborns [3,4]. W-FCs *in situ* are well tolerated by infants [4] and are commonly in use for nasogastric feeding and thus are accessible to clinicians. On the other hand, transducer microtip catheters may drift with changes in the temperature or the fluid nature of the surrounding intra-esophageal medium [5]. They are markedly more sensitive to intra-esophageal cardiac artifacts than A-BCs [6] and may overestimate dynamic pleural pressures in infants [7]. The A-BC balloon length is advantageous for measuring intra-esophageal pressure over a large portion of the lower esophagus, while current availability of disposable pressure transducers [8] makes the robust [9] W-FCs and A-BCs affordable manometer options.

The presence of high-frequency respiratory mechanics in newborns makes formal frequency response assessment of fluid-filled catheters a necessity [10, 11]. This assessment may be performed using the *in vitro* swept sine-wave generator technique, or the *in vitro* (burst-balloon) or *in vivo* (fast-flush) square-wave response techniques. Square-wave response techniques usually invoke equations that assume catheter frequency responses are a second-order system, thereby enabling prediction of the catheters' frequency response curves and the frequency up to which the catheters exhibit a near uniform response [12, 13]. The theory of typical equations used to analyze square-wave responses and to predict underdamped liquid-filled catheter frequency responses is extensively published [14-20]. However, experimental evidence to support the assumption of an adequate second-order fit, inherent to most of these equations, is sparse and only found for certain intra-arterial liquid-filled catheters [9, 21, 22]. The validity of assuming a second-order system frequency response for liquid- and gas-filled polyvinyl chloride (PVC) nasogastric feeding catheters (NGC) used to measure infant dynamic intra-esophageal pressure is untested. Nevertheless, the square-wave response technique, typically reliant upon this assumption, is used to obtain the frequency responses of these fluid-filled NGCs [23].

In this article, we discuss our study that quantitatively tests the validity of the assumption that fluid-filled NGC frequency responses adequately fit a second-order system. This assumption is inherent to equations commonly used to predict frequency responses from square-wave response techniques. We review our experiment in which we determined the frequency response of different catheter brands with a sine-wave generator, and we present the results.

Materials and Methods

Catheters and Frequency Response Measurements

Data presented in this study were obtained from experiments performed by the authors to determine the frequency responses of infant air-balloon versus equivalent liquid-filled PVC feeding catheters as used to measure dynamic intra-esophageal pressure in infants (data not yet published). Infant A-BCs were laboratory manufactured by attaching suitable latex balloons [24] to PVC NGCs. A commercially available adult A-BC (Erich Jaeger, Germany) was also included in the experiment (Table 1).

Eight samples each of differing brands and FG (French Gauge) size A-BCs and W-FCs of similar lengths (Table 1), connected to a Gould P10EZ pressure transducer and disposable diaphragm dome (Viggo-Spectramed Gould TA1019, Oxnard, CA) and 4-way stopcocks, were inserted into a water-filled chamber kept at 37°C. W-FCs were flushed with carbon dioxide followed by degassed water at 37°C prior to testing [25]. A-BCs were operated within their determined optimal volume working range [24]. A sine-wave generator (Hewlett Packard 3562A, USA) linked to a DC-coupled amplifier and loudspeaker (Bose 4.5" 802, Bose Corporation, MA) generated sinusoidal pressure waveforms inside the chamber between -5.5 and +10 cmH_2O pressure from 1-100

Craig G. Hartford[1], Johan M. van Schalkwyk[2], Geoffrey G. Rogers[1], and Martin J. Turner[3]
Departments of Physiology[1], Anaesthetics[2] and Electrical Engineering[3]
Johannesburg Hospital, University of the Witwatersrand Medical School

 0739-5175/97/$10.00©1997

Table 1. Catheter types.

Nasogastric Catheter	FG	ID, mm	Length, cm
Portex W-FC + A-BC (Portex, Kent, UK)	10	2.3	60
Ven W-FC + A-BC (Ven Products, SA)	10	2.3	50
Portex W-FC + A-BC	8	1.8	50
Ven W-FC + A-BC	8	1.8	50
Portex W-FC + A-BC	6	1.4	50
Ven W-FC + A-BC	6	1.2	50
Adcock Ingram W-FC (Sabax Division, SA)	5	0.8	50
Ven W-FC	5	0.8	50
Portex W-FC	4	0.6	50
Vygon Nutrisafe W-FC (Vygon Laboratories, France)	4	0.8	50
Erich Jaeger A-BC (Erich Jaeger, GE)	8	1.5	50

FG, French gauge; ID, internal diameter; W-FC, water-filled catheter; A-BC, air-balloon catheter; UK, United Kingdom; SA, South Africa; GE, Germany.

Hz, averaged for 10 s at each 1 Hz interval. Catheter amplitude and phase-frequency responses were determined (Hewlett Packard Dynamic Signal Analyser 3562A, USA) by comparison with the output from a temperature-compensated reference pressure transducer (Honeywell Microswitch 170PC, USA) located above the catheter tip.

Frequency Response Ratios and Variables

The original recorded curves (ORC) of amplitude and phase-frequency responses obtained from the sine-wave generator technique were further analyzed by fitting second-order system curves (2 poles, no zeros) to the ORC traces, using the curve-fit function of the HP3562A analyzer. Curves were fitted between 1 Hz and the frequency at which the amplitude was 1 dB down from the maximum recorded amplitude. The ORCs and second-order fitted curves (SOFC) were then divided through by their amplitudes at 1 Hz (regarded as the DC response).

The values of five variables (commonly quoted by researchers to describe the frequency responses of their catheter-manometer systems) were obtained from each SOFC and ORC tracing (Fig. 1). The SOFC:ORC ratio (for amplitude-frequency responses) and the SOFC-ORC difference (for phase-frequency responses) were determined for each variable as follows:

SOFC:ORC ratios from the amplitude-frequency response tracings:

- SOFC:ORC of f_{A5}: Ratio of the SOFC and ORC tracings' frequency values at which $A = 1.05$ (A refers to the linear amplitude gain of the catheter-manometer under test over that of the reference transducer. f_{A5} is thus the frequency up to which the catheter has a near uniform amplitude-frequency response [12, 17] (Fig. 1).
- SOFC:ORC of f_r: Ratio of the SOFC and ORC tracings' damped resonance frequency values (frequency at maximum amplitude gain)
- SOFC:ORC of A_r: Ratio of the SOFC and ORC tracings' maximum amplitude gain values (linear gain at f_r)

SOFC-ORC phase-shift differences from the phase-frequency response tracings:

- SOFC-ORC of P_{A5}: Difference between the SOFC and ORC tracings' phase-shift values at f_{A5}
- SOFC-ORC of Pf_r: Difference between the SOFC and ORC tracings' phase-shift values at f_r

Statistical Analysis

For amplitude-frequency response variables, confidence intervals (95%) for SOFC:ORC ratios were calculated [26]. SOFC:ORC ratios with confidence intervals that excluded the ideal ratio of 1.0 and that additionally had mean ratios less than or equal to 0.95 or greater than or equal to 1.05 were regarded as significantly different. SOFC-ORC phase-shift variables were compared using the Student two-tailed paired t-test.

Significant differences between samples of A-BC and W-FC FG sizes and brands were determined by one-way (independent variables: A-BC or W-FC

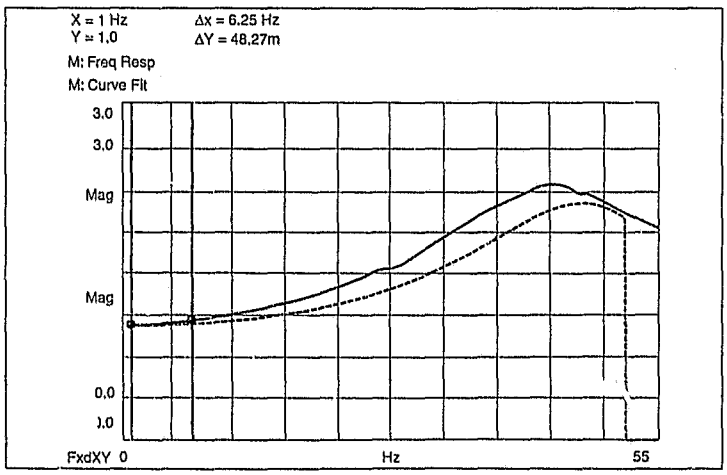

1. Sample plot of second-order fitted curve (SOFC, dashed line) versus original recorded curve (ORC, solid line) for Ven FG-size 8 water-filled catheter (W-FC) amplitude-frequency response trace. First marker circle represents baseline amplitude (Y-axis, Ya = 1.0 Mag) and baseline frequency (X-axis, X = 1 Hz). Second marker circle shows frequency at which $A = 1.05$ Mag on the ORC trace (X-axis, $f_{A5} = X + \Delta X = 7.4$ Hz). The SOFC's f_{A5} is extended upwards relative to the ORC's f_{A5}, yielding a SOFC:ORC f_{A5} ratio of 1.5. Mag: linear gain over reference transducer; Hz: hertz.

catheter types) multivariate (5 dependent SOFC:ORC amplitude or phase-frequency response variables) analysis of variance (MANOVA F-test, StatisticaTM software, Statsoft, OK) and a post-analysis Tukey Significant Difference test-correction applied to significant differences [27]. All displayed values are mean ±SD, and P-values less than 0.05 are regarded as statistically significant.

Results

SOFC:ORC ratios for the amplitude-frequency response variables are depicted in Fig. 2. SOFCs of both the A-BC and W-FC groups significantly overvalued the frequency at which the amplitude gain was 1.05 (or f_{A5}), as evidenced from the mean SOFC:ORC ratios of f_{A5} being significantly greater than 1.0 for all but one (wPor4) catheter sample (Fig. 2, top graph). Between the A-BC and W-FC catheter groups, for the same FG size and brand of catheter, the SOFC of the W-FC group's samples overvalued f_{A5} to a significantly greater degree than did the SOFCs of the A-BC group's samples (e.g., compare the ratios of wVen10 and aVen10). Within the W-FC group there was a significant decrease in the mean SOFC:ORC ratio of f_{A5} (toward the ideal ratio of 1.0) with decreasing catheter FG size, but this decrease was less noticeable within the A-BC group. Within both A-BC and W-FC groups, for the same sample FG sizes, the SOFC:ORC ratio of f_{A5} was unaffected by the brand of catheter tested (e.g., compare the ratio of wPor10 with wVen10).

In contrast to the SOFC:ORC ratios of f_{A5} above, the SOFC:ORC ratio of f_r (Fig. 2, middle graph) was not significantly different from the ideal ratio of 1.0 in all of the A-BC group's samples, while SOFCs of only a few of the W-FC group's samples significantly overvalued the f_r (to a small degree). However, SOFCs of most W-FC and A-BC group's samples significantly undervalued the amplitude magnitude at resonance frequency (A_r), as evidenced by the SOFC:ORC of A_r being significantly less than 1.0 (Fig. 2, bottom graph). This SOFC undervaluation of A_r was similar between the A-BC and W-FC groups, and in several catheter samples the magnitude of undervaluation significantly decreased with decreasing catheter FG-size in both groups. Within the A-BC and the W-FC groups, for the same FG-size samples, the SOFC:ORC ratio of A_r was not significantly affected by the brand of catheter tested. Only one (wPor4) catheter's SOFC:ORC did not differ significantly from ideal across all three amplitude-frequency response variables.

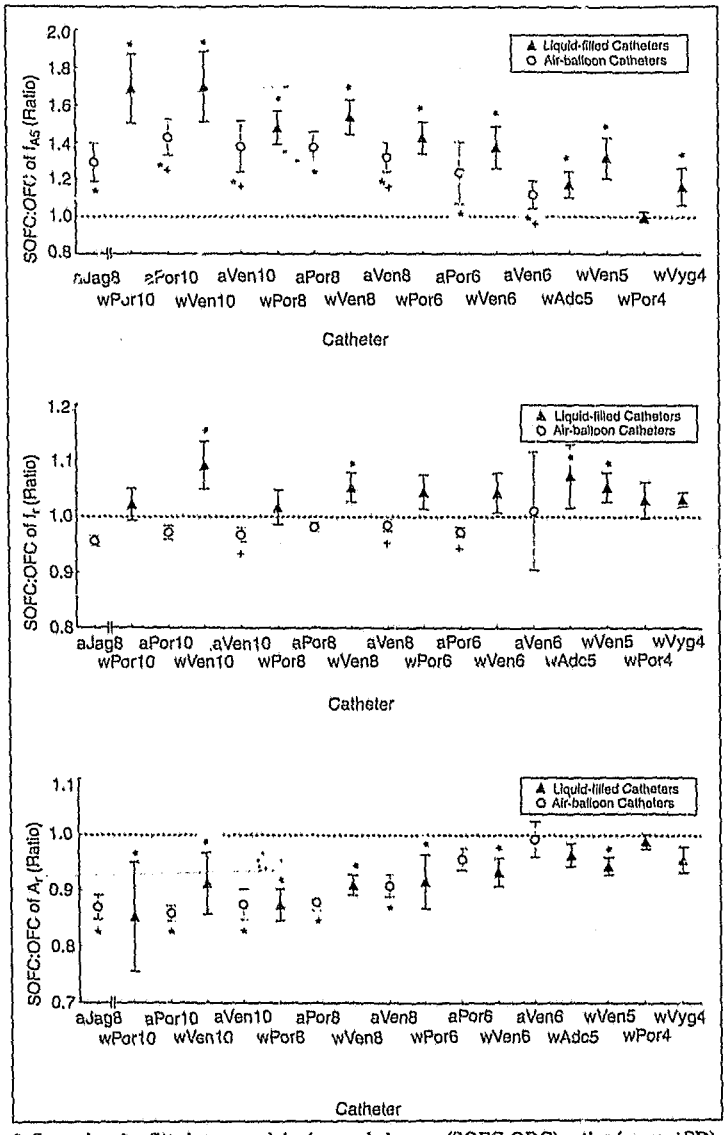

2. Second-order fitted curve:original recorded curve (SOFC:ORC) ratios (mean ±SD) for amplitude-frequency response trace variables. Horizontal dashed line depicts ideal SOFC:ORC ratio of 1.0. X-scale break separates commercial Jaeger adult from laboratory-made air-balloon catheters. SOFC:ORC of f_{A5}: SOFC:ORC ratio at the frequency at which $A = 1.05$; SOFC:ORC of f_r: SOFC:ORC ratio at damped resonance frequency; SOFC:ORC of A_r: SOFC:ORC ratio at maximum amplitude gain. Catheter: catheter brand and French Gauge size; aPor or wPor: air-balloon or water-filled Portex catheter. *: SOFC:ORC ratio significantly different from ideal 1.0 (see criteria in methods). +: $P < 0.05$ for A-BC vs. W-FC of same FG-size and brand.

SOFC-ORC differences for phase-frequency response variables are depicted in Fig. 3 (a negative phase-shift difference implies that the SOFC phase-shift is greater than the corresponding ORC

Table 2. SOFC:ORC ratios; statistical summary table.

Catheter	(1)	(2)	(3)	(4)	(5)	(6)	(7)	(8)	(9)	(10)	(11)	(12)	(13)	(14)	(15)	(16)	(17)
wPor10 (1)																	
aPor10 (2)	ade																
wVen10 (3)	abde	abde															
aVen10 (4)	ade	-	abde														
wPor8 (5)	a	de	abde	e													
aPor8 (6)	ade	-	abde	-	de												
wVen8 (7)	-	bde	-	bde	-	bde											
aVen8 (8)	ade	-	abde	-	de	-	abde										
wPor6 (9)	ac	bde	ad	bde	-	de	-	de									
aPor6 (10)	acde	c	abde	c	acde	c	adbd	-	bde								
wVen6 (11)	ac	bcde	ad	bde	-	de	-	de	-	bde							
aVen6 (12)	acd	ace	abcd	acde	acde	ac	acde	ac	acde	-	ade						
wAdc5 (13)	acde	abce	ad	abce	ac	bce	ad	be	ad	be	d	de					
wVen5 (14)	ac	bcde	ad	bce	c	bcde	a	bde	-	bde	-	de	-				
wPor4 (15)	acd	acde	acde	acde	acd	acde	acd	ace	acd	ae	ad	-	de	ad			
wVyg4 (16)	acd	ace	ad	ace	ac	ace	ad	e	ad	e	ad	de	-	-	d		
aJag8 (17)	ade	-	abde	-	de	-	abde	-	bde	c	bde	ce	bce	bcde	abce	bce	

SOFC, Second Order Fitted Curve; ORC, Original Recorded Curve; a, SOFC:ORC ratio of f_{A5}; b, SOFC:ORC ratio of f_r; c, SOFC:ORC ratio of A_r; d, SOFC-ORC phase-shift difference of P_{A5}; e, SOFC-ORC phase-shift difference of Pf_r; w/aPor-Adc-Ven Jag, water-filled/air-balloon Portex Adcock Ven Erich-Jaeger catheter brands and FG size; Variables a-e indicated are $P < 0.05$ between any two catheters; -, no significant difference.

phase-shift). SOFCs of the A-BC and W-FC groups overvalued the phase-shift at f_{A5} (= P_{A5}), as evidenced by the SOFC-ORC phase-shift difference of P_{A5} being significant for most catheter samples (Fig. 3, top graph). Between the A-BC and W-FC catheter groups, for the same FG-size and brand of catheter, the SOFC of all the W-FC group's samples overvalued P_{A5} to a significantly greater degree than did SOFCs of the A-BC group's samples (e.g., compare the SOFC-ORC phase-shift difference of wPor8 with aPor8).

There was a trend, significant in several samples, for the magnitude of the phase-shift difference overvaluation by SOFCs to decrease with decreasing FG size in the W-FC group. Within the A-BC group, for the same FG size, the SOFC-ORC phase-shift difference of P_{A5} was unaffected by the brand of catheter tested (e.g., compare the phase-shift difference of aPor8 with aVen8). However, catheter brand significantly affected the W-FC group's samples (e.g., compare wPor10 with wVen10). SOFCs significantly overvalued the phase-shift difference at f_r (= Pf_r) in the W-FC group, but significantly undervalued Pf_r in the A-BC group (Fig. 3, bottom graph).

SOFC:ORC ratios and SOFC-ORC phase-shift differences for the commercially available Erich-Jaeger A-BC did not differ significantly from those of our similar FG-sized laboratory-manufactured A-BCs. The variance of SOFC:ORC ratios and of the SOFC-ORC phase-shift differences within most catheter samples were generally large (see standard deviation bars in Figs. 2 and 3). Table 2 summarizes the SOFC:ORC ratios' and the SOFC-ORC phase-shift differences' significant differences between differing A-BC and W-FC FG sizes and brands.

Discussion

The assumption that fluid-filled catheter-manometer systems adequately approximate second-order systems is motivated by the advantages thereof, such as the derivation of relatively simple mathematical equations that allow prediction of catheter frequency responses from square-wave response measurement techniques. Additionally, the electrical correction of incorrect information from an imperfect catheter-manometer system may be accomplished using second-order system models. The square-wave response technique is used by clinicians to assess *in vivo* the frequency response of underdamped catheter-manometer systems *in situ*, as well as by researchers who do not have ready access to suitable sine-wave pressure generators.

The construction of an appropriate